BIOMARKERS IN CARTILAGE REPAIR AND OSTEOARTHRITIS

Mass spectrometry (imaging) for the detection of possible diagnostic and therapeutic biomarkers for cartilage repair and osteoarthritis development

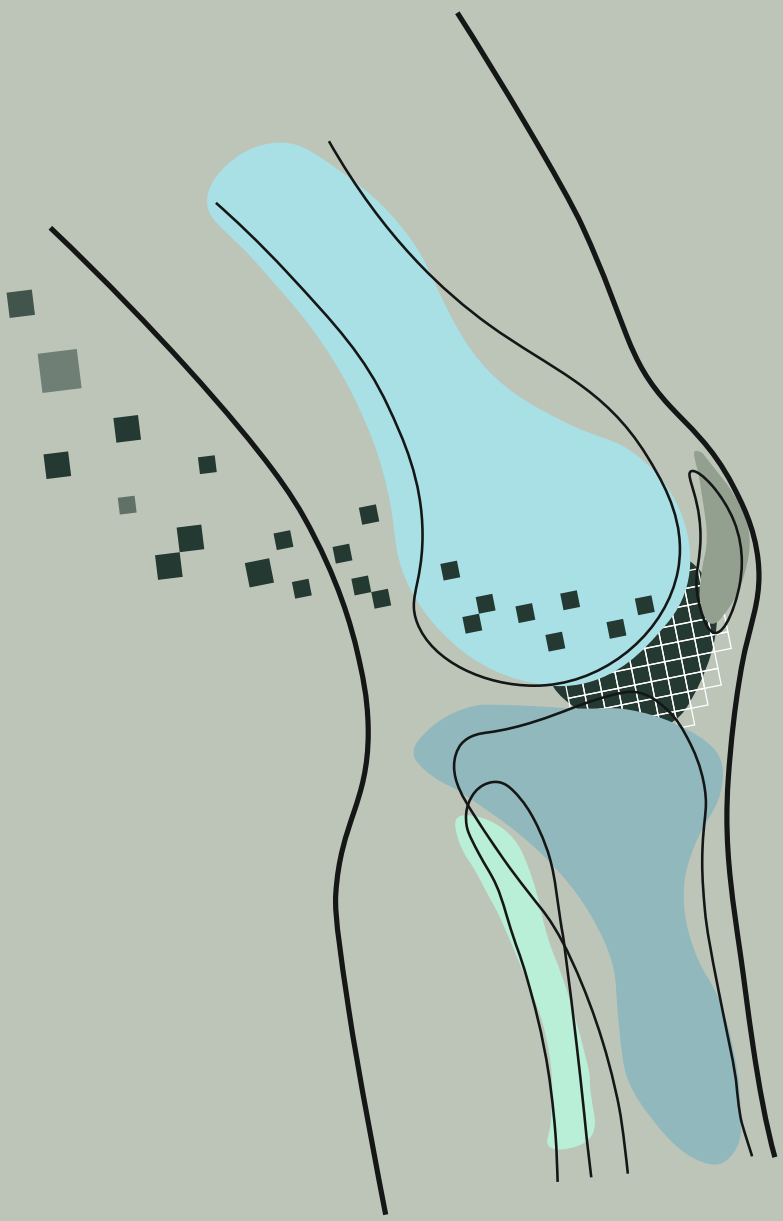

Mirella Haartmans

Biomarkers in cartilage repair and osteoarthritis

Mass spectrometry (imaging) for the detection of possible diagnostic and therapeutic biomarkers for cartilage repair and osteoarthritis development

Mirella J.J. Haartmans

ISBN: 978-94-6483-725-4

Ph.D. thesis Maastricht University

Biomarkers in cartilage repair and osteoarthritis
Mass spectrometry (imaging) for the detection of possible diagnostic and therapeutic biomarkers for cartilage repair and osteoarthritis development

Cover design: Dagmar Versmoren
Layout: Mirella Haartmans
Printed by: Ridderprint

The research reported in this dissertation was carried out at the Laboratory for Experimental Orthopedics, Department of Orthopedic Surgery and Maastricht Multimodal Molecular Imaging Institute (M4i), Maastricht University, Universiteitssingel 50, 6229ER, Maastricht, the Netherlands.

Biomarkers in cartilage repair and osteoarthritis

Mass spectrometry (imaging) for the detection of possible diagnostic and therapeutic biomarkers for cartilage repair and osteoarthritis development

PROEFSCHRIFT

ter verkrijging van de graad van doctor aan de Universiteit Maastricht,

op gezag van de Rector Magnificus, Prof. dr. Pamela Habibović

volgens het besluit van het College van Decanen,

in het openbaar te verdedigen

op dinsdag 20 februari 2024 om 10.00 uur

door

Mirella Josephina Johanna Haartmans

Geboren op 24 januari 1995 te Heerlen

Promotor

Prof. dr. R.M.A. Heeren

Copromotores

Dr. P.J. Emans
Dr. B. Cillero-Pastor

Assessment Committee

Prof. dr. M. Poeze, voorzitter
Prof. dr. A.E.R.C.H. Boonen
Dr. L.B. Creemers (UMC Utrecht)
Prof. dr. M. van Griensven
Prof dr. H.B.J. Karperien (Universiteit Twente)

This research was part of a collaboration between the Laboratory for Experimental Orthopaedics at Maastricht University, the Department of Orthopaedic Surgery of the MUMC+ and Maastricht MultiModal Molecular Imaging Institute (M4i) and part of the NWO William Hunter Revisited consortium (P15-23).

The M4i research program is financially supported by the province of Limburg (the Netherlands) via the LINK program. ReumaNederland financially supported the work conducted at the department of Orthopaedic Surgery (MUMC+) and the Laboratory for Experimental Orthopaedics at Maastricht University.

Financial support for the publication of this Thesis was provided by Anna Fonds | NOREF.

Voor papa ♥

Table of contents

Chapter 1

General introduction & scope of this Thesis

Osteoarthritis of the knee, a burden of disease

Osteoarthritis (OA) is one of the most important causes of disability in the elderly population, affecting over 500 million people worldwide[1]. With an ageing population, increase in prevalence of obesity[1], and additional increasing numbers of sports injuries contributing to OA, the burden of knee OA is expected to increase even further in the future. Although hand OA is the most common type of OA[2-4], knee OA accounts for almost 80% of the burden of OA worldwide[5, 6], as it affects the patient's locomotive and consequently the patient's overall body health. Physical inactivity, as a result of affected locomotion, is a primary cause of chronic diseases[7]. In addition, these co-existing conditions such as heart disease, diabetes, or mental health problems are associated with increasing morbidity and mortality rates[1, 8].

Healthy joint homeostasis

The human knee joint makes our body mobile, allowing us to walk, run, and play different types of sports. Inside the knee, multiple intra-articular tissues, maintaining healthy joint homeostasis, can be recognized (**Figure 1.1**). Joint homeostasis is determined by complex interactions between tissues, cells, and molecules involved in signaling pathways regulating remodeling, restoration, and destruction[9, 10]. A healthy joint requires a balance between these molecular signals, which is determined by cells, tissues, and cell- and/or tissue interactions within the joint[10]. If the joint is damaged, such as with OA, healthy joint homeostasis is disturbed and tissue destruction is enhanced[10].

The knee joint connects the femur (upper bone of the leg) with the tibia (lower bone of the leg). The connecting ends of these bones are covered by a layer of 2 to 4 mm articular hyaline cartilage that provides a smooth, shock-absorbing surface for articulation and load transmission[11]. This cartilage is a type of connective tissue, consisting of water (65-80% of wet weight), collagens (60% of dry weight), proteoglycans (10-15% of wet weight), and other glycoproteins[11]. For extension of the knee, the patella forms the anterior compartment of the knee joint. This patella is covered with one of the thickest layers of articular cartilage in the human body.

Two other fibrocartilaginous tissues inside the joint lay between the tibia and the femur: the menisci. These menisci function as additional protection of the articular cartilage by spreading the load, absorbing shocks, as well as stabilizing and lubricating the joint[12]. For anterior-posterior rotational stability of the joint, the anterior and posterior cruciate ligaments connect the tibia with the femur[13]. The inner surface of the joint is covered by a synovial membrane or synovium. It provides a non-adherent movable surface while lubricating the cartilage surface (synovial fluid) and providing nutrients[14]. The synovial membrane is also involved in the

inflammatory response, producing chemokines and cytokines[14]. The infrapatellar fat pad (IPFP), or Hoffa's fat pad (HFP), is located outside the synovial cavity, inside the knee capsule, and underneath the patella tendon[15, 16]. The function of this highly vascularized adipose tissue is not completely known[15], but has been shown to be involved in inflammatory processes by secretion of inflammatory mediators[16]. It is therefore expected to play an important role in maintaining healthy joint homeostasis.

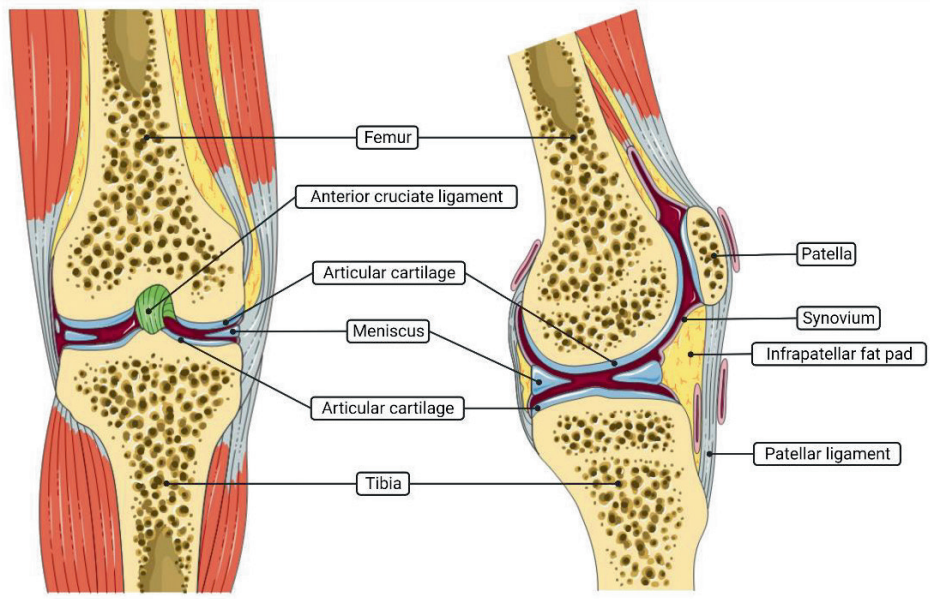

Figure 1.1. Anatomy of the knee: frontal (left) and parasagittal (right) view of the knee. The human knee consists of two long bones (femur and tibia), connected by the anterior crucial ligaments, and the patella. These bones are covered with a layer of articular hyaline cartilage. In between those articular cartilage layers lay two menisci, also consisting of cartilage. A lubricant that facilitates movement, synovial fluid, fills up the synovial cavity, sealed by the synovium or synovial membrane. The infrapatellar fat pad or Hoffa's fat pad is located outside the synovial membrane under the patellar ligament. *The image was created with permission from Servier Medical Art, licensed under a Creative Common Attribution 3.0 Generic License. http://smart.servier.com/. Created with BioRender.com.*

Every articular joint has one of these well-vascularized fat pads[17]. Throughout the body, white adipose tissue in general has been acknowledged as metabolically active organ[17, 18]. Alongside its function in joint stability and shock absorbance, it stores lipids and controls the metabolic balance by functioning as endocrine organ[17, 19]. Within the joint, the articular fat pad has been associated with joint pathologies including OA[20]. Its role however, in maintaining healthy joint homeostasis, remains unknown[17]. The largest articular fat pad in the knee joint, the IPFP, has been

described as endocrine organ due to its high vascularity[17, 19] and has been suggested to play an important role as sensory organ due to the presence of nerve fibers[17]. The IPFP has been shown an important contributor to anterior knee pain after joint trauma[17, 21], as well as inflammation and progression of knee OA[17, 22].

Disturbed joint homeostasis: osteoarthritis

William Hunter once stated in 1743: "If we consult the standard Chirurgical Writers from Hippocrates down to the present age, we shall find, that an ulcerated cartilage is universally allowed to be a very troublesome disease; that it admits of a cure with more difficulty than carious bone; and that, when destroyed, it is not recovered"[23]. The breakdown of cartilage and underlying bone, with the lack of regenerative potential of cartilage, is the leading cause of a degenerative disease called OA[24]. OA's increasing prevalence and incidence are associated with age, making it one of the most common joint diseases in the world[25].

Patients suffer from progressive pain, swelling, (morning) stiffness, and mobile disability, reducing the quality of life[24, 26, 27]. OA affects the whole joint and is characterized by inflammatory pathogenesis[24], synovial thickening, and cartilage degradation among others[24] (**Figure 1.2**).

Progressive loss of cartilage may eventually lead to patient's disability. Alongside age[25], genetics[28], obesity[29], gender[30], (sports) injury[31, 32], ethnicity[33], and joint abnormalities[33] are the most common risk factors for its development. OA can develop in any joint with articular cartilage, but is most prevalent in hand and fingers, hip, and knee[33]. For OA in the knee, factors such as overweight, obesity, and lifestyle play an important role in its development due to its loadbearing capabilities. Diagnosis and treatment of OA, already in or before the early stages of its development, towards the end-stage of OA, can have a huge societal impact for the patient and even improve quality of life.

Osteoarthritis: diagnosis and current treatment options

Clinically, OA is diagnosed using a standing knee radiograph, showing joint space narrowing, osteophyte formation, thickening of the bone, and bone cysts[24]. The severity of OA can be determined for example by using the Kellgren-Lawrence (KL) grading scale[24, 34] (**Figure 1.3**). The first line of joint-preserving treatment options for OA focuses on exercise, diet, and weight loss[35-37], the use of braces[38], and/or pharmacological treatment of symptoms such as pain or inflammation by non-steroidal anti-inflammatory drugs (NSAIDs)[39].

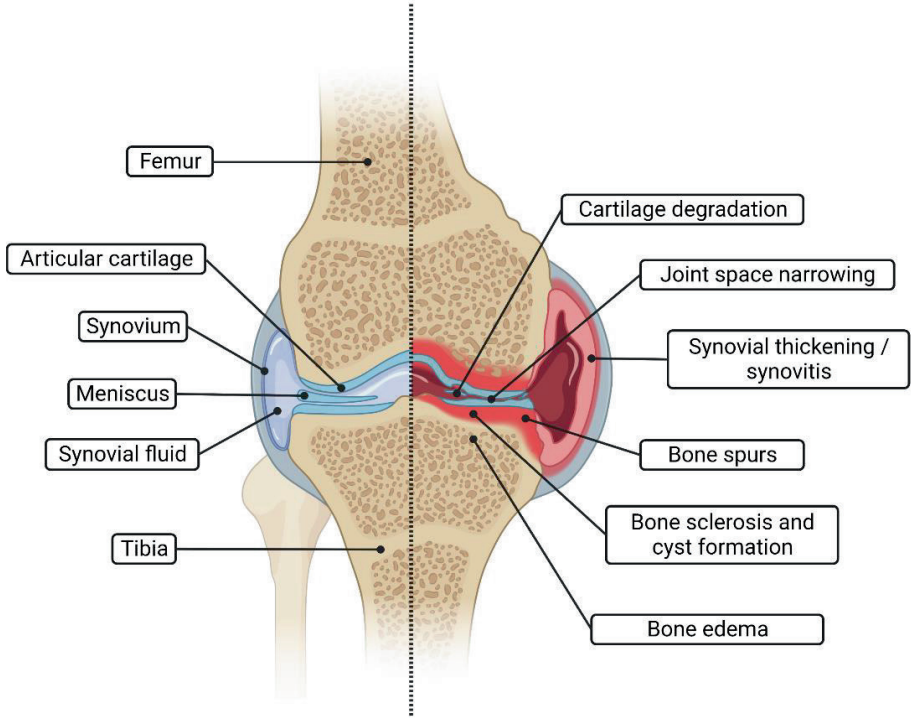

Figure 1.2. Representation of a healthy knee (left) vs osteoarthritic knee (right). Synovial thickening and inflammation, cartilage degradation, formation of bone spurs, bone sclerosis and cyst formation, and bone edema characterize osteoarthritis in the knee. *Created with BioRender.com*.

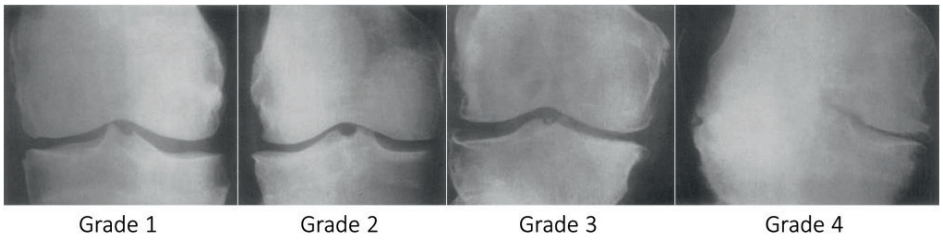

Figure 1.3. Radiographic representation of the original (1957) Kellgren-Lawrence (KL) classification for osteoarthritis in the knee[34]. A healthy knee is described as a joint without joint space narrowing (KL 0), a knee with minor-mild osteoarthritis (KL 1-2) shows joint space narrowing with osteophyte formation, and a knee with mild-advanced osteoarthritis (KL 3-4) shows joint space narrowing with osteophyte formation and bone deformation. Eventually, bone will get sclerotic (KL 4). *Used with permission*.

One of these NSAIDs is celecoxib. Celecoxib is a selective cyclooxygenase (COX) 2 inhibitor, known for its inhibition of prostaglandins (PGs), a class of molecules involved in inflammation[40, 41] (**Figure 1.4**). The chondroprotective effect of celecoxib is disputed, with studies showing its chondroprotective effect *ex vivo* and *in vivo*[42-47] or, on the contrary, the lack of chondroprotective effect[48-50]. Contradiction of the effect of celecoxib on cartilage, and the results found in currently existing literature, might be dependent on differences in study design, way of administration, or dosage, among other factors[51].

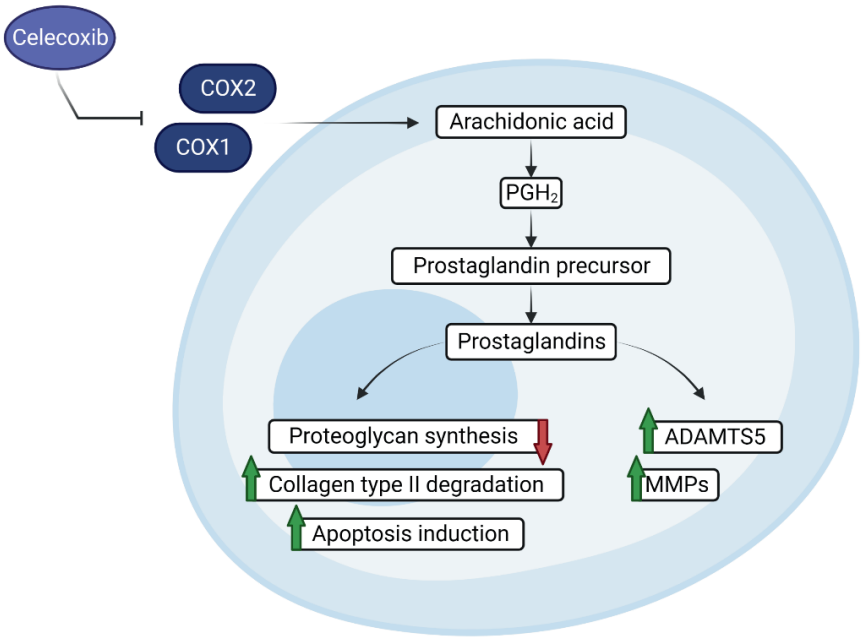

Figure 1.4. Simplified overview of the working mechanism of Celecoxib on cyclooxygenase 2 (COX-2) and its underlying pathway. Celecoxib is known to inhibit prostaglandins, resulting in a decrease in proteoglycan synthesis and an increase in collagen type II and apoptosis[41]. Additionally, it alters gene expression in osteoarthritis patients, inducing the release of proteolytic enzymes like a disintegrin and metalloproteinase with thrombospondin motifs 5 (ADAMTS5) and matrix metalloproteinases (MMPs). *Created with BioRender.com.*

Numerous studies, showing a variety in study design and inconsistency in results, have been studying intra-articular administration of celecoxib and its chondroprotective effect on cartilage. In **this Thesis**, in **Chapter 3**, the effect of celecoxib on cartilage after a single bolus intra-articular injection was studied. This technique has not been used in the clinic yet, but might have its advantages over possible severe side effects after oral administration[47]. The use of NSAIDs can be

accompanied by possible adverse events such as gastrointestinal or cardiovascular complication due to inhibition of COX-2 and COX-1[47, 52]. Local, intra-articular administration of celecoxib could have a more effective chondroprotective effect on cartilage and possibly prevent adverse events already known for oral administration of celecoxib.

If the use of NSAIDs such as celecoxib or other painkillers such as opioids, lifestyle changes, and physiotherapy are insufficient to treat the symptoms of OA, often intra-articular injections of corticosteroids or hyaluronic acid are executed until total joint arthroplasty[53].

The (lack of) regenerative potential of cartilage

OA prevalence is not only increasing in our elderly population[33], but also in the younger population[54] due to the increasing incidence of risk factors such as obesity and intra-articular defects (e.g. osteochondral trauma, cruciate ligament tear, or patella luxation)[28, 33, 54]. Early detection of OA, phenotyping of OA, as well as prediction of OA development are of great value for maintaining a patient's mobility and herewith prevent other chronic diseases. In addition, early detection and phenotyping of OA might contribute to (the development of novel) targeted therapies and personalized medicine.

Currently, there is no disease-modifying therapy for OA. Joint-preserving surgery and improvements in lifestyle, including weight loss, have been described to slow down, stop, or even (partially) reverse the course of OA (**Figure 1.5**). Total joint arthroplasty is the unique treatment for end-stage OA. At this moment, a total joint prosthesis has the highest positive impact on quality of life as it promotes the patient's mobility[55].

With an increasing incidence of OA in the younger population[54] and a total joint prosthesis' limited lifespan, it is even more important that joint damage is treated properly, OA is detected early, and the need for total joint arthroplasty is postponed. It has been shown that with joint replacement before the age of 55, the chances of revision surgery increase up to 35% in the following 10 years[56]. This causes a treatment gap between ages 40-60, in which total joint replacement is not the solution, though the better options are lifestyle changes or joint preserving surgery (e.g. cartilage repair, osteotomy, or meniscus repair/replacement), preferably before OA progresses[57] (**Figure 1.5**).

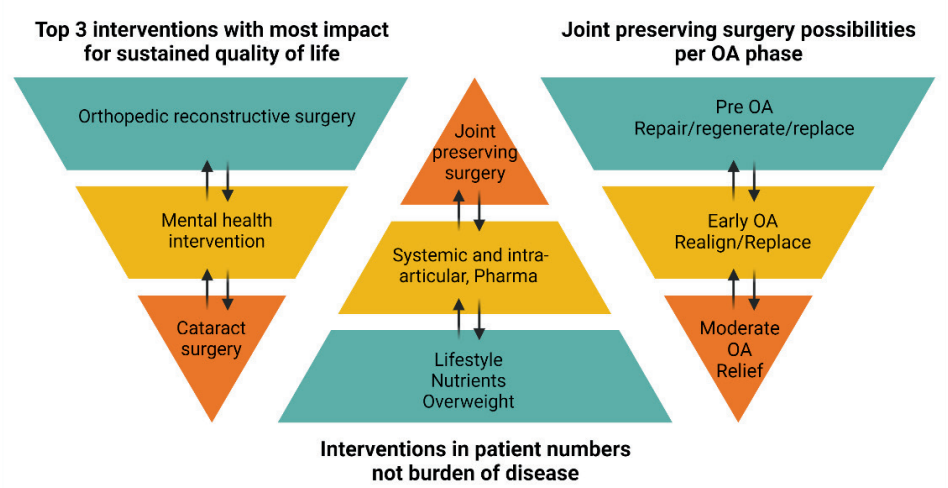

Figure 1.5. The three triangles in this figure show the top three interventions (from left to right) that have the most impact on the quality of life, burden of disease, and the surgical options available per osteoarthritis (OA) phase[55]. *Created with BioRender.com.*

The extracellular matrix (ECM) of articular cartilage is made up of differently abundant and aligned chondrocytes and collagen type II fibers in each of the cartilage zones: superficial-, transitional- (middle-), deep-, and calcified zone[58] (**Figure 1.6**). In the superficial zone, chondrocytes lay flattened along the surface[58]. Likewise, the orientation of the collagen (COL) type II fibers are condensed and parallel to the joint[58].

Few proteoglycans are present in the superficial zone[58]. Both transitional and deep zones contain round chondrocytes, which produce large amounts of proteoglycans, gradually declining towards the tidemark[58]. Furthermore, hypertrophic chondrocytes in the calcified zone produce different (ratio) of ECM components, such as COL-X. Chondrocytes in the calcified zone are responsible for mineralization[58], maintaining the interface between cartilage and bone[59].

Articular cartilage does not regenerate because it lacks blood vessels, nerves, and lymph vessels[11]. It therefore still remains a challenge to develop methods to regenerate cartilage (e.g. after a defect), delay OA progression, or reverse the OA development process [60]. A better understanding of the (molecular) pathophysiology of OA and its development after e.g. intra-articular damage including (osteo)chondral defects has led to the development of a wider variety of joint preserving and/or cartilage repair therapies to relieve symptoms and postpone OA development and joint replacement surgery[61].

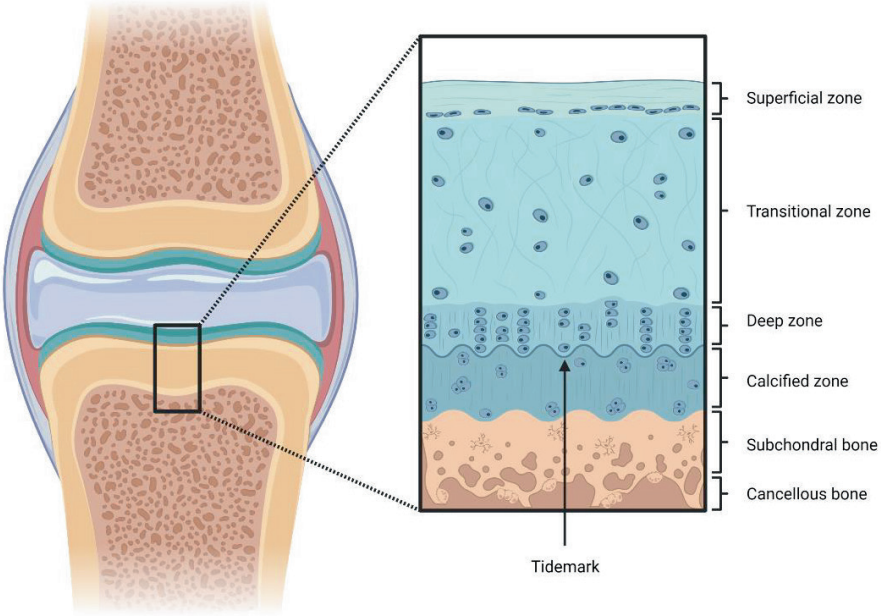

Figure 1.6. Schematic representation of the structure of the articular cartilage and underlying bone. The articular cartilage consists of four zones: the superficial zone, consisting of a layer of flattened chondrocytes parallel to the surface, the transitional zone (middle zone), containing isolated round chondrocytes, the deep zone, consisting of round, nicely arranged layers of chondrocytes, and the calcified zone, containing hypertrophic chondrocytes. The tidemark is situated between the deep zone and the calcified zone. *Created with BioRender.com.*

From cartilage defect towards development of osteoarthritis: phenotypes

While not only intra-articular trauma and damage are contributing to OA development, intra-articular surgery by itself causes intra-articular damage as well, contributing to OA. It is even more important to have insight in the phase and phenotype of OA to be able to indicate the proper joint-preserving treatment (**Figure 1.5**) and thereby preventing early joint replacement and complex revision surgery[57]. Joint-preserving intra-articular surgery by removal of the affected tissue followed by inserting an (metal, autograft, or allograft) implant is one option to resurface the cartilage at the site of the defect[61]. However, other regenerative options have been developed to reduce pain or stimulate cartilage growth[61]. These regenerative options include palliative techniques, such as chondroplasty, that focus on the treatment of cartilage lesions by smoothing or trimming the degenerative cartilage to reduce the patient's pain and prevent worsening of the defect[62]. Other

regenerative treatments include bone marrow stimulation techniques, cell-based techniques, and other bone-based techniques such as osteochondral allograft or autograft transplantation[61].

Bone marrow stimulating techniques such as microfracture surgery can often be performed arthroscopically. During the procedure, holes are created at the site of injury to recruit blood and stem cells from the bone marrow and fill up the cartilage defect with a blood clot that eventually forms a cartilage-like material called fibrocartilage[63]. Cell-based techniques on the other hand, focus on the transplantation of previously obtained autologous articular cartilage material that has been expanded in a laboratory setting (e.g. autologous chondrocyte transplantation)[64]. Not only cells, but also part of the cartilage, including a piece of subchondral bone, an osteochondral autograft or allograft, can be collected from a less essential, less weight bearing part of the joint and transplanted into the defect (e.g. mosaicplasty)[65].

Sanders et al. have described that treatment of osteochondral defects, as described above, will delay the progress of OA[66]. Which treatment is used in each patient is dependent on effectiveness, considering age, severity and magnitude of the defect, as well as the expected outcome[61]. In the Netherlands specifically, Jeuken et al. showed in a survey study that not all treating surgeons are aware of the latest insights concerning the treatment of a defect and that the characteristics of the defect (e.g. size) as well as the patient (e.g. age or body mass index (BMI)) should be taken into consideration[67]. In addition, better knowledge, and the availability of state-of-the-art treatments will lead to better patient outcomes and possibly preservation of the joint[67, 68].

OA development after an injury such as a cartilage defect is defined as post-traumatic OA (PTOA) and is accounting for nearly 12% of the symptomatic OA cases[31, 69]. Within seconds after injury, structural changes within the cartilage take place: cartilage starts swelling, cells get necrotic, collagen ruptures and glycosaminoglycans (GAGs) are lost[69]. Within years, mechanobiological, cellular and molecular changes in the joint can lead to an inflammatory reaction, which might eventually develop into OA[69]. Specifically for the knee, 13.9% of the patients with a history of joint injury develop OA[69]. This type of OA development is particularly affecting patients with relative young age[69, 70]. PTOA has been integrated in the mechanical overload OA phenotype, as it is hard to distinguish a micro-trauma worsening over years from a traumatic defect. Mechanical OA also includes osteochondral defects (especially around an age above 40), as well as varus and valgus misalignments[71], and patellar tracking disorders[72], and is accounting for 12-22% of the knee OA cases[73]. Also for other phenotypes, it is important that OA is detected early in its development, as a change in lifestyle, such as changes in diet,

physical activity, and use of NSAIDs might have an inhibitory effect on further development of OA[74, 75]. A patient's potential phenotype can be determined based on multiple factors including bone marrow lesions, inflammation, biochemical markers, and pain[76, 77]. A total of six phenotypes for OA can be identified according to a systematic literature review by Dell'Isola et al. in 2016 including 1) chronic pain, 2) inflammation, 3) metabolic syndrome (e.g. diabetes or obesity), 4) alterations in bone and cartilage metabolism, 5) mechanical (e.g. overload, malalignment, or medial compartment disease), and 6) minimal joint disease (e.g. minor clinical symptoms and progression over time)[73, 77, 78]. A better insight in these phenotypes and their changes during OA aids proper treatment of a specific patient.

Biomarkers for osteoarthritis

A biomarker, or biological marker, can refer to a broad range of predictive, diagnostic, or prognostic indications for a certain medical status, which can be measured in an accurate and reproducible way[79]. There is no well-established categorical system for biomarkers, nevertheless, several classification systems are used in literature[80]. One classification is the subdivision of biomarkers into "wet biomarkers" and "dry biomarkers"[80]. Wet biomarkers include measureable genetic and molecular factors, such as molecules present in tissues (e.g. cartilage, synovium, or meniscus)[81] and fluids (e.g. synovial fluid[82], or blood)[79, 80, 83, 84]. Dry biomarkers on the other hand include imaging (e.g. magnetic resonance imaging (MRI) or X-ray), as well as scoring systems or questionnaires[80]. Another way of categorizing biomarkers is based on their purpose and includes competitive, efficacy, pharmacodynamics, pharmaco-economic, predictive, prognostic, safety, and stratification biomarkers[80]. Although these biomarkers often not exclusively fit to one class[80] and are not always objective measures, they may represent the early development of OA or possibly predict cartilage regenerative outcome[81, 85]. Biomarkers may thus play an important role in surgical decision-making. It is even more important if joint-preserving (e.g. intra-articular vs extra-articular surgery and when intra-articular surgery is conducted, should it be regenerative or resurfacing?) surgery or joint-replacement surgery is indicated and a decision on treatment has to be made. This clinical decision-making can theoretically be guided by biomarkers that can be obtained using non-invasive techniques such as quantitative MRI[86] or visually during (arthroscopic) surgery. An example of a biomarker detected with MRI is the GAG content in cartilage. GAG content can be measured using MRI because it attracts water into the ECM[86, 87]. During early cartilage degeneration, this GAG content in cartilage is lost, which renders the MRI result, a measure of the cartilage quality[86]. MRI is a well-developed method to measure cartilage quality and improve surgical decision-making. At this moment, the technique is time consuming (patients have to lay still for extensive periods), expensive and requires an additional appointment. Novel developments, such as low-field MRI in combination with e.g. artificial

intelligence or digital technologies, address the shortcomings of MRI, as mentioned above, making it an interesting objective measurement-control in the field of intra-articular injury and OA. In addition, visual evaluation of the cartilage during surgery might be subjective or inconclusive.

Current decision-making on whether or not to operate, and whether or not to preserve the joint, is mostly based on MRI and/or X-ray, combined with clinical aspects such as medical history, age, BMI, and expectations of the patient. Which (group of) biomarker(s) eventually can help with this decision-making and play an important role in the prediction of OA development remains unknown. In **this Thesis**, we addressed this knowledge gap by giving an overview of the currently known molecular biomarkers for OA by mass spectrometry (MS) in literature in **Chapter 2**. Additionally, **this Thesis** addresses novel approaches for biomarker discovery for OA development (**Chapter 4, Chapter 5,** and **Chapter 6**), as well as their possible implication as prognostic tool for cartilage repair patients in the clinic (**Chapter 6**).

The infrapatellar fat pad as novel biomarker source

Compared to cartilage, synovial fluid or synovium, the IPFP is a less studied tissue within the field of OA research[81]. It has been suggested as novel biomarker source for early OA detection, development and progression, as it is highly available as waste material and can be obtained from almost every knee-related surgery[81]. Additionally, biopsy taking would be minimally invasive as it is easy to reach[81]. The IPFP contains a variety of molecules among which lipids, which already have been shown of importance in the inflammatory response in OA. Previous work on the biomarkers for OA showed a diversity of proteins, lipids, and metabolites upregulated in cartilage, meniscus, synovium, and synovial fluid of OA patients compared to control patients[81]. The application of the IPFP as a possible novel biomarker source for OA and cartilage regeneration will be further explored in **this Thesis** in **Chapter 4**, **Chapter 5**, and **Chapter 6**.

A variety of proteins (including complement component C9, complement factor B, fibrinogen β and γ chains, and fibronectin), and lipids and metabolites (including multiple fatty acids and vitamin D3 fragments), in a variety of intra-articular tissues (cartilage, meniscus, synovium, and synovial fluid) have been shown of importance in the search for OA related biomarkers. It therefore has been suggested that a combination of molecules in a biomarker profile for OA is of greater importance than one single particular biomarker[81]. This hypothesis will be tested thoroughly with the technological advances described in **this Thesis**.

In **this Thesis**, the IPFP's molecular profile and the feasibility of its use in biomarker discovery for OA development were investigated. The molecular profile of the IPFP

has not been studied as a potential diagnostic and predictive tool for early OA detection. Taking into account the IPFP's intra-tissue heterogeneity, the samples were analyzed using a technique that preserves the molecular spatial distribution throughout the tissue (mass spectrometry imaging, MSI) in **Chapter 4** and **Chapter 5**, and a technique that might be implementable in the clinic (rapid evaporative ionization mass spectrometry, REIMS), in combination with a proteomics approach in **Chapter 6**.

Mass spectrometry (imaging)

One technique that can be used for the detection and discovery of (novel) diagnostic or predictive biomarkers, or a biomarker profile, is MS. MS is a label-free analytical tool[88], able to detect molecules including lipids, metabolites, proteins or peptides, in a variety of samples such as tissues, fluids or gasses[88, 89]. MSI is a MS technique for rapid detection of the on-tissue spatial distribution of a variety of molecules and combines localization and identification[90]. It gives us a detailed understanding of the body's biological processes and development of certain diseases (such as OA) at tissue- and even cellular level[91, 92]. In addition, near real-time techniques using MS were developed for the analysis of tissues and fluids, with the potential to be used in out-patient clinic or intra-operatively. Alongside biomarker discovery, MS(I) has been used in many other clinical applications. It has been used for diagnostic purposes and to build models to predict patient outcome, across a variety of medical specialties and research areas, including oncology, cardiovascular diseases, and rheumatology[93].

A mass spectrometer consists of different elements, including an ion source, mass analyzer, and detector[89, 94]. The ionization source volatilizes and ionizes molecules from a solid or liquid sample, into gas phase ions[94]. A variety of ionization sources are available, including hard ionization sources (e.g. secondary ion mass spectrometry, SIMS), utilizing a high amount of energy causing fragmentation of molecules, and soft ionization sources (e.g. matrix-assisted laser desorption/ionization, MALDI, or electrospray ionization, ESI) allowing the analysis of the molecular ion, rather than fragment ions[88, 89, 95]. Ambient ionization techniques, such as REIMS, coupled to a surgical tool such as a diathermic knife, were developed to explore the use of MS *in vivo*[96, 97]. The mass analyzer subsequently separates the ionized molecules based on their mass-to-charge ratio (*m/z*) using magnetic or electric fields. There are many types of mass analyzers, including time-of-flight (TOF), ion trap, Orbitrap, and quadrupole (e.g. Q-TOF). In a TOF system, molecules accelerate through a high voltage electrical field towards the detector. The time until these molecules reach the detector is dependent on the mass of the ion[89, 94]. A detector detects ionized molecules and provides us with an

electrical signal, which can be transformed into a mass spectrum, visualizing relative abundancies of the detected *m/z* values (**Figure 1.7**).

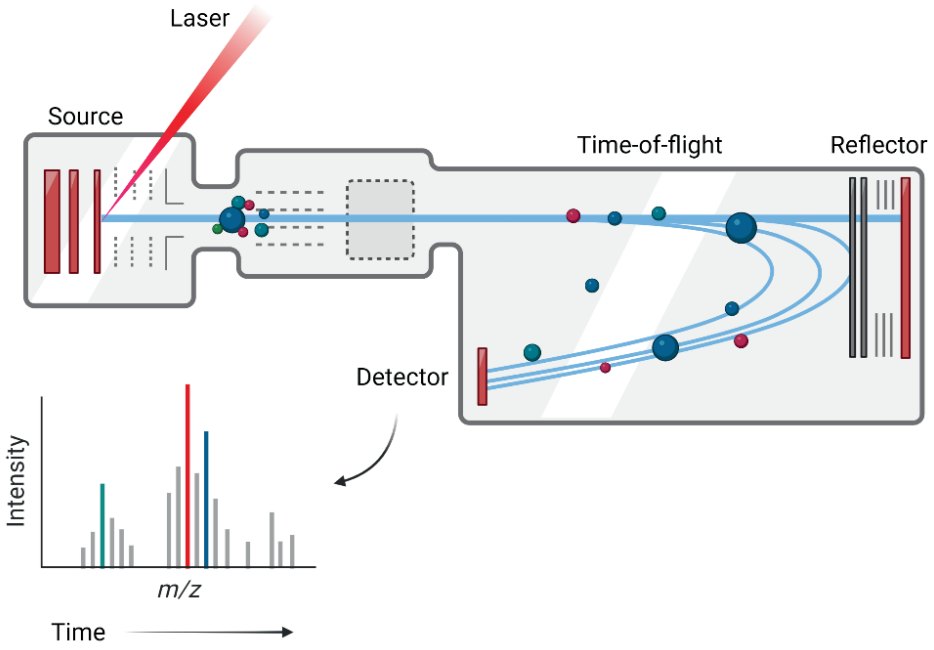

Figure 1.7. Simplified overview of a MALDI-TOF system, running in reflectron mode. A sample is irritated with a laser pulse, creating a plume of ionized molecules that enter a TOF MS system running in reflector mode where ionized molecules are separated based on their mass-to-charge ratio (*m/z*). The detector detects the ionized molecules and creates a mass spectrum. *Created with BioRender.com.*

In **this Thesis**, the MALDI-TOF system was used in reflectron mode. The reflectron is an electrostatic field at the end of the flight tube, which works like a mirror, reflecting ions towards the detector[89, 94, 98, 99]. The time necessary for a molecule to reach the detector, is dependent on the penetration depth of the ionized molecule[98, 99]. The higher the kinetic energy of the ion, the further the ion penetrates the reflectron. This method compensates for differences in flight times of ions with the same *m/z* (**Figure 1.7**).

Molecular identification

Tandem mass spectrometry (MS/MS or MS^2) is used to gather additional information on a molecule of interest for identification[88, 89, 94]. With MS^2, at least two mass analyzers (e.g. ion trap, Orbitrap, or (Q-)TOF) are coupled together to form a hybrid

system. Sample molecules get ionized as described above (MS^1) and get separated based on their *m/z*. These so-called precursor ions[88, 89, 94], are then trapped in the second mass analyzer, where they are fragmented into so-called product-ions by collision induced dissociation (CID)[89, 94, 100]. These fragments can then be analyzed by MS^2, resulting in a mass spectrum. These fragment *m/z* provide additional information, essential for identification of the precursor molecule.

Within the biomedical and clinical field of MS research, the most widely used ionization technique is MALDI[88]. MALDI-MSI with a TOF mass analyzer (**Chapter 4** and **Chapter 5**), ESI-liquid chromatography tandem MS (LC-MS/MS) (**Chapter 3** and **Chapter 6**), and REIMS with Q-TOF mass analyzer (**Chapter 6**), were applied in **this Thesis** and will be discussed in more detail in next paragraphs.

MALDI-MSI

MALDI is one of the most frequently used ionization (negative and positive) techniques for MSI (**Figure 1.8**). It has been widely used as a technique for the detection of (bio) molecules such as lipids, metabolites, proteins, and peptides, as well as a variety in drugs[101] and polymers[102] in a wide variety of applications[103] along with compound or drug detection, (clinical) diagnostics, biomarker discovery, and identification of potential targets for treatment. Its application involves single cells[104, 105] and cell cultures[106, 107], organoids[108, 109], animal- and human organs[110-112], as well as plants and food[113-115], among other.

Although the workflow for MALDI-MSI (**Figure 1.9**) might differ among tissue type and molecule of interest, a general MALDI-MSI workflow starts with the collection of fresh frozen (snap-frozen and stored at -80°C) or formalin-fixed and paraffin-embedded (FFPE, for proteins and peptides) tissue samples. It is important that tissue samples are collected and stored adequately to preserve tissue morphology, and prevent molecules from degrading or delocalizing. Subsequently, sections are made and transferred to indium tin oxide (ITO) coated glass slides. There are multiple approaches to get a thin and flat tissue section, with variations in thickness (usually between 10-20 µm) and mounting (e.g. thaw-mounting or tape transfer) dependent on the tissue type used. Dependent on the molecule of interest, a specific matrix is applied. This can either be done by spraying, sublimation, spotting or nebulization. This matrix extracts the molecules (analytes) of interest from the tissue section, has a photon absorbance in the wavelength range of the laser used, and allows analyte desorption and ionization, as well as prevents delocalization of molecules by crystalizing on the tissue surface[116].

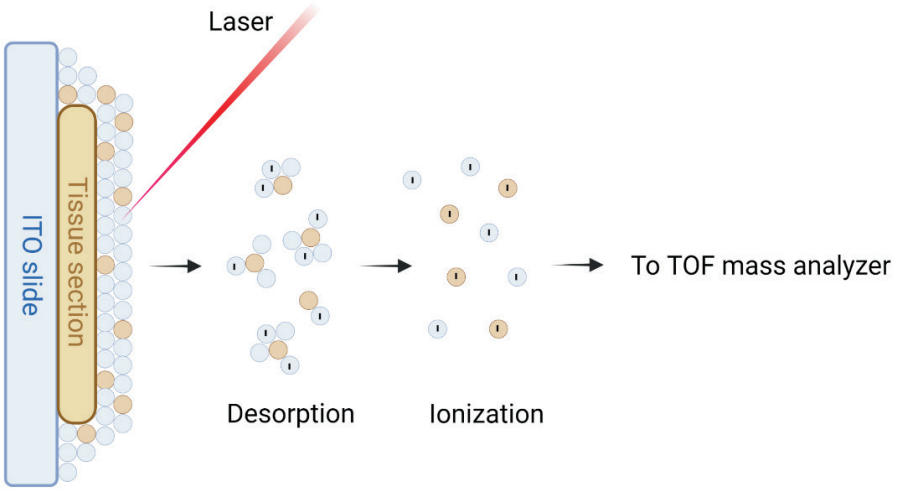

Figure 1.8. Schematic representation of matrix-assisted laser desorption/ionization (MALDI) in negative ionization mode. A fresh-frozen tissues section on an indium tin oxide (ITO) glass slide is covered with a layer of matrix. This layer of matrix extracts molecules of interest out of the tissue section and crystalize on the surface. A laser irradiates the crystals, causing the molecules to vaporize. In this gas phase, ions are formed, which are transmitted to the mass analyzer. *Created with BioRender.com.*

After matrix application, the coated slide is introduced into the MALDI source of the mass spectrometer. A focused laser irradiates the matrix-analyte crystals on the tissue surface (region of interest, ROI), without damaging the tissue underneath, volatizing them into the vacuum of the mass spectrometer (desorption). The resulting ionization of negative or positive charged molecules is dependent on the type of matrix applied. Each laser pulse, each pixel, generates a mass spectrum. The analyzed slide is subsequently stained with Hematoxylin and Eosin (H&E) for co-registration of the MSI data to the sample histology. Specific identifications can be obtained by MS^2 experiments described earlier.

MALDI-MSI is used to analyze and visualize lipids in the IPFP of patients with a cartilage defect or OA in **Chapter 4** and **Chapter 5** of **this Thesis**.

LC-MS/MS

Although LC-MS has been developed in the 1960's[117], since the beginning of 2000, LC-MS and LC-MS/MS have been used routinely in clinical applications, such as laboratory diagnostics or toxicology[118]. In the past decades, several methods for protein- and peptide analysis, metabolites, and lipids among others, have been

developed and optimized for multi-purpose application, including pharmacology and food-related projects.

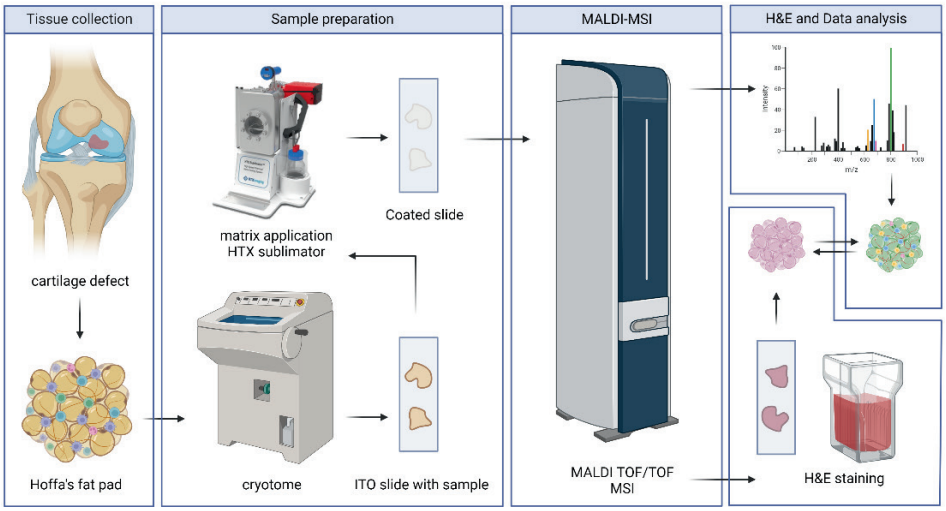

Figure 1.9. General workflow for matrix-assisted laser desorption/ionization mass spectrometry imaging (MALDI-MSI). *Created with BioRender.com.*

LC-MS/MS is an analytical technique in which molecules in liquid (biological) samples are separated based on their interaction capability to the LC-column connected (e.g. ultra high performance liquid chromatography, UHPLC) (**Figure 1.10**). Molecules of interest can be extracted from tissue samples, as well as fluids such as culture medium, blood, urine, or synovial fluid. Sample preparation may include cell lysis, tissue homogenization, filtration, or precipitation and extraction steps. Molecules with a stronger interaction to the column, move more slowly through the column than molecules with weaker interaction. These molecules are subsequently transferred to an ion source (e.g. ESI, atmospheric pressure chemical Ionization (APCI), or atmospheric pressure photoionization (APPI)). The mass spectrometer provides information on detection and identification of each molecule or component in the mixture.

LC-MS is used to analyze the protein secretome of cartilage after celecoxib treatment in **Chapter 3** and to analyze the protein profile of the IPFP in **Chapter 6** of **this Thesis**.

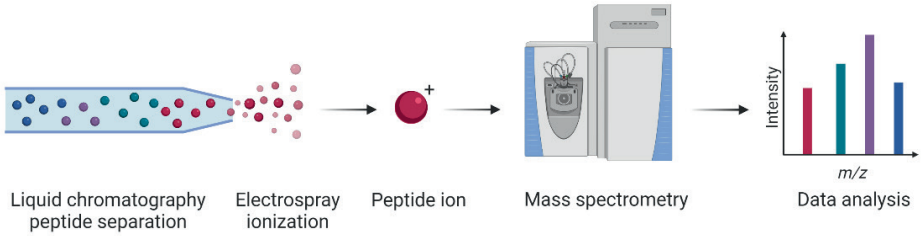

Figure 1.10. Simplified Liquid chromatography mass spectrometry (LC-MS) workflow. Peptides are separated on a column, ionized and analyzed in the mass spectrometer, generating a mass spectrum. *Created with BioRender.com.*

REIMS

REIMS is a relatively new MS technique, which involves the aspiration and thermal ionization of molecules in aerosols generated from evaporation by electrocautery or laser irradiation, of biological samples or liquids without the need for sample preparation[119]. Smoke that consists of these diagnostic aerosols can be generated by e.g. a hand piece such as electrocautery/diathermic blade/knife or needle, routinely used in the operating theater during a variety of surgeries[120] (**Figure 1.11**). When connected to a mass spectrometer, this translational technology generates a molecular profile of a specific tissue type, or affected tissue. REIMS requires minimal sample preparation, which makes it a promising tool for clinical application.

REIMS has high potential for future application in the clinic. The technique can be applied *in vivo*, during surgery, to provide the surgeon with near real-time molecular profiling of the patient. This patient profiling might in the future contribute to better surgical decision-making and better patient outcome.

REIMS is used to analyze the lipid profile of the IPFP in **Chapter 6** of **this Thesis**.

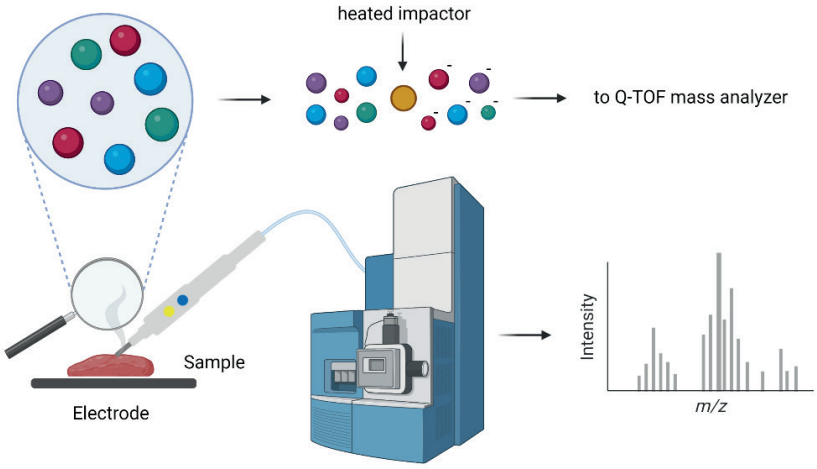

Figure 1.11. Schematic representation of the rapid evaporative ionization mass spectrometer (REIMS) system. The REIMS system can be coupled to a surgical instrument, such as an electrocautery knife. Smoke generated during the procedure is led into the REIMS system, providing a direct visualization of the state of the tissue or disease. *Created with BioRender.com.*

Scope of this Thesis

It is of great importance that OA is detected early in its development to delay the disease progression and postpone total knee arthroplasty (TKA). To achieve this, additional knowledge on the (molecular) pathophysiology, (molecular) OA-phenotyping, and possible (molecular) prediction models should be obtained. This can in turn improve clinical decision-making, and prevent or postpone OA development. Therefore, **this Thesis** aims to develop and test MS-tools to identify biomarkers for cartilage regeneration and OA by measuring the molecular changes or profiles that can predict or relate to disease status (regeneration and degeneration).

In **Chapter 2,** the currently known MS-based biomarkers (lipids, metabolites and proteins) for knee OA and knowledge gaps in the field of biomarker research in OA are systemically reviewed. At this moment, there is no biomarker available for OA development. Therefore, surgical decision-making is mostly based on MRI and X-ray, in combination with clinical aspects such as age and BMI. The finding of a (panel of) (molecular) biomarker(s) for OA development might contribute to better surgical decision-making and patient outcome. In the search for a molecular biomarker profile, we provide an overview of possible biomarkers in a variety of tissue types of OA and non-OA patients. In addition, we discussed the current limitations and give

some future suggestions for the use of MS as a tool for the identification of possible prognostic and diagnostic biomarkers, and possible therapeutic targets.

The first line of joint-preserving treatment for OA includes lifestyle-changes, the use of a brace, and/or pharmacological treatment to reduce pain and inflammation (NSAIDs). One of these NSAIDs is celecoxib, which has been shown in literature to act chondroprotective, as also its shortcoming on acting chondroprotective. The use of celecoxib as a possible chondroprotective drug in the development of OA can be of great importance in patients who develop OA at young age (before the age of 55). Other than the contradictive results on the chondroprotective effect of celecoxib, the drawback of the oral use of celecoxib is that it can be accompanied by negative side effects such as cardiovascular disease. In **Chapter 3** the possibility of intra-articular administration of celecoxib is addressed. This study focusses on the effects of celecoxib on the secretome of cartilage, as well as its possible chondroprotective effect. **This Chapter** contributes novel information to the unresolved discussion on the potential chondroprotective effect of celecoxib. We describe the effect of celecoxib treatment on secreted molecules by human cartilage *ex vivo* and investigated the chondroprotective effect of celecoxib on cartilage *in vivo* in an OA rat model.

Lipids have already to be shown important molecules regarding OA development. In **Chapter 3,** the importance of lipids was acknowledged by showing that the secretion of pro-inflammatory prostaglandins by cartilage after celecoxib treatment is reduced. **This Thesis** further focusses on a less studied tissue type, full of "unknown" lipids: the IPFP. In **Chapter 4,** we focus on the development of a MSI method applicable for biomarker research on the IPFP. A sample preparation method for the detection of lipids in the IPFP using MALDI-MSI was described. Sample handling and preparation for MALDI-MSI on adipose-like tissue can be challenging because adipose tissue is susceptible to melt, leading to delocalization of molecules and loss of spatial information. We developed and optimized a protocol for cryosectioning and matrix application for MALDI-MSI on the IPFP.

Using the protocol developed in **Chapter 4**, we analyzed the lipidome of the IPFP of cartilage repair and OA patients to find possible novel biomarkers for OA development in **Chapter 5**. We applied this previously developed protocol to the IPFP of OA and cartilage defect patients undergoing TKA and cartilage repair surgery respectively. We identified different lipid profiles for OA and cartilage defect patients and found specific lipids for each patient group. In addition, intra-tissue heterogeneity had been shown of importance. Each specific tissue type within the IPFP (adipose tissue and connective tissue) showed a different lipid distribution. We were able to discriminate OA patients from cartilage defect patients at the molecular level using their lipid profiles.

MALDI-MSI is at this moment not likely to be used in an *in vivo* clinical setting as it requires sample preparation and there is no validated clinical assay approved for diagnostics. However, in Chapter 6, we investigate the potential application of another MS-based technique (REIMS), which does not require extensive sample preparation and provides near real-time molecular profiling, on the IPFP *ex vivo* as a potential prognostic and diagnostic tool for cartilage regeneration and future development of personalized treatment, as well as its possible implementation in the clinic. We focused on the differences in lipid profiles of the IPFP of OA vs cartilage repair patients and correlated our findings to patients' questionnaires, IPFP fibrosis scores (scored on MRI), and histology. Secondly, we investigated the IPFP's proteome. Proteomics is a well-established technique in biomarker discovery. Similarly to the lipid profiles, proteins of OA and cartilage repair patients were correlated to patients' questionnaires, IPFP fibrosis, and histology.

In conclusion, the work in this Thesis contributes information towards the discovery of novel biomarkers for OA and/or cartilage regeneration. A better prediction model for surgical outcome will improve surgical decision-making and patient outcome, and might even lead to personalized treatment strategies. OA's prevalence is not only expected to increase due to the ageing population, but as important is the fact that patients develop OA at younger age due to a variety of factors including obesity and sports injuries. The development of a clinically applicable method for the early diagnosis of OA, as well as the prediction of patient outcome before cartilage repair surgery can improve surgical decision-making and patient outcome. More personalized treatment and early diagnosis of OA might delay OA development, which leads to better and longer mobility, and improved quality of life.

Chapter 2

Mass spectrometry-based biomarkers for knee osteoarthritis – a systematic review

Mirella J.J. Haartmans, Kaj S. Emanuel, Gabrielle J.M. Tuijthof, Ron M.A. Heeren, Pieter J. Emans, Berta Cillero-Pastor

Expert Review of Proteomics 2021

Abstract

Knee osteoarthritis (OA) is a joint disease, affecting multiple tissues in the joint. Early detection and intervention may delay OA development and avoid total knee arthroplasty. Specific biomarker profiles for early detection and guiding clinical decision-making of OA have not yet been identified. One technique that can contribute to the finding of this 'OA biomarker' is mass spectrometry (MS), which offers the possibility to analyze different molecules in tissues or fluids. Several proteomic, lipidomic, metabolomic and other – omic approaches aim to identify these molecular profiles; however, variation in methods and techniques complicate the finding of promising candidate biomarkers. In this systematic review, we aim to provide an overview of molecules in knee OA patients. Possible biomarkers in several tissue types of OA and non-OA patients, as well as current limitations and possible future suggestions will be discussed. According to this review, we do not believe one specific biomarker will function as predictive molecule for OA. Likely, a group of molecules will give insight in OA development and possible therapeutic targets. For clinical implementation of MS-analysis in clinical decision-making, standardized procedures, large cohort studies and sharing protocols and data is necessary.

Introduction

Knee osteoarthritis (OA) is a total joint disease, characterized by cartilage degeneration, thickening and inflammation of the synovium, and osteophyte formation, leading to pain and immobility among patients[28]. The incidence of knee OA in the human population has been increasing over the past decades and is expected to increase even further[33]. Not only the increasing elderly population, but also the younger population is confronted with OA more frequently[54]. Risk factors such as osteochondral damage and obesity are identified[28, 33, 54].

Current treatment options for OA focus on diet and moderate physical activity, as well as the reduction of pain and inflammation with non-steroidal anti-inflammatory drugs (NSAIDs)[74]. OA affects multiple, if not all, tissues inside the joint. Its features make it hard to find targeted therapies, leaving total knee arthroplasty (TKA) as inescapable treatment option. Early detection and intervention have been shown to postpone rigorous treatment[121]. This makes it even more important to find biomarkers or molecular factors that contribute to OA development and disease progression, not only to gain insight in disease pathogenesis, but also to guide clinical decision-making and treatment discovery.

Treatments that prevent OA progression or OA from developing are lacking. The development of disease modifying OA drugs (DMOADs) requires knowledge on the structure and homeostasis of the joint[122]. This information can for example be obtained from molecular imaging analysis and might contribute to the development of personalized treatments. OA has been described as a total joint disease, implicating that all tissues inside the joint are or can be affected[123] and is often the result of trauma or injury. OA is not limited to the knee. It can appear in all joints of the human body. However, knee OA is the most prevalent[33]. In addition, most research is done on knee OA, as waste tissue from the knee after replacement surgery is usually available.

The human knee consists of different tissue types and fluids. Both femur and tibia, as well as the patella, are covered with a layer of hyaline cartilage, supporting subtle movement of the knee. Between these layers of cartilage, a thin layer of synovial fluid is lubricating the cartilage surface for smooth movement. Several ligaments, such as the anterior cruciate ligament (ACL), limit these movements, giving the knee its stability. To prevent bone-to-bone friction and absorb some of the impact on the knee, the menisci are located between the edges of the cartilage layers. All these tissues are surrounded by a layer of synovial membrane, the knee capsule. Finally, yet importantly, underneath the patellar ligament, Hoffa's fat pad (HFP) or the infrapatellar fat pad (IPFP) is located (**Figure 2.1**). The IPFP has been proven an important metabolic organ, involved in OA's inflammatory response[20, 124]. In the OA

knee, the cartilage is damaged, synovium thickened and inflamed, and there is more synovial fluid present.

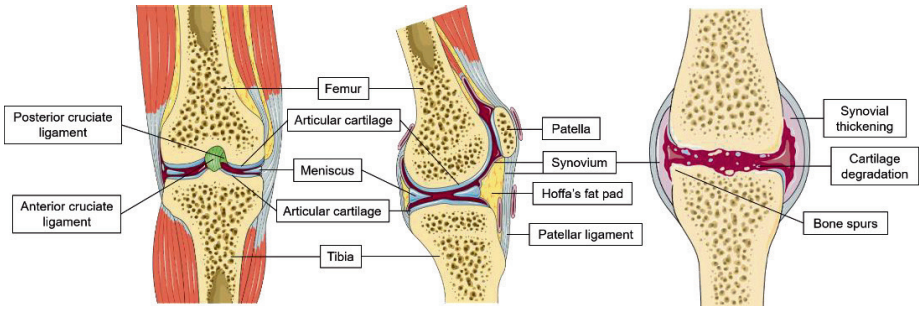

Figure 2.1. Frontal (left) and parasagittal (middle) view of the knee's anatomy, as well as a visualization of the osteoarthritic knee (right) with osteoarthritic features such as synovial thickening, cartilage degradation and development of bone spurs. The bones in the human knee are covered by a layer of hyaline cartilage. This cartilage, in combination with the menisci and a layer of lubricating synovial fluid, facilitates the movement of the knee. Other tissues such as synovium and Hoffa's fat pad are there to maintain joint homeostasis. *Image was modified with permission from Servier Medical Art, licensed under a Creative Common Attribution 3.0 Generic License. http://smart.servier.com/*

From all techniques employed for biomarker discovery, mass spectrometry (MS) offers the possibility of analyzing thousands of different molecules in a single experiment. Other methods such as microarrays, for DNA, RNA or protein analysis, can also measure thousands of different molecules simultaneously, however this is a more targeted approach compared to most of MS studies. It has been evolving as technique to detect (and locate) possible biomarkers for OA by measurement of the mass to charge ratio of the detected molecules. Proteomic, lipidomic, metabolomic and other – omic approaches aim to identify molecular profiles or signatures of different tissues (cartilage, bone, synovium, meniscus, tendon, IPFP) or liquids (synovial fluid) inside the OA knee joint, hoping to find certain predictive molecules or molecular classes responsible for OA development, disease progression or possible therapeutic targets. However, differences in MS approaches, targeted molecular classes and tissue sources make it difficult to appreciate which method and molecules are the most promising candidates as OA biomarkers.

Due to the plethora of available techniques, as well as target compounds, we aimed to look for common molecular signatures that could be used for future research, disease prognosis or treatment. Therefore, in this systematic review, we aim to provide an overview of molecules in the knee that distinguish between (several

degrees of) OA and non-OA patients. Possible biomarkers for knee OA, current limitations, and possible future suggestions will be discussed.

Methods

Literature search and article selection

The literature search and article selection was conducted following the Preferred Reporting Items for Systematic Reviews and Meta-Analysis (PRISMA)[125]. The PubMed database was searched for eligible articles on 28 January 2021. The search included topics on OA, MS, proteomics, lipidomics, and metabolomic approaches, including underlying terms (MesH terms) and terms in title and abstract (tiab) (**Supplementary Table 2.1**). Two blinded researchers (MH and KE), individually evaluated all records using 'Rayyan QCRI'[126]. Conflicts were solved by a third researcher (BCP) after discussion.

Studies were included if the article covered 1) the use of samples directly derived from patients with knee OA, 2) the analysis of local molecular markers in intra-articular fluid or tissue (including IPFP) of the knee, 3) a comparison of patients with different stages of OA, 4) a comparison of OA patients with either healthy subjects or patients with other knee injuries and 5) the use of untargeted MS analysis. Exclusion criteria included 1) abstracts only and reviews, 2) the use of non-local fluids like blood/serum or urine, 3) lack of a non-OA control group, 4) tissue and cell culture, 5) full text not in English and 6) lack of reporting of molecular differences between groups.

All data on use of subjects, tissue collection, tissue type, methodological approach, and molecular class of interest, as well as used databases for identification were extracted from the articles of interest (**Tables 2.1** and **2.2**). In this review, we focused on, already hard to find, local markers in the knee, rather than markers in serum, plasma or blood because we believe it is important to unravel the local changes of OA before translating it to systemic changes. In addition, with the exclusion of systemic markers, we prevent possible co-factors of other diseases to interfere with the results.

PRISMA results and data extraction

From our search in PubMed, 701 records were identified and screened based on abstract according to the mentioned inclusion and exclusion criteria. From these, 636 records were excluded, whereas 64 records were assessed for eligibility based on full text. In total, 32 and 24 studies were included in the qualitative synthesis and quantitative synthesis (pathway analysis) respectively (**Figure 2.2**).

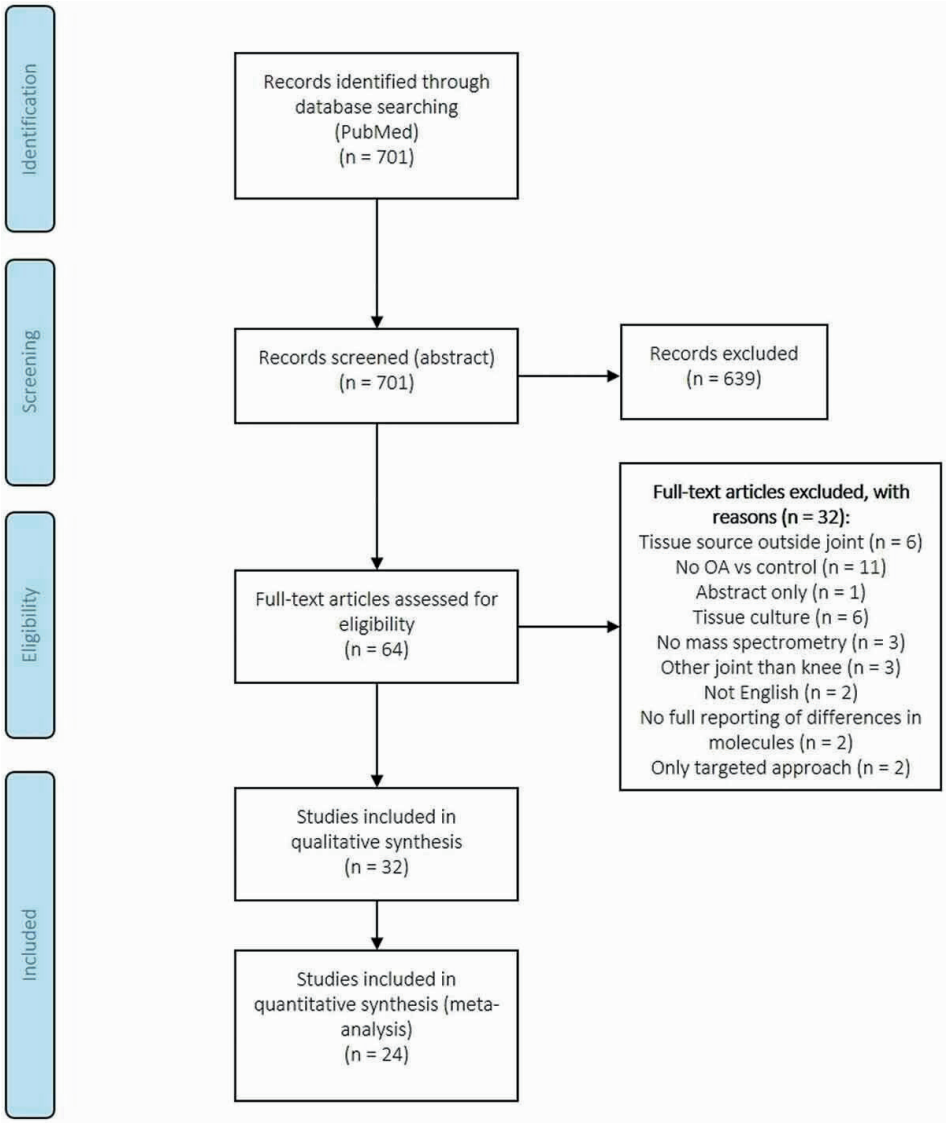

Figure 2.2. PRISMA flow diagram, screened abstracts and articles. A total of 32 and 24 articles were used for qualitative and quantitative analysis respectively in this systematic review.

Table 2.1. Data extraction and study characteristics of selected articles: proteins analyzed in synovial fluid, cartilage, synovium or meniscus, sorted on tissue type and mass spectrometry method.

Author[ref]	Year	Subjects (n)	MS(/MS) method and ionization source (if stated)	Identification database
Synovial fluid				
Ahmed et al.[127]	2016	eOA (46) lOA (17)	LC-MS/MS	Cross references
Ahrman et al.[128]	2014	Non-OA (35) OA (20)	LC-MS/MS	UniProtKB
Brophy et al.[129]	2019	Non-OA (6) OA (3)	LC-MS/MS	UniProt
Gobezie et al.[130]	2007	Non-OA (20) eOA (21) lOA (18)	LC-MS/MS	NCBI RefSeq Human
Kamphorst et al.[131]	2007	Non-OA (1) OA (1)	LC-MS/MS	Human FASTA
Liao et al.[132]	2018	Non-OA (10) lOA (10)	LC-MS/MS, SWATH	NS
Roller et al.[133]	2016	Non-OA (16) OA (5)	RP-LC-MS/MS	NS
Steinbeck et al.[134]	2007	Non-OA (4) eOA (11) lOA (18)	LC-MS	NS
Timur et al.[135]	2021	Non-OA (10) OA (10)	ESI-LC-MS/MS	Unihuman Reviewed
Corigliano et al.[136]	2017	eOA (13) lOA (12)	MALDI-MS and MS/MS	UniProtKB
Liao et al.[137]	2013	Non-OA (12) eOA (5) lOA (7)	MALDI-MS	NCBInr
Liao et al.[138]	2015	Non-OA (10) OA (10)	MALDI-MS and MS/MS	NCBInr

2D-DIGE-MS = two-dimensional difference gel electrophoresis mass spectrometry, eOA = early osteoarthritis, ESI = electrospray ionization, (RP)-LC-MS(/MS) = (reversed phase) (tandem) liquid chromatography mass spectrometry, lOA = late osteoarthritis, MALDI-MS(I) = matrix-assisted laser desorption/ionization mass spectrometry (imaging), NS = not stated, OA = osteoarthritis, SWATH-MS = SWATH-mass spectrometry.

Table 2.1 (continued). Data extraction and study characteristics of selected articles: proteins analyzed in synovial fluid, cartilage, synovium or meniscus, sorted on tissue type and mass spectrometry method.

Author[ref]	Year	Subjects (n)	MS(/MS) method and ionization source (if stated)	Identification database
Synovial fluid				
Ritter et al.[139]	2013	Non-OA (10) eOA (10) lOA (10)	2D-DIGE-MS and MS/MS	UniProt
Cartilage				
Cillero-Pastor et al.[140]	2013	Non-OA (10) lOA (10)	MALDI-MSI and MS/MS	UniProt
Guo et al.[141]	2008	Non-OA (3) OA (3)	ESI and MS/MS	UniProt
Hsueh et al.[142]	2016	Non-OA (NS) OA (NS)	Nano-spray LC-MS/MS	UniProt
Rosenthal et al.[143]	2011	Non-OA (10) OA (10)	Nano-spray LC-MS/MS	UniProt
Wu et al.[144]	2007	Non-OA (7) OA (7)	Nano-spray LC-MS/MS	NCBInr
Synovium				
Cillero-Pastor et al.[145]	2015	Non-OA (3) lOA (3)	MALDI-MSI and MS/MS	UniProt
Tang et al.[146]	2018	Non-OA (3) OA (4)	LC-MS/MS	UniProt
Meniscus				
Folkesson et al.[147]	2020	Non-OA (10) lOA (9)	LC-MS/MS	Human protein database
Roller et al.[148]	2015	Non-OA (6) eOA (6) lOA (3)	LC-MS/MS	NS

2D-DIGE-MS = two-dimensional difference gel electrophoresis mass spectrometry, eOA = early osteoarthritis, ESI = electrospray ionization, (RP)-LC-MS(/MS) = (reversed phase) (tandem) liquid chromatography mass spectrometry, lOA = late osteoarthritis, MALDI-MS(I) = matrix-assisted laser desorption/ionization mass spectrometry (imaging), NS = not stated, OA = osteoarthritis, SWATH-MS = SWATH-mass spectrometry.

Table 2.2. Data extraction and study characteristics of selected articles analyzing metabolites and lipids in synovial fluid and cartilage.

Author[ref]	Year	Subjects (n)	Sample type	MS(/MS) method and ionization source (if stated)	Identification database
Metabolites					
Carlson et al.[149]	2018	Non-OA (5) OA (5)	Synovial fluid	LC-MS	METLIN
Carlson et al.[150]	2019	Non-OA (7) eOA (55) lOA (17)	Synovial fluid	LC-MS	NS
Kim et al.[151]	2017	eOA (8) lOA (7)	Synovial fluid	ESI-GC-MS	BinBase (in-house)
Mickiewicz et al.[152]	2015	Non-OA (13) OA (55)	Synovial fluid	H-NMR, GC-MS	GOLM, NIST
Zheng et al.[153]	2017	Non-OA (21) OA (49)	Synovial fluid	ESI-GC-MS, LC-MS/MS	NIST, LECO
Lipids					
Cillero-Pastor et al.[154]	2012	Non-OA (3) lOA (3)	Cartilage	SIMS	LIPIDMAPS
Kosinska et al.[155]	2013	Non-OA (9) eOA (17) lOA (13)	Synovial fluid	ESI-MS/MS	Lipidomic Net
Kosinska et al.[156]	2014	Non-OA (9) eOA (17) lOA (13)	Synovial fluid	ESI-MS/MS, LC-MS/MS	LIPIDMAPS
Kosinska et al.[157]	2015	Non-OA (16) eOA (26) lOA (22)	Synovial fluid	ESI-MS/MS, GC-MS	LIPIDMAPS
Vyver et al.[158]	2020	Non-OA (6) OA (23)	Synovial fluid	ESI-LC-MS	Authentic standards

eOA = early osteoarthritis, ESI-MS/MS = electrospray ionization tandem mass spectrometry, GC-MS = gas chromatography mass spectrometry, LC-MS(/MS) = (tandem) liquid chromatography mass spectrometry, lOA = late osteoarthritis, NS = not stated, OA = osteoarthritis.

The topics of interest 'first author name,' 'number of subjects,' 'sample type,' 'molecule of interest,' 'MS method' and 'identification database' were extracted from each article and sorted based on molecular class (**Table 2.1** for proteins and **Table 2.2** for lipids and metabolites). Subjects were classified as non-OA ((postmortem) healthy, trauma/amputation, knee pain, (sub-) acute ACL, meniscus injury), early OA (eOA, Ahlbäck grades 1 and 2, Kellgren-Lawrence (KL) 1 and 2), late OA (lOA, Ahlbäck grades 3, 4 and 5, KL 3 and 4), and OA without classification.

In addition, we used the data retrieved from the reviewed articles to conduct a joint pathway analysis (Homo Sapiens (human), integrated metabolic and gene pathways) on all upregulated-highlighted proteins (UniProt Protein ID, n = 35), lipids and metabolites (compound name, n = 13) (**Supplementary Tables 2.2** and **2.3**) in OA, using the web tool MetaboAnalyst 5.0[159] to see which pathways, rather than single molecules, are involved in OA pathophysiology. The pathway analysis was conducted using a human (Homo sapiens) database (KEGG), including metabolic and gene pathways. Additionally, for enrichment analysis, topology measure and integration method, a hypergeometric test, degree centrality and combined queries were used respectively.

Proteins in osteoarthritis

Twenty-three articles included the terms 'protein' and 'biomarkers.' Of these, 13 focused on proteins in synovial fluid, 5 in cartilage, 2 in synovium and 2 in meniscus. All authors compared proteins in a non-OA group to either early OA, late OA or OA in general, except for Ahmed et al. (2016) and Corigliano et al. (2017) who only compared early OA vs late OA (**Table 2.1**).

Liquid chromatography tandem mass spectrometry

Liquid chromatography tandem mass spectrometry (LC-MS/MS) coupled to electrospray ionization (ESI), was the predominant MS technique used for the detection of peptides and proteins in these samples. To a lesser extent, matrix-assisted laser desorption/ionization MS (imaging) (MALDI-MS(I)) was used to analyze proteins, especially in tissues like cartilage and synovium. MALDI-MSI allows us to, not only detect molecules inside the tissue, but also to determine the spatial distribution of these molecules throughout the tissue. This makes MALDI-MSI a significant tool to analyze tissues that consist of multiple structures, layers or cells, such as cartilage, and understand intra-tissue remodeling[140, 160].

Supplementary Table 2.2 summarizes the proteins that were highlighted in two or more studies. Of these, 35 proteins were upregulated in multiple tissue types and/or fluids of OA patients (**Supplementary Table 2.2** and **Figure 2.3**). Interestingly,

fibronectin was found to be upregulated in all measured tissues/fluids (synovial fluid, synovium, meniscus and cartilage) of OA patients (**Figure 2.3**). Only one protein, transaldolase, was downregulated in the synovial fluid of OA patients (measured by at least two studies, **Supplementary Table 2.2**). In addition, histone H2B and serum amyloid A1 (isoform 1) were upregulated in control patients (**Supplementary Table 2.2**). Many others suggest important proteins, such as annexin A2, apolipoprotein A-1 (precursor), cartilage oligomeric matrix protein (COMP), versican core protein and collagen α1(II) isoforms but showed contradictive results (variations in up- or down-regulation of proteins) between articles (**Supplementary Table 2.2**).

Small molecules in osteoarthritis: metabolites and lipids

Compared to proteins, the number of studies on small molecules like lipids or metabolites is limited. Five articles that focused on the detection and identification of metabolites in OA vs healthy/non-OA patients and five articles that focused on lipid species were found (**Table 2.2**).

All metabolite studies analyzed synovial fluid, collected from healthy patients (postmortem or during amputation) and patients with (several degrees of) knee OA (either during treatment or postmortem). The number of samples used varied from 5–21 in the healthy groups and 5–69 in the OA groups (early OA and late OA). All five articles used either untargeted LC-MS or gas chromatography MS (GC-MS) methods for the detection of metabolites in these synovial fluid samples (**Table 2.2**). The use of standard operating procedures, or SOPs, is clearly important in these type of studies for method standardization and inter or intra-laboratory reproducibility. In addition to these methods, Mickiewicz et al. added a targeted 1 H nuclear magnetic resonance (1 H NMR) spectroscopy approach to their analysis method for an NMR/GC-MS combined dataset to develop a prediction model of OA[152]. All studies were able to distinguish healthy subjects from those with OA using principal component analysis (PCA) and/or orthogonal partial least squares discriminant analysis (OPLS-DA). Interestingly, two phenotypes each for early OA and late OA were identified by Carlson et al.[150].

Although synovial fluid is found to be the preferred source in the search for lipid biomarkers, Cillero-Pastor et al.[154] were the only authors that analyzed cartilage samples, as well as the spatial distribution of molecules. Different number of patient samples with different age ranges were used for lipidomic analysis in each article: 3–16 healthy donors (postmortem), 17–26 early OA patients (during arthroscopy) and/or 3–22 late OA patients (during TKA). Lipid species were either detected with the use of time-of-flight secondary ion MSI (TOF-SIMS), high-performance LC-MS (HPLC-MS) or electrospray ionization tandem MS (ESI-MS/MS) and GC-MS (**Table 2.2**).

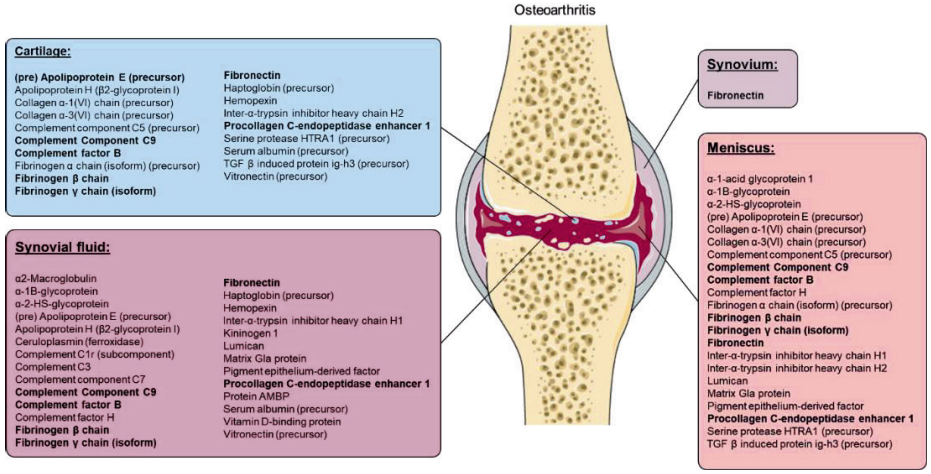

Figure 2.3. Upregulated proteins in cartilage, synovial fluid, synovium and meniscus of osteoarthritis patients, identified by at least two authors, without contradiction. Recurring proteins measured in at least three tissue types are highlighted in bold. *Image was modified with permission from Servier Medical Art, licensed under a Creative Common Attribution 3.0 Generic License. http://smart.servier.com/*

The use of multiple biomarkers, rather than one, increases the power of discriminating OA from non-OA patients. The authors suggested multiple metabolites or lipids in the synovial fluid (or cartilage) of OA patients as possible biomarkers for OA (**Supplementary Table 2.3** and **Figure 2.4**). Several amino acids, amines, sugar (alcohols), organic acids, (mono-un) saturated and omega-6) fatty acids), phosphates, (lyso)phospholipid(s) (classes), sphingomyelins, and ceramides, among others, were shown to be different between early OA and/or late OA patients and controls (**Supplementary Table 2.3**). Remarkably, all molecules found to be upregulated in cartilage of OA patients, were also upregulated in the synovial fluid of OA patients, except for the group fatty acids (**Figure 2.4**).

Osteoarthritis phenotyping

Several OA phenotypes have been described in literature: among others, the senescent phenotype, inflammatory phenotype, metabolic phenotype, genetic phenotype and endocrine phenotype[76, 78]. These phenotypes might be important when developing personalized OA treatments. For example, synovitis can be treated with anti-inflammatory drugs[76] or reducing mechanical loading in a mechanical overload phenotype[78]. Also at the molecular level, different OA phenotypes can be identified. For example, Eveque-Mourroux et al. found differences in lipid and protein profiles in patients with or without Type 2 Diabetes Mellitus (T2DM)[160]. Briefly, phospholipase A2 and lysolipids were in general associated to the OA group

with T2DM whereas phosphatidylcholine and sphingomyelin species were associated to the group of OA patients without T2DM[160].

Interestingly, arachidonic acid, ethanolamine and malate were decreased in the OA group when compared to non-OA patients[152, 158], but increased in the late OA group when compared to early OA[151]. In addition, Kim et al. found differences in metabolites between patients with OA KL grade 1, 2, 3, and 4 specifically[151]. Levels of sugar (alcohols) such as arabitol, galactose, glucose, mannose and tagatose were increased in KL grade 1 compared to other stages. Urate, β-alanine, pyruvate, and terephthalate levels were increased in KL grade 2 patients and fatty acids, proline, phenylalanine, squalene, and trehalose-6-phosphate were increased in KL grade 3 and 4[151].

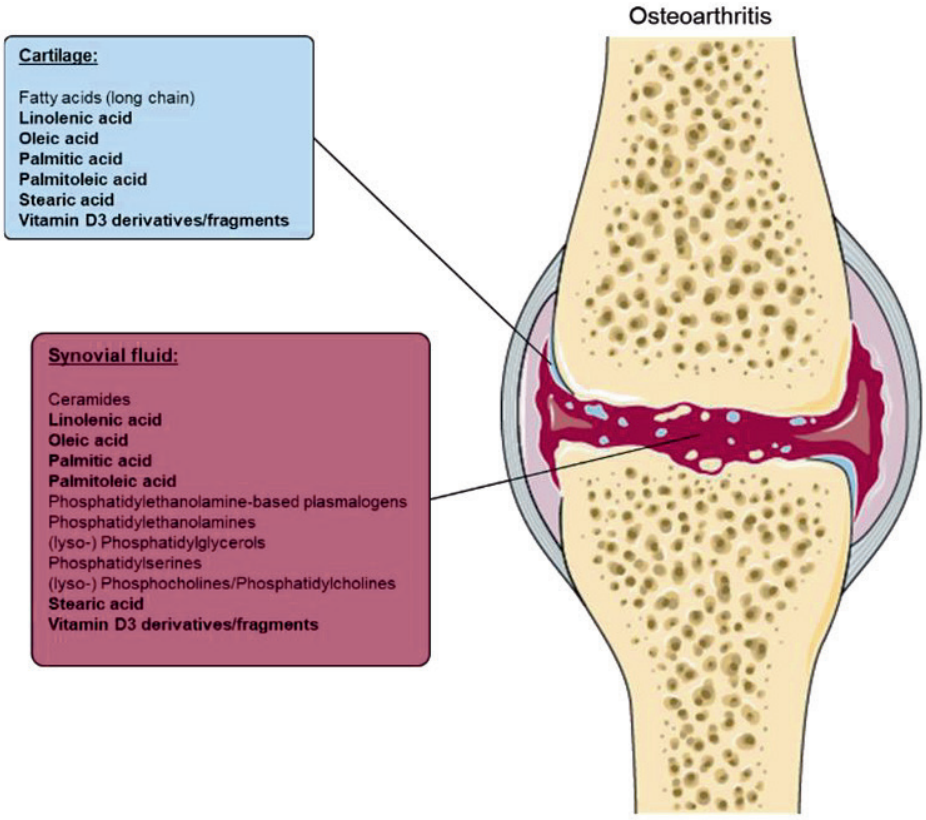

Figure 2.4. Upregulated metabolites and lipids in cartilage and synovial fluid of osteoarthritis patients, identified by at least two authors, without contradiction. Lipid or metabolite species that were found in cartilage and synovium are highlighted in bold. *Image was modified with permission from Servier Medical Art, licensed under a Creative Common Attribution 3.0 Generic License. http://smart.servier.com/*

Several metabolisms and metabolic pathways were found to be altered in (different stages of) OA: amino acid metabolism, central energy metabolism (gluconeogenesis, glycolysis and citric acid cycle), extracellular matrix component metabolism (including ascorbate metabolism, galactosamine and glucosamine biosynthesis, keratin sulfate metabolism and N-glycan metabolism), fatty acid (biosynthesis) and lipid metabolism (carnitine shuttle, glycerol(phospho)lipid and glycosphingolipid metabolism), inflammation (leukotriene metabolism), oxidative stress (glutathione and vitamin E metabolism) and vitamin C, E, B1, B3, B6, B9 metabolism. In addition, Carlson et al.[150] also found two different phenotypes (inflammatory and structural deterioration) associated to early and late OA groups.

Joint pathway analysis in MetaboAnalyst 5.0

Twenty-three pathways were significantly upregulated ($p < 0.05$) in OA patients according to our analysis. These included complement and coagulation cascades (highest significance) and inflammatory pathways among others (**Figure 2.5** and **Table 2.3**).

When comparing these pathways to the pathways described in the articles of this review, there were some similarities. OA was associated with altered extracellular matrix (ECM) component metabolism, lipid and fatty acid metabolism, vitamin metabolism, inflammation and complement and coagulation pathways among many others[139, 147, 149, 150].**Table 2.3** describes all significant ($p < 0.05$) pathways involved with the highlighted upregulated proteins, lipids, and metabolites in OA. Complement and coagulation cascades, ECM-receptor interaction and multiple inflammatory pathways were associated with OA (**Table 2.3**). In addition, false-discovery rate (FDR) and impact are described (**Table 2.3**).

In summary, our results describe a variety of possible biomarkers for OA. Multiple patient groups, tissues and analysis methods were described by the authors of included articles. These differences will be elaborated and discussed below.

Discussion: Inter-patient variability, tissue types and molecules

Inter-patient variability

Healthy patient material as control is crucial in the search for potential OA biomarkers. However, healthy 'living' material is either not usually available or material is collected postmortem, which might influence analysis results due to the occurrence of degradation products (some authors correct for this). Postmortem samples are suggested as a valid alternative for healthy material, if tissue sampling occurs within foreseeable time and researchers correct for tissue degradation. In the

included papers in this review, several non-OA patient groups (trauma, knee pain and ACL or meniscus injury) were used as control group. Some articles did not use a non-OA control, but distinguished between early OA and late OA patients. In addition, the willingness of healthy individuals to undergo synovial fluid, or intra-articular tissue sampling can be an issue as it is rather invasive.

Control groups often consist of a limited sample size (n = 1 or n = 3). Controversially, the OA group is often of bigger magnitude as collection of rest material during surgery occurs more often. The results of this review emphasize the importance of OA grade, as several lipid or metabolite biomarkers showed contradictive results when OA grade is considered a distinguishing factor. It is problematic that most control groups have a traumatic incident in their joint, as this may induce inflammatory or OA-like features[69]. This might also influence the results, as these joint defects often result in the development of OA when not treated sufficiently.

Therefore, the results of this review should be interpreted as markers that are different in a chronic inflammatory and degenerative state (OA) compared to an acute inflammatory state due to a traumatic event. True healthy control tissue is necessary to confirm that these differences are also representative to distinguish OA from non-affected tissue. As ethical consideration may prohibit collection of such tissue from a general population, possible sources may be during healthy knee allograft collection for ankle defects, surgery of bony structures where the knee is unaffected or contra-lateral biopsy during TKA.

Tissue types and molecules

Synovial fluid is the most frequently used biopsy source for OA biomarkers. It is easily accessible (in most cases), can be harvested from non-OA patients (postmortem or alive) and can be measured by one of the most used and sensitive MS techniques: LC-MS. Synovial fluid, if not contaminated with blood, is easy to process, and requires limited actions before analysis. Authors often use 2D gel electrophoresis (2DE) and/or sodium dodecyl sulfate polyacrylamide gel electrophoresis (SDS-PAGE) to separate proteins before LC-MS analysis to measure proteins in synovial fluid.

Synovial fluid can be aspirated from the joint using a syringe prior to or during surgery. This technique is already been used in clinic to reduce swelling or infection, as well as for diagnostic purposes[161]. Aspiration of synovial fluid is an invasive technique, puncturing the knee capsule, which often needs echography guidance. The OA knee often contains more synovial fluid compared to the healthy knee. To detect biomarkers for OA and be able to intervene in its development, synovial fluid should be aspirated early in the disease. However, patients with early stages of OA often do not experience symptoms or seek medical help.

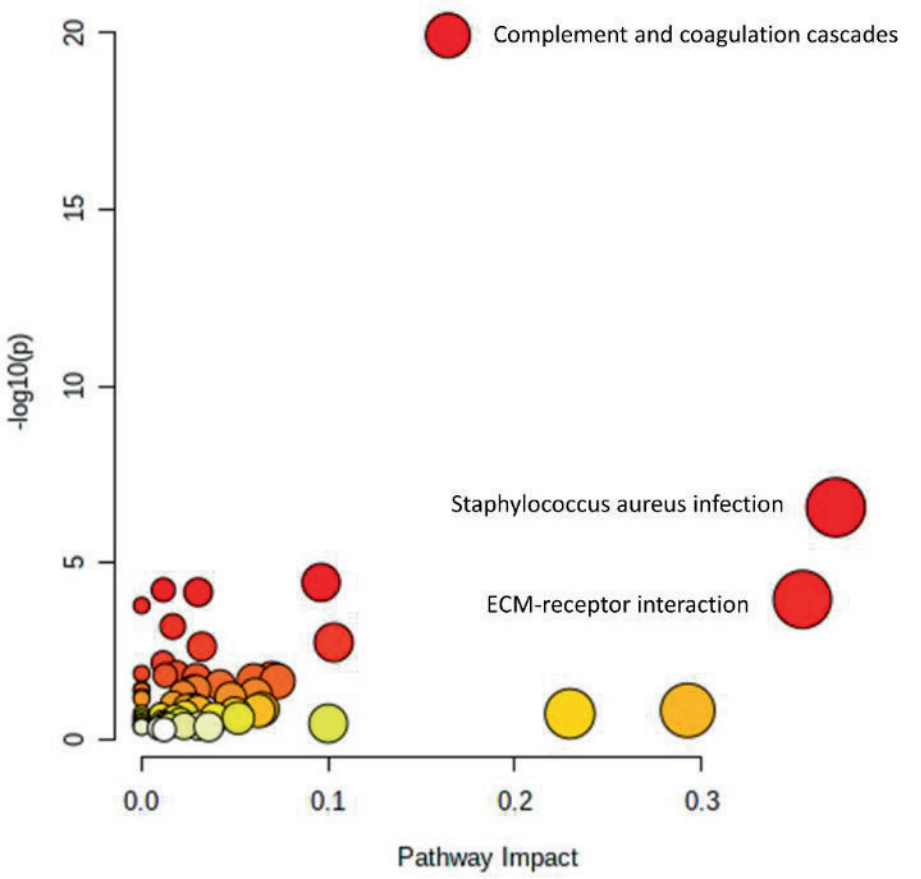

Figure 2.5. The Pathway Enrichment vs -log10 (p) with $p < 0.05$ cutoff for proteins, lipids, and metabolites in osteoarthritis patients. P-values are subdivided on a white to red color scheme, red indicating higher significance ($p < 0.05$). Circle size is determined based on Enrichment Ratio (ER), with small circles representing low ER and big circles representing high ER. ECM = extracellular matrix.

Cartilage is the second most-explored tissue of the human knee and is often harvested postmortem or during TKA. In severe cases of OA, the cartilage is degraded to the bone, making it hard to harvest late-stage OA cartilage. The use of cartilage and other tissue types in combination with LC-MS requires protein extraction from the tissue. Other techniques like MALDI-MS(I) are favored for these 'solid' tissue types, as it gives researchers the opportunity to visualize the location of the detected molecule by spatial analysis. Healthy cartilage is even more difficult to obtain. Harvest of healthy human cartilage is only possible postmortem or after trauma. Therefore, most studies use damaged tissues from the knee as control.

These tissues are often removed or replaced during surgery and are therefore more likely to acquire.

Table 2.3. Pathway analysis in MetaboAnalyst 5.0 using all upregulated-highlighted proteins (n = 35), lipids and metabolites (n = 13) in OA patients, found in the article search of this review. Pathways with high impact (impact > 0.1) are highlighted in bold. These pathways include complement and coagulation cascades, extracellular matrix receptor interaction and multiple inflammatory pathways.

Pathway name	p-value	FDR	Impact	Database
Complement and coagulation cascades	1.19E-20	3.95E-18	0.16	KEGG
Staphylococcus aureus infection	2.69E-07	4.45E-05	0.37	KEGG
Systemic lupus erythematosus	3.57E-05	0.0039	0.1	KEGG
Fatty acid biosynthesis	5.79E-05	0.0045	0.01	KEGG
Biosynthesis of unsaturated fatty acids	6.75E-05	0.0045	0.03	KEGG
ECM-receptor interaction	1.07E-04	0.0059	0.35	KEGG
Prion diseases	1.61E-04	0.0076	0	KEGG
Cholesterol metabolism	6.25E-04	0.026	0.02	KEGG
Pertussis	0.0018	0.065	0.1	KEGG
Focal adhesion	0.0023	0.077	0.03	KEGG
Platelet activation	0.0067	0.2	0.01	KEGG
Vitamin digestion and absorption	0.014	0.35	0	KEGG
Human papillomavirus infection	0.014	0.35	0.02	KEGG
Fatty acid elongation	0.015	0.36	0.01	KEGG
PI3K-Akt signaling pathway	0.017	0.38	0.03	KEGG
Adipocytokine signaling pathway	0.019	0.4	0.07	KEGG
Proteoglycans in cancer	0.021	0.41	0.06	KEGG
Leishmaniasis	0.022	0.41	0.07	KEGG
Fatty acid degradation	0.029	0.5	0.04	KEGG
Chagas disease (American trypanosomiasis)	0.037	0.57	0.03	KEGG
Choline metabolism in cancer	0.038	0.57	0	KEGG
AGE-RAGE signaling pathway in diabetic complications	0.038	0.57	0.03	KEGG
Amoebiasis	0.041	0.6	0	KEGG

ECM = extracellular matrix, FDR = false discovery rate.

While we already know that ACL and/or meniscus rupture contributes to the development of OA in the future[162, 163], the use of ACL and/or meniscus tissue in the search for biomarkers with MS is limited or absent. Also limited/absent is the search for biomarkers in synovium and IPFP, though both tissue types play an important

role in the inflammatory and molecular signature of OA[164, 165]. In addition, bone, or the bone-cartilage interface, and tendon (injury) are in this search not even suggested as tissue of interest, while these tissues might also be contributing to inflammation or OA development[166-168].

Most articles in our search focus on the analysis of proteins. Proteins fulfill multiple functions in the human body, such as tissue growth, maintenance, and cell/tissue communication. Dysregulation of protein synthesis or expression is often associated with disease pathology[169]. Therefore, it is not surprising that proteins are predominantly used as diagnostic or therapeutic target for OA. Proteins are known to interact with other proteins, but also with lipids in cell membranes[170].

Lipids and metabolites are less studied in disease pathologies such as OA. For example, lipids have been shown to play an important role in the pro-inflammatory phenotype of OA[171]. This suggests that these molecules might also function as diagnostic or therapeutic targets for OA and that more research needs to be done. An important feature of the reviewed articles focusing on lipids is that they often provide sum compositions, whereas possible different lipid isomers might also play different signaling roles in OA.

Discussion: Molecular signature dependent on sample preparation and mass spectrometry technique

Sample preparation

The techniques used for sample preparation varied among authors and are dependent on the MS technique used for analysis. Not only the MS technique has to be taken into account, but also the purpose of the study (homogenate or local analysis), sample volume, sample concentration or composition, and the preparation method/solution are important[172]. In addition, external factors such as inter-person variabilities, (storage) temperature, and humidity can play a roll.

Before analyzing tissues or fluids with MS, it is important to consider enhancing the performance of protein digestion and reduce the complexity of the proteome by using several enzyme (protease) combinations for protein digestion. Proteases such as (chymo)trypsin, or alternative proteases such as endoproteinases glutamic-C, lysine-C, lysine-N, or aspartic-N, can generate unique peptide sequences and improve protein sequence coverage in different MS applications[173].

Post-translational modifications of proteins could also be of interest while searching for biomarkers. Top-down proteomics allows the detection of specific post-translational modifications such as phosphorylation, glycosylation, ubiquitination,

nitrosylation, methylation, or acetylation, and typically involves purification steps. Glycoprotein modifications in the cartilage for instance have been described[174]. In many cases these modifications cannot be detected. Chromatographic separation or previous protein purification are often needed. In addition, protocols that disrupt collagen fibers are recommended since the access to proteins with specific roles and post-translational modifications can be better digested then. For example, Hsueh et al. used a strong guanidine extraction buffer for protein extraction in cartilage[142].

Mass spectrometry and data analysis

Using currently available MS techniques, it is possible to detect molecules including peptides and proteins, lipids, metabolites and other (bio) chemical compounds. The majority of articles in our search focuses on the detection and analysis of peptides and proteins, rather than lipids or metabolites. Hereby, every ionization method (ESI, MALDI, etc.) has a different effect on sample and final analysis result, as sensitivity and detection method are different. In addition, the mass resolution and accuracy of the instrument are important when comparing data between articles.

A mass spectrometer consists of an ion source for sample ionization, a mass analyzer for mass separation and a detector for ion detection. There are several types of mass analyzers available, which separate ionized masses based on mass-to-charge ratio (*m/z*) which can be detected by the detector: quadrupole (ion trap), time-of-flight (TOF), magnetic or electrostatic double sector, and ion cyclotron resonance mass analyzers[175-177]. Which mass analyzer to use is dependent on the application.

In addition, the ionization source also has an influence on the detected molecules. As could be shown from this review, ESI is mainly used in combination with LC-MS instruments. In contrast to ESI, electron ionization (EI) and collision induced (CI) are mainly used in GC-MS techniques. With these ionization techniques, electrons or chemicals are used to ionize or charge molecules in the mass spectrometer[178].

Alternatively, some MS techniques make use of ion-mobility to separate ions based on their interaction with collision gas, which leads to an increased number of identifications.

LC-MS, combined with dedicated bioinformatics strategies, is highly specific and well developed over the past years and has become one of the widely used techniques in MS. LC-MS analysis of tissues and fluids give us a detailed overview on the molecular/protein profiles in OA patients. In addition, most LC-MS analyses focus on the detection and identification of proteins in particularly fluids. More specific for synovial fluid; available from different OA patients (TKA surgery) or healthy phenotypes can be purchased. Other tissue types are less available and need

multiple processing steps before LC-MS analysis. Different analytical results might be due to differences in sample preparation or type of database used. Protein databases such as UniProt/SwissProt include a high variety of proteins. Still, there can be differences between databases and protein content, resulting in more or less identifications dependent on the database used.

Other techniques such as MALDI-MS(I), GC-MS and SIMS have shown to be a promising addition to the field of biomarker discovery too. Whereas proteins appear to be very important in the development of OA, more and more is known about other tissue types, as well as other molecules, such as lipids and metabolites and their involvement in OA development[179, 180]. What techniques such as MALDI-MSI discriminate from techniques such as LC-MS is the ability to study molecular distributions within the tissue and the associated tissue heterogeneity. Analysis is performed on-tissue directly and only needs minor sample processing by matrix application. This is of particular importance when analyzing for instance very heterogeneous tissues, such as IPFP[181].

Several imaging software, such as Lipostar[182] and SCILS are then able to visualize molecules and determine their distribution throughout the tissue. In addition, with these programs, tissue typing, segmentation and classification of molecules is possible. It gives detailed information on tissue types, cells and molecules within the tissue. For example, Cillero-Pastor et al. addresses the importance of the location of molecules within the tissue, as well as the importance to measure molecules in multiple polarities (negative and positive), which is not usually applied throughout the reviewed articles[140]. Considering these techniques, analytical programs and databases are less developed and used, the information gathered might be of high importance, but not given consideration due to lack of molecule identification. For example, an unknown molecule is detected, but not present in one of the databases.

Discussion: A molecular signature for osteoarthritis?

The need for biomarkers in the development of DMOADs and personalized treatment is high[122]. Ideally, a treatment for OA would reduce symptoms and modify disease development[122]. However, the progression of OA causes biomarker fluctuations between phases of high and low disease activity[122]. It is therefore unlikely that a single biomarker will be specific and sensitive enough to detect, predict, or monitor the disease, rather than a combination of molecular biomarkers[122].

Although several studies show contradictive results (differences in up- or down-regulation of measured molecules), various proteins, lipids, and metabolites were found to play an important role in distinguishing OA patients from control patients.

Differences in molecular signature between articles might be due to differences in patients, methods, analysis, or interpretation. Several isoforms of collagen, as well as fragments from the complement system are well known factors in OA[183, 184]. In addition, some less known factors have been shown to play an important role in OA development. For example, several lipid species (e.g. prostanoids) have been shown to be involved in inflammation[185]. These species might be different in acute patients (e.g. patients suffering from cartilage defect or ACL rupture), rather than patients with a chronic inflammatory profile such as in OA. Remarkably, most candidate biomarkers for OA were upregulated molecules, rather than downregulated molecules. We suspect this is related to increased tissue degradation, tissue remodeling and inflammation in the OA knee joint. Relevant proteins, such as cytokines would be produced and transported to the affected joint.

MS has been shown a promising tool for the detection of molecular signatures responsible for OA development, prognosis or treatment. However, its translation to the (outpatient-) clinic is difficult. The lack of concrete molecular phenotypes, as well as manageability of the MS systems available, makes it still challenging for routine usage in a clinical setting. A clinical setting might for example be the direct analysis of taken biopsies. These biopsies could be obtained during surgery, to guide treatment decision making on the spot (e.g. damaged cartilage, is the patient able to regenerate?), or in outpatient clinic, to decide on next steps for treatment (e.g. biopsy of IPFP).

Biopsy taking of critical tissues such as cartilage and synovium, as well as its storage in an accessible biobank, would facilitate research in large study cohorts and contribute to our knowledge on OA development. However, it would be very invasive, entering the knee capsule and often lacks a healthy control. One other possibility is the use of IPFP. IPFP has already been shown to contribute to the inflammatory phenotype in OA and is more easily accessible as it is located outside the knee capsule. Fat tissue is already known to contribute to diseases such as obesity and diabetes. More and more evidence is gathered that this is also true for fat tissue inside the knee joint of OA patients[186].

According to our results, we would suggest a combination of proteins, lipids and metabolites as biomarker profile for OA. These include (pre) apolipoprotein E (precursor), complement component C9, complement component factor B, fibrinogen β chain, fibrinogen γ chain (isoform), fibronectin, procollagen C-endopeptidase enhancer 1, linolenic acid, oleic acid, palmitic acid, palmitoleic acid, stearic acid and vitamin D3 derivatives or fragments. Whereas synovial fluid is the most studied and accessible source for biomarker discovery in OA, future research on the discovered biomarker profile according to this review is needed. Nevertheless, other tissue types such as the IPFP, are also interesting.

Conclusion

Early detection of OA is important to predict disease progression and outcome. It also gives the opportunity to intervene and treat early in the disease stage, prolonging the development of OA and TKA. Protein, lipid and metabolite profiles have been shown to differ in OA from control patients and have therefore the potential to be used as (diagnostic) biomarkers. Different usage of patient information, patient material and MS techniques herein, increases the variation in the detection of molecules, complicating the discovery of potential biomarkers for OA, as well as the development of targeted treatment options.

OA is a multifactorial disease, affecting the whole joint. This review shows that a combination of proteins, lipids and metabolites might contribute to a biomarker profile for OA rather than one single biomarker. To identify a biomarker profile for OA, which can be implicated in the clinic, experiments should be conducted on large patient cohorts, with standardized methods, combined with shared databases.

Expert opinion

The ultimate goal of the use of diagnostic MS is to find a molecular profile that can be used to predict OA development, early diagnosis, the search for new therapeutic targets, and the development of personalized treatments. Early diagnosis of OA and better clinical decision-making can contribute to more efficient treatments. With the use of joint-preserving therapies, such as lifestyle interventions and weight loss, as well as nutritional and pharmacological interventions, intra-or-extra articular biomechanics can be restored; TKA can be postponed, leading to fewer revisions and more mobility among patients.

In this review, we concluded that MS is able to separate disease states based on the difference in molecular signatures. However, due to the limited size of the studies, using different techniques, targets and sources, inconsistency of results is inevitable. To be able to translate these preclinical results towards a clinical application, results should be validated and confirmed by different labs.

In addition, the use of alternative tissues such as IPFP (highly available because it is routinely removed with every knee-related surgery and biopsy taking would be minimally invasive), might be more applicable for a biomarker profile for OA. Further analysis on multiple tissue types of patients with multiple disease states, might contribute to the finding of a molecular (biomarker) profile for early OA detection, as well as OA development and progression. This might also contribute to the development of personalized therapeutic strategies and molecular targets.

However, this review highlighted many obstacles on the way to these well-needed clinical goals. Almost all included papers studied the difference between OA and control. However, in clinical practice, the need for predictive or phenotyping molecular profiles is just as large as for diagnostic profiling. To truly aid clinical decision-making, the MS analysis should provide the clinician with information on the prognosis of disease or how well a patient would respond to a certain treatment. Only then, it can contribute to personalized medicine. As it is well known from *in vitro* studies that the chondrocytes in the cartilage are very responsive to e.g. inflammatory signaling molecules[187], the homeostasis of the joint can be predictive of recovery or degeneration of the cartilage. If analysis of an upregulated pathway is shown, such as the complement and coagulation pathway or several inflammatory pathways, there could be an indication for anti-inflammatory treatment.

Recommendations for biomarker discovery with mass spectrometry

With the heterogeneity of the different approaches, as highlighted in this review, we are still a long way from validating the clinical value of molecular markers. We would like to propose several recommendations to the field:

First, experiments for biomarker analysis should be conducted on large cohorts, including patients with early and late OA, but also patients with cartilage defects. To gain more insight in OA progression after treatment or intervention, it would be optimal if these patients were followed over time using questionnaires and MRI.

Secondly, one of the striking features of this review is that each article uses different protocols and methods. Standardization of protocols for biopsy taking, sample preparation and MS analysis is necessary to combine and compare datasets of biomarkers. In addition, it is not clear for all reviewed articles what exact method was used for molecule ionization or identification. MS/MS analysis is necessary for proper identification of measured molecules. Authors likely assume that the reader already knows what ionization or identification method they have used. The use of standardized procedures for biopsy taking (of multiple tissue types) and biomarker discovery would facilitate the finding of a specific molecular profile for OA or its development. Other methods than LC-MS such as GC-MS, MALDI-MSI and SIMS are promising, but more research needs to be done. Also outstanding, is the use of multiple names for the same molecule. If databases would merge their knowledge, molecular identifiers or accession numbers, there will be less confusion on molecule identification. A standardized method to describe the molecules in articles would also contribute to that.

In addition, single cell analysis and spatially resolved – omics techniques will give more insight in the positional context of cells within a tissue. For example, specific

inflammatory cells and tissues in cartilage, IPFP or synovium of OA patients are responsible for the secretion of pro-inflammatory factors or cartilage degradation factors[188, 189].

Thirdly, we should work towards clinical implementation and point-of-care analysis for early detection and intervention of OA. If the molecular signature of multiple tissue types within the knee are known and related to OA progression, blood analysis (not included in the article search of this review) would possibly be a good alternative for the invasive biopsy/surgical methods currently used. The focus now is mainly on synovial fluid, which is close to the source of the problem. However, other tissue types such as meniscus, cartilage and synovium have shown promising results. In addition, LC-MS has already evolved to a very reliable technique for the detection of biomarkers. Newer advanced, technologies, such as MSI will possibly evolve to highly contributing techniques in the near future, but more research is needed.

Finally, it should be possible to combine data sets using several data analyzing programs and databases. There are several databases available on the internet to analyze proteins (UniProt/SwissProt, NCBInr, DDBJ, etc.)[190], lipids (LIPID MAPS, Lipidomic Net, etc.) or metabolites (METLIN, GOLM, etc.). Each database makes use of a different search technique and includes a different number of proteins or genes. Some make use of the protein name, which can differ even for the same protein; others make use of the gene name or protein accession, which is more reliable and avoids potential mismatches. Protein names can be divided in recommended name (often recommended by database) or alternative name (synonyms, abbreviations, acronyms). The International Protein Nomenclature Guidelines are written to prevent these name differences among databases[191]. In addition, lipid and metabolite databases are of high quality and nomenclature and classification is comparable with proteomic databases[192, 193].

Techniques in development

The possibility of on-tissue analysis of biopsies or possibly during surgery would facilitate clinical decision-making on the spot. This would be feasible with techniques like rapid evaporative ionization MS (REIMS), connected to an intelligent knife: the iKnife. This iKnife generates smoke when in contact with tissue during surgery, which is analyzed in a REIMS system, giving molecular information directly to the surgeon[194]. Direct on- or in-tissue analysis *in vivo* or on biopsies, would increase our knowledge on OA. However, not much is known about this technique in orthopedic research. In addition, there is currently no clear molecular profile for OA development or progression available. This might be due to the variety in methods, patients, lack of healthy/control samples and lack of molecule identification.

All these steps will eventually lead to better prediction models for OA development, better prediction models for patients after injury and better treatment decisions. Systems such as REIMS/iKnife are promising technologies that might be used at the surgical theater in the near future, contributing to better clinical decision making, less revision surgery, better patient health and decreased health costs. From now on, we expect that all mentioned techniques will develop towards highly recommended and useful techniques to determine patient profiles. For this, standardized methods, bigger patient groups and accessible biobanking of clinical data will make patient profiling more reliant and accessible.

Not one biomarker for osteoarthritis

In conclusion, we do not believe that one particular biomarker will function as predictive molecule for OA development or early detection. Most likely, a group of molecules (proteins, lipids, metabolites and possibly other molecules combined) will give a better insight in the development OA and possible therapeutic targets. To reach clinical implementation of MS analysis in treatment decision making, standardizing procedures, large relevant cohort studies and sharing of protocols and data are necessary.

Supplementary information

Supplementary Table 2.1. PubMed Advanced Search conducted on January 28, 2021.

#	PubMed Advanced Search	Results 28.01.2021
1	mass spectrometry[MesH] OR proteomics[MesH] OR lipidomics[MesH] OR metabolomics[MesH] OR mass spectrometry[tiab] OR metabonomic*[tiab] OR proteomic*[tiab] OR lipidomic*[tiab] OR metabolomic*[tiab] OR glycomic*[tiab]	441987
2	osteoarthritis[MesH] OR osteoarthritis[tiab]	93208
3	#1 AND #2	701

Supplementary Table 2.2. Potential protein or peptide biomarker(s) up (↑) or down (↓) regulated in osteoarthritis (OA) or control patients, described by ≥ two studies without contradictive results. Pathway analysis in MetaboAnalyst 5.0 was conducted on all upregulated-highlighted proteins (n = 35) in OA patients.

Biomarker[ref]	Tissue/fluid	Specific for	
α2-Macroglobulin[132, 144]	Synovial fluid	↑	OA
α-1-acid glycoprotein 1[153, 157]	Meniscus	↑	OA
α-1B-glycoprotein[144, 157]	Synovial fluid, meniscus	↑	OA
α-2-HS-glycoprotein[137, 157]	Synovial fluid, meniscus	↑	OA
(pre) Apolipoprotein E (precursor)[132, 148, 153, 157]	Synovial fluid, meniscus, cartilage	↑	OA
Apolipoprotein H (β2-glycoprotein I)[132, 153]	Synovial fluid, cartilage	↑	OA
Ceruloplasmin (ferroxidase)[132, 144]	Synovial fluid	↑	OA
Collagen α-1(VI) chain (precursor)[145, 148, 157]	Meniscus, cartilage	↑	OA
Collagen α-3(VI) chain (precursor)[148, 157]	Meniscus, cartilage	↑	OA
Complement C1r (subcomponent)[134, 144]	Synovial fluid	↑	OA
Complement C3[132, 134, 144]	Synovial fluid	↑	OA
Complement component C5 (precursor)[148, 157]	Meniscus, cartilage	↑	OA
Complement component C7[134, 144]	Synovial fluid	↑	OA
Complement Component C9[134, 144, 153, 157]	Synovial fluid, meniscus, cartilage	↑	OA
Complement factor B[137, 144, 153, 157]	Synovial fluid, meniscus, cartilage	↑	OA
Complement factor H[144, 153, 157]	Synovial fluid, meniscus	↑	OA

OA= osteoarthritis

Supplementary Table 2.2 (continued). Potential protein or peptide biomarker(s) up (↑) or down (↓) regulated in osteoarthritis (OA) or control patients, described by ≥ two studies without contradictive results. Pathway analysis in MetaboAnalyst 5.0 was conducted on all upregulated-highlighted proteins (n = 35) in OA patients.

Biomarker[ref]	Tissue/fluid	Specific for	
Fibrinogen α chain (isoform) (precursor)[148, 153, 157]	Meniscus, cartilage	↑	OA
Fibrinogen β chain[144, 153, 157]	Synovial fluid, meniscus, cartilage	↑	OA
Fibrinogen γ chain (isoform)[132, 144, 153, 157]	Synovial fluid, meniscus, cartilage	↑	OA
Fibronectin[127, 137, 144, 155, 157]	Synovial fluid, meniscus, cartilage, synovium	↑	OA
Haptoglobin (precursor)[132, 143, 148]	Synovial fluid, cartilage	↑	OA
Hemopexin[144, 153]	Synovial fluid, cartilage	↑	OA
Inter-α-trypsin inhibitor heavy chain H1[137, 144, 157]	Synovial fluid, meniscus	↑	OA
Inter-α-trypsin inhibitor heavy chain H2[153, 157]	Meniscus, cartilage	↑	OA
Kininogen 1[133, 137, 144]	Synovial fluid	↑	OA
Lumican[144, 157]	Synovial fluid, meniscus	↑	OA
Matrix Gla protein[133, 157]	Synovial fluid, meniscus	↑	OA
Pigment epithelium-derived factor[144, 157]	Synovial fluid, meniscus	↑	OA
Procollagen C-endopeptidase enhancer 1[144, 146, 157]	Synovial fluid, meniscus, cartilage	↑	OA
Protein AMBP[134, 144]	Synovial fluid	↑	OA
Serine protease HTRA1 (precursor)[148, 157]	Meniscus, cartilage	↑	OA
Serum albumin (precursor)[134, 144, 148]	Synovial fluid, cartilage	↑	OA
Transaldolase[134, 144]	Synovial fluid	↓	OA
Transforming growth factor-beta-induced protein ig-h3 (precursor)[148, 157]	Meniscus, cartilage	↑	OA
Vitamin D-binding protein (group specific component)[132, 144, 157]	Synovial fluid, meniscus	↑	OA
Vitronectin (precursor)[144, 148]	Synovial fluid, cartilage	↑	OA
Histone H2B[133, 148]	Synovial fluid, cartilage	↑	Control
Serum amyloid A1 (isoform 1)[131, 133]	Synovial fluid	↑	Control

OA= osteoarthritis

Supplementary Table 2.3. Potential lipid and metabolite biomarker(s) (group) up (↑) regulated in early (eOA) or late (lOA) osteoarthritis (OA) patients, described by ≥ two authors without contradictive results. Pathway analysis in MetaboAnalyst 5.0 was conducted on all upregulated-highlighted lipids and metabolites (n = 13) in OA patients.

Biomarker[ref]	Tissue/fluid	Specific for	
Fatty acids			
Fatty acids (long chain)[78, 152]	Cartilage	↑	OA
Linolenic acid[152, 154]	Synovial fluid, cartilage	↑	lOA
Oleic acid[152, 154]	Synovial fluid, cartilage	↑	lOA
Palmitic acid[152, 154]	Synovial fluid, cartilage	↑	lOA
Palmitoleic acid[152, 154]	Synovial fluid, cartilage	↑	lOA
Stearic acid[152, 154]	Synovial fluid, cartilage	↑	lOA
Phospholipids			
Phosphatidylethanolamine-based plasmalogens[78, 151]	Synovial fluid	↑	OA
Phosphatidylethanolamines[78, 150, 151]	Synovial fluid	↑	OA
(lyso-) Phosphatidylglycerols[150, 151, 158]	Synovial fluid	↑	OA
Phosphatidylserines[150, 151]	Synovial fluid	↑	OA
(lyso-) Phosphatidylcholines/ Phosphatidylcholines[78, 150, 151]	Synovial fluid	↑	OA
Other			
Ceramides[150, 158]	Synovial fluid	↑	OA
Vitamin D3 derivatives/fragments[150, 152]	Synovial fluid, cartilage	↑	OA

lOA = late osteoarthritis, OA = osteoarthritis.

Chapter 3

Evaluation of the anti-Inflammatory and chondroprotective effect of celecoxib on cartilage *ex vivo* and in a rat osteoarthritis model

Mirella J.J. Haartmans*, Ufuk Tan Timur*, Kaj S. Emanuel, Marjolein M.J. Caron, Ralph M. Jeuken, Tim J.M. Welting, Gerjo J.V.M. van Osch, Ron M.A. Heeren, Berta Cillero-Pastor†, Pieter J. Emans†

* = shared first author, † = equal contribution

Cartilage 2022

Abstract

The potential chondroprotective effect of celecoxib, a nonsteroidal anti-inflammatory drug (NSAID) and selective cyclooxygenase (COX) 2 inhibitor used to reduce pain and inflammation in knee osteoarthritis (OA) patients, is disputed. This study aimed at investigating the chondroprotective effects of celecoxib on (1) human articular cartilage explants and (2) in an *in vivo* OA rat model. Articular cartilage explants from 16 OA patients were cultured for 24 hours with celecoxib or vehicle. Secreted prostaglandins (PGs, prostaglandin E2, prostaglandin F2α, prostaglandin D2) and thromboxane B2 (TXB2) concentrations were determined in medium by enzyme-linked immunosorbent assay ELISA, and protein regulation was measured with label-free proteomics. Cartilage samples from 7 of these patients were analyzed for gene expression using real-time quantitative polymerase chain reaction. To investigate the chondroprotective effect of celecoxib *in vivo*, 14 rats received an intra-articular injection of celecoxib or 0.9% NaCl after osteoarthritis induction by anterior cruciate ligament transection and partial medial meniscectomy (ACLT/pMMx model). Histopathological scoring was used to evaluate OA severity 12 weeks after injection. Secretion of PGs, target of Nesh-SH3 (ABI3BP), and osteonectin proteins decreased, whereas tissue inhibitor of metalloproteinase 2 (TIMP-2) increased significantly after celecoxib treatment in the human (*ex vivo*) explant culture. Gene expression of a disintegrin and metalloproteinase with thrombospondin motifs 4 and 5 (ADAMTS4/5) and metalloproteinase 13 (MMP13) was significantly reduced after celecoxib treatment in human cartilage explants. Cartilage degeneration was reduced significantly in an *in vivo* OA knee rat model. Our data demonstrated that celecoxib acts chondroprotective on cartilage *ex vivo* and a single intra-articular bolus injection has a chondroprotective effect *in vivo*.

Introduction

Knee osteoarthritis (OA) patients suffer from joint pain and immobility, which is usually treated by nonsteroidal anti-inflammatory drugs (NSAIDs) and physical therapy, with total knee arthroplasty (TKA) as an end-stage disease solution[195, 196]. Over the years, several disease-modifying OA drugs came to attention[197]. Selective cyclooxygenase 2 (COX-2) inhibitors are a type of disease-modifying OA drugs and are investigated for their effect on the inhibition of prostaglandins (PGs). PGs, secreted by intra-articular tissues, are an important class of signaling molecules present in synovial fluid and involved in inflammation[40, 41].

The family of eicosanoids consists of 5 different subtypes: prostaglandin E2 (PGE2), prostaglandin D2 (PGD2), prostaglandin I2 (PGI2), prostaglandin F2α (PGF2α), and thromboxane A2 (TXA2)[198]. Inhibition of their production has been shown to provide pain-reducing effects[198]. It has been suggested that PGE2 acts catabolic and induces cartilage degradation by inhibiting proteoglycan synthesis and stimulating matrix degradation[199, 200]. Studies on the actions of prostanoids on articular tissues have focused mainly on cartilage and PGE2, proposing it as a catabolic or anti-anabolic factor[199-201], while also anti-catabolic effects on chondrocytes have been reported[202-204].

An effective way to target prostanoid synthesis is by blocking COX activity[198]. At least 2 COX isoforms have been described, COX-1 and COX-2, the latter being considered to be associated with inflammation[205]. COX-2 inhibitors have been designed to target the inflammatory COX-2 while circumventing inhibition of COX-1[205]. An example of a specific COX-2 inhibitor is celecoxib, which is currently used as an analgesic by patients with inflammatory arthritic diseases[206]. Besides being a drug with analgesic properties, evidence on the OA disease-modifying effects of celecoxib is now increasing, with *ex vivo* and *in vivo* data showing chondroprotective effects[42-47], including beneficial effects on cartilage matrix turnover and suppression of pro-inflammatory factors. However, other studies report contradictory data showing the absence of a chondroprotective effect of celecoxib in a groove OA-model in dogs[48], in human patients with knee OA[49], or in a ligament transection and meniscectomy mouse model[50]. This may be related to differences in OA severity, timing of administration after OA induction, or lower local concentrations of celecoxib in the knee joint due to oral administration and insufficient patient compliance[207].

Whereas oral administration of celecoxib can be accompanied by negative side effects such as cardiovascular disease[47], the effect of intra-articular administration, which has not been used in clinic yet, has been studied briefly[45, 208-210]. Whereas some studies report improvement in cartilage degeneration scores[45, 208], others do not report improvement[209, 210]. Differences in study design, including dosage, timing

of treatment, or way of administration (with or without the use of dose delivery systems), and use of scoring system might be related to the outcome of results.

Due to the controversy of previous literature and to further clarify the chondroprotective effect of celecoxib; this work aims at studying the effect of celecoxib *in vitro* and *in vivo*. In the current study, we aimed at investigating (1) the *ex vivo* biomolecular mechanism and chondroprotective effect of celecoxib in cartilage biopsies by measuring (a) prostaglandin and protein secretion in the culture medium and (b) gene expression in the cartilage explants. In addition, (2) the *in vivo* effect of an intra-articular celecoxib injection on cartilage was investigated in an OA-induced rat model.

We hypothesize that celecoxib acts chondroprotective by reducing the release of inflammatory prostaglandins and that it might act as an anti-proteolytic drug by reducing the gene expression of specific proteolytic enzymes (such as metalloproteinases (MMPs))[211] and altering secreted proteins. To test this hypothesis, we analyzed the prostaglandin release by cartilage explants treated with celecoxib or dimethyl sulfoxide (DMSO) and performed gene expression analysis of important proteolytic enzymes known to be involved in knee OA pathophysiology. Subsequently, we analyzed the protein secretome in cartilage-conditioned medium.

We expect that the intra-articular injection of celecoxib has a chondroprotective effect and that a local administration would have a larger effect compared with oral administration. Thus, we investigated the chondroprotective capacity of a single intra-articular bolus injection of celecoxib in an *in vivo* surgically induced rat OA model.

Method – *Ex vivo* study

Human tissue explant cultures

From 16 human subjects with knee OA who underwent TKA, full-thickness cartilage explants were obtained (MEC approval 11-4-040). Cartilage pieces from femoral condyles and tibia plateaus were cut into small pieces, washed thoroughly with 0.9% NaCl 3 times, and cultured at 37°C and 5% CO2 in suspension for 24 hours with a concentration of 100 mg tissue/ml in Dulbecco's modified Eagle's medium (DMEM-F12 low glucose; Invitrogen, Carlsbad, CA) supplemented with 1% insulin-transferrin-selenite media supplement (ITS) (Invitrogen) and 1% antibiotic/antimycotic (Invitrogen)[16]. In addition, celecoxib (LC Laboratories, Woburn, MA) was dissolved in DMSO (vehicle, DMSO; Sigma-Aldrich, St Louis, MO) and added to the culture medium in a 10 µM final concentration. The concentration of celecoxib was determined based on earlier dose-response experiments[16, 46]. DMSO was added

1:1,000 to cultures without celecoxib as a control. After 24 hours, cartilage-conditioned medium was harvested, centrifuged at 1200 RPM for 8 minutes, and the supernatant was frozen at −80°C. Media were stored for a maximum of 4 weeks before prostanoid analysis. After 24 hours of culture, tissue explants were snap-frozen in liquid nitrogen and stored at −80°C until being processed for RNA isolation.

Prostanoid measurement in conditioned media

PGE2, PGF2α, PGD2, and TXB2 (a stable metabolite of TXA2) concentrations were determined in OA cartilage-conditioned medium by a competitive enzyme-linked immunosorbent assay (ELISA) according to the manufacturer's instructions (Cayman Chemicals, Ann Arbor, MI). ELISA for PGI2 was not performed in these experiments, as PGI2 is unstable in culture medium and previous experiments showed that it could not be measured reliably. PG concentrations in the samples were calculated from a calibration curve using standards supplied by the manufacturer.

Gene expression analysis: RNA isolation and RT-qPCR

Frozen cartilage samples from 7 patients were homogenized with a Mikro-Dismembrator S (B. Braun Biotech International GmbH, Melsungen, Germany) and suspended in 1 ml TRIzol (Thermo Fisher Scientific, Waltham, MA)/100 mg tissue. RNA extraction, purification, and quantification have been published earlier, as was the complementary DNA (cDNA) synthesis using both commercially available Rneasy Micro Kit (QIAGEN, Hilden, Germany) and Eurogentec kits (Eurogentec, Seraing, Belgium)[16]. Gene expression was analyzed using quantitative real-time polymerase chain reaction (RT-qPCR) as described earlier[16]. Validated primer sequences of 28S ribosomal RNA (rRNA), PPIA (peptidylprolyl isomerase A), GAPDH (glyceraldehyde 3-phosphate dehydrogenase), MMP13 (matrix metalloproteinase 13), COL2A1 (collagen type 2 alpha 1), ACAN (aggrecan), ADAMTS4 (a disintegrin and metalloproteinase with thrombospondin motifs 4), and ADAMTS5 (a disintegrin and metalloproteinase with thrombospondin motifs 5) were published earlier[16]. Amplification efficiencies of the primers were between 0.9 and 1.05. Gene expression analysis was performed based on normalization to the best housekeeper index, based on gene expression levels of 28S, PPIA, and GAPDH, as previously described[212]. These housekeeping genes were selected before as reliable[16].

Mass spectrometry analysis of conditioned media

An untargeted proteome analysis on OA cartilage-conditioned medium with and without celecoxib treatment was performed. For protein precipitation, the samples were centrifuged for 5 minutes at 1,200 RPM to remove potential cells and for 10 minutes at 13,000 RPM to remove potential macromolecular aggregates.

Subsequently, 10 µl of 0.2% sodium deoxycholate (DOC; Sigma-Aldrich) was added to each sample, vortexed, and incubated for 10 minutes at 4°C. Then, 10 µl of trichloroacetic acid (TCA; Sigma-Aldrich) was added, vortexed, and incubated for 1 hour at 4°C. The samples were centrifuged for 10 minutes at 13,000 RPM and the supernatant was removed. The remaining pellet was washed with 1 ml of cold acetone (−20°C) 3 times with intermediate centrifugation (13,000 RPM for 10 min) and removal of the supernatant. Dried protein pellets were dissolved in 50 µl of 5 M urea (GE Healthcare, Chicago, IL)/50 mM ammonium bicarbonate (Sigma-Aldrich) sample buffer and stored at −20°C until further processing. The protein content of each sample was measured using Bradford Protein Assay (Bio-Rad Laboratories, Hercules, CA) according to the manufacturer's protocol. Absorption was determined at 595 nm (optical density). A total of 6.6 µg protein per sample was used for protein digestion. Five microliters of 20 mM dithiothreitol (Sigma-Aldrich) in ULC/MS grade water (Biosolve, Valkenswaard, the Netherlands) was added to each sample, vortexed, and incubated for 45 minutes at room temperature. Subsequently, 6 µl of 40 mM iodoacetamide (Sigma-Aldrich) in ULC/MS grade water (Biosolve) was added, vortexed, and incubated for 45 minutes at room temperature in the dark. Ten microliters of 20 mM dithiothreitol (Sigma-Aldrich) was added to the solution, vortexed, and incubated at room temperature for 45 minutes to stop the reaction. A trypsin/Lys-C solution in resuspension buffer (Promega, Leiden, the Netherlands) was added in an enzyme to protein ratio of 1:25. The samples were vortexed and incubated in a water bath (37°C) for 2 hours, before spinning the samples down and adding 200 µl of 50 mM ammonium bicarbonate (Sigma-Aldrich) sample buffer. Again, samples were vortexed and incubated in a water bath (37°C) overnight.

Finally, 30 µl of 20% acetonitrile (ACN) (Biosolve)/10% formic acid (FA) (Biosolve) was added and samples were vortexed to stop the reaction. Samples were centrifuged for 30 minutes at 13,000 RPM to remove possible particles and were stored at −20°C until liquid chromatography-tandem mass spectrometry (LC-MS/MS).

Proteomic analysis was performed on a Thermo Scientific Ultimate 3000 Rapid Separation UHPLC system (Dionex, Amsterdam, the Netherlands), coupled to a Q-Exactive HF mass spectrometer (Thermo Fisher Scientific). The UHPLC system was equipped with a PepSep C18 analytical column (15 cm, ID 75 µm, 1.9 µm Reprosil, 120Å). Samples were desalted on an online installed C18 trapping column and then separated on an analytical column with a 90-minute linear gradient (5%-35% ACN with 0.1% FA, flow rate 300 nl/min). The scans were performed in data-dependent acquisition mode (DDA). Full mass spectrometry (MS) scans were executed from 250 to 1250 *m/z* (mass to charge ratio) at a resolution of 120,000, followed by tandem MS (MS/MS) scans on the 15 most intense ions at a resolution of 15,000[160].

Method – *In vivo* study

Surgery for induction of osteoarthritis

The chondroprotective effect of celecoxib was investigated in a rat OA model, anterior cruciate ligament (ACL) transection in combination with a partial medial meniscectomy (ACLT/pMMx). The primary outcome measure was the cartilage degeneration score according to the Osteoarthritis Research Society International (OARSI) histopathology initiative for the rat[213]. The study was performed in accordance with the ARRIVE (Animal Research: Reporting of *In Vivo* Experiments) guidelines[214]. All animal experimental protocols were approved by the Maastricht University Animal Ethics Committee (DEC13-052).

Sample size was calculated according to the formula of L. Sachs[215] with $\alpha = 0.05$, power = 0.80 ($\beta = 0.20$), spread of $\sigma = 20\%$, and an effect size of $\delta = 33\%$[216], resulting in n = 6 knees per group. We expected a 10% dropout for all groups. Therefore, we included 7 knees per group.

Fourteen 3-month-old, male Lewis rats (Charles River, 's-Hertogenbosch, the Netherlands) were allowed to acclimatize for 1 week, before the start of the experiments. Animals were housed in pairs, kept on a 12-hour dark/light cycle, and fed ad libitum. OA was surgically induced in the right knee by the ACLT/pMMx OA model[213]. The left knees were used as healthy controls. Only male rats were included in this study to prevent an influence of hormonal fluctuation during menstrual cycle of female rats.

In brief, rats were anesthetized in a chamber containing 1% isoflurane (Isoflo; Abbott Laboratories, Chicago, IL). The right knee joint of each rat was shaved, cleaned, and disinfected with iodine (Eurovet Animal Health, Bladel, the Netherlands). The skin was incised with a longitudinal incision on the medial side of the joint. Then, the joint capsule was incised on the medial side of the patellar tendon, which provided access to the joint space. The patella was dislocated laterally and the ACL was transected using a surgical blade (size 11). Transection was confirmed by a manually performed anterior drawer test. In addition, the anterior part of the medial meniscus was removed using a surgical scissor. The joint capsule and skin were closed with Vycril 4-0 sutures. Left knees were kept intact.

Animals were allowed to move freely in their cage and were checked daily for general health and experiment-related discomfort for 3 weeks. Four weeks after surgery, rats were randomly assigned to 2 experimental groups using the block randomization method. The treatment group received an intra-articular injection of 25 µl of 0.9% NaCl containing 92.25 ng of celecoxib in both the operated (group 1a:

OA celecoxib) and nonoperated leg (group 1b: healthy celecoxib). The control group received an intra-articular injection of 25 µl of 0.9% NaCl in both legs (group 2a and group 2b, respectively: OA control and healthy control). This amount of celecoxib was based on previous literature[16, 46]. Twelve weeks after injection, rats were anesthetized with 1% isoflurane and killed by cervical dislocation. OA severity was assessed by scoring histological sections of rat knee joints using the OARSI histopathology initiative for the rat by 2 blinded observers[213].

Tissue preparation and histology Rat knee joints were carefully resected and fixed with 3.7% paraformaldehyde (VWR International, Radnor, PA) in 0.1 M phosphate-buffered saline (PBS) at 4°C for 1 week. Next, tissues were decalcified in 0.5 M ethylenediamenetetraacetic acid (EDTA) solution (pH 7.8) for 8 weeks. After confirmation of decalcification on x-ray, knee joints were cut in halves along the medial collateral ligament in the frontal plane to directly get access to the central weightbearing region of the joint. The posterior half of the knees was dehydrated by transferring through solutions of increasing ethanol concentration up to 100% ethanol. After a final 24-hour dehydration step in cold 100% acetone at 4°C, specimens were infiltrated with Technovit 8100 (VWR International) at 4°C for 4 weeks. After this, specimens were placed into polyethylene-embedding molds. Polymerization solution (hardner), prepared according to the protocol of the manufacturer, was poured into the molds and air contact was prevented by covering the cavities with plastic films. The embedding form was placed on a thin layer of ice, and polymerization was allowed for 24 hours at 4°C. After hardening was complete, specimens were blocked with Histobloc and Technovit 3040 (VWR International) and removed from the molds. Sections (5-10 µm) were cut from the blocks using a rotation microtome (Leica Biosystems, Nussloch, Germany), stretched on distilled water, and mounted on uncoated glass slides at 80°C. Slides were subjected to thionine staining for routine histological examination by light microscopy (Axio Vert A1 microscope, Axiovision LE release 4.8.2; Carl Zeiss AG, Oberkochen, Germany).

As lesions in the ACLT/pMMx model develop mainly at the outer one-third of the medial tibial plateau, thionine-stained sections of the medial tibial plateau were scored using the cartilage degeneration score according to the OARSI histopathology initiative for the rat[213]. Scoring was performed by 2 blinded observers (U.T.I. and R.M.J.). Measurements of parameters needed for the cartilage degeneration score were made using Axiovision Software (Axiovision LE release 4.8.2; Carl-Zeiss).

Statistics and data analysis

ELISA and RNA measurements

GraphPad Prism 8 (GraphPad Software, San Diego, CA) was used for statistical analysis. Per donor, explants were obtained, pooled, and randomly divided over the different conditions. All samples for gene expression analysis and prostanoid measurements in the medium were processed and analyzed individually with a single measurement per donor. Continuous variables were tested for normality using the Kolmogorov-Smirnov test and normality plots were visually assessed for skewness. No normal distribution was identified. Effects of celecoxib on gene expression and prostanoid release by different intra-articular tissues were evaluated using a Wilcoxon matched-pairs signed-rank test. Statistical differences in histology scores in OA-induced knees or non-OA-induced knees injected with 0.9% NaCl or a bolus celecoxib were analyzed using a Mann-Whitney U test.

Proteome analysis

The acquired spectra were analyzed for protein identification and quantification using Proteome Discoverer (PD) Software version 2.2 (Thermo Fisher Scientific). Protein identification was conducted using the Sequest HT search engine with SwissProt (Human) database (Homo sapiens, Tax ID 9606). Analysis settings for this search included: enzyme trypsin, a maximum of 2 missed cleavage sites, a minimum peptide length of 6 and maximum of 144, a precursor mass tolerance of 10 ppm, and fragment mass tolerance of 0.02 Da. In addition, dynamic modifications of methionine oxidation (+15.995 Da) and protein N-terminus acetylation (+42.011 Da), and static modification of carbamidomethylation (+57.021 Da) were used. A false discovery rate of ≤1% was applied.

Protein quantification was performed using label-free quantification settings in PD version 2.2. Peptide precursor intensities were used for peptide abundance and total peptide amount was used for normalization. The difference in protein secretion (proteins with high confidence) between treatment groups was determined using a Wilcoxon signed-rank test with Benjamini-Hochberg correction for multiple testing[217] in MATLAB 2018a for Windows (MathWorks, Natick, MA) with $\alpha = 0.05$.

Results

Celecoxib reduces prostanoid release by cartilage e*x vivo*

All 4 prostanoid subtypes were detected in medium conditioned by OA cartilage (**Figure 3.1**). The average concentration of PGE2, PGF2α, PGD2, and TXB2 by cartilage

in the control group was, respectively, 23 ng/ml, 5 ng/ml, 3 ng/ml, and 0.4 ng/ml (Figure 3.1). In conditioned medium acquired from celecoxib-treated OA cartilage, a significantly reduced PGE2 ($P < 0.001$; 60-fold), PGF2α ($P < 0.001$; 14-fold), PGD2 ($P < 0.001$; 21-fold), and TXB2 ($p = 0.0092$; 2-fold) concentration was measured (Figure 3.1).

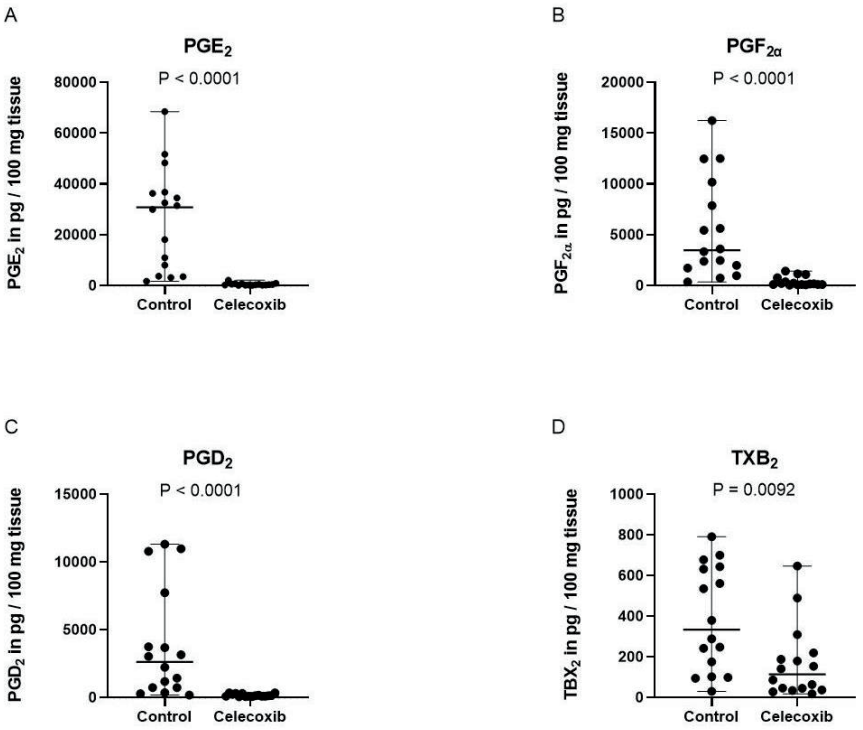

Figure 3.1. Celecoxib reduced prostanoid release by cartilage *ex vivo*. PGE2 (A), PGF2α (B), PGD2 (C) and TXB2 (D) release by cartilage after 24 hours of culture. Each dot represents absolute prostanoid values (in pg/100 mg tissue) per individual patient. The median and range are plotted in the figures. p-values are depicted in the figure. n = 16. PGE2 = prostaglandin E2, PGD2 = prostaglandin D2, PGF2α = prostaglandin F2α, TXB2 = thromboxane B2.

Celecoxib reduces gene expression of proteolytic enzymes in cartilage *ex vivo*

To evaluate the chondroprotective effects of celecoxib on cartilage *ex vivo*, we evaluated the effect of celecoxib on the gene expression levels of COL2A1 and ACAN, which are major structural proteins of the cartilage matrix[218]. We have also evaluated the effect of celecoxib on the gene expression levels of proteolytic enzymes MMP13, ADAMTS4, and ADAMTS5, which are known to be involved in knee

OA pathophysiology[218]. The expression of COL2A1, ACAN, MMP13, ADAMTS4, and ADAMTS5 could be detected in all cartilage donors. Celecoxib treatment did not alter the gene expression of COL2A1 ($p = 0.5781$) and ACAN ($p = 0.9375$). However, it significantly reduced gene expression levels of ADAMTS4 ($p = 0.0156$; 4-fold), ADAMTS5 ($p = 0.0156$; 3-fold), and MMP13 ($p = 0.0156$; 3-fold) in cartilage (**Figure 3.2**).

Celecoxib changes protein secretion by cartilage *ex vivo*

Cartilage-conditioned media were analyzed using LC-MS/MS to get a broader insight into the actions of celecoxib on cartilage on secreted proteins. A total protein input of 6.6 µg/µl per sample was used for the detection of 154 proteins with high confidence in cartilage-conditioned media. COL2A1 and AGC core protein (aggrecan, ACAN) were detected in our analysis; however, there were no significant differences between groups (**Figure 3.3**). A significant increase (after p-value correction) in normalized abundance of tissue inhibitor of metalloproteinase 2 (TIMP-2; $p = 0.0009$; 5-fold) and reduction of target of Nesh-SH3 (ABI3BP; $p = 0.0010$; 6-fold) and osteonectin ($p = 0.0010$; 39-fold) was observed after treatment with celecoxib (**Figure 3.3**).

Celecoxib acts chondroprotective *in vivo*

Based on the *ex vivo* results showing the anti-catabolic effect of celecoxib, we investigated the effect of a single intra-articular bolus injection with celecoxib *in vivo* on OA development in a trauma-induced OA rat model (ACLT/pMMx model)[213]. No wound infection was noticed after ACLT and pMMx surgery in any of the animals. We had a dropout of one of the rats in the control group. The wounds healed within 1 week with no difference between the operated and non-operated leg. All rats had a similar weight gain over 16 weeks. The cartilage degeneration score[213] was significantly reduced in OA-induced knees treated with celecoxib compared with OA-induced knees injected with 0.9% NaCl, as scored by observer 1 (median cartilage degeneration score: 0.9% NaCl 5 [range 3-7] and celecoxib 0 [range 0-5]; $p = 0.0169$; **Figure 3.4**) and observer 2 (median cartilage degeneration score: 0.9% NaCl 4.5 [range 4-7] and celecoxib 2 [0-7]; $p = 0.245$; **Figure 3.4**). Contralateral knees without OA induction did not have significant cartilage pathology in both the 0.9 % NaCl group and bolus celecoxib group (**Figure 3.4**). Histological images representing the difference between OA-induced and healthy rat knees injected with 0.9 % NaCl and a bolus celecoxib are shown in **Figure 3.4**.

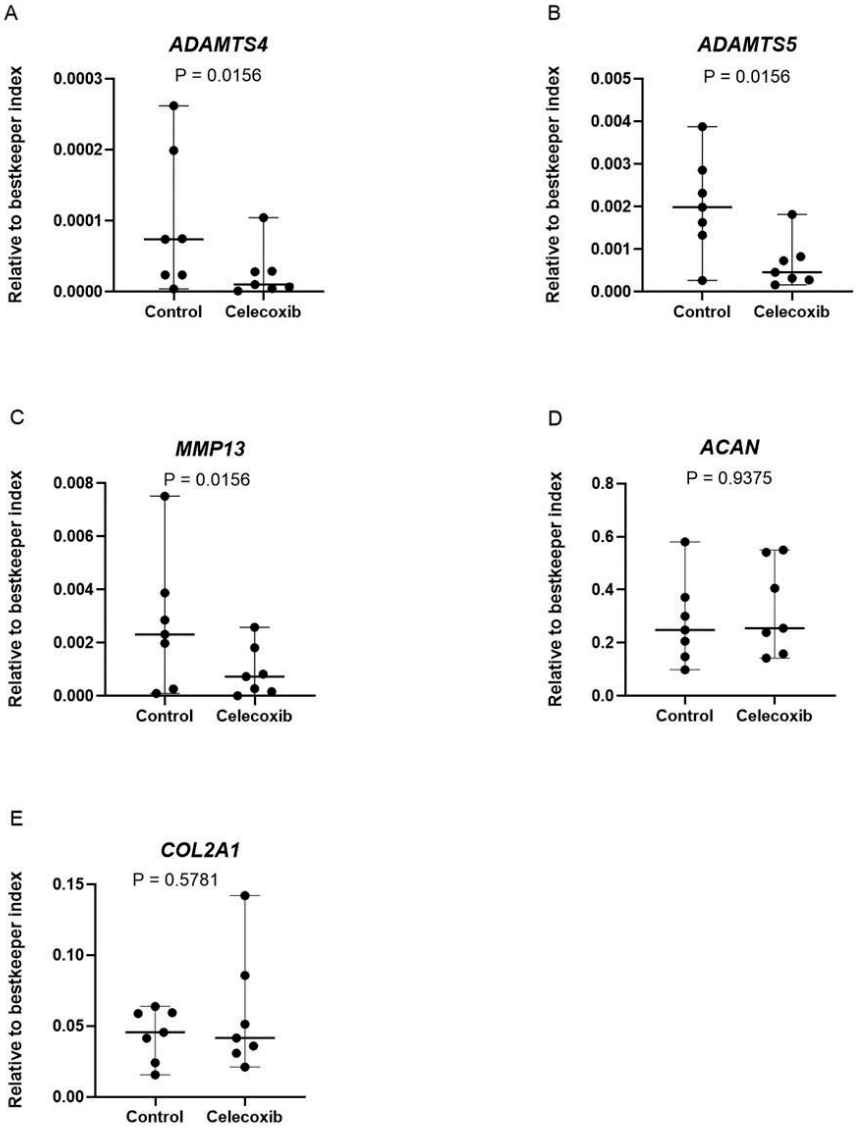

Figure 3.2. Celecoxib reduces gene expression of proteolytic enzymes in cartilage *ex vivo*. ADAMTS4 (A), ADAMTS5 (B), MMP13 (C), AGC (D), and COL2A1 (E) mRNA expression levels in cartilage explants from OA patients treated with or without celecoxib. The median and range are plotted in the figures. Absolute p-values are depicted in the figure. n = 7. ADAMTS4 = a disintegrin and metalloproteinase with thrombospondin motifs 4, ADAMTS5 = a disintegrin and metalloproteinase with thrombospondin motifs 5, MMP13 = metalloproteinase 13, AGC = aggrecan (protein), COL2A1 = collagen type 2 alpha 1, OA = osteoarthritis.

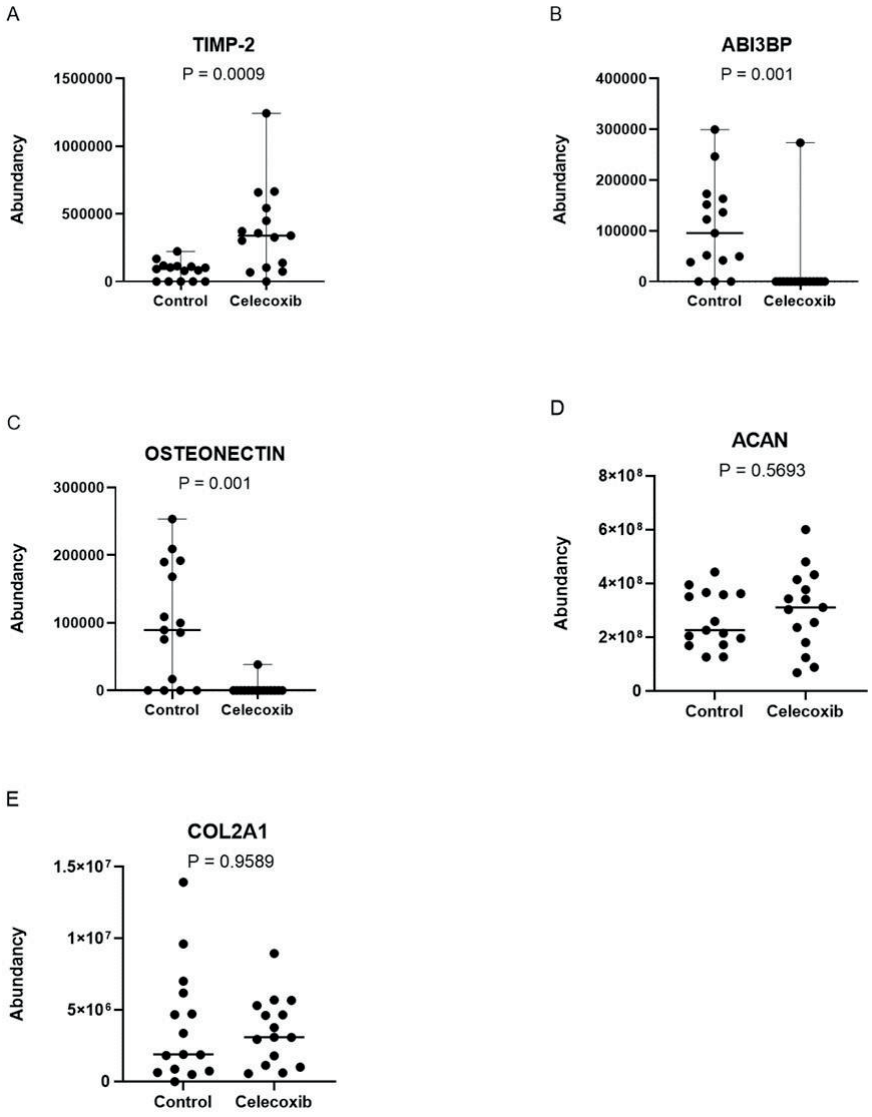

Figure 3.3. Significantly different secreted proteins by cartilage after celecoxib treatment. Changes in osteonectin (A), TIMP-2 (B), and ABI3BP (target of Nesh-SH3) (C) after celecoxib treatment. ACAN (D) and COL2A1 (E) did not change. The median and range are plotted in the figures. Absolute p-values are depicted in the figure. n = 15. TIMP-2 = tissue inhibitor of metalloproteinase 2, ABI3BP = target of Nesh-SH3, ACAN = aggrecan, COL2A1 = collagen type 2 alpha 1.

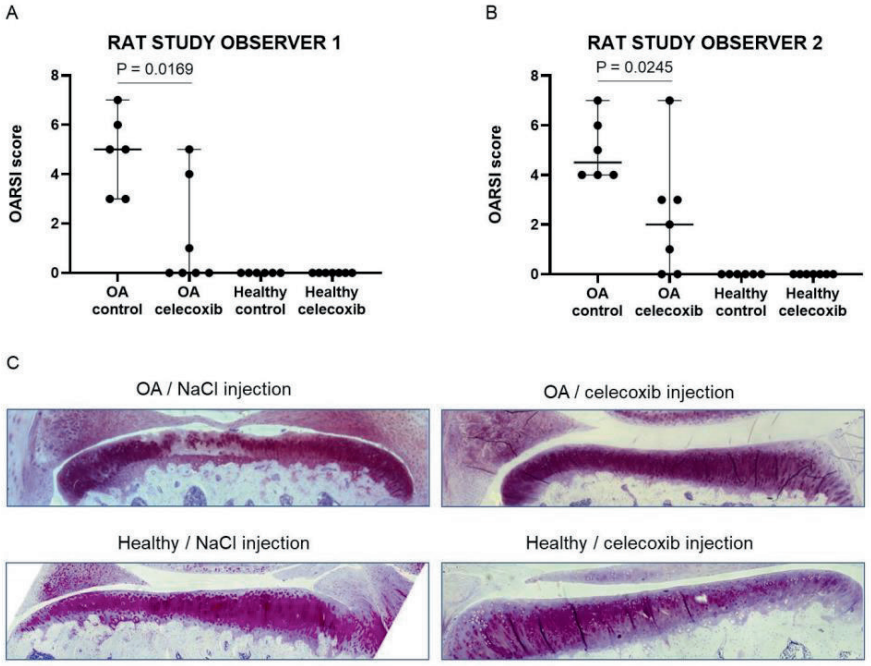

Figure 3.4. Cartilage degeneration scores of rat knees treated with celecoxib or NaCl. Cartilage degeneration scoring of rat knees by observer 1 (A) and observer 2 (B), including histological images representing the largest difference of a rat knee injected with NaCl or celecoxib (C). The median and range are plotted in figures A and B. Absolute p-values are depicted in the figure. n = 6 for OA and healthy with NaCl treatment. n = 7 for OA and healthy celecoxib. OA = osteoarthritis.

Discussion

As hypothesized in this study, cartilage prostanoid (PGE2, PGF2α, PGD2, and TXB2) levels in cartilage-conditioned medium were reduced after treatment with celecoxib. In addition, celecoxib altered gene expression levels of proteolytic enzymes in cartilage *ex vivo*, but did not alter gene expression of COL2A1 and ACAN. Celecoxib did significantly reduce gene expression levels of MMP13, ADAMTS4, and ADAMTS5 in cartilage, suggesting an anti-proteolytic effect. In addition, an untargeted LC-MS/MS analysis was conducted on medium samples of all explant cultures to confirm that the changes in gene expression led to different protein secretion profiles. Three proteins showed significant upregulation (TIMP-2) or downregulation (ABI3BP and osteonectin) in the conditioned medium treated with celecoxib. Finally, we found an OA-modulatory effect *in vivo*. The cartilage degeneration score was significantly reduced in OA-induced knees treated with

celecoxib compared with OA-induced knees injected with 0.9% NaCl. Overall, in accordance with our hypothesis, the data indicate a chondroprotective role of celecoxib *ex vivo* and *in vivo*.

In this work, we combined analysis on the effect of celecoxib on cartilage on different levels: the secretion of prostaglandins and proteins, gene expression, and its effect *in vivo* in an OA rat model. Prostanoid-reducing actions of celecoxib on cartilage have been shown earlier[219]. In addition, as the specific COX-2 inhibitor celecoxib was able to significantly reduce prostanoid release in cartilage, prostanoid synthesis in cartilage seems to be mainly COX-2-driven. These data are in accordance with a study performed by Hardy et al.[200], where COX-2 induction was detected in cartilage after an inflammatory stimulus. We and others have also found that prostanoid subtypes differentially influence chondrogenic differentiation, indicating that prostanoids have an anti-catabolic function, and influence the chondrogenic differentiation of progenitor cells[220, 221]. The detection of all prostanoid subtypes in cartilage and their inhibition by celecoxib suggest that they are all COX-2-driven. Future experiments can focus on whether specific subtypes have different functions in cartilage and may aid in developing novel therapeutic strategies to target inflammatory and catabolic processes in knee OA.

In the current work, we provide further evidence of the chondroprotective effects of celecoxib via the modulation of other important proteolytic enzymes involved in knee OA such as ADAMTS4 and ADAMTS5[222]. ADAMTS4 and ADAMTS5 have been shown to play an important role in OA development by the degradation of ACAN (a critical cartilage component)[223]. In addition, MMPs (especially MMP13)[224] contribute to this process by degrading collagen[223, 225]. Yang et al.[226] found that celecoxib can reduce the expression of gelatinases in different joint tissues such as cartilage. These enzymes are involved in knee OA pathophysiology[226]. The decrease of secretion of these enzymes by cartilage after celecoxib treatment suggests that celecoxib acts anti-proteolytic by regulation of the expression of these enzymes. In addition, it has been shown that celecoxib inhibits the production of MMPs via nuclear factor-κB and mitogen-activated protein kinases, unrelated to PGE2[227].

In our study, celecoxib increased the secretion of TIMP-2. According to these results and given literature[224, 228, 229], this suggests the confirmation that celecoxib treatment might also lead to a decrease in MMP activity, inhibiting cartilage degradation and inflammation[224, 230]. Although a direct connection between TIMP-2 and MMP-13 was not made in this experimental setting, the data support the indications that celecoxib may act anti-proteolytic and thus contribute to the chondroprotective effect on cartilage.

The untargeted LC-MS/MS analysis revealed a reduction in ABI3BP, an extracellular matrix structural constituent that has been associated with inducing cell senescence in different cell types[231]. Senescence has been associated with OA[232, 233], although little is known about the mechanisms involved in chondrocytes. ABI3BP might be one of the factors promoting cellular senescence in articular chondrocytes[234], and its downregulation in articular cartilage supports the potential chondroprotective effect of celecoxib. Similarly, osteonectin (secreted protein acidic and rich in cysteine [SPARC]) is an extracellular matrix protein, playing an important role in collagen binding and modulating cell-matrix interactions[235, 236]. Osteonectin binds calcium and is involved in cartilage calcification, leading to the progression of OA[237]. Its downregulation after treatment with celecoxib further bolsters insights into a potential chondroprotective effect of celecoxib.

In the *in vivo* rat model for OA, we used one single bolus injection of celecoxib to ensure only local administration, in line with our previous data[46]. Previously performed animal studies[45, 208-210] using intra-articular injection of celecoxib show contradictive results, dependent on dosage and way of administration (drug delivery system or single bolus injection), initiation, and duration of treatment and scoring system. In our study, we do not make use of any drug delivery system or repeated intra-articular injections. In addition, our study initiates celecoxib treatment at 4 weeks after surgery, suggesting that OA was developed further than when started directly after OA induction by surgery. Although our data imply a positive outlook for the use of celecoxib as chondroprotective drug in OA patients, the discussion remains whether this contrasting evidence is due to factors such as celecoxib concentration, timing of injection, or the fact that celecoxib might function analgesic, leading to improved mobility (and increased cartilage wear and OA development) of the treated animal[207]. Overall, according to our results, we speculate that celecoxib might cause an effective reduction of local inflammation and that this might be accompanied by an anti-proteolytic effect downstream of the inflammatory signaling.

As our results suggest that celecoxib can be used as a chondroprotective drug in the treatment of osteoarthritis, it should be noted that this only includes the beneficial effects and that certain side effects, ranging from gastrointestinal problems to cardiovascular diseases and high blood pressure, should be taken into account[47, 238]. In addition, we hypothesize for future studies that local administration of celecoxib, by intra-articular injection, might not only have a positive influence on its chondroprotective effect, but might also limit certain systemic side effects that have been seen with the use of celecoxib[47]. With the application of local administration, it could be easily regulated how much celecoxib eventually ends up at the affected location in the joint, rather than the rest of the body. With this, we reopen the

discussion and try to close the knowledge gap on the best way for celecoxib to be administrated.

One limitation of our study is the use of a rodent animal model. Nevertheless, we were still able to conclude that celecoxib acts chondroprotective *in vivo* when administrated locally using a single intra-articular injection. Future studies should focus on bigger animal models such as goat, sheep, or horse, in general more similar to humans. Our data suggest the importance of implementing local drug administration for osteoarthritis treatment.

Conclusion

In conclusion, our data indicate a chondroprotective effect of celecoxib via a reduction in inflammation and proteolytic enzyme expression. A single bolus injection of celecoxib showed a protective effect against cartilage degeneration in a rat model for OA. These data suggest that local, intra-articular administration of celecoxib might be more effective in OA treatment and that celecoxib should be reconsidered as a chondroprotective drug in OA patients. However, certain side effects should be taken into account when prescribing this drug. Future experiments should therefore focus on local administration and gathering more *in vivo* data, especially from bigger animal models and human studies.

Chapter 4

Sample preparation for lipid analysis of intra-articular adipose tissue by using matrix-assisted laser desorption/ionization imaging

Mirella J.J. Haartmans, Britt S.R. Claes, Kaj S. Emanuel, Gabrielle J.M. Tuijthof, Ron M.A. Heeren, Pieter J. Emans, Berta Cillero-Pastor

Analytical Biochemistry 2023

Abstract

Mass spectrometry imaging (MSI) is a powerful technique enabling the visualization of the spatial distribution of different molecules in tissue biopsies with different pathologies. Sample handling and preparing adipose tissue for MSI is challenging and prone to molecular delocalization due to tissue melting. In this work, we developed a method for matrix-assisted laser desorption/ionization (MALDI)-MSI to study lipids in human infrapatellar fat pad (IPFP), a biomarker source in musculoskeletal pathologies, while preserving molecular spatial distribution. Cryosectioning at 15 µm with a temperature below -30°C, thaw mounting, and sublimation, was demonstrated to preserve IPFP's heterogeneous appearance and spatial distribution of lipids.

Introduction

Mass spectrometry imaging (MSI) is a powerful technique that enables the visualization of the spatial distribution of molecules, such as lipids, metabolites, and proteins in thin sample sections[90]. Matrix-assisted laser desorption/ionization (MALDI) MSI is the MSI method most commonly used within the biomedical field[239]. Molecular distributions can be used to measure a variety of pathological conditions in biological samples (e.g. biomarkers)[240-242], drugs or compounds[101, 243], and can be useful for the development of targeted treatments[22, 101]. The analysis of lipids in adipose tissue with MS is already an expanding field of research[244-246]. Adipose tissue does contain healthy adipocytes, however in some cases, like visceral fat in obesity or the infrapatellar fat pad (IPFP) in osteoarthritis, it can be inflamed, secreting multiple pro-inflammatory mediators[186, 247]. Immune cells, like macrophages or T-cells, infiltrate the adipose tissue and mediate this inflammatory response[248, 249]. In IPFP, or Hoffa's fat pad (the fat pad underneath the patella tendon in the knee[16]), a strong inflammation in relation to some diseases in the knee joint has been observed[16, 250]. Therefore, the IPFP can be considered a rich source of biomarkers. As the tissue is heterogeneous in nature, consisting of adipose, fibrous, and synovial tissue, MSI analysis is preferred to study the spatial distribution of potential biomarkers. However, sample handling and preparation are important factors to consider when analyzing adipose tissue using MSI techniques. Usually, snap-frozen samples are sectioned at a few micrometers and low temperatures, before being mounted on glass slides using thaw mounting, slide coating, gluing, or tape transfer methods[251-253]. When tissue sections stay at room temperature, for either matrix application or co-registration, molecules can delocalize[254]. Existing protocols using tape transfer methods[251] do not work for the IPFP due to polymer contamination (transparent tape, Cryofilm Type 3C (16UF), Section-Lab Co. Ltd., Hiroshima, Japan) or other practicalities (e.g. commonly used double-sided copper tape is limited in width and interferes with tissue staining and light microscopy). Therefore, we needed a different workflow applicable to IPFP. Furthermore, we needed to overcome the challenge of matrix application on fatty tissues without the delocalization of molecules, as can be seen with spray deposition[252].

To our knowledge, to date, no MSI working protocol to study IPFP has been described. Therefore, in this methodological paper, we developed and evaluated a method for MALDI-MSI for IPFP.

Materials and methods

Tissue collection, storage and cryosectioning

For this methodological development, human IPFP was collected as waste material from a patient undergoing cartilage repair surgery at Maastricht University Medical Center (MUMC+) in the Netherlands. Samples were collected in accordance with the Medical Ethics Committee (MEC) assigned non-WMO (wet medisch-wetenschappelijk onderzoek, law for medical-scientific research in humans in the Netherlands) approval for the collection of waste material during cartilage repair surgery (ID: MEC 2018-0963, 2018). Directly after dissection at the surgical theater, tissue sections were washed in phosphate-buffered saline (PBS), snap-frozen in liquid nitrogen, and stored at −80°C until further processing. Adipose tissue, or fat tissue, has been shown a difficult tissue type to analyze using MSI without molecular delocalization. Tissue degradation was prevented by snap freezing the tissues directly at the surgical theater. IPFP needs to be washed using PBS due to the amount of blood (vessels) present in the tissue. Blood can have a major effect on the outcome of the measurement, as heme and hemoglobin hamper the ionization of other molecules of interest. Washing tissue with salty solutions such as PBS is not optimal for mass spectrometry (MS) analysis[255], however, it did not cause disturbance of our analysis in negative ion mode. The use of alternative washing solutions might be more favorable; however, we were limited by the regulations and strict protocols at the operating theater. Tissues were stored at −80°C in an ultra-low temperature freezer until use, to prevent molecular degradation. Subsequently, tissues were transported to the cryotome on dry ice to prevent melting.

Although frozen, we noticed that cryosectioning of IPFP at −20°C to −30°C (for high lipid content containing tissues)[256] and at 5–10 µm[26] thickness was not optimal due to thawing/melting. We tried several tape-transfer methods[251], including transparent tape and double-sided copper tape. However, the transparent tape (Cryofilm Type 3C (16UF), Section-Lab) caused polymer contamination, whereas the copper tape prevented us from performing multi-modal –omics approaches[257] and/or histological staining and microscopy. Finally, the frozen IPFP was sectioned at 15 µm thickness with a cryostat (Leica Microsystems Cryotome, Wetzlar, Germany) covered with dry ice to maintain the temperature in the cryotome between −30°C and −35°C, while keeping the stage, knife, slides, and other tools at the same temperature (**Figure 4.1A**). We kept the stage and knife in the cryotome cooled by using dry ice, as it heats up while cutting (e.g. due to environmental temperature and humidity, body heat (breathing or hands, and friction of the tissue moving over the knife). This would make the tissue sticky and proper sectioning difficult (**Figure 4.1B**). The obtained IPFP tissue sections (2 sections per slide) were thaw-mounted on a cooled indium tin oxide (ITO) coated glass slide (4–8 Ω

resistance, Delta Technologies, CO, USA) using body heat, and were immediately refrozen using the cooled stage in the cryotome to avoid delocalization of molecules (**Figure 4.1C**), prior to storage in the freezer. Both actions, thaw-mounting and refreezing, were performed within 5–10 s. Importantly, in contrast to other methods, we do not need tape to transfer our sample to a slide[251] or any type of additional slide coating[252]. For transportation of tissue sections to the desiccator (to dry) and mass spectrometer, slides were placed in in-house developed silica carrier boxes[258, 259]. These closable metal boxes with a glass lid and a silica box inside prevent condensation from thawing and thus delocalization of molecules. All slides were transferred to an ultra-low temperature freezer (−80°C) horizontally in a slide box on dry ice until MALDI-MSI analysis. Nevertheless, different fat sources may need different approaches.

Matrix application

Tissues were transported from the ultra-low temperature freezer (−80°C) in a cooled silica carrier box[258, 259] as horizontal as possible to a desiccator and dried inside the opened carrier box for 30 min under vacuum to ensure that the tissue was dry before application of the matrix. Then, the box containing the slide was closed for transportation and matrix application was performed using sublimation (HTX Sublimator, HTX Imaging, Chapel Hill, NC, USA) with 55 mg Norharmane matrix (Sigma-Aldrich, Zwijndrecht, the Netherlands) dissolved in 2 mL MeOH to extract lipids. We used Norharmane as a matrix to analyze lipids (analytes of interest) in both negative and positive polarities. Preheating of the sublimator was performed at 60°C, the pressure was set at < 0.04 mBar and sublimation was performed at 140°C for 200 s. Matrix application using sublimation is preferred as the sublimation process occurs under a vacuum and the slide is cooled using a water-cooling system. Both prevent molecules from delocalizing. Although spraying of the matrix could be more efficient on analyte extraction and thus enhance the signal compared to sublimation[253], the use of spraying solvents can cause melting of the tissue and delocalization of molecules[252]. After matrix application, the slide was placed back in the silica carrier box for transportation.

MALDI-MSI

MALDI-MSI experiments were performed on a RapifleX Tissuetyper (Bruker Daltonics, Bremen, Germany) at 50 µm of lateral resolution in negative ion mode, running in reflector mode with a mass range of 100–2000, 60 laser shots/pixel, and laser frequency of 10 kHz. Red phosphorus was used for instrument calibration prior to the measurement. MALDI-MSI on a RapifleX Tissuetyper is a relatively fast (up to 40 pixels/second) and sensitive method to measure and locate small molecules such as lipids, metabolites or peptides at high spatial resolution (up to 5 µm). However,

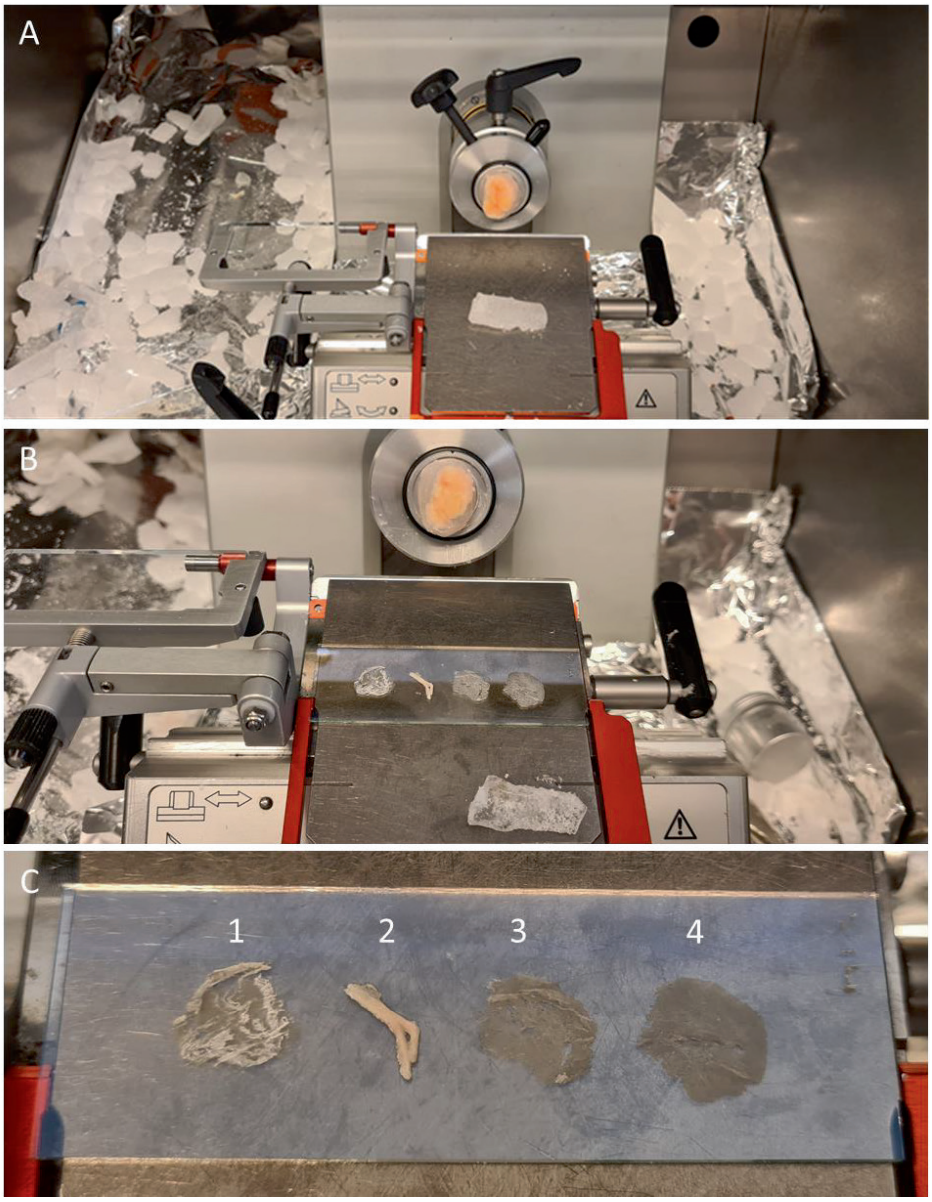

Figure 4.1. Instrumental (Leica) set-up. The cryotome chamber was cooled below −30°C using dry ice (A). In addition, this cooled stage was used to immediately re-freeze the section after thaw mounting on the slide (B). In (C) an indium tin oxide slide with sections of the infrapatellar fat pad (IPFP), sectioned at 15 µm with a temperature of −20°C (1 and 2) and −30°C (3 and 4) with (2 and 4) or without (1 and 3) the use of an anti-roll system.

the use of a time-of-flight (TOF)/TOF analyzer lacks sufficient mass resolution for proper lipid identifications.

Therefore, we performed additional MALDI-MSI MS/MS analysis on an Orbitrap-Elite hybrid ion trap MS instrument (Thermo Fisher Scientific GmbH, Bremen, Germany) running in data-dependent acquisition (DDA) mode[260] in negative ion polarity (*m/z* 200–2000) on a consecutive slide with a step size of 50 × 100 µm to gather MS^2 data for identification. In the Orbitrap, MS^1 data of *m/z* 200–2000 were acquired at a nominal mass resolution of 240 k (at *m/z* 400) and an injection time of 250 ms. MS^2 data were acquired using an ion trap with an isolation width of 0.7 *m/z* and a collision-induced dissociation of 38.0 (manufacturer units) with an activation q value of 0.25.

Histology

Matrix was removed from the same slide used for MALDI-MSI following ethanol series incorporated in the staining protocol. These tissue sections were then stained with Mayer's Hematoxylin (Dako, Agilent Technologies, Glostrup, Denmark) and Eosin (Merck KGaA, Darmstadt, Germany) (H&E) using standard protocols to reveal the anatomical features. Microscopic images were taken with an M8 microscopic scanner (Precipoint, Freising, Germany) with a 20x objective. MS results are usually co-registered to H&E images of the same (or consecutive) tissue section to confirm the (tissue-specific) molecular distributions. Standardized protocols for H&E staining are sufficient when including matrix removal in ethanol series (>70%).

Data analysis

H&E images were co-registered to the MALDI-MSI data in FlexImaging v5.0 (Bruker Daltonics). SCiLS lab MVS, version 2022a (SCiLS GmbH, Bremen, Germany) was used for principal component analysis (PCA) on the MS^1 data. Lipid spectra of the MS^1 results after PCA were acquired using in-house ChemomeTricks for MATLAB (The MathWorks, Natick, MA, USA). Recalibration of the DDA data was performed using RecalOffline software (Thermo Fisher Scientific GmbH), using Norharmane (*m/z* 333.11457 $[2M - 3H]^-$) and *m/z* 885.54985 (PI 38:4 $[M - H]^-$. Lipid assignments were performed with Lipostar MSI version 1.1.0b26 (LIPID MAPS database, 3- and 4-star rating, Molecular Horizon, Bettona, PG, Italy)[261] and Thermo Scientific FreeStyle 1.8 SP1 software version 1.8.51.0 (Thermo Fisher Scientific GmbH) in combination with the web application ALEX123 lipid calculator[262].

Results and discussion

Visualization of lipids

Multivariate analysis of the MALDI-MSI data revealed different tissue types within the IPFP. Comparing this finding with the H&E staining, it could be seen that some principal components (PCs) represented specific tissue types such as connective tissue (red, PC 9), synovium (blue, PC 2), and adipose tissue (green, PC 10) (**Figure 4.2**). For example, we were able to visualize a specific lipid for adipose tissue in the IPFP without delocalization: *m/z* 698.57 (RapifleX). This lipid could be identified as ether-linked phosphatidylethanolamine (PE O-) PE O-34:3 [M − H]- (**Figure 4.2**). Additional ion images and lipid assignments can be found in the supplementary information, **Supplementary Figure 4.1** and **Supplementary Table 4.1**. Repeated experiments showed similar results.

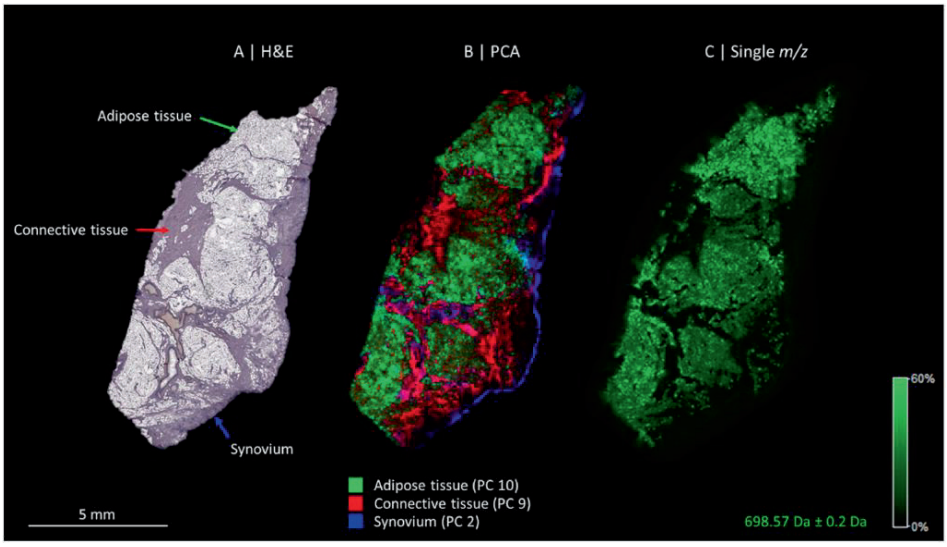

Figure 4.2. Results overview. Hematoxylin and Eosin (H&E) image (A) of a tissue section of the infrapatellar fat pad (IPFP). Principal component analysis (PCA, B), based on the spectra gathered during matrix-assisted laser desorption/ionization mass spectrometry imaging (MALDI-MSI) showed different lipid distributions of connective tissue (red, PC 9), synovium (blue, PC 2) and adipose tissue (green, PC 10) within the IPFP. In image (C) an adipose tissue-specific lipid (*m/z* 698.5, RapifleX) represented. *m/z* 698.5 could be identified as glycerophospholipid PE O-34:3 $[M - H]^-$ (*m/z* 698.5131 (Orbitrap)). H&E = hematoxylin and eosin, *m/z* = mass-to-charge ratio, PCA = principal component analysis, PC = principal component, PE = phosphatidylethanolamine. (For interpretation of the references to color in this figure legend, the reader is referred to the Web version of this article).

IPFP's intra-tissue heterogeneity

At the cellular level, adipose tissue consists of adipocytes, progenitor cells, immune cells, and fibroblasts, as well as connective tissue matrix and vasculature[263]. All these compositional factors can influence the tissue structure and ability to process it. For example, the more adipocytes with fat droplets, the higher the chances of delocalization of molecules from the tissue. IPFP or fat can contain pro-inflammatory cells (early osteoarthritis development[264], obesity[248], etc.) and undergo fibrosis as a reaction to injury or disease[265], which might change its appearance, structure, and lipid signature. Other protocols, such as (copper/conductive) tape transfer[251] or specific glass slide coatings[252] are suggested for adipose tissue containing a high adipocyte/low fibroblast ratio such as abdominal fat. However, using our protocol, while decreasing the chamber temperature in the cryotome and keeping the material as cold as possible using dry ice, we do not need these steps to acquire tissue sections and prevent molecules from delocalizing.

Conclusions

This paper presents for the first time a method for MALDI-MSI lipid analysis on IPFP. Important considerations for the experimental design include washing and freezing in the operating theater, as well as IPFP's adipose-like structure and additional problems regarding cryosectioning, matrix application, and MS. We have observed that the IPFP consists of different tissue types with distinctive lipid profiles and that its composition has an influence on the ability to obtain good quality sections and subsequently data. The protocol describes a method for tissue sectioning without the use of additional tape or coating for MALDI-MSI. Most importantly, cryosectioning below −30°C, fast thaw-mounting and refreezing, and keeping the sample in a desiccator box when possible, helps to acquire MALDI-MSI data of lipids without delocalization.

Supplementary information

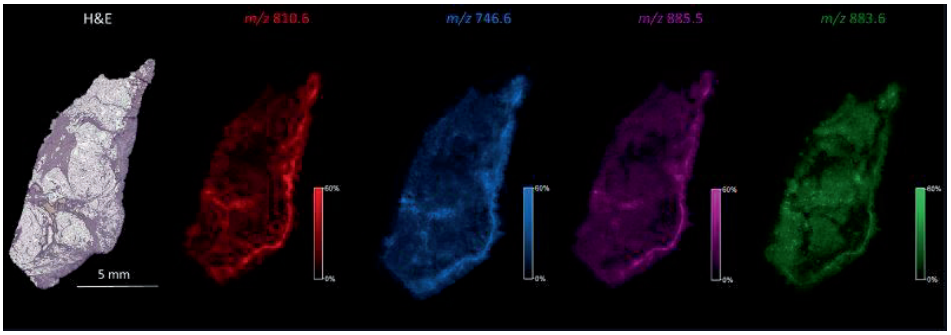

Supplementary Figure 4.1. Representation of multiple ion-images displaying multiple lipid-associated *m/z* within one single tissue section of the infrapatellar fat pad, measured in negative ion mode.

Supplementary Table 4.1. Lipid assignments.

MALDI-TOF MS^1 (*m/z*)	Orbitrap MS^1 (*m/z*)	Δppm	ms/ms fragments		ID	Adduct
698.6	698.5130	0.0	253.2	FA 16:1(+O)	PE O-34:3	$[M-H]^-$
			279.2	FA 18:2(+O)		
			418.2	-FA 18:2(+HO)		
			436.3	-FA 18:2(-H)		
746.6	746.5130	0.0	255.2	FA 20:6(-CO)	PE O-38:7	$[M-H]^-$
			259.2	FA 20:4(-CO)		
			283.2	FA 22:6(-CO)		
			303.2	FA 20:4(+O)		
			327.2	FA 22:6(+O)		
			418.3	-FA 22:6(+HO)		
			436.3	-FA 22:6(-H)		
			442.3	-FA 20:4(+HO)		
			460.3	-FA 20:4(-H)		

FA = Fatty acid, MALDI-TOF MS = Matrix-assisted laser desorption/ionization – time of flight mass spectrometry, *m/z* = mass-to-charge ratio, PE = phosphatidylethanolamine, PI = phosphatidylinositol, ppm = parts per million, PS = phosphatidylserine.

Supplementary Table 4.1 (continued). Lipid assignments.

MALDI-TOF MS^1 (*m/z*)	Orbitrap MS^1 (*m/z*)	Δppm	ms/ms	fragments	ID	Adduct
810.6	810.5279	1.4	283.2	FA 18:0(+O)	PS 38:4	$[M-H]^-$
			303.2	FA 20:4(+O)		
			419.2	-FA 20:4(+HO) -PS(87)		
			437.3	-FA 20:4(-H) -PS(87)		
			439.2	-FA 18:0(+HO) -PS(87)		
			457.2	-FA 18:0(-H) -PS(87)		
			723.5	-PS(87)		
883.6	883.5341	0.1	259.2	FA 20:4(-CO)	PI 38:5	$[M-H]^-$
			281.2	FA 18:1(+O)		
			303.2	FA 20:4(+O)		
			417.2	FA 18:1 ($+C_3H_5O_5P$)		
			435.2	FA 18:1 ($+C_3H_7O_6P$)		
			439.2	FA 20:4 ($+C_3H_5O_5P$)		
			457.2	FA 20:4 ($+C_3H_7O_6P$)		
			579.3	-FA 20:4(+HO)		
			597.3	-FA 20:4(-H)		
			601.3	-FA 18:1(+HO)		
			619.3	-FA 18:1(-H)		
885.5	885.5497	0.2	259.2	FA 20:4(-CO)	PI 38:4	$[M-H]^-$
			283.2	FA 18:0(+O)		
			303.2	FA 20:4(+O)		
			419.3	FA 18:0 ($+C_3H_5O_5P$)		
			437.3	FA 18:0 ($+C_3H_7O_6P$)		
			439.2	FA 20:4 ($+C_3H_5O_5P$)		
			581.3	-FA 20:4(+HO)		
			599.3	-FA 20:4(-H)		
			601.3	-FA 18:0(+HO)		
			619.3	-FA 18:0(-H)		

FA = Fatty acid, MALDI-TOF MS = Matrix-assisted laser desorption/ionization – time of flight mass spectrometry, *m/z* = mass-to-charge ratio, PE = phosphatidylethanolamine, PI = phosphatidylinositol, ppm = parts per million, PS = phosphatidylserine.

Chapter 5

Matrix-assisted laser desorption/ionization mass spectrometry imaging (MALDI-MSI) reveals lipid markers in infrapatellar fat pad biopsies of osteoarthritis and cartilage defect patients

Mirella J.J. Haartmans, Britt S.R. Claes, Gert B. Eijkel, Kaj S. Emanuel, Gabrielle J.M. Tuijthof, Ron M.A. Heeren, Pieter J. Emans, Berta Cillero-Pastor

Analytical and Bioanalytical Chemistry, 2023

Abstract

The incidence of osteoarthritis (OA) has been expected to increase due to an ageing population, as well as an increased incidence of intra-articular (osteo-) chondral damage. Lipids have already been shown to be involved in the inflammatory process of OA. This study aims at revealing region-specific lipid profiles of the infrapatellar fat pad (IPFP) of OA or cartilage defect patients by matrix-assisted laser desorption/ionization mass spectrometry imaging (MALDI-MSI), which could be used as biomarkers for early OA detection. A higher presence of phospholipids was found in OA patients compared to cartilage defect patients. In addition, a higher abundance of ether-linked phosphatidylethanolamines (PE O-s) containing arachidonic acid was specifically found in OA patients compared to cartilage defect patients. These lipids were mainly found in the connective tissue of the IPFP. Specific lipid species were associated to OA patients compared to cartilage defect patients. PE O-s have been suggested as possible biomarkers for OA. As these were found more abundantly in the connective tissue, the IPFP's intra-tissue heterogeneity might play an important role in biomarker discovery, implying that the amount of fibrous tissue is associated with OA.

Introduction

Knee osteoarthritis (OA) is one of the leading causes of disability in the elderly population due to its high prevalence [266]. While OA is affecting millions of patients already, its incidence is expected to increase over the next years due to our aging population [267, 268]. OA development early in life is often related to an increased incidence of diabetes mellitus type 2 and obesity [267, 268], but also to an increase in intra-articular or osteochondral damage caused by (sport) injuries or trauma [269, 270]. As a result, total knee replacement surgery is being conducted at a younger age, resulting in higher chances of prosthesis revision [56] and immobility later in life. Considering this, the urge for joint-preserving or preventive therapy has never been stronger.

Cartilage has a limited ability to regenerate due to a lack of vasculature and a low abundance of cells [271]. When treated insufficiently, cartilage damage may lead to the development of OA [31]. This could be the result of changes in the cartilage matrix structure, leading to degradation of matrix or collagen type II [272, 273]. Additionally, accompanying inflammation, the release of pro-inflammatory cytokines [272, 274] accelerate cartilage degradation, resulting in OA development.

Currently used (surgical) treatments after a cartilage defect, to prevent OA from developing, focus on regeneration (minced cartilage, autologous chondrocyte transplantation, or hedgehog) or resurfacing (autograft or allograft transplantation and metal implant) [275-278]. Less common, but not less important, are treatments like osteotomy, joint distraction, or pharmaceuticals to prevent further OA development [279-281]. The major hurdle for successful treatment is the early detection of cartilage damage and finding the right treatment for the right patient. Therefore, biomarker research is needed to fill this gap [81]. These biomarkers can be derived invasively from tissues or fluids inside the knee (proteins, peptides, metabolites, lipids, genes) but also non-invasively from follow-up imaging (magnetic resonance imaging (MRI) or radiographic imaging) or questionnaires [282]. A clear predictive biomarker, indicating if and which joint-preserving treatments might have an OA disease-modifying effect, could further facilitate the clinical decision-making of these joint-preserving treatments and improve patient outcomes.

OA has been acknowledged as a whole joint disease, affecting not only cartilage, but also other intra-articular tissues such as the meniscus, synovial membrane, or infrapatellar fat pad (IPFP) [16, 283, 284]. The IPFP, or Hoffa's fat pad, is a piece of fat tissue located underneath the patella (tendon) [16, 285] and is often removed (partially) to gain access to the knee capsule during surgery. It is already known to be involved in the inflammatory process of OA by secretion of pro-inflammatory factors such as

prostaglandins [16, 286] and might therefore be a potential source for biomarker discovery.

Since IPFP can be used as an accessible biopsy target, molecular markers found in the IPFP may have potential as diagnostic biomarkers in the use of joint-preserving treatments and the development of (early) OA. Histologically, the IPFP is a heterogeneous tissue, containing adipose-, fibrous- and synovial tissue, as well as blood vessels. Due to its heterogeneous composition, matrix-assisted laser desorption/ionization mass spectrometry imaging (MALDI-MSI), a technique to study the spatial distribution of molecules and possible detection of biomarkers, could reveal local tissue-specific molecular changes [91].

MALDI-MSI has already been used in the past in the field of biomedical research [239], enabling the visualization of the spatial distribution of molecules in sections of tissues, to identify possible diagnostic compounds or biomarkers [240-242]. The analysis of lipids is already a growing area in the MSI field [244-246]. OA in the knee has been associated with an increased inflammatory profile and increased secretion of pro-inflammatory factors by the IPFP [16, 250]. Lipids have been shown to play an important role in OA [287] in which lipid deposits are stored in chondrocytes of OA articular cartilage [179, 287] and elevated levels of fatty acids have been associated with histological severity of OA [287]. Additionally, it has been hypothesized that an altered lipid metabolism could lead to a variety of changes related to OA [288].

This study aims to identify the differences in lipid profiles of the IPFP between OA and cartilage defect patients; and to identify OA and cartilage defect-specific lipids which could be used as a biomarker for OA development. In addition, the influence of the two main tissue types in the IPFP (adipose tissue and connective tissue) on the lipid profile, and its effect on characterizing OA and cartilage defect patients was investigated.

Materials and Methods

Patient inclusion and tissue collection

Human IPFP was collected as surgical waste material from seven patients with moderate-late-stage OA undergoing total knee arthroplasty (TKA), and seven control patients undergoing cartilage repair surgery for an osteochondral defect in a femoral condyle. Patients were matched for age (median 50.4 (OA) and 43.9 (cartilage defect), ns), gender (4 (OA) vs 3 (cartilage defect), ns), and body mass index (BMI, median 27.3 (OA) and 27.1 (cartilage defect), ns) as accurately as possible regarding the availability of tissue. The Medical Ethics Committee (MEC) assigned non-WMO

(wet medisch-wetenschappelijk onderzoek, law for medical-scientific research in humans in the Netherlands) approval for the collection of waste material during TKA (ID: MEC 2017-0183, 2017) or cartilage repair surgery (ID: MEC 2018-0963, 2018). In addition, patients signed informed consent for the use of this waste material for experimental purposes. Patients were graded for radiographic OA severity using Kellgren-Lawrence (KL) score (3.3 (OA) vs 0.3 (cartilage defect), $p < 0.001$) by an orthopedic surgeon (PE).

Sample preparation and mass spectrometry imaging

The sample preparation workflow has been previously described in detail [91]. In summary, directly after dissection, every IPFP was washed in phosphate-buffered saline (PBS), snap-frozen in liquid nitrogen, and stored at -80°C until further processing. Frozen IPFPs were sectioned at 15 µm thickness with a cryostat (Leica Microsystems Cryotome, Wetzlar, Germany) in the presence of dry ice (cryotome temperature below -30°C) and mounted onto indium tin oxide (ITO) coated glass slides (Delta Technologies, CO, USA). All tissue sections were sublimed (HTX Sublimator, HTX Imaging, Chapel Hill, NC, USA) with 55 ± 2 mg Norharmane matrix (Sigma-Aldrich, Zwijndrecht, the Netherlands) to extract lipids (preheating at 60°C, pressure at < 0.04 mBar, sublimation at 140˚C for 200 seconds). Lipid analysis was performed by MALDI-MSI in positive and negative ion modes on consecutive sections at a lateral resolution of 50 µm on a RapifleX Tissue Typer (Bruker Daltonics, Bremen, Germany), running in reflectron mode. The instrument was calibrated using a standard mixture of red phosphorous (Sigma-Aldrich, Saint Louis, MO, USA). Lipids were detected over a mass range of *m/z* (mass-to-charge ratio) 100-2000 Da.

Lipid identifications

Identification of lipids was performed on an Orbitrap-Elite mass spectrometer (Thermo Fisher Scientific, Waltham, MA, USA) running in data-dependent acquisition (DDA, positive and negative) mode [91, 260], on consecutive sections at a spatial resolution of 100 µm and a laser repetition rate of 1000 Hz. Here, mass spectrometry $(MS)^1$ data of *m/z* 200-2000 were acquired at a nominal mass resolution of 240,000 (FWHM *m/z* 400) with an injection time of 250 ms. In parallel, MS^2 data were acquired in the ion trap with collision-induced dissociation (CID) using an isolation window of 0.7 Da. A normalized collision energy (NCE) of 30 (manufacturer units) and an activation Q of 0.17 were used in positive mode, and 38 and 0.25 in negative mode, respectively. A selected number of lipids with inclusive spectra were manually fragmented in the higher-energy collisional dissociation (HCD) cell using an injection

time of 2000 ms and an NCE between 25 and 30 for 30 scans, while continuously moving the stage.

Histology

To correlate the tissue structure to the MSI data, the same tissue sections were stained with Mayer's Hematoxylin (Dako, Agilent Technologies, Glostrup, Denmark) and Eosin (Merck KGaA, Darmstadt, Germany) (H&E) after MALDI-MSI using a standard protocol to correlate the IPFP's tissue structure to the MSI data. In brief, the matrix was removed from the slide by incubating the slide in 70% ethanol for 5 minutes. Subsequently, slides immersed in distilled water for 3 minutes. Then, the tissue sections were stained with Mayer's Hematoxylin (Dako, Agilent Technologies, Glostrup, Denmark) for 3 minutes before being rinsed under running tap water for 3 minutes. After rinsing the slide in distilled water for 30 seconds, tissue sections were stained with Eosin (Merck KGaA, Darmstadt, Germany) for another 30 seconds. To remove an excess of Eosin, the slides were dipped 10 times in 70% ethanol. Subsequently, the slides were dehydrated in 100% for 5 min twice. Then the slides equilibrated in xylene for 5 minutes twice. The sections were mounted with Histomount (Sigma-Aldrich) and covered with a glass coverslip. Microscopic images were taken with an Aperio CS2 with a 20x objective (Leica Biosystems, Wetzlar, Germany).

Data analysis

Using a Kolmogorov-Smirnov normality test with Dallal-Wilkinson-Lillie for p-value ($p < 0.05$) normal distribution was tested. Differences between groups regarding age, gender, BMI, left or right knee, and KL score were determined using an unpaired nonparametric Mann-Whitney test in GraphPad Prism version 8.1.2 (GraphPad Software, San Diego, CA, US) to compare ranks ($p < 0.05$).

All files were exported from FlexImaging 5.0 (MS^1, Bruker Daltonics, Bremen, Germany) as imzML and loaded in SCiLS lab 2019b (SCiLS lab, GmbH, Bremen, Germany) software. From here, data were exported to MATLAB 2016b (The MathWorks, Natick, MA, USA). A region of interest (ROI), including the tissue types of interest (adipose tissue or connective tissue), based on histological examination, was selected for each tissue section using in-house ChemomeTricks data analysis tool for MATLAB.

Additionally, tissue sections were assigned to either OA or cartilage defect groups- for spectrum-based principal component analysis (PCA), followed by linear discriminant analysis (LDA) to analyze the differences between patient groups and

tissue types (**Figure 5.1**). Score projections were performed in the same program. A region of interest, based on the H&E images of both adipose tissue and connective tissue, was selected for further analysis. Lipid species were manually assigned using MS^1 and MS^2 spectra acquired from DDA measurements using Freestyle software (Thermo Fischer Scientific), Lipostar MSI version 1.1.0b26 (MS^2, Molecular Discovery, Borehamwood, UK) using the LIPID MAPS database (3- and 4-star rating, Molecular Horizon, Bettona, PG, Italy) [261], and the ALEX123 web application [262]. The top 20 lipids showing the highest loading for each group (OA, cartilage defect, adipose tissue, or connective tissue) in negative and positive ion mode after PCA and LDA were selected for identification.

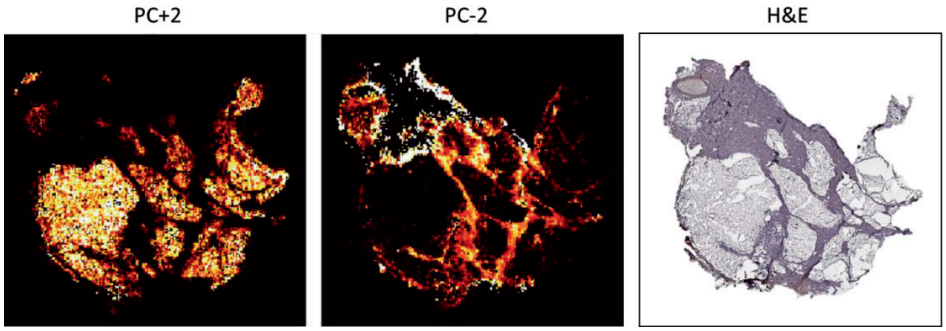

Figure 5.1. An example in which adipose tissue (PC+2) and connective tissue (PC-2) could be separated using principal component analysis (PCA) and linear discriminant analysis (LDA), showing the distribution of lipids based on Hematoxylin and Eosin (H&E) staining in negative ion mode.

Results

Patient characteristics

In this study, lipid profiles in the IPFP of patients with late-stage OA were compared to patients undergoing cartilage repair surgery for a cartilage defect. Patient characteristics, including age, BMI, gender, and KL score were depicted in **Table 5.1**. In addition, found lipid species were identified and IPFP intra-tissue heterogeneity was evaluated. An example of IPFP intra-tissue heterogeneity is visualized in **Figure 5.2**.

The data regarding patient characteristics did not show a normal distribution. Gender, age, and BMI were not statistically different between groups ($p > 0.05$). The KL score was significantly decreased in the cartilage defect group compared to the OA group ($p < 0.001$).

Table 5.1. Characteristics of osteoarthritis (n = 7) and cartilage defect (n = 7) patients undergoing total knee arthroplasty or cartilage repair surgery.

Patient	OA/CD	Gender	Age	BMI	KL grade	Female (n)	Age (med.)	BMI (med.)	KL (med.)
1	OA	Male	56	26.9	3	4	50.4	27.3	3.3
2	OA	Male	42	29.6	3				
3	OA	Female	60	25.7	4				
4	OA	Female	54	28.3	4				
5	OA	Male	52	23.2	4				
6	OA	Female	58	26.0	3				
7	OA	Female	40	31.5	2				
8	CD	Male	47	23.7	1	3 (ns)	43.9 (ns)	27.1 (ns)	0.3 ***
9	CD	Male	38	34.3	0				
10	CD	Female	49	24.3	0				
11	CD	Male	48	26.6	0				
12	CD	Male	33	31.0	0				
13	CD	Female	56	27.2	0				
14	CD	Female	36	22.5	1				

OA = osteoarthritis, CD = cartilage defect, BMI = body mass index, KL = Kellgren-Lawrence, ns = not significant, med. = median, *** = $p < 0.001$.

MALDI-MSI approach on the IPFP

As described before [91], the main challenge of the use of MALDI-MSI on the IPFP is the IPFP's adipose-like structure. Sample handling and sample preparation are of importance while applying MALDI-MSI on the IPFP to prevent delocalization of molecules. The most important aspects of the working method included cryosectioning at 15 µm below a temperature of -30°C, the use of an anti-roll system, quick thaw-mounting and refreezing, and matrix application by sublimation. Furthermore, it has been shown of importance that the slides were transported inside a silica carrier box and dried thoroughly in a desiccator before matrix application.

Patient profiling based on IPFP lipid composition in negative ion mode

Data analysis, after PCA and LDA, showed a separation between the group of patients with OA (n = 7) and the group of patients with a cartilage defect (n = 7) in negative ion mode. Discriminant function 1 (DF1) was differentially distributed in OA and cartilage defect patients according to the IPFP's lipid profile, independent from

tissue type (adipose tissue or connective tissue) (**Figure 5.3A**). Likewise, in DF2, adipose tissue separated from connective tissue, independent from disease pathology (OA or cartilage defect) (**Figure 5.3B**). The differences in DF1 can be appreciated in the score projections as well (**Figure 5.4**), independent from tissue type (yellow-to-red representing cartilage defect patients and light-to-dark blue representing OA patients), as well as a clear separation between adipose tissue (yellow-to-red) and connective tissue (light-to-dark blue) in DF2 (**Figure 5.5**).

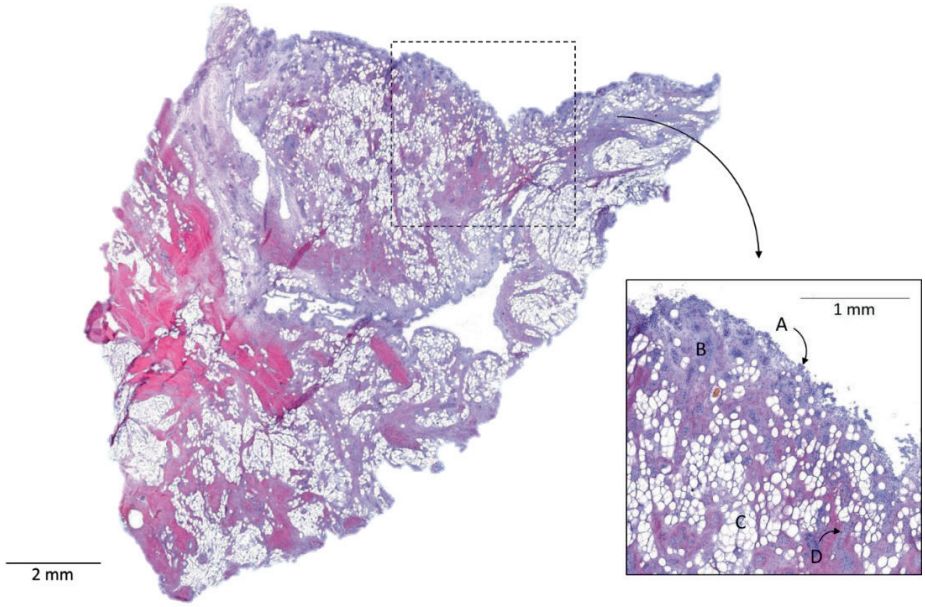

Figure 5.2. Example of a Hematoxylin and Eosin stained microscopic image of the infrapatellar fat pad. The synovial membrane (A), connective tissue (B), adipose tissue (C) and blood vessels (D) could be identified from tissue sections.

In general, a higher abundance of lipids was present in the OA patient IPFP samples compared to cartilage defect patient IPFP samples, independently from tissue type, measured by MALDI-MSI in negative ion mode (**Table 5.2**). In the OA patient group specifically, ether-linked phosphatidylethanolamines (PE O-38:6, PE O-38:7, PE O-36:5, and PE O-40:7) and phosphatidylethanolamines (PE 38:4 and PE 36:1) could be identified with the highest loadings (**Table 5.2**), driving the LDA as has been shown in **Figure 5.3**. No lipids specific for cartilage defect patients could be identified after PCA and LDA within the 20 lipids with the highest loading.

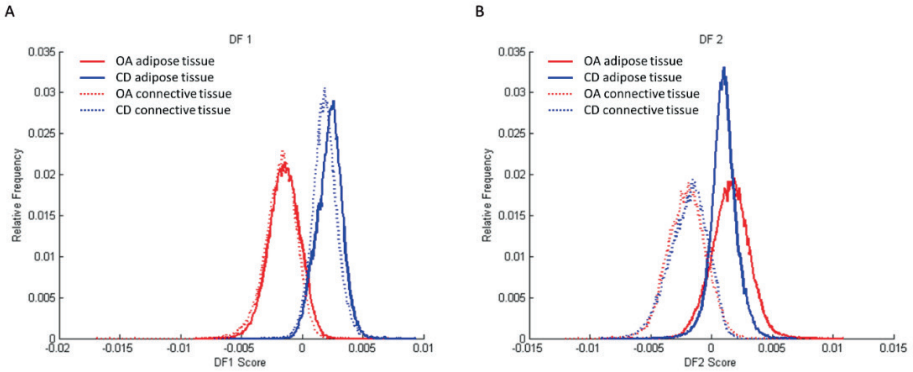

Figure 5.3. Discriminant function 1 (DF1) discriminates between osteoarthritis (OA) and cartilage defect (CD) patients, independently from tissue type (adipose tissue or connective tissue) after principal component analysis (PCA) and discriminant analysis (DA) in negative ion mode (A, between/within (B/W) = 2.4). Additionally, DF2 showed discrimination between adipose tissue (AT) of OA and CD patients and connective tissue (CT), independently from patients' disease pathology (B, B/W = 1.3).

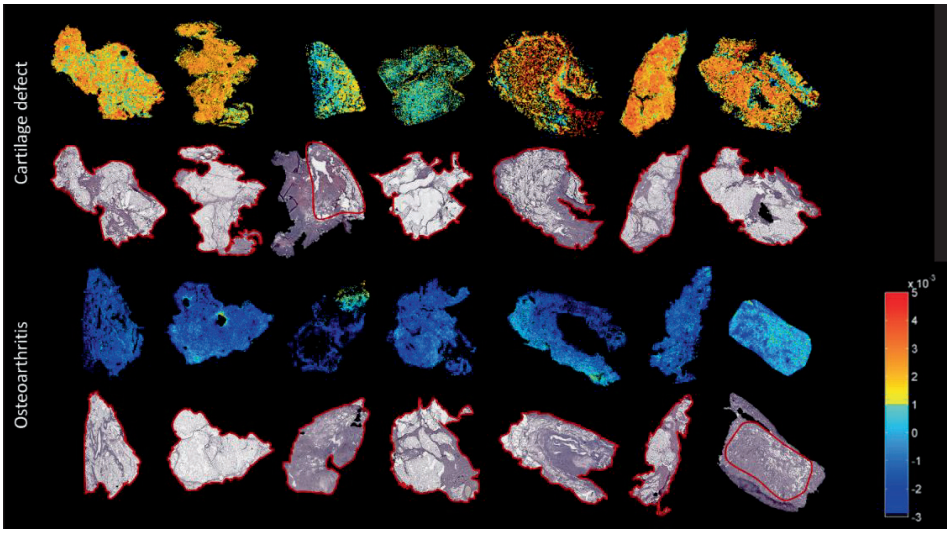

Figure 5.4. Score projection figures (discriminant function 1 (DF1)) of osteoarthritis (OA) and cartilage defect (CD) patients in negative ion mode. A separation in CD (yellow-to-red) and OA (blue) patient groups was visualized (A). The red line displays the ROI used for analysis.

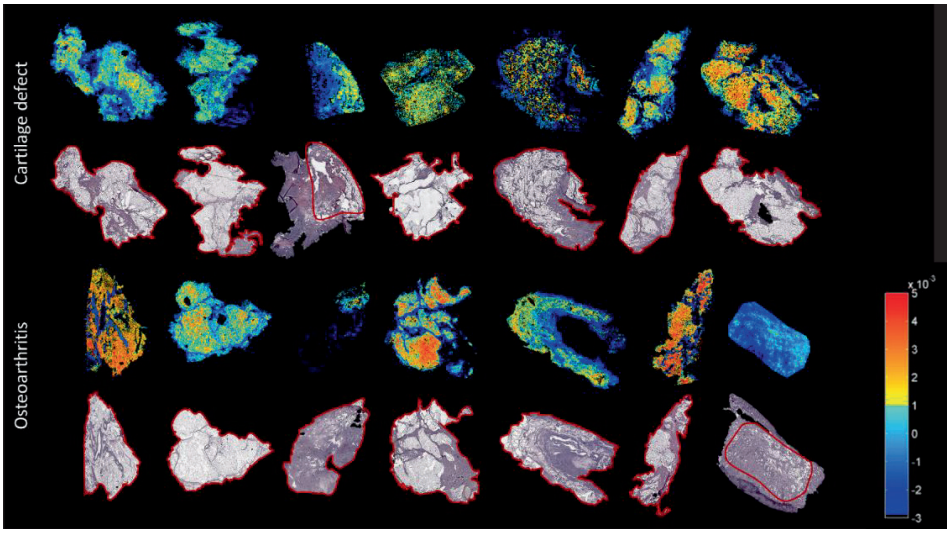

Figure 5.5. Score projection figures (discriminant function 2 (DF2)) of osteoarthritis (OA) and cartilage defect (CD) patients in negative ion mode. A separation in connective tissue (blue) and adipose tissue (yellow-to-red) was visualized (A). The red line displays the ROI used for analysis.

Tissue specific lipid profiles in negative ion mode

When comparing adipose tissue with connective tissue, PEs, PE O-s, and phosphatidylserines (PSs) were highly abundant in both tissue types. Phosphatidic acid (PA) 36:2 and phosphatidylinositol (PI) 38:3 specifically, were more abundant in adipose tissue in negative ion mode (**Table 5.3** and **5.4**). More specifically, for adipose tissue, PE O-34:3, PE O-36:3, PE O-36:2, PE O-36:4, PE O-34:2, PE 34:4, PI 38:3, PA 36:2, PS 36:2, and PS 38:5 could be identified (**Table 5.3**). For connective tissue, PE O- 40:6, PE O-40:7, PE O-40:5, PE O-38:7, PE O-38:5, PE O-40:8, PE 38:4, PE 40:4, PS 36:1, PS 40:5 were identified (**Table 5.4**).

Table 5.2 Lipid assignments for osteoarthritis patients (DF1) based on MS^2 data in negative ion mode. The *m/z* values were collected on an Orbitrap Elite running in data-dependent acquisition mode.

Type	Ion mode	Rapiflex MS^1 (*m/z*)	Loading	Orbitrap MS^1 (*m/z*)	Δ ppm	Lipid ID	Adduct
OA	Negative	748.6	-0.351	748.5286	0.1	PE O-38:6 PE O-18:2_20:4 PE O-16:1_22:5	$[M-H]^-$
OA	Negative	766.6	-0.351	766.5391	0.1	PE 38:4 PE 18:0_20:4	$[M-H]^-$
OA	Negative	746.6	-0.343	746.5130	0.0	PE O-38:7 PE O-16:1_22:6 PE O-18:3_20:4	$[M-H]^-$
OA	Negative	722.6	-0.328	722.5130	0.0	PE O-36:5 PE O-16:1_20:4	$[M-H]^-$
OA	Negative	744.6	-0.314	744.5548	0.1	PE 36:1 PE 18:0_18:1 PE 16:0:20:1	$[M-H]^-$
OA	Negative	774.6	-0.291	774.5442	0.1	PE O-40:7 PE O-18:1_22:6 PE O-22:6_18:1 PE O-18:2_22:5 PE O-20:3_20:4	$[M-H]^-$

MS = mass spectrometry, *m/z* = mass to charge ratio, OA = osteoarthritis, PE = phosphatidylethanolamine, PE O- = ether-linked phosphatidylethanolamine, ppm = parts per million.

Table 5.3. Lipid assignments for adipose tissue in osteoarthritis and cartilage defect patients (DF2) based on MS^2 data in negative ion mode. The *m/z* values were collected on an Orbitrap Elite running in data-dependent acquisition mode.

Type	Ion mode	Rapiflex MS^1 (*m/z*)	Loading	Orbitrap MS^1 (*m/z*)	Δ ppm	Lipid ID	Adduct
AT	Negative	698.6	0.662	698.5130	0.0	PE O-34:3 PE O-16:1_18:2 PE O-18:2_16:1	$[M-H]^-$
AT	Negative	726.6	0.648	726.5443	0.0	PE O-36:3 PE O-18:1_18:2 PE O-18:2_18:1	$[M-H]^-$
AT	Negative	699.6	0.636	699.4971	0.1	PA 36:2 PA 18:0_18:2 PA 18:1_18:1	$[M-H]^-$
AT	Negative	786.6	0.568	786.5290	0.1	PS 36:2 PS 18:0_18:2 PS 18:1_18:1	$[M-H]^-$
AT	Negative	728.6	0.553	728.5599	0.1	PE O-36:2 PE O-18:1_18:1 PE O-18:0_18:2	$[M-H]^-$
AT	Negative	724.6	0.547	724.5286	0.1	PE O-36:4 PE O-18:2_18:2 PE O-16:1_20:3	$[M-H]^-$
AT	Negative	808.6	0.459	808.5112	2.7	PS 38:5 PS 18:0_20:5 PS 18:1_20:4 PS 16:1_22:4 PS 18:2_20:3	$[M-H]^-$

AT = adipose tissue, MS = mass spectrometry, *m/z* = mass to charge ratio, PA = phosphatidic acid, PE = phosphatidylethanolamine, PE O- = ether-linked phosphatidylethanolamine, PI = phosphatidylinositol, ppm = parts per million, PS = phosphatidylserine.

Table 5.3 (continued). Lipid assignments for adipose tissue in osteoarthritis and cartilage defect patients (DF2) based on MS^2 data in negative ion mode. The *m/z* values were collected on an Orbitrap Elite running in data-dependent acquisition mode.

Type	Ion mode	Rapiflex MS^1 (*m/z*)	Loading	Orbitrap MS^1 (*m/z*)	Δ ppm	Lipid ID	Adduct
AT	Negative	700.6	0.443	700.5287	0.1	PE O-34:2 PE O-16:1_18:1 PE O-16:0_18:2 PE O-18:1_16:1 PE O-18:2_16:0	$[M-H]^-$
AT	Negative	883.6	0.428	883.5341	0.1	PI 38:3 PI 38:1_20:4	$[M-H]^-$
AT	Negative	714.6	0.399	714.5080	0.1	PE 34:2 PE 16:0_18:2 PE 16:1_18:1	$[M-H]^-$

AT = adipose tissue, MS = mass spectrometry, *m/z* = mass to charge ratio, PA = phosphatidic acid, PE = phosphatidylethanolamine, PE O- = ether-linked phosphatidylethanolamine, PI = phosphatidylinositol, ppm = parts per million, PS = phosphatidylserine.

Table 5.4. Lipid assignments for connective tissue in osteoarthritis and cartilage defect patients (DF2) based on MS^2 data in negative ion mode. The *m/z* values were collected on an Orbitrap Elite running in data-dependent acquisition mode.

Type	Ion mode	Rapiflex MS^1 (*m/z*)	Loading	Orbitrap MS^1 (*m/z*)	Δ ppm	Lipid ID	Adduct
CT	Negative	810.6	0.459	810.5279	1.4	PS 38:4 PS 18:0_20:4 PS 18:1_20:3	$[M-H]^-$
CT	Negative	776.6	0.439	776.5598	0.2	PE O-40:6 PE O-20:2_20:4 PE O-18:2_22:4 PE O-18:1_22:5	$[M-H]^-$
CT	Negative	774.6	0.427	774.5442	0.1	PE O-40:7 PE O-18:1_22:6 PE O-22:6_18:1 PE O-18:2_22:5 PE O-20:3_20:4	$[M-H]^-$
CT	Negative	778.6	0.426	778.5754	0.2	PE O-40:5 PE O-20:2_20:4 PE O-18:2_22:4 PE O-18:1_22:5	$[M-H]^-$
CT	Negative	766.6	0.403	766.5391	0.1	PE 38:4 PE 18:0_20:4	$[M-H]^-$
CT	Negative	746.6	0.399	746.5130	0.0	PE O-38:7 PE O-16:1_22:6 PE O-18:3_20:4	$[M-H]^-$

CT = connective tissue, MS = mass spectrometry, MMPE = monomethyl-phosphatidylethanolamine, *m/z* = mass to charge ratio, PE = phosphatidylethanolamine, PE O- = ether-linked phosphatidylethanolamine, PG = phosphatidylglycerol, ppm = parts per million, PS = phosphatidylserine.

Table 5.4 (continued). Lipid assignments for connective tissue in osteoarthritis and cartilage defect patients (DF2) based on MS^2 data in negative ion mode. The *m/z* values were collected on an Orbitrap Elite running in data-dependent acquisition mode.

Type	Ion mode	Rapiflex MS^1 (*m/z*)	Loading	Orbitrap MS^1 (*m/z*)	Δ ppm	Lipid ID	Adduct
CT	Negative	750.6	0.386	750.5442	0.1	PE O-38:5 PE O-18:1_20:4 PE O-16:1_22:4	$[M-H]^-$
CT	Negative	794.6	0.385	794.5703	0.2	PE 40:4 PE 20:0_20:4 PE 18:0_22:4	$[M-H]^-$
CT	Negative	788.6	0.383	788.5446	0.1	PS 36:1 PS 18:0_18:1	$[M-H]^-$
CT	Negative	836.6	0.347	836.5445	0.3	PS 40:5 PS 18:0_22:5	$[M-H]^-$
CT	Negative	772.6	0.342	772.5286	0.2	PE O-40:8 PE O-18:2_22:6	$[M-H]^-$

CT = connective tissue, MS = mass spectrometry, MMPE = monomethyl-phosphatidylethanolamine, *m/z* = mass to charge ratio, PE = phosphatidylethanolamine, PE O- = ether-linked phosphatidylethanolamine, PG = phosphatidylglycerol, ppm = parts per million, PS = phosphatidylserine.

Patient profiling based on IPFP lipid composition in positive ion mode

In positive ion mode, one IPFP section of the OA group and one IPFP section of the cartilage defect group were excluded from analysis because a comparison between adipose tissue and connective tissue was not possible due to the lack of or absence of either one of the tissues. Data analysis, after PCA and LDA, showed a separation between the group of patients with OA (n = 6) and the group of cartilage defect patients (n = 6) in positive ion mode. DF1 was differentially distributed between OA and cartilage defect patients according to the IPFP's lipid profile, independent from tissue type (adipose tissue or connective tissue) (**Figure 5.6A**). Likewise, in DF2, adipose tissue separated from connective tissue, independent from disease pathology (OA or cartilage defect) (**Figure 5.6B**). In addition, score projections show the same distribution of OA vs cartilage defect (**Figure 5.7**), independent from tissue type, as well as a clear separation between adipose tissue and connective tissue (**Figure 5.8**).

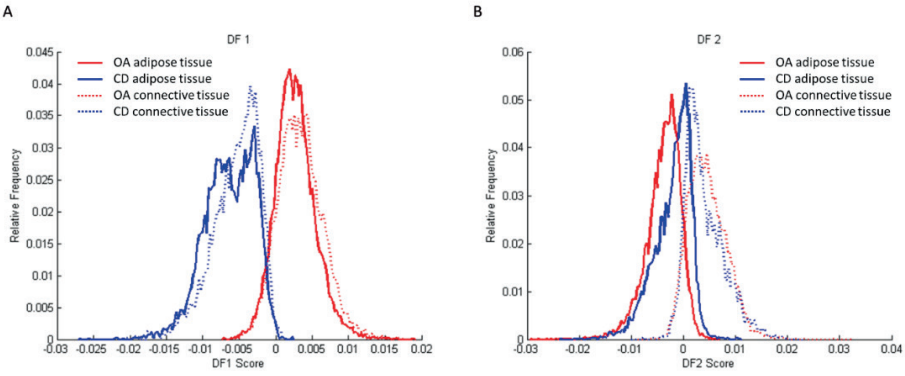

Figure 5.6. Discriminant function 1 (DF1) discriminates osteoarthritis (OA) and cartilage defect (CD) patients, independently from tissue type (adipose tissue or connective tissue) after principal component analysis (PCA) and discriminant analysis (DA) in positive ion mode (A, B/W = 2.0). Additionally, DF2 showed discrimination between adipose tissue (AT) of OA and CD patients and connective tissue (CT), independently from patients' disease pathology (B, B/W = 1.2).

Tissue specific lipid profiles in positive ion mode

Whereas sphingomyelin (SM) SM 40:2;O2 and PC 36:3 were identified in the OA group in positive ion mode, only PC 36:3 could be identified for cartilage defect in the highest 20 loadings (**Table 5.5** and **5.6**). PC 36:3 was thus non-specific as it was found in both OA and cartilage defect patient groups.

Table 5.5. Lipid assignments for osteoarthritis patients (DF1) based on MS^2 data in positive ion mode. The *m/z* values were collected on an Orbitrap Elite running in data dependent acquisition mode.

Type	Ion mode	Rapiflex MS^1 (*m/z*)	Loading	Orbitrap MS^1 (*m/z*)	Δ ppm	Lipid ID	Adduct
OA	Positive	785.7	0.169	785.6529	0.2	SM 40:2;O2	$[M+H]^+$
OA	Positive	806.7	0.178	806.5670	0.0	PC 36:3	$[M+Na]^+$
OA	Positive	784.7	0.163	784.5847	0.5	PC 36:3	$[M+H]^+$

OA = osteoarthritis, MS = mass spectrometry, *m/z* = mass to charge ratio, PC = phosphatidylcholine, ppm = parts per million, SM = sphingomyelin

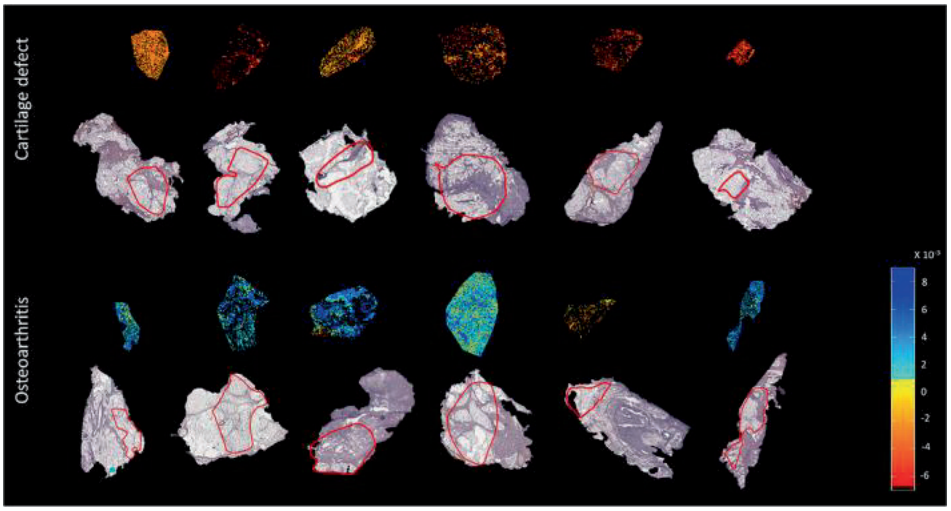

Figure 5.7. Score projection figures (discriminant function 1 (DF1)) of the tissue-specific separation in positive ion mode. A separation in cartilage defect (CD, yellow-to-red) and osteoarthritis (OA, blue) patient groups was observed.

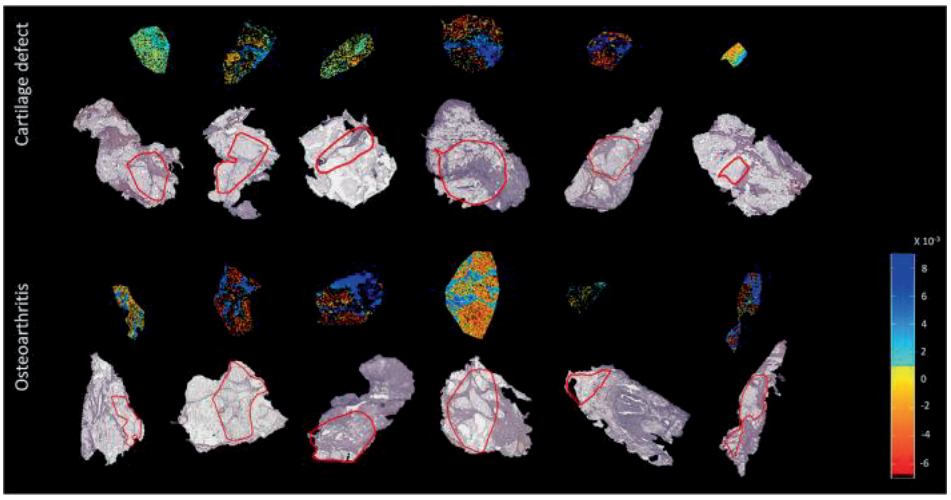

Figure 5.8. Score projection figures (discriminant function 2 (DF2)) of the tissue-specific separation in positive ion mode. A separation in connective tissue (blue) and adipose tissue (yellow-to-red) was observed.

In positive ion mode, (ether-linked) PCs (PC O-34:2, PC O-34:3, PC O-34:3, PC O-32:2, PC O- 36:3, PC 32:2, and PC 34:2) were highly abundant in the adipose tissue (**Table 5.7**), whereas PCs (PC 38:4, PC 38:5, and PC 36:4), together with two SM (SM 42:2;O2 and SM 34:1;O2) were more abundant in the connective tissue (**Table 5.8**).

Table 5.6. Lipid assignments for cartilage defect patients (DF1) based on MS^2 data in positive ion mode. The *m/z* values were collected on an Orbitrap Elite running in data dependent acquisition mode.

Type	Ion mode	Rapiflex MS^1 (*m/z*)	Loading	Orbitrap MS^1 (*m/z*)	Δ ppm	Lipid ID	Adduct
CD	Positive	806.5	-0.253	806.5670	0.0	PC 36:3	$[M+Na]^+$

CD = cartilage defect, MS = mass spectrometry, *m/z* = mass to charge ratio, PC = phosphatidylcholine, ppm = parts per million.

Table 5.7. Lipid assignments for adipose tissue in osteoarthritis and cartilage defect patients (DF2) based on MS^2 data in positive ion mode. The *m/z* values were collected on an Orbitrap Elite running in data dependent acquisition mode.

Type	Ion mode	Rapiflex MS^1 (*m/z*)	Loading	Orbitrap MS^1 (*m/z*)	Δ ppm	Lipid ID	Adduct
AT	Positive	744.5	0.566	744.5900	0.2	PC O-34:2	$[M+H]^+$
AT	Positive	742.7	0.472	742.5744	0.2	PC O-34:3	$[M+H]^+$
AT	Positive	764.7	0.419	764.5563	0.1	PC O-34:3	$[M+Na]^+$
AT	Positive	730.6	0.416	730.5380	0.2	PC 32:2	$[M+H]^+$
AT	Positive	758.5	0.393	758.5690	0.3	PC 34:2	$[M+H]^+$
AT	Positive	716.6	0.373	716.5588	0.1	PC O-32:2	$[M+H]^+$
AT	Positive	770.7	0.372	770.6055	0.4	PC O-36:3	$[M+H]^+$

AT = adipose tissue, MS = mass spectrometry, *m/z* = mass to charge ratio, PC = phosphatidylcholine, PC O- = ether-linked phosphatidylcholine, ppm = parts per million.

Table 5.8. Lipid assignments for connective tissue in osteoarthritis and cartilage defect patients (DF2) based on MS^2 data in positive ion mode. The *m/z* values were collected on an Orbitrap Elite running in data dependent acquisition mode.

Type	Ion mode	Rapiflex MS^1 (*m/z*)	Loading	Orbitrap MS^1 (*m/z*)	Δ ppm	Lipid ID	Adduct
CT	Positive	832.7	-0.317	832.5827	0.0	PC 38:4	$[M+Na]^+$
CT	Positive	830.7	-0.304	830.5670	0.0	PC 38:5	$[M+Na]^+$
CT	Positive	813.8	-0.292	813.6843	0.2	SM 42:2;O2	$[M+H]^+$
CT	Positive	725.7	-0.291	725.5567	0.1	SM 34:1;O2	$[M+Na]^+$
CT	Positive	804.7	-0.279	804.5513	0.1	PC 36:4	$[M+Na]^+$

CT = connective tissue, MS = mass spectrometry, *m/z* = mass to charge ratio, PA = phosphatidic acid, PC = phosphatidylcholine, ppm = parts per million, SM = sphingomyelin

Discussion

This study compared for the first time the lipid profiles in the IPFP of OA and cartilage defect patients as well as specific lipids for adipose and connective tissues, using MALDI-MSI. Different lipid profiles for OA and cartilage defect patients were revealed. The IPFP phenotype of OA patients was characterized by a great plethora of phospholipids, which also has been demonstrated in the synovial fluid of early and late OA patients by Kosinska et al. [155].

Phospholipids contribute to the maintenance of homeostasis in a healthy joint. They function as cell membrane elements and play an important role in facilitating lubrication of the joint in synovial fluid [289-291]. Phosphocholines are essential components of the lubricating layer in the joint [291]. However, the increase of phospholipids in the synovial fluid of the OA joint results in the formation of aggregates, such as micelles [291] that disturb the lubrication of the joint. Also in line with our findings, most phospholipids show increased levels in OA synovial fluid [289, 291], contributing to OA pathogenesis by modulating inflammatory responses [155, 289].

PE O-s, including arachidonic acid (fatty acid 20:4), were highly abundant in OA patients (**Table 5.2**). Ether-linked lipids such as PE O- contain high amounts of arachidonic acid and have been shown to be involved in the pro-inflammatory response in diseases like obesity [292]. Eicosanoids, including prostaglandins, derived from arachidonic acid, are important inflammatory factors [293, 294], and have been shown involved in the inflammatory response in OA [51, 198, 292, 295]. Additionally, SM 40:2;O2 was identified as highly abundant in OA patients. Sphingolipids have been suggested as possible biomarker species in OA, as they are involved in synovial inflammation and joint repair responses [156]. An increase of SMs has been shown to be involved in the down-regulation of type II collagen by disruption of the articular cartilage matrix homeostasis in vitro [296] and in bovine articular chondrocytes [297]. As example, Kosinska et al. reported SM 42:2;O2 upregulated in patients with late OA, suggesting it as possible biomarker for (early) OA [156].

The IPFP shows tissue heterogeneity within and between samples. Adipose tissue, connective tissue, synovial tissue, and blood vessels (dependent on tissue section) were identified using H&E histological staining (**Figure 5.2**). Here, we focused on the two main tissues present in the IPFP, namely adipose tissue and connective tissue. The consistency and proportion of these tissues inside the IPFP determine which lipids are detected, as well as what their importance is in disease discrimination.

The PE O-s highly present in the adipose tissue part of the IPFP did not contain arachidonic acid (**Table 5.3**). Contrarily, the majority of the PE O-s found in the connective tissue of the IPFP did contain arachidonic acid (**Table 5.4**), suggesting that

the pro-inflammatory phenotype of OA is represented in the connective tissue of the IPFP. In general, in the tissue samples measured in this work, the IPFP of OA patients contained more connective tissue and was thus more fibrotic compared to the IPFP of cartilage repair patients. Fibrosis of especially cartilage and synovial tissue of the joint has been shown associated to OA [298, 299]. Likewise in the IPFP, fibrosis was found as a typical characteristic in OA patients, indicating that changes in the IPFP due to molecular and biomechanical alterations, influence the OA development process [124, 300].

The IPFP is not commonly studied in OA research, where the focus is predominantly on synovial fluid, cartilage, or synovial membrane [81]. The importance of the IPFP in OA has already been acknowledged [16, 20, 124, 300]. However, the knowledge on the IPFP's lipid profile and its role in OA development is limited. Because IPFP is not located inside the knee joint capsule and therefore accessible with limited infection risk and the IPFP is often removed (partly or as a whole) during knee surgery, it is suggested as promising biopsy target for diagnostic and as a predictive source for OA or cartilage regenerative biomarker discovery [81]. The lipids found as specific biomarkers for OA in this research, might contribute to future diagnostic applications for early OA and OA development.

By unraveling the lipidome of IPFP, we emphasize its importance, in combination with MALDI-MSI, in possible clinical diagnostic or predictive research regarding OA or cartilage regeneration. MALDI-MSI gives us a clear visualization of the lipid profile of the IPFP, taking into account the IPFP intra-tissue heterogeneity. Additional research on the lipid profile of the IPFP is necessary before a specific biomarker (profile) for OA can be identified and implementation in the clinic would be possible.

Limitations and future research

To identify OA markers in IPFP for predictive biomarkers and possible treatment purposes, the analysis of lipid profiles in early OA patients would be of importance. Certainly, a healthy control would be optimal, although this is not feasible due to ethical reasons. This study analyzed the lipid profile of the IPFP of end-stage OA patients, undergoing TKA. As control tissue, waste IPFP of cartilage repair surgery was analyzed. Cartilage repair patients can be considered as patients who are early in the process of OA development. Therefore, the IPFP collected from these patients is an interesting alternative. Whereas this IPFP of cartilage repair patients has been suggested healthier than OA IPFP, there might already be an inflammatory response present in these patients' joints influencing the acquired results. Additionally, although patients' IPFP were selected with care, age, BMI, gender, or the presence of synovial tissue can play a considerable role in lipid distribution. In addition, whereas MALDI-MSI gives us important information on the spatial distribution of

molecules throughout the tissue, differences in ionization or signal intensity per pixel prevents us from measuring the amount of the analyte of interest present. Validation of our results is necessary and can possibly be done by cutting out the region of interest (e.g. connective tissue) within the IPFP using laser microdissection (LMD) prior to quantitative liquid chromatography tandem MS (LC-MS/MS) [301].

The IPFP is suggested as potential source for biomarkers for OA. Compared to more favorably explored fluids or tissues such as synovial fluid or cartilage, the IPFP is (almost) always present in the affected knee, easy to biopsy with limited infection risk, and commonly removed as waste material during cartilage repair surgery or TKA, thus highly available for research purposes. It is suggested that future experiments should be performed on larger patient groups and that not only inter-patient variability, but also intra-tissue heterogeneity should be taken into account. Possible biomarkers within the IPFP might relate to the genesis of OA and lead to possible novel interventions, treatments, or drug targets.

Conclusion

In conclusion, several lipid species were identified that are characteristic of OA and cartilage defect phenotypes. Highly expressed PE O-s, containing arachidonic acid, in the connective tissue of the IPFP, suggested a connection of these lipids to the OA phenotype. Intra-tissue heterogeneity has been shown of importance and might be associated with the different phenotypes.

Chapter 6

Towards the clinical implementation of mass spectrometry as diagnostic and prognostic tool in cartilage defect and osteoarthritis patients:

Lipid and protein analysis to identify possible biomarkers in the infrapatellar fat pad

Mirella J.J. Haartmans*, Kaj S. Emanuel*, Javier Sanmartin Martinez, Benjamin Balluff, Sylvia P. Nauta, Frank M. Zijta, Ron M.A. Heeren, Pieter J. Emans, Berta Cillero-Pastor

* = shared first author

Manuscript in preparation

Abstract

Young adults following knee injury, such as cartilage defects, have a severely increased risk for development of osteoarthritis (OA) later in life if not treated accordingly. Adequate treatment of these defects and better phenotyping of these patients can contribute to early detection of OA and is critical for a delay in OA development later in life. In this study, we 1) analyzed the lipid profiles in the infrapatellar fat pad (IPFP) of cartilage defect and OA patients using Rapid Evaporative Ionization Mass Spectrometry (REIMS) for analysis of electrosurgical vapors associated to patient outcome and 2) analyzed the protein profile of the IPFP to identify potential biomarkers. To validate the use of REIMS, snap-frozen IPFP explants, collected during cartilage defect surgery or total knee arthroplasty, were analyzed using a diathermic knife linked to a REIMS ionization source to collect lipid spectral profiles. Then, 53 snap-frozen IPFPs of cartilage defect patients were collected and measured using the same method. Diagnostic variables based on magnetic resonance imaging (MRI), patient reported outcome measures (PROMs) and patient history were collected from the patient's pre-operative, and treatment outcome state at 1-year follow-up. The status of the IPFP according to its lipid profile was evaluated using these MRIs and PROMs. Additionally, these 53 IPFPs were cryosectioned and used for liquid-chromatography mass spectrometry (LC-MS) to analyze the proteome. Specific *m/z* (lipids) were found to be distinctive for OA and cartilage defect patients. In addition, specific proteins were found as possible biomarker profile for clinical outcome after cartilage repair surgery, including an upregulation of cartilage intermediate layer protein 2 (CILP-2) and hematopoietic progenitor cell antigen CD34 (CD34), and a downregulation of aggrecan core protein and proteoglycan 4 (PRG4) in patients with bad surgical outcome. The finding of these proteins in the IPFP suggests an interaction between the IPFP and cartilage. CILP-2, CD34, aggrecan and PRG4 (lubricin) are proteins involved in maintaining tissue structure (CILP-2 and aggrecan), cell adhesion and division (CD34), and lubrication of the joint (PRG4). (A combination of) these protein biomarkers can possibly be used as potential prognostic factors to predict patient outcome after cartilage repair surgery. In addition, the finding of these therapeutic targets might also contribute to the development of novel (personalized) therapeutic or surgical strategies, improve patient outcome, and delay OA development.

Introduction

Young adults following knee injury such as osteochondral and cartilage defects, have an increased risk at the development of osteoarthritis (OA) later in life if not treated adequately[302]. Current knowledge on which type of cartilage repair surgery to perform on which patient it lacking and the treatment options available are often limited or with insufficient effectiveness[67]. Examples of osteochondral/cartilage repair surgeries are microfracture (in which holes are drilled in the underlying bone to release bone marrow derived stem cells), minced cartilage or hedgehog techniques (in which a loosened cartilage body is placed back in the defect using stitches or glue (e.g. Chondrofiller)), autologous chondrocyte transplantation (in which chondrocytes are harvested, cultured, and transplanted in the defect), osteochondral autograft (mosaicplasty)/allograft transplantation (in which an osteochondral graft is harvested and transplanted in the defect), or (metal) implant[67]. Current decision making on the treatment used after an osteochondral injury is mainly dependent on the availability of surgical tools and therapy, or the opinion and experience of the performing surgeon[67]. Nonetheless, patient outcome after cartilage repair surgery might be related to the type of treatment, the patient's cartilage regenerative potential, compliance to adequate rehabilitation, and/or other influencing factors such as age and body mass index (BMI), fibrosis, or previous surgery.

The infrapatellar fat pad (IPFP) is a type of adipose tissue inside the knee joint. This highly potential source for the identification of potential diagnostic or prognostic target for biomarkers and future treatment options is easily accessible as it is located outside of the knee capsule, and plays an important role in OA pathology and development[303]. The IPFP is generally (partial) removed as waste material during total knee arthroplasty (TKA) or cartilage repair surgery to improve visibility into the joint.

Rapid evaporative ionization mass spectrometry (REIMS) is a mass spectrometry (MS) technique that provides on-the-spot molecular information of the measured tissue. Connected to a diathermic knife, similar to the one already used in the operating theater, REIMS has great potential to be used intraoperatively (point-of-care) as diagnostic or prognostic tool. The smoke generated during surgical incision making is aspirated into the mass spectrometer, providing us with a molecular profile of the tissue of interest. Using this molecular information, specific software can be used to build diagnostic or prediction models, which can be used for clinical decision-making or personalized patient care. REIMS has already been utilized as a

method for drug detection[304], tissue identification[194], and tissue classification[96]. The potential of REIMS being used as diagnostic intraoperative tool has already been described in, for example, cancer research[305, 306]. However, its potential use as prediction tool for patient outcome after cartilage repair surgery remains unexplored.

In this Chapter, the IPFP's potential as possible (biomarker/biopsy) target for diagnosis and/or classification of OA and possible prognosis of cartilage repair after an (osteo)chondral defect were investigated. Patient characteristics such as gender, BMI, or age, as well as IPFP fibrosis, pre-operative patient reported outcome measures (PROMs) and patient outcome after surgery were correlated to the IPFP's lipid and protein profile. Pre- and post-operative pain- and clinical performance scores were determined using self-reported questionnaires based on the visual analogue scale (VAS) and knee injury and osteoarthritis outcome score (KOOS) respectively. A VAS score is determined based on a 10-point scale in which a patient can indicate pain intensity with zero defining "no pain", towards "worst pain" at a score of 10[307]. The KOOS score evaluates short- and long-term consequences of knee-specific injury and consists of 42 items distributed over five subscales: pain, additional symptoms (including swelling, range of motion restriction, and mechanical symptoms), situation in daily life (ADL), situation in sport/recreation, and knee-related quality of life (QOL)[308].

In this Chapter, first, the application of MS in the form of REIMS was explored as potential tool to predict patient outcome after cartilage repair surgery based on lipid-based biomarkers. Additionally, a protocol for laser capture microdissection (LMD) on the IPFP was tested. Using LMD, a specific tissue type of interest can be cut from a cryosection with a laser, captured in an Eppendorf tube and analyzed using liquid chromatography tandem mass spectrometry (LC-MS/MS) for label-free proteomics.

As a proof of concept, regarding the results showed in Chapter 5 of this Thesis, the differences in the IPFP lipid profile of OA and cartilage defect patients were investigated using REIMS connected to a diathermic knife. To investigate the potential of this technique on prediction patient outcome after cartilage repair surgery in the clinic, the lipid profile of the IPFP of a cohort of patients undergoing cartilage repair surgery was investigated. Although REIMS is a very promising technique for the *in situ* analysis of a variety of tissue samples in a diversity of disease pathologies, REIMS connected to a diathermic knife is a relatively destructive technique, burning away tissue to generate smoke for analysis. In combination with

the IPFP, a tissue that has not only a fatty, but also an adhesive signature, keeping the morphological information after analysis is difficult. LMD in a multi-omics approach would give us the opportunity to not only evaluate the identification and spatial distribution of lipids in the IPFP after matrix-assisted laser desorption/ionization mass spectrometry imaging (MALDI-MSI), as has been described in **Chapter 4** and **Chapter 5**. In addition, LC-MS/MS proteomic analysis would also give us additional information on the proteome of (specific parts of) the IPFP. Therefore, an LMD protocol for the IPFP, in combination with LC-MS/MS, was optimized to evaluate whether proteins might be a better target for the classification of patients based on their characteristics (e.g. gender, age, or BMI) and pre- and post-operative clinical state or outcome (VAS and KOOS).

Altogether, this study aimed to identify possible diagnostic and prognostic biomarkers (or biomarker profiles) that might lead to a better understanding of post-traumatic OA development, possible personalized treatment, and better surgical outcomes after cartilage repair surgery. Using REIMS as a potential *in situ* analysis technique, **this Chapter** briefly touches upon the use of this system as a tool to predict patient outcome after cartilage repair surgery. In parallel, we identified protein biomarkers associated to patient response after which might serve as novel targets for clinical decision-making on therapy and surgical strategies.

Methods

Tissue sampling and sample preparation: osteoarthritis vs cartilage defect

IPFP was collected as waste material from 14 cartilage repair (7 patients > 35 years and 7 patients < 35 years) and seven TKA patients (all patients > 35 years, but < 60 years of age) at Maastricht University Medical Center (MUMC+) in the Netherlands. Non-WMO (Wet Medisch-Wetenschappelijk Onderzoek, law for medical-scientific research in humans in the Netherlands) approval for the collection of waste material during TKA (ID: MEC 2017-0183, 2017) or cartilage repair surgery (ID: MEC 2018-0963, 2018) was assigned by the Medical Ethics Testing Committee (METC). In addition, informed consent was signed by each patient. Patients were matched for cartilage damage/OA grade (Kellgren-Lawrence (KL) grade, graded based on MRI or X-ray by an orthopedic surgeon (PE)) and age. In **Chapter 1**, it was described that a treatment gap for OA exist between the ages of 40-60 years, in which TKA is not the solution[56,57]. However, to prevent age-related differences between the study groups as much as possible in this analysis, a cut-off age of 35 was used: 7 OA patients below the age of 59, 7 cartilage defect patients above the age of 35 years, and 7 cartilage

defect patients below the age of 35 years. Directly after dissection at the surgical theater, IPFPs were washed in phosphate-buffered saline (PBS) to remove possible blood residue. Samples were snap-frozen in liquid nitrogen and stored at -80°C until further analysis.

Tissue sampling and sample preparation: cartilage repair patient cohort

53 IPFP of patients with a cartilage defect undergoing any type of cartilage repair surgery at the MUMC+ were collected as waste material with non-WMO approval for the collection of waste material during cartilage repair surgery, assigned by the METC (ID: MEC 2018-0963, 2018). Of each patient, pre- and post-operative MRI and questionnaires, including patient characteristics and scores for pain (VAS) and KOOS, were collected. MRI images were scored by an experienced musculoskeletal radiologist on a 3-point scale (none, normal-mild, moderate-severe) for levels of IPFP fibrosis. As described above, after dissection at the surgical theater, IPFPs were washed in PBS to remove possible blood residue. Samples were snap-frozen in liquid nitrogen and stored at -80°C until further analysis. When frozen, prior to REIMS and LC-MS/MS analysis, each IPFP explant was cut in two pieces and placed back in the -80°C. One piece was used for REIMS analysis, one piece for cryosectioning and LMD prior to LC-MS/MS analysis.

Rapid Evaporative Ionization Mass spectrometry (REIMS)

IPFPs were cauterized *ex vivo* using a hand-held iKnife disposable device (Waters Research Center, Hungary) supplied with a 1.7 cm diameter blade, connected to an electrosurgical heat generator (Force FX, Covidien) operating in CUT mode. The electrocautery device was connected to a mobile REIMS Xevo G2-XS Q-ToF mass analyzer (Waters Corporation, Wilmslow, UK), aspirating the smoke generated.

Experiments were performed in a laminar flow class II biosafety cabinet (Biowizard Xtra Line, Kojair Blue Series Technologies). The IPFP of each patient thawed on ice and was placed on a chemically inert wipe (Kimtech, Kimberly Clark) on a silicone counter electrode (Erbe) and wetted with deionized water. Samples were cauterized at least five times using cut modality with a power of 30W. Generated vapors were aspirated into the REIMS Xevo G2-XS Q-ToF mass analyzer (Waters Corporation, Wilmslow, UK) via a polytetrafluoroethylene tube, connected to the electro-cauterization device. Aspiration was improved using an aspiration system (ZERO SMOG 2, Weller FT), connected to the venture in the REIMS system to avoid excessive smoke nuisance. The lock mass solution (0.075 µg/ml Leucine-Encephalin

(Leu-Enk, Sigma-Aldrich, The Netherlands) in isopropanol (Biosolve, Honeywell, Germany), *m/z* 554.26, was infused at 150 µL/min (31194519 and 33208813) and acquisition was performed in negative ionization mode and sensitivity mode with mass range *m/z* 50-1500.

Histology

To keep the morphology of the IPFP after REIMS analysis and to identify in which specific tissue type within the IPFP the cut was made, the IPFP explants measured were embedded in paraffin and stained with Hematoxylin and Eosin (H&E) using standard protocols as described in Chapter 5.

Data analysis (REIMS)

Abstract Model Builder (AMX) software version 0.9.2092.0 (Waters Research Center, Budapest, Hungary) was used for data analysis. Of each tissue, five correctly performed scans were selected for additional analysis (*m/z* 600-1000). For the model used, 0.1 binning, lock-mass correction, background subtraction, and normalization were performed. Patient groups were analyzed using built-in linear discriminant analysis (LDA) and cross-validation (20% out) with confusion matrix was performed to test the model for correct classification rate.

Cryosectioning and laser capture microdissection (LMD)

15 µm cryosections of the IPFP of 53 cartilage defect patients were obtained as described in Chapter 4 and Chapter 5 of this Thesis. Next to thaw-mounting the tissue section on indium tin oxide (ITO) slides (4–8 Ω resistance, Delta Technologies, CO, USA), polyethylene naphthalate (PEN) membrane slides (2.0 µm, Leica Biosystems, Nußloch, Germany) and metallic frame polyphenylene sulfide (PPS) (FRAME) membrane slides (1.2 µm, Leica Biosystems, Nußloch, Germany) were used to test multiple LMD approaches. Subsequently, the slides were stored at -80°C until use.

Prior to LMD, the slides went through a variety of washing steps to remove excessive lipid content. The washing protocols included 1) desiccation only; 2) three minutes in milliQ water, two minutes in 100% ethanol; 3) two minutes each in 50%, 70%, 95%, 100%, and 100% ethanol; 4 three minutes in milliQ, two minutes in 100% ethanol, and two minutes in chloroform; and 5) two minutes each in 50%, 70%, 95%, 100%, and 100% ethanol, and two minutes in chloroform. All slides air-dried for 10 minutes after washing.

For testing purposes, different areas (0.15 cm^2 and 0.25 cm^2) of adipose tissue inside the IPFP sections on either ITO, PEN or FRAME slides were cut using a Leica LMD 7000 system (Leica Biosystems) for LC-MS/MS analysis. The LMD system were set as follows: a wavelength of 349 nm, a power of 40, aperture of 38, speed of 17, specimen balance of 0, line spacing of 5, head current of 60%, and a pulse frequency of 310 Hz. Slightly different for PEN membrane and FRAME slides, power was set at 60, speed at 9, specimen balance at 20 and head current at 100%, with a pulse frequency of 119 Hz.

Due to insufficient protein amounts in the tested samples, for the cartilage defect patient cohort, a minimum of 20 sections of 15 µm thickness were collected in an Eppendorf tube prior to protein extraction and LC-MS/MS analysis. All sections were stored at -80°C until protein digestion.

Protein extraction and quantification

Proteins were extracted from the IPFP through an in-house developed protocol, taking into account the considerations of Feist et al.[309], using 50 µL 5 M Urea (GE Healthcare, Chicago, IL)/50 mM ammonium bicarbonate (ABC, Sigma-Aldrich, Saint Louis, MO) buffer. After briefly spinning down the sample, three freeze-thaw cycles were performed using dry ice and water bath sonication, followed by a quick vortexing step between each cycle. The samples were then centrifuged for 30 minutes at 15,000 x g at 10°C. Total protein content was determined through Bradford Protein Assay (Bio-Rad Laboratories, Hercules, CA) according to the manufacturer's protocol. Absorption was measured at 595 nm (optical density) using a Spark 10M microplate reader (Tecan, Männedorf, Switzerland).

Protein digestion

Protein digestion, as has been described before in **Chapter 3** of **this Thesis**, was performed using a protein amount of 50 µg in 50 µl 5 M Urea/50 mM ABC buffer. In brief, the samples incubated for 45 minutes at room temperature with 5 µl 20 mM dithiothreitol (DTT, Sigma-Aldrich)/50 mM ABC (Sigma-Aldrich) buffer. Then, 6 µl 40 mM iodoacetamide (IAM, Sigma-Aldrich) was added to the samples and incubated for 45 minutes at room temperature in the dark, before 10 µl of 20 mM DTT was added and incubated at room temperature for 45 minutes. A trypsin/Lys-C solution in resuspension buffer (Promega, Leiden, the Netherlands) was added in an enzyme to protein ratio of 1:25 and incubated in a Thermoshaker (Eppendorf, Hamburg, Germany) for 2 hours at 250 rpm and 37°C. Hereafter, 200 µl of 50 mM ABC (Sigma-Aldrich) sample buffer was added to the samples and incubated overnight in a

Thermoshaker (Eppendorf) at 250 rpm and 37°C. Finally, 30 µl of 20% acetonitrile (ACN, Biosolve)/10% formic acid (FA, Biosolve) was added to the samples and vortexed to stop the reaction. Samples were centrifuged for 30 minutes at 15,000 x g to remove possible particles and the supernatant were stored at −20°C until LC-MS/MS analysis.

Liquid chromatography tandem mass spectrometry (LC-MS/MS)

Proteomic analysis was performed on a Thermo Scientific Ultimate 3000 Rapid Separation UHPLC system (Dionex, Amsterdam, the Netherlands), coupled to a Q-Exactive HF mass spectrometer (Thermo Fisher Scientific), equipped with a PepSep C18 analytical column (15 cm, ID 75 µm, 1.9 µm Reprosil, 120 Å). Samples were desalted on a C18 trapping column and separated on an analytical column with a 90-minute linear gradient (5%-35% ACN with 0.1% FA, flow rate 300 nl/min). Mass spectra were acquired in positive ion mode and in data-dependent acquisition mode (DDA) using a mass-to-charge ratio (*m/z*) of 250-1250 at a 12,000 resolution. MS/MS scans were acquired from the 15 most intense ions at a 15,000 resolution[51, 160].

Data analysis (LC-MS/MS)

The data acquired was analyzed using Proteome Discoverer (PD) Software version 2.2 (Thermo Fisher Scientific, Waltham, MA). Proteins were identified and quantified using the built-in Sequest HT search engine with SwissProt (Human) database (Homo sapiens, Tax ID 9606) as described in **Chapter 3** of **this Thesis**. Only proteins present in 60% of the patients in one group with an abundance ratio ≤ 0.67 or ≥ 1.5 (-0.58 < log2 > 0.58) and abundance ratio adjusted p-value < 0.05 were considered differentially expressed between groups. Subsequent pathway analysis was conducted in String-db[310] version 11.5 for clinical outcome parameters ΔKOOS and ΔVAS. The description of each parameter used for evaluation, based on the minimal clinically important difference (MCID) (age, BMI, fibrosis, KOOS and VAS), as well as the cut-off values used are depicted in **Table 6.1**. All descriptive statistics (including calculations of averages and calculations of differences between groups (one-way ANOVA with post-hoc Tukey test)) were performed in SPSS Statistics 27 (IBM Corp., Armonk, NY).

Table 6.1. Cut-off values for age, body mass index (BMI), fibrosis, knee injury and osteoarthritis outcome score (KOOS) and visual analogue scale (VAS).

Parameter	description	cut-off
Age [61, 311]	Biological age in years	Young ≤ 35 Old > 35
BMI [312, 313]	Body mass index: body weight (kg) divided by square height (m^2).	Low BMI ≤ 25 High BMI > 25
Fibrosis [299, 314, 315]	Thickening or scarring of the IPFP on MRI.	Subjective grouping into a non-fibrosis group, mild fibrosis, and moderate fibrosis
KOOS [308, 316, 317]	Self-reported questionnaire related to knee pain and function on a 100-point scale (knee injury and osteoarthritis outcome score).	Pre-operative KOOS ≤ 45 Pre-operative KOOS > 45 Post-operative KOOS ≤ 70 Post-operative KOOS > 70 ΔKOOS ≤ 10 ΔKOOS > 10
VAS [318, 319]	Visual analogue scale for self-reported measure of pain on a 10-point scale.	Pre-operative VAS ≤ 5.8 Pre-operative VAS > 5.8 Post-operative VAS ≤ 2.4 Post-operative VAS > 2.4 ΔVAS ≤ 2.7 ΔVAS > 2.7

IPFP = infrapatellar fat pad, MRI = magnetic resonance imaging, KOOS = knee injury and osteoarthritis outcome score, VAS = visual analogue scale.

Results

Osteoarthritis vs cartilage defect (REIMS analysis)

For the analysis of the data collected using REIMS on the IPFP of OA or a cartilage defect patients, patients were matched for age and BMI regarding the patient material available (**Table 6.2**).

The LDA results of OA and cartilage defect showed a trend towards a separation between the three groups (**Figure 6.1**). According to this analysis, the old cartilage defect group showed the highest discrimination from OA and young cartilage defect groups (**Figure 6.1**).

Table 6.2. Characteristics osteoarthritis patients vs "old and young" cartilage defect patients.

Patient	OA / CD	Gender	Age	Left/right	BMI	KL grade
1	OA < 60	Male	56	Left	26.9	3
2	OA < 60	Male	42	Right	29.6	3
3	OA < 60	Male	58	Left	27.1	4
4	OA < 60	Female	54	Right	28.3	4
5	OA < 60	Male	52	Left	23.2	4
6	OA < 60	Female	58	Left	26	3
7	OA < 60	Female	40	Left	31.5	2
1	CD > 35	Male	48	Left	25.2	0
2	CD > 35	Male	47	Left	23.7	1
3	CD > 35	Male	38	Left	34.3	0
4	CD > 35	Female	49	Left	24.3	0
5	CD > 35	Male	48	Right	26.6	0
6	CD > 35	Female	56	Left	27.2	0
7	CD > 35	Female	36	Right	22.5	1
1	CD < 35	Male	21	Left	25.1	0
2	CD < 35	Female	20	Right	22.8	0
3	CD < 35	Male	20	Left	26.1	0
4	CD < 35	Female	21	Right	21.4	0
5	CD < 35	Female	19	Left	24.1	0
6	CD < 35	Male	22	Right	27.4	1
7	CD < 35	Male	19	Left	26.9	0

OA = osteoarthritis, CD = cartilage defect, BMI = body mass index, KL = Kellgren-Lawrence.

A cross validation (20% out) with confusion matrix showed an overall classification rate of 62.9%, meaning that 62.9% (66 out of 105) of the cuts made in the IPFP were correctly classified. The highest correct classification rates were acquired in the cartilage defect > 35 years (71.4%) and cartilage defect < 35 years (80%) (**Table 6.3**).

Each group of patients (OA, cartilage defect > 35, and cartilage defect < 35) was characterized by a specific lipid profile when compared to either one of the patient groups (**Figures 6.2 – 6.4**). The top 20 *m/z* with the highest loadings contributing to the discrimination between each group were depicted in **Tables 6.4 – 6.6**.

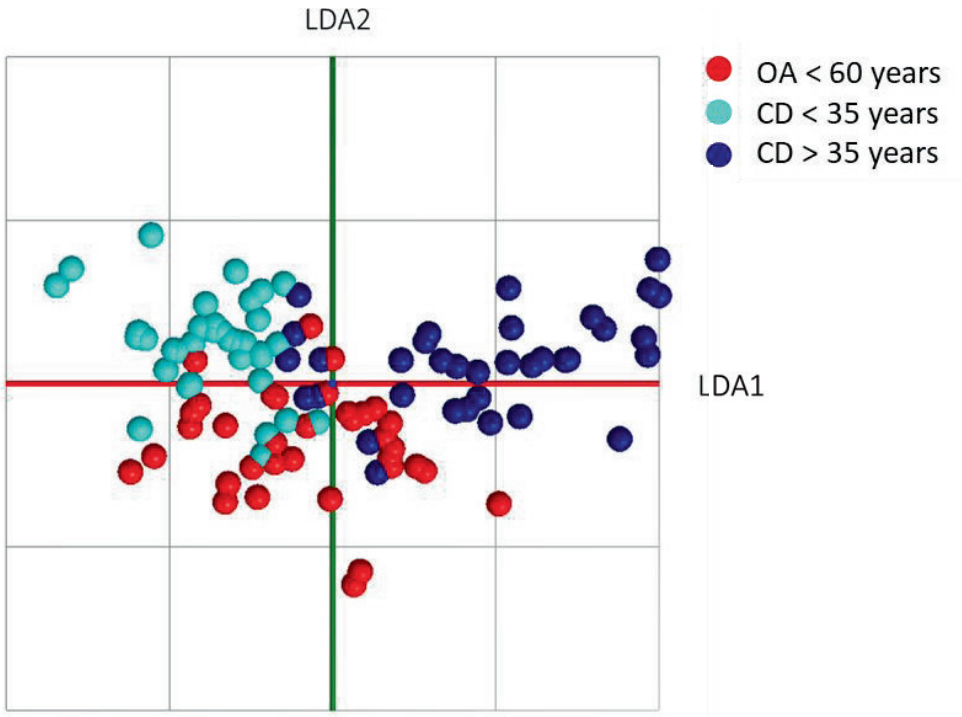

Figure 6.1. Linear discriminant analysis (LDA, per burn) of osteoarthritis (OA) and cartilage defect (CD, < 35 years and > 35 years) patients. The confusion matrix (20% out) showed an overall correct classification rate of 62.9%.

Table 6.3. Classification rates of cartilage defect patients > 35 years, cartilage defect patients < 35 years, and OA patients.

Patient group	Classified correctly (%)	Classified incorrectly in … group (%)
Overall	66 / 105 cuts (62.9%)	Overall 37.1%
CD > 35 years	25 / 35 cuts (71.4%)	CD < 35 (17.1%)
		OA (11.4%)
CD < 35 years	28 / 35 cuts (80%)	CD > 35 (0%)
		OA (20%)
OA	13 / 35 cuts (37.1%)	CD < 35 (31.4%)
		CD > 35 (31.4%)

CD = cartilage defect, OA = osteoarthritis

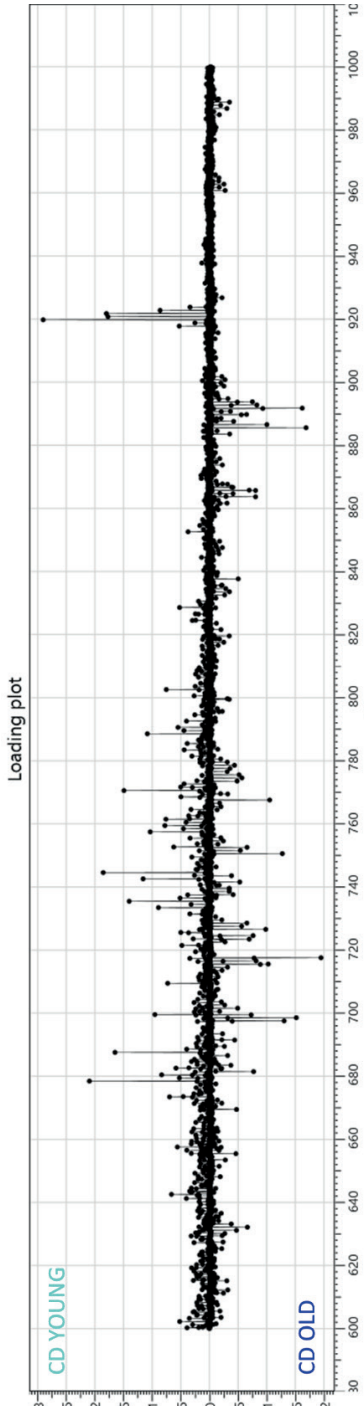

Figure 6.2. Loading plot of LD1, separating cartilage defect (CD) patients < 35 years from CD patients > 35 years.

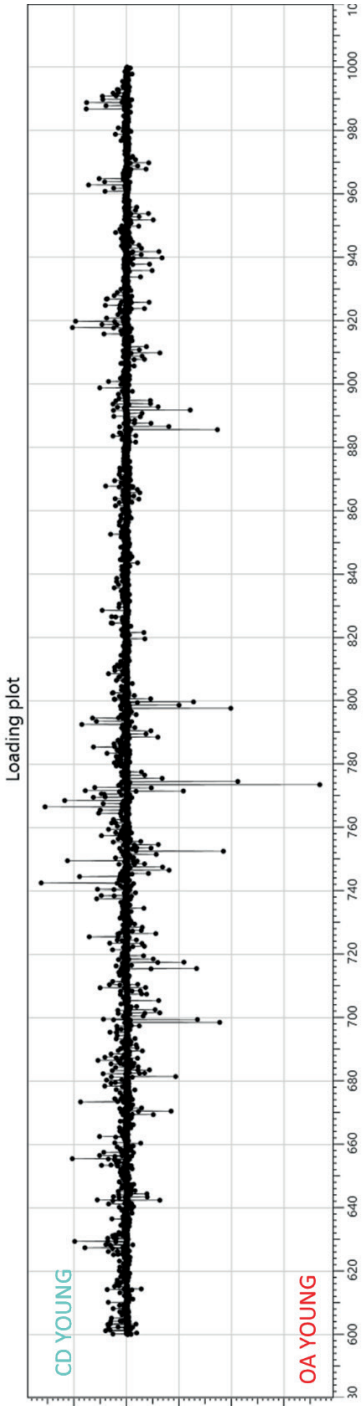

Figure 6.3. Loading plot of LD1, separating cartilage defect (CD) patients < 35 years from osteoarthritis (OA) patients.

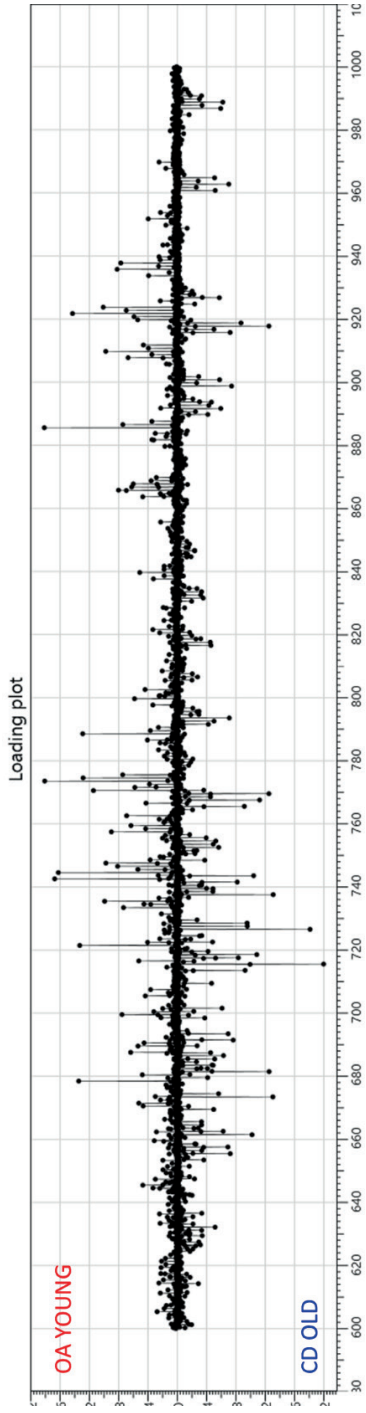

Figure 6.4. Loading plot of LD1, separating cartilage defect (CD) > 35 years patients from osteoarthritis (OA) patients.

Table 6.4. The top 20 *m/z* with highest loadings corresponding to cartilage defect patients < 35 years and cartilage defect patients > 35 years.

CD < 35 years		CD > 35 years	
m/z	Loading	*m/z*	Loading
919.75	0.290406	717.55	0.19477
678.45	0.209656	885.55	0.16872
744.55	0.185506	891.75	0.16203
921.75	0.179975	698.55	0.15164
920.75	0.177214	697.55	0.13047
687.55	0.164929	750.55	0.12724
770.55	0.149358	767.55	0.10517
735.45	0.140175	715.55	0.10261
742.55	0.115902	886.55	0.10035
788.55	0.108539	726.55	0.0983
757.45	0.103484	891.65	0.09318
699.55	0.095331	715.45	0.08884
733.45	0.088999	892.75	0.08274
922.75	0.086216	716.55	0.08144
680.45	0.083501	863.65	0.08049
759.45	0.077837	865.65	0.08049
761.45	0.076077	717.45	0.07796
802.55	0.075334	681.45	0.07705
709.45	0.072937	724.55	0.07616
673.45	0.069633	893.75	0.07505

CD = cartilage defect, *m/z* = mass-to-charge ratio.

Table 6.5. The top 20 *m/z* with highest loadings corresponding to cartilage defect patients < 35 years and OA patients.

CD < 35 years		OA	
m/z	Loading	*m/z*	Loading
742.55	0.162135	773.55	0.36781
766.55	0.154785	774.55	0.21184
768.55	0.117489	797.65	0.19856
749.55	0.112191	752.55	0.18446
655.55	0.102957	698.55	0.17751
917.75	0.102745	885.55	0.17307
629.45	0.098395	699.45	0.13512
919.75	0.096676	715.55	0.13336
744.55	0.089203	799.65	0.12768
673.45	0.087215	891.75	0.12136
792.55	0.084819	717.55	0.10942
627.45	0.078987	771.55	0.10841
771.65	0.078201	798.65	0.10007
986.75	0.076426	681.45	0.0937
988.75	0.075683	670.55	0.08495
962.75	0.072076	746.55	0.08111
725.55	0.070747	886.55	0.0807
794.55	0.064444	747.55	0.06883
769.55	0.062895	775.55	0.068
785.45	0.062671	939.75	0.06773

CD = cartilage defect, OA = osteoarthritis, *m/z* = mass-to-charge ratio.

Table 6.6. The top 20 *m/z* with highest loadings corresponding to cartilage defect patients > 35 years and OA patients.

CD > 35 years		OA	
m/z	Loading	*m/z*	Loading
715.55	0.19952	885.55	0.181598
726.55	0.18105	773.55	0.18107
737.55	0.13072	742.55	0.167505
673.45	0.13028	744.55	0.162459
681.45	0.12514	921.75	0.14312
917.75	0.12491	678.45	0.134635
769.55	0.1249	721.45	0.133211
767.55	0.11222	788.55	0.129197
718.55	0.10837	774.55	0.128693
743.55	0.104	770.55	0.114589
661.45	0.10189	923.75	0.101201
715.45	0.09921	735.45	0.09927
727.55	0.09543	909.75	0.097712
728.55	0.09518	747.55	0.097561
713.55	0.09237	757.45	0.090112
765.55	0.09139	935.75	0.082247
918.75	0.08681	746.55	0.081568
717.55	0.08315	865.75	0.080347
741.55	0.08171	937.75	0.077268
691.45	0.07617	699.55	0.075634

CD = cartilage defect, OA = osteoarthritis, *m/z* = mass-to-charge ratio.

Cartilage defect patient cohort – REIMS analysis

To evaluate if certain patient groups with less distinctive profiles could be identified based on their lipid profile, lipid analysis was performed on the IPFP of 53 cartilage defect patients (Table 6.7). Per patient five cuts were made (with the exception of one cut that was not taken into account due to low intensity (not recognized as cut in the program used)). A list of the top 20 lipids responsible for the discrimination between groups is shown if the cross validation (20% out) confusion matrix was above 65%.

For all patients in this cohort, information on gender, age, and BMI were available (Table 6.7). The majority of patients in the cartilage defect patient cohort (n = 53) were male (35 compared to 18 female). The mean age and BMI of the population measured were 29.4 ± 11.7 years and 24.3 ± 3.6 kg/m^2 respectively. Pre- and post-operative (1 year after surgery) questionnaires (KOOS and VAS) were filled in by 43 of 53 patients. Pre-operatively, an average of 44.7 ± 18.1 for KOOS and 5.5 ± 2.3 cm for VAS were calculated; post-operatively, average scores of 67.1 ± 20.3 (KOOS) and 3.0 ± 2.9 cm (VAS). Both pre- and post-operative KOOS and VAS were available from 34 patients (ΔKOOS, mean 24.5 ± 23.1; ΔVAS, mean -2.9 ± 2.8 cm) (Table 6.7).

Dependent on the type of surgery performed, patients were allocated in one of three groups: 1) regenerative (loosened cartilage body was glued or used to fill up the cartilage defect using e.g. minced cartilage or hedgehog techniques combined with stitches or glue such as Chondrofiller), 2) biological resurfacing (the defect was filled with the patient's own material collected from a different, less weight-bearing part of the joint (e.g. mosaicplasty), cultured cells (articular chondrocyte transplantation, ACT), or derived from bone marrow derived stem cells (microfracture)), or 3) metal resurfacing (metallic implant). Average age, BMI, pre- and post- operative KOOS and VAS, and ΔKOOS and ΔVAS were depicted in Table 6.8. A one-way ANOVA ($F = 50.75$ and $p < 0.001$) with post-hoc Tukey test showed statistical significance between age groups based on the different types of surgery ($p < 0.001$) (Table 6.8).

Information on previous trauma was available from 53 patients. 32 patients have had previous knee-related trauma, compared to 21 patients without previous trauma (Table 6.7). In addition, information on previous knee surgery was available from 52 of 53 patients. 23 patients already underwent surgery prior to the surgical treatment for the (osteo)chondral defect, compared to 29 without previous surgery (Table 6.7).

In addition, fibrosis scored by a radiologist through MRI were available from 51 of 53 patients based on a 0-2 scale with 0) no fibrosis, 1) normal-mild fibrosis, and 2) moderate-severe fibrosis. 12 patients did not show IPFP fibrosis on the MRI prior to surgery. 39 patients, of which 28 patients showed normal-to-mild fibrosis and 11 patients moderate-to-severe fibrosis showed signs of IPFP fibrosis on the MRI prior to surgery (**Table 6.7**).

Patient profiling based on lipid profile in the infrapatellar fat pad

Table 6.9 gives an overview of the correct classification rates of cartilage defect patients after LDA and cross validation analysis (20% out) based on gender (53.4%), age (65.5%), and BMI (43.9%). The highest correct classification rate was found for the group of cartilage defect patients < 35 years (**Figure 6.5**), matching previous results (**Table 6.3**). The top 20 *m/z* with highest loading in each of the group (cartilage defect patients < 35 years and cartilage defect patients > 35 years) are depicted in **Table 6.10**.

It was not possible to discriminate cuts made in the IPFP of patients that already had previous knee-related trauma and/or underwent surgery based on their lipid profile (**Table 6.9**). In addition, it was not possible to discriminate IPFP fibrotic profiles based on the IPFP lipid profile (**Table 6.9**).

Responders and non-responders (unrelated to type of surgery)

Based on the pre- and post-operative KOOS and VAS scores it was determined if patients responded well (responders) or not (non-responders) to cartilage repair surgery. For pre- and post-operative KOOS and VAS scores, it was not possible to discriminate cuts made in the IPFP of responders from non-responders (**Table 6.11**). The same was true for the difference between pre- and post-operative KOOS and VAS scores (ΔKOOS and ΔVAS) (**Table 6.11**).

Table 6.7. Patient characteristics of cartilage defect patient cohort (n = 53).

Patient	PT nr	Gender	Age	BMI	VAS T0	VAS 1Y	KOOS T0	KOOS 1Y	Previous trauma	Previous surgery	Type of surgery	Fibrosis IPFP (MRI)
1	P18-129	Female	16	23.31		7.00		40.64	Yes	No	Regenerative (Chondrofiller)	0
2	P18-137	Male	48	25.21	8.00	7.90	19.45	26.44	Yes	Yes	Metal resurfacing	1
3	P18-145	Male	47	23.72	5.40	2.70	69.34	78.68	Yes	Yes	Metal resurfacing	0
4	P18-147	Female	29	27.18	6.20	5.30	48.8	42.08	Yes	Yes	Metal resurfacing	2
5	P19-015	Male	32	35.49		4.40		48.61	Yes	No	Regenerative (Chondrofiller)	0
6	P19-016	Male	16	17.53		0		86.3	Yes	Unknown	Regenerative (Hedgehog)	2
7	P19-030	Female	26	28.34	6.90		56.91		Yes	Yes	Fulkerson osteotomy	1
8	P19-032	Female	16	26.12	6.40	0.20	32.62	69.47	No	No	Regenerative (Hedgehog)	0
9	P19-037	Male	29	22.26	7.40	2.00	24.55	84.24	Yes	Yes	Regenerative (Microfracture)	1

ACT = articular chondrocyte transplantation, BMI = body mass index, IPFP = infrapatellar fat pad, KOOS = knee injury and osteoarthritis outcome score, MRI = magnetic resonance imaging, PT = patient, VAS = visual analogue score, Y = year.

Table 6.7 (continued). Patient characteristics of cartilage defect patient cohort (n = 53).

Patient	PT nr	Gender	Age	BMI	VAS T0	VAS 1Y	KOOS T0	KOOS 1Y	Previous trauma	Previous surgery	Type of surgery	Fibrosis IPFP (MRI)
10	P19-039	Female	15	26.99		6.90		77.54	Yes	Yes	Regenerative (Minced cartilage)	0
11	P19-045	Male	24	19.08	6.30	1.20	30.6	71.63	No	No	Regenerative (Minced cartilage)	1
12	P19-054	Male	38	34.32	7.30	2.70	43.5	72.29	Yes	Yes	Metal resurfacing	1
13	P19-055	Male	27	25.08	6.80	6.00	34.96	45.14	Yes	Yes	Regenerative (Minced cartilage)	0
14	P19-071	Male	35	23.92	0.50		38.8		No	No	Regenerative (Minced cartilage)	NA
15	P19-079	Female	18	24.38		6.30		42.59	No	No	Regenerative (Minced cartilage)	1
16	P19-080	Male	37	25.98	3.50		62.53		No	No	Regenerative (Minced cartilage)	1
17	P19-081	Male	16	21.91	7.50	0	45.37	97.14	Yes	No	Regenerative (Minced cartilage)	0
18	P19-089	Female	16	21.45		5.70		62.55	Yes	No	Regenerative (Hedgehog + osteotomy)	0

ACT = articular chondrocyte transplantation, BMI = body mass index, IPFP = infrapatellar fat pad, KOOS = knee injury and osteoarthritis outcome score, MRI = magnetic resonance imaging, PT = patient, VAS = visual analogue score, Y = year.

Table 6.7 (continued). Patient characteristics of cartilage defect patient cohort (n = 53).

Patient	PT nr	Gender	Age	BMI	VAS T0	VAS 1Y	KOOS T0	KOOS 1Y	Previous trauma	Previous surgery	Type of surgery	Fibrosis IPFP (MRI)
19	P19-118	Female	13	20.76		1.90		72.39	No	No	Regenerative (Hedgehog)	1
20	P19-119	Male	21	22.86	8.00	2.50	34.95	77.21	No	No	Regenerative (Minced cartilage)	1
21	P19-120	Male	33	28.93	5.50	8.50	56.92	39.3	Yes	Yes	Biological resurfacing (Mosaicplasty)	1
22	P19-123	Male	24	23.77	5.70	0.70	31.5	78.93	No	No	Regenerative (Hedgehog)	1
23	P19-124	Male	42	26.01	5.00	0	61.9	99.29	Yes	No	Metal resurfacing	1
24	P19-125	Female	36	20.80	5.00	1.90	15.02	66.01	Yes	Yes	Metal resurfacing	1
25	P19-133	Female	30	26.06	0.50	1.00	84.99	82.15	Yes	Yes	Biological resurfacing (Mosaicplasty)	1
26	P19-134	Male	16	25.46	4.20	0.20	65.18	81.94	No	No	Regenerative (Minced cartilage)	2
27	P19-135	Male	23	21.85	2.40	0.20	74.06	90.52	No	No	Regenerative (Minced cartilage)	1

ACT = articular chondrocyte transplantation, BMI = body mass index, IPFP = infrapatellar fat pad, KOOS = knee injury and osteoarthritis outcome score, MRI = magnetic resonance imaging, PT = patient, VAS = visual analogue score, Y = year.

Table 6.7 (continued). Patient characteristics of cartilage defect patient cohort (n = 53).

Patient	PT nr	Gender	Age	BMI	VAS T0	VAS 1Y	KOOS T0	KOOS 1Y	Previous trauma	Previous surgery	Type of surgery	Fibrosis IPFP (MRI)
28	P19-136	Male	25	25.62	1.30		68.06		Yes	No	Regenerative (Minced cartilage)	1
29	P19-181	Female	49	24.51	7.00		25.35		Yes	Yes	Metal resurfacing	1
30	P19-182	Male	38	26.47		0.60		78.48	Yes	No	Biological resurfacing (Mosaicplasty)	1
31	P20-014	Male	14	19.05	8.50		46.57		No	No	Regenerative (Hedgehog)	1
32	P20-019	Male	39	24.06	3.30	0.40	39.01		No	No	Metal resurfacing	0
33	P20-057	Male	48	26.42	5.00	3.80	36.31	43.76	Yes	Yes	Metal resurfacing	2
34	P20-058	Male	33	31.02	8.00	7.60	44.71	28.01	Yes	Yes	Metal resurfacing	2
35	P20-063	Male	15	21.20	6.70		56.21		No	No	Regenerative (Minced cartilage)	1
36	P20-064	Male	38	24.16	4.90		52.8		Yes	Yes	Biological resurfacing (ACT)	1

ACT = articular chondrocyte transplantation, BMI = body mass index, IPFP = infrapatellar fat pad, KOOS = knee injury and osteoarthritis outcome score, MRI = magnetic resonance imaging, PT = patient, VAS = visual analogue score, Y = year.

Table 6.7 (continued). Patient characteristics of cartilage defect patient cohort (n = 53).

Patient	PT nr	Gender	Age	BMI	VAS T0	VAS 1Y	KOOS T0	KOOS 1Y	Previous trauma	Previous surgery	Type of surgery	Fibrosis IPFP (MRI)
37	P20-065	Female	27	20.20	5.90	0.80	33.56	73.01	Yes	No	Biological resurfacing (ACT)	2
38	P20-083	Male	29	24.84		5.90		66.42	No	No	Biological resurfacing (Mosaicplasty)	0
39	P20-084	Male	26	25.49	4.80	2.20	61.7	67.52	Yes	Yes	Biological resurfacing (ACT)	1
40	P20-086	Male	31	24.74	1.70	2.80	56.69	57.16	Yes	Yes	Biological resurfacing (ACT)	2
41	P21-001	Male	15	16.98	0.80	0	75.65	91.96	No	No	Regenerative (Hedgehog)	NA
42	P21-002	Female	56	27.18	7.00	6.80	20.27	33.13	Yes	Yes	Metal resurfacing	0
43	P21-003	Male	18	20.88	5.20	1.00	58.79	73.82	Yes	Yes	Regenerative (Hedgehog)	2
44	P21-004	Female	36	22.46	4.60	2.90	23.53	67.44	No	No	Metal resurfacing	1
45	P21-005	Male	20	25.08	7.30	0	37.06	78.86	No	No	Regenerative (Hedgehog)	1

ACT = articular chondrocyte transplantation, BMI = body mass index, IPFP = infrapatellar fat pad, KOOS = knee injury and osteoarthritis outcome score, MRI = magnetic resonance imaging, PT = patient, VAS = visual analogue score, Y = year.

Table 6.7 (continued). Patient characteristics of cartilage defect patient cohort (n = 53).

Patient	PT nr	Gender	Age	BMI	VAS T0	VAS 1Y	KOOS T0	KOOS 1Y	Previous trauma	Previous surgery	Type of surgery	Fibrosis IPFP (MRI)
46	P21-007	Male	23	18.91	7.90	1.30	27.09	76.53	No	No	Biological resurfacing (ACT)	1
47	P21-008	Female	21	21.05	5.70	6.30	54.49	52.73	Yes	Yes	Biological resurfacing (ACT)	2
48	P21-009	Female	19	24.09	2.20	0	54.52	94.29	No	No	Regenerative (Minced cartilage)	0
49	P21-017	Male	29	28.33	7.40		44.49	73.07	Yes	Yes	Biological resurfacing (Mosaicplasty)	1
50	P21-018	Female	42	26.23					No	No	Biological resurfacing (Mosaicplasty)	1
51	P21-019	Female	52	22.59	8.40	10.00	11.73	25.97	Yes	Yes	Metal resurfacing	2

ACT = articular chondrocyte transplantation, BMI = body mass index, IPFP = infrapatellar fat pad, KOOS = knee injury and osteoarthritis outcome score, MRI = magnetic resonance imaging, PT = patient, VAS = visual analogue score, Y = year.

Table 6.7 (continued). Patient characteristics of cartilage defect patient cohort (n = 53).

Patient	PT nr	Gender	Age	BMI	VAS T0	VAS 1Y	KOOS T0	KOOS 1Y	Previous trauma	Previous surgery	Type of surgery	Fibrosis IPFP (MRI)
52	P21-034	Male	49	24.86	6.80	7.00	48.88	72.6	No	No	Metal resurfacing	1
53	P21-035	Male	45	23.89	6.90	7.90	13.78	96.19	Yes	Yes	Metal resurfacing	2
Mean (if applicable)			29.4 ± 11.7	24.3 ± 3.6	5.5 ± 2.3	3.0 ± 2.9	44.7 ± 18.1	67.1 ± 20.3				

ACT = articular chondrocyte transplantation, BMI = body mass index, IPFP = infrapatellar fat pad, KOOS = knee injury and osteoarthritis outcome score, MRI = magnetic resonance imaging, PT = patient, VAS = visual analogue score, Y = year.

Table 6.8. Patient characteristics and statistical analysis.

Parameter	Regenerative	Biological resurfacing	Metallic resurfacing
N	24	13	15
Age***	20.46 ± 6.7	30.46 ± 6.04	43.13 ± 7.69
BMI	23.29 ± 3.79	24.44 ± 3.05	25.62 ± 3.42
KOOS0	49.85 ± 15.58 (n = 17)	49.73 ± 18.12 (n = 10)	34.77 ± 18.02
KOOS3	72.71 ± 17.53 (n = 19)	68.24 ± 13.69 (n = 11)	57.84 ± 26.07 (n = 13)
ΔKOOS	31.3 ± 15 (n = 12)	17.91 ± 27.04 (n = 9)	22.67 ± 26.32 (n = 13)
VAS0	4.9 ± 2.65 (n = 17)	5.17 ± 2.41 (n = 10)	6.26 ± 1.48
VAS3	2.33 ± 2.73 (n = 19)	3.14 ± 2.76 (n = 10)	3.89 ± 3.14 (n = 14)
ΔVAS	-4.23 ± 2.31 (n = 12)	-1.81 ± 3.59 (n = 8)	-2.32 ± 2.3 (n = 14)

BMI = body mass index, CD = cartilage defect, KOOS = knee injury and osteoarthritis outcome score, OA = osteoarthritis, VAS = visual analogue scale, *** = $p < 0.001$.

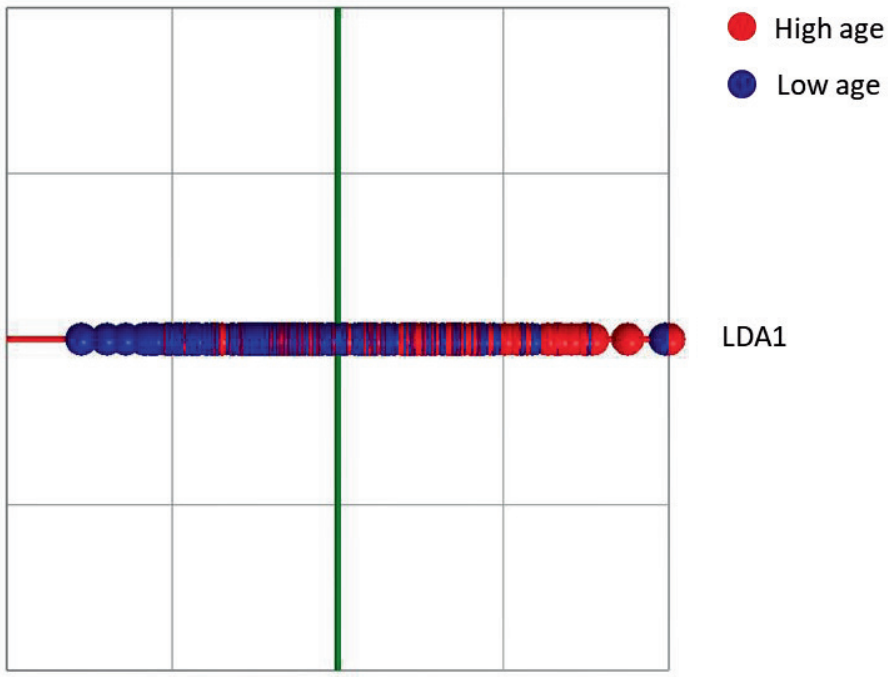

Figure 6.5. Linear discriminant analysis (LDA) of the age-related differences in the lipid profile of the infrapatellar fat pad (IPFP). A cross validation analysis (20% out) showed an overall classification rate of 65.5%. An age above or equal to 35 has been categorized as high; an age below 35 has been categorized as low.

Table 6.9. Correct classification rate of gender, age, and body mass index (BMI) after linear discriminant analysis (LDA) and cross validation with confusion matrix (20% out).

Parameter	Correct classification type	Correct classification rate
Gender	Overall (n = 53)	53.4% (141 of 264 cuts)
	Female (n = 18)	51.1% (46 of 90 cuts)
	Male (n = 35)	54.6% (95 of 174 cuts)
Age	Overall (n = 53)	**65.5% (173 of 264 cuts)**
	Age > 35 (n = 17)	61.9% (52 of 84 cuts)
	Age < 35 (n = 36)	**67.2% (121 of 180 cuts)**
BMI	Overall (n = 53)	43.9% (116 of 264 cuts)
	BMI > 25 (n = 31)	45.9% (50 of 109 cuts)
	BMI < 25 (n = 22)	42.6% (66 of 155 cuts)
Previous trauma	Overall (n = 53)	56.1% (148 of 264 cuts)
	No previous trauma (n = 21)	52.9% (55 of 104 cuts)
	Previous trauma (n = 32)	58.1% (93 of 160 cuts)
Previous surgery	Overall (n = 52)	51.1% (134 of 259 cuts)
	No previous surgery (n = 29)	52.8% (76 of 144 cuts)
	Previous surgery (n = 23)	50.4% (58 of 115 cuts)
Fibrosis (3 groups)	Overall (n = 51)	41.3% (105 of 254 cuts)
	None (n = 12)	28.3% (17 of 60 cuts)
	Normal-mild (n = 28)	41% (57 of 139 cuts)
	Moderate-severe (n = 11)	56.4% (31 of 55 cuts)
Fibrosis (yes/no)	Overall (n = 53)	51.6% (131 of 254 cuts)
	No (n = 12)	51.7% (31 of 60 cuts)
	Yes (n = 49)	51.5% (100 of 194 cuts)

BMI = body mass index.

Table 6.10. The top 20 *m/z* with highest loadings discriminating between cartilage defect patients > 35 years and cartilage defect patients < 35 years.

Age > 35		Age < 35	
m/z	Loading	*m/z*	Loading
893.75	0.230998	919.75	0.19423
750.55	0.212063	700.55	0.19041
885.55	0.196176	742.55	0.17309
642.45	0.192793	611.25	0.1674
766.55	0.187951	698.55	0.15113
794.55	0.167064	920.75	0.13147
900.75	0.136513	687.55	0.09868
895.75	0.117847	701.55	0.09778
901.75	0.11666	716.55	0.09509
751.55	0.113136	863.65	0.09261
615.15	0.111595	865.65	0.07981
767.55	0.111367	728.55	0.07839
792.55	0.110379	935.75	0.07422
721.45	0.100634	726.55	0.07394
886.55	0.098939	743.55	0.06986
894.75	0.098588	892.75	0.06769
749.55	0.093295	724.55	0.06669
797.65	0.09022	714.55	0.06548
790.55	0.086624	909.75	0.05902
926.75	0.083528	740.55	0.05522

Table 6.11. Correct classification rate of pre- and post-operative knee injury and osteoarthritis outcome score (KOOS) and visual analogue scale score (VAS) after linear discriminant analysis (LDA) and cross validation with confusion matrix (20% out).

Parameter	Correct classification type	Correct classification rate
Pre-op KOOS	Overall (n = 43)	53.7% (115 of 214 cuts)
	KOOS > 45 (n = 21)	53.8% (56 of 104 cuts)
	KOOS < 45 (n = 22)	53.6% (59 of 110 cuts)
Post-op KOOS	Overall (n = 43)	55.4% (119 of 215 cuts)
	KOOS > 70 (n = 24)	55.8% (67 of 120 cuts)
	KOOS < 70 (n = 29)	54.7% (52 of 95 cuts)
Pre-op VAS	Overall (n = 43)	52.8% (113 of 214 cuts)
	VAS > 5.8 (n = 22)	54.5% (60 of 110 cuts)
	VAS < 5.8 (n = 21)	51.0% (53 of 104 cuts)
Post-op VAS	Overall (n = 41)	44.4% (91 of 205 cuts)
	VAS > 2.4 (n = 20)	47% (47 of 100 cuts)
	VAS < 2.4 (n = 21)	41.9% (44 of 105 cuts)
ΔKOOS	Overall (n = 34)	51.8% (88 of 170 cuts)
	ΔKOOS > 10 (n = 24)	51.3% (59 of 115 cuts)
	ΔKOOS < 10 (n = 10)	52.7% (29 of 55 cuts)
ΔVAS	Overall (n = 34)	52.9% (90 of 170 cuts)
	ΔVAS > -2.7 (n = 16)	53.3% (48 of 90 cuts)
	ΔVAS < -2.7 (n = 18)	52.5% (42 of 80 cuts)

Pre-op = pre-operative, Post-op = post-operative, KOOS = knee injury and osteoarthritis outcome score, VAS = visual analogue scale.

Responders and non-responders (in relation to type of surgery)

The results acquired from patient outcome scores ΔKOOS and ΔVAS were matched with the type of surgery performed. Based on the results described in **Table 6.12**, it could be acknowledged that one patient with a ΔKOOS < 10, or bad clinical outcome, of the group in which the own cartialge was used to fill the defect could be classified in the correct group with a correct classification rate of 80%. However, it should be noted that this is only one patient.

Table 6.12. Correct classification rate of delta knee injury and osteoarthritis outcome score (KOOS) with a certain type of surgery (autograft resurfacing, regenerative, or prosthesis) after linear discriminant analysis (LDA) and cross validation with confusion matrix (20% out).

Parameter	Correct classification type	Correct classification rate
ΔKOOS	Overall (n = 34)	26.5%
	ΔKOOS > 10 + biological resurfacing (n = 4)	5%
	ΔKOOS > 10 + regenerative (n = 11)	9.1%
	ΔKOOS > 10 + metal resurfacing (n = 8)	32.5%
	ΔKOOS < 10 + biological resurfacing (n = 5)	40%
	ΔKOOS < 10 + regenerative (n = 1)	**80%**
	ΔKOOS < 10 + metal resurfacing (n = 5)	48%
ΔVAS	Overall (n = 34)	17.1%
	ΔVAS < -2.7 + biological resurfacing (n = 3)	6.7%
	ΔVAS < -2.7 + regenerative (n = 8)	0%
	ΔVAS < -2.7 + metal resurfacing (n = 7)	2.9%
	ΔVAS > -2.7 + biological resurfacing (n = 5)	40%
	ΔVAS > -2.7 + regenerative (n = 4)	40%
	ΔVAS > -2.7 + metal resurfacing (n = 7)	25.7%

KOOS = knee injury and osteoarthritis outcome score, VAS = visual analogue scale

Infrapatellar fat pad intra-heterogeneity

In addition, histological scoring was performed to address in which tissue type (adipose tissue or connective tissue) the cuts in the IPFP were made. An estimation of the amount of adipose tissue or connective tissue was made of the whole IPFP tissue section in 53 patients on a 1-5 scale with 1) mostly adipose tissue (90-100%), 2) predominantly adipose tissue (60-90%), 3) equal amount of adipose tissue and connective tissue (40-60%), 4) predominantly connective tissue (60-90%), and 5) mostly connective tissue (90-100%).

Overall, evaluating the whole IPFP biopsy section, 119 cuts were estimated to be 60-90% of adipose tissue, 100 cuts were estimated to be equal adipose tissue and connective tissue (40-60%), 40 cuts were estimated to be predominantly connective tissue (60-90%), and 5 cuts were estimated to be connective tissue (90-100%) (**Table 6.14** and **Figure 6.6**). No discrimination in lipid profile after LDA was shown based on tissue type (**Figure 6.6**).

A cross validation (20% out) with confusion matrix showed an overall correct classification rate of 42.4% (112 of 264 cuts). For the cuts made in predominantly adipose tissue (60-90%), 66 of 119 cuts were correctly classified (55.5%), 13 were classified incorrectly as equally adipose tissue and connective tissue (40-60%), 19 were incorrectly classified as predominantly connective tissue (60-90%), and 21 were incorrectly classified as mostly connective tissue (90-100%). For the cuts classified as having an equal amount of adipose tissue and connective tissue, 21 of 100 cuts (21%) were correctly classified, compared to 29 incorrectly classified as predominantly adipose tissue, 20 incorrectly classified as predominantly connective tissue and 30 incorrectly classified as mostly connective tissue. Next, for the cuts made in predominantly connective tissue, 22 of 40 were correctly classified (55%), compared to 7 incorrectly classified as predominantly adipose tissue, 4 as equally adipose tissue or connective tissue, and 7 mostly connective tissue. Finally, for the cuts made in the connective tissue, 3 of 5 were correctly classified (60%), compared to 1 incorrectly classified as mostly adipose tissue, and 1 incorrectly classified as predominantly connective tissue.

Additionally an estimation of the tissue type of each cut was made using the same scale. Out of a total of 265 cuts, 23 were not found and 55 were inconclusive. A total of 187 cuts were used for LDA and cross validation analysis. 11 cuts were classified as mostly adipose tissue (90-100%), 70 cuts were classified as predominantly adipose tissue (60-90%), 66 cuts were classified as equal amount of adipose tissue and connective tissue (40-60%), 73 cuts were classified as predominantly connective tissue (60-90%), and 20 cuts were classified as mostly connective tissue (90-100%) (**Figure 6.6**).

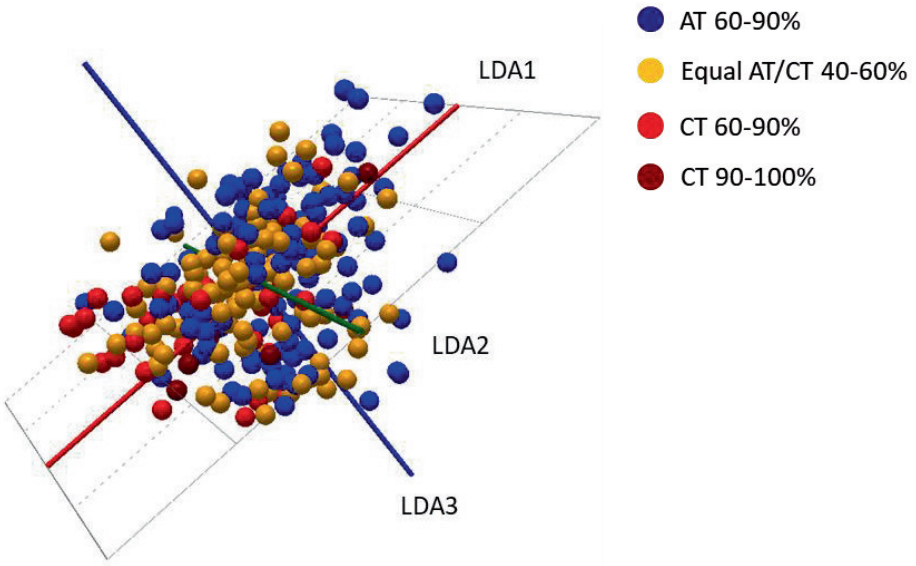

Figure 6.6. Linear discriminant analysis (LDA) of the differences in the lipid profile of the infrapatellar fat pad (IPFP) related to intra-tissue heterogeneity. A cross validation analysis (20% out) showed an overall classification rate of 42.4%. AT = adipose tissue, CT = connective tissue.

For LDA and cross validation (20% out) the 2 most distinctive profiles (adipose tissue and connective tissue 90-100%) were used. 11 cuts were characterized as adipose tissue, divided over 7 patients. In comparison, 19 cuts were characterized as connective tissue, divided over 9 patients. LDA (**Figure 6.7**) and cross validation (20% out) with confusion matrix showed an overall correct classification rate of 90% (27 of 30 cuts). 9 of 11 cuts (81.8%) were classified correctly as adipose tissue, whereas 18 of 19 cuts (94.7%) were classified correctly as connective tissue. The top 20 lipids corresponding to adipose tissue or connective tissue after LDA were depicted in **Table 6.13**.

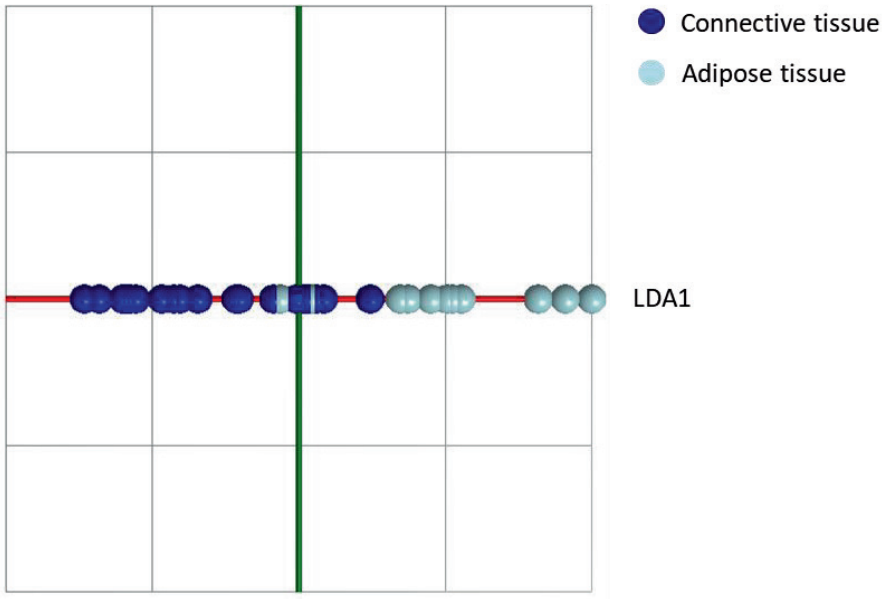

Figure 6.7. Linear discriminant analysis (LDA) of the differences in the lipid profile of the infrapatellar fat pad (IPFP) related to intra-tissue heterogeneity. A cross validation analysis (20% out) showed an overall classification rate of 90% for the comparison of adipose tissue vs connective tissue.

Taking into account IPFPs intra-tissue heterogeneity

Additionally, the IPFPs tissue heterogeneity was taken into account while running the analysis (only cuts classified as 90-100% adipose tissue or connective tissue). Looking at the three most important measures for patient outcome, post-operative KOOS (adipose tissue or connective tissue) and post-operative VAS (connective tissue) give overall correct classification rates of ≥ 70% (**Table 6.14**). However, it has to be taken into account that the sample size for these analyses was very low. Out of all cuts made in 53 patients (= 265), only 11 cuts were with confidence classified as adipose tissue and 19 cuts were classified as connective tissue (90-100% adipose tissue or connective tissue). Whereas not scores were available for all patients, low numbers of patients or cuts were used for analysis.

Table 6.13. Loadings corresponding to LD1 depicted in Figure 6.7, discriminating adipose tissue from connective tissue.

Adipose tissue		Connective tissue	
m/z	Loading	*m/z*	Loading
615.15	0.395762	687.55	0.05958
919.75	0.316416	600.25	0.05128
893.75	0.315596	717.35	0.04726
616.15	0.249757	744.55	0.04645
891.75	0.235283	601.25	0.04537
617.15	0.235109	601.35	0.04254
917.75	0.198516	643.35	0.04214
920.75	0.184062	602.25	0.04208
921.75	0.172514	629.35	0.04095
894.75	0.15439	602.35	0.03795
892.75	0.129241	628.35	0.03737
918.75	0.125189	630.35	0.03704
612.25	0.124764	641.35	0.03698
895.75	0.119912	629.25	0.03676
618.15	0.11469	628.25	0.03438
659.15	0.111297	718.55	0.03407
610.15	0.097067	770.55	0.03389
922.75	0.066484	615.35	0.03347
697.45	0.065953	627.25	0.03344
661.15	0.063116	642.35	0.03321

m/z = mass-to-charge ratio

Table 6.14. Correct classification rate of pre- and post-operative knee injury and osteoarthritis outcome score (KOOS) and visual analogue scale (VAS) taking only one tissue type (adipose tissue or connective tissue) into account after linear discriminant analysis (LDA) and cross validation with confusion matrix (20% out).

Parameter	AT or CT	Overall correct classification rate
Pre-op KOOS	Adipose tissue	11%
Pre-op KOOS	Connective tissue	53%
Post-op KOOS	Adipose tissue	**70%**
Post-op KOOS	Connective tissue	**73%**
Pre-op VAS	Adipose tissue	33%
Pre-op VAS	Connective tissue	33%
Post-op VAS	Adipose tissue	33%
Post-op VAS	Connective tissue	**73%**
ΔKOOS	Adipose tissue	50%
ΔKOOS	Connective tissue	**70%**
ΔVAS	Adipose tissue	50%
ΔVAS	Connective tissue	Not enough data
Fibrosis	Adipose tissue	45%
Fibrosis	Connective tissue	50%

AT = adipose tissue, CT = connective tissue, Pre-op = pre-operative, Post-op = post-operative, KOOS = knee injury and osteoarthritis outcome score, VAS = visual analogue scale.

Considering the described method and according to the results described above, we were not able to discriminate patients who responded well to cartilage repair treatment (responders) from patients who responded poorly to cartilage repair patients (non-responders) based on their lipid signature using REIMS. It was shown that the IPFP's intra-tissue heterogeneity (the appearance of adipose tissue or connective tissue) might have an influence on the lipid signature measured, although this was based on very low sample numbers (**Table 6.14**). Therefore, in the next section of **this Chapter**, the use of a method utilizing LMD in combination with a well-understood proteomics approach was investigated to identify the proteome of either adipose tissue or connective tissue in the IPFP of cartilage repair patients. Because of the fact that LMD has not been utilized on the IPFP according to our knowledge, a protocol had to be optimized.

Laser capture microdissection (LMD)

The IPFPs adipose like, fatty, and sticky nature has been demonstrated to cause problems during the cutting and collecting part of the LMD procedure, including burning of the tissue or lack of detachment. To overcome this, multiple slides (ITO, PEN membrane and FRAME) and washing steps were tested for dehydration of the tissue and the removal of lipids within the IPFP and facilitate cutting with LMD.

After LMD on tissue sections treated with desiccation only or slides which were not completely dehydrated, tissue was not detached from the slides or captured. It was acknowledged that the membrane of PEN and FRAME slides loosened after chloroform washing. Although the membrane detaches from the slide alongside the edges, sections, which were dehydrated through ethanol series followed by chloroform, were best cut and captured. Using LMD on IPFP on ITO slides, as has been described by Mezger et al. for multi-omics approaches[257], would have been favored, however was not possible due to the amount of IPFP tissue necessary for LC-MS/MS analysis and the time necessary for tissue ablation. In addition, the tissue on ITO slides is prone to burn, the time needed might cause molecule delocalization or breakdown.

An area of 0.15 cm^2 of adipose tissue of IPFP led to a concentration of 1.62 µg/µl protein and the identification of 33 proteins with high confidence. Additionally an area of 0.2 cm^2 led to a protein concentration of 4.14 µg/µl and the identification of 71 proteins with high confidence. Alternatively, concentrations of 3.1 (15 sections) and 3.5 (20 sections) µg/µl were obtained using cryosectioning and collection in an Eppendorf tube only instead of LMD. Here, 809 and 955 proteins were identified with high confidence respectively (**Figure 6.8**).

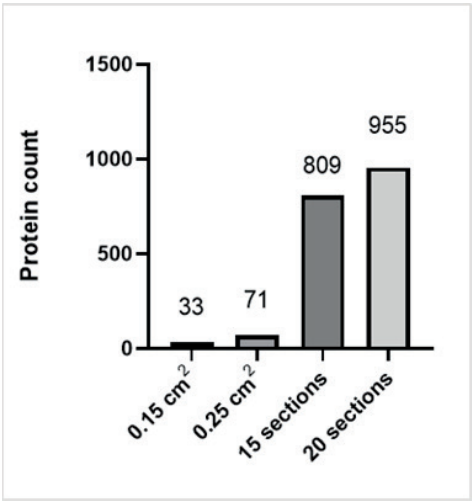

Figure 6.8. Protein count with high confidence in the adipose tissue of the infrapatellar fat pad (IPFP) after cutting 0.15 cm^2 or 0.25 cm^2 with LMD, or 15 or 20 cryosections of the whole IPFP, not taking into account the IPFPs intra-tissue heterogeneity.

In conclusion, it was not feasible to cut enough IPFP tissue using LMD for proteomics analysis and acquire a sufficient amount of proteins for analysis. Therefore, in the next section of this Chapter, proteomic analysis of whole tissue sections of the IPFP of cartilage repair patients was performed.

Proteomic analysis identified prognostic biomarkers in the infrapatellar fat pad of cartilage defect patients

Proteomic analysis was conducted to evaluate the proteome of the IPFP and to evaluate whether proteins might be a better target for the classification of patients based on their characteristics and pre- and post-operative clinical state or outcome.

Despite the fact that a big variety (341-898 proteins, average 601.6 ± 124.1) in protein numbers was measured in this sample cohort, no batch effect (ANOVA with F value 0.411 and p-value 0.665) or outlier (interquartile range (IQR = Q3 - Q1) stating that values > Q3 + 1.5*IQR or values < Q1 – 1.5*IQR are considered outliers) could be detected.

Patients with different gender, age, and BMI show distinctive protein abundancies in the infrapatellar fat pad of cartilage defect patients

Gender related differences in protein profiles of cartilage defect patients

Looking at gender-related differences, 12 proteins were found to be significantly upregulated in female patients compared to male patients, including a top three of hematopoietic progenitor cell antigen CD34 (CD34), cytochrome c (CytC), and serum amyloid A-4 protein (SAA4) with the highest abundance ratio's (**Table 6.15**). On the contrary, four proteins were found significantly downregulated in female patients compared to male patients, including hemoglobin subunit zeta (HBZ), nucleoside diphosphate kinase A (NDPKA), aggrecan core protein (ACAN), and 40S ribosomal protein S27 (MPS1) (**Table 6.15**).

Age related differences in protein profiles of cartilage defect patients

In addition, seven proteins were found to be in patients above 35 years compared to patients below the age of 35, among which a top three of cartilage intermediate layer protein 2 (CILP-2), protein S100-A9 (S100A9/ MRP14), and neutrophil defensin 1 (DEFA1) (**Table 6.16**). Contrarily, six proteins were found significantly downregulated in older patients compared to younger patients, including myelin basic protein 7 (MBP7), microfibril-associated glycoprotein 4 (MAGP4), and desmin (**Table 6.16**).

BMI related differences in protein profiles of cartilage defect patients

Furthermore, seven proteins were found to be upregulated in patients with high BMI (BMI > 25), compared to low BMI (BMI < 25) among which a top three of CILP-2, CILP-1, and tenascin-X (TNX) (**Table 6.17**). Moreover, 13 proteins were found significantly downregulated in patients with high BMI compared to low BMI, including a top three of tubulin beta-4A chain (TUBB4A), coatomer subunit epsilon (COPE), and ubiquitin-60S ribosomal protein L40 (**Table 6.17**).

Table 6.15. Significant up- and down-regulated proteins in the infrapatellar fat pad of female patients compared to male patients.

Accession	Description	Abundance ratio	Abundance ratio (log2)	Abundance ratio adj. p- value
Upregulated				
P28906	Hematopoietic progenitor cell antigen CD34	100	6.64	5.27E-16
P99999	Cytochrome c	2.44	1.28	3.47E-07
P35542	Serum amyloid A-4 protein	2.18	1.12	1.46E-05
P07099	Epoxide hydrolase 1	2.09	1.06	5.08E-05
P01019	Angiotensinogen	1.84	0.88	1.65E-03
P00738	Haptoglobin	1.64	0.72	0.02
P06702	Protein S100-A9	1.63	0.70	0.02
P08185	Corticosteroid-binding globulin	1.62	0.70	0.02
P00450	Ceruloplasmin	1.61	0.69	0.02
Q03135	Caveolin-1	1.61	0.69	0.02
P62987	Ubiquitin-60S ribosomal protein L40	1.57	0.65	0.04
Q99707	Methionine synthase	1.57	0.65	0.04
Downregulated				
P02008	Hemoglobin subunit zeta	0.39	-1.35	6.44E-07
P15531	Nucleoside diphosphate kinase A	0.47	-1.08	2.13E-04
P16112	Aggrecan core protein	0.53	-0.93	2.99E-03
P42677	40S ribosomal protein S27	0.60	-0.74	0.04

Table 6.16. Significant up- and down-regulated proteins in the infrapatellar fat pad of patients with an age above 35 compared to patients with an age below 35.

Accession	Description	Abundance ratio	Abundance ratio (log2)	Abundance ratio adj. p- value
Upregulated				
Q8IUL8	Cartilage intermediate layer protein 2	2.09	1.06	2.09E-03
P06702	Protein S100-A9	1.81	0.86	6.22E-03
P59665	Neutrophil defensin 1	1.70	0.76	0.02
P00918	Carbonic anhydrase 2	1.69	0.75	0.03
P00915	Carbonic anhydrase 1	1.66	0.73	0.03
P68871	Hemoglobin subunit beta	1.65	0.72	0.04
P35542	Serum amyloid A-4 protein	1.61	0.69	0.04
Downregulated				
P02686	Myelin basic protein	0.33	-1.58	3.42E-05
P55083	Microfibril-associated glycoprotein 4	0.37	-1.42	8.88E-05
P17661	Desmin	0.44	-1.20	2.96E-03
P29536	Leiomodin-1	0.47	-1.09	0.03
Q08170	Serine/arginine-rich splicing factor 4	0.49	-1.02	0.03
Q8N474	Secreted frizzled-related protein 1	0.52	-0.94	0.03

Table 6.17. Significant up- and down-regulated proteins in the infrapatellar fat pad of patients with a BMI above 25 compared to patients with a BMI below 25.

Accession	Description	Abundance ratio	Abundance ratio (log2)	Abundance ratio adj. p-value
Upregulated				
Q8IUL8	Cartilage intermediate layer protein 2	2.72	1.44	9.42E-13
O75339	Cartilage intermediate layer protein 1	1.71	0.78	5.62E-04
P22105	Tenascin-X	1.61	0.69	3.28E-03
P35443	Thrombospondin-4	1.55	0.63	8.38E-03
Q99972	Myocilin	1.52	0.6	0.01
Q8N474	Secreted frizzled-related protein 1	1.51	0.6	0.02
Q9BXN1	Asporin	1.50	0.58	0.02
Downregulated				
P04350	Tubulin beta-4A chain	0.01	-6.64	7.23E-16
O14579	Coatomer subunit epsilon	0.385	-1.38	1.81E-09
P62987	Ubiquitin-60S ribosomal protein L40	0.47	-1.09	9.92E-06
P02686	Myelin basic protein	0.492	-1.02	5.15E-05
P69891	Hemoglobin subunit gamma-1	0.536	-0.9	8.94E-04
P49327	Fatty acid synthase	0.581	-0.78	7.88E-03
P15531	Nucleoside diphosphate kinase A	0.591	-0.76	0.01
Q14767	Latent-transforming growth factor beta-binding protein 2	0.616	-0.7	0.03

Table 6.17 (continued). Significant up- and down-regulated proteins in the infrapatellar fat pad of patients with a BMI above 25 compared to patients with a BMI below 25.

Accession	Description	Abundance ratio	Abundance ratio (log2)	Abundance ratio adj. p-value
Downregulated				
P08571	Monocyte differentiation antigen CD14	0.616	-0.7	0.03
P09486	SPARC	0.619	-0.69	0.03
P30047	GTP cyclohydrolase 1 feedback regulatory protein	0.626	-0.68	0.04
O95399	Urotensin-2	0.632	-0.66	0.05
Q93077	Histone H2A type 1-C	0.634	-0.66	0.05

Effect of previous trauma or surgery on the protein profile of the infrapatellar fat pad of cartilage defect patients

Previous trauma was associated with a significant upregulation of five proteins, including CD34, CILP-2, and dynamin-2 (**Table 6.18**). Contrarily, previous surgery was associated with a significant downregulation of 11 proteins, including MBP, fatty acid synthase (FAS), and glutathione hydrolase 5 proenzyme (P36269) (**Table 6.18**).

Similarly, patients with a history of previous surgery show a significant upregulation of four proteins, among which CD34, CILP-2, and CILP-1 (**Table 6.19**). On the other hand, 10 proteins were significantly downregulated, including beta-actin-like protein 2 (ACTBL2), NDPKA, and GTP cyclohydrolase 1 feedback regulatory protein (GFRP).

Infrapatellar fat pad fibrosis affects protein appearance in the IPFP of cartilage defect patients

The fibrotic state of the IPFP, based on the patients' MRI, was associated with a significant upregulation of 10 proteins, including CD34, dynamin-2, and microsomal glutathione S-transferase 1 (MGST1) (**Table 6.20**). 14 proteins were found to be significantly downregulated in the group of patients with high IPFP fibrosis, including S100A9, apoliprotein C-II (APOC-II), and von Willebrand factor A domain-containing protein 5A (VWA5A) (**Table 6.20**).

Table 6.18. Significant up- or down-regulated proteins in the infrapatellar fat pad of patients with a history of previous trauma.

Accession	Description	Abundance ratio	Abundance ratio (log2)	Abundance ratio adj. p-value
Upregulated				
P28906	Hematopoietic progenitor cell antigen CD34	100	6.64	5.01E-16
Q8IUL8	Cartilage intermediate layer protein 2	2.08	1.05	1.15E-05
P50570	Dynamin-2	1.91	0.93	1.53E-03
O75339	Cartilage intermediate layer protein 1	1.58	0.66	7.13E-04
P49747	Cartilage oligomeric matrix protein	1.51	0.6	1.42E-03
Downregulated				
P02686	Myelin basic protein	0.434	-1.2	7.45E-08
P49327	Fatty acid synthase	0.476	-1.07	2.50E-07
P36269	Glutathione hydrolase 5 proenzyme	0.566	-0.82	9.88E-03
P30047	GTP cyclohydrolase 1 feedback regulatory protein	0.586	-0.77	0.01
P40261	Nicotinamide N-methyltransferase	0.608	-0.72	0.05
P11413	Glucose-6-phosphate 1-dehydrogenase	0.627	-0.67	0.03
P07108	Acyl-CoA-binding protein	0.645	-0.63	0.03
P16930	Fumarylacetoacetase	0.646	-0.63	0.03

Table 6.18 (continued). Significant up- or down-regulated proteins in the infrapatellar fat pad of patients with a history of previous trauma.

Accession	Description	Abundance ratio	Abundance ratio (log2)	Abundance ratio adj. p-value
Downregulated				
P55083	Microfibril-associated glycoprotein 4	0.649	-0.62	0.03
P33121	Long-chain-fatty-acid--CoA ligase 1	0.652	-0.62	0.03
P35568	Insulin receptor substrate 1	0.665	-0.59	0.05

Table 6.19. Significant up- or down-regulated proteins in the infrapatellar fat pad of patients with a history of surgery.

Accession	Description	Abundance ratio	Abundance ratio (log2)	Abundance ratio adj. p-value
Upregulated				
P28906	Hematopoietic progenitor cell antigen CD34	100	6.64	6.73E-16
Q8IUL8	Cartilage intermediate layer protein 2	3.03	1.6	3.15E-10
O75339	Cartilage intermediate layer protein 1	1.74	0.8	6.87E-06
Q14956	Transmembrane glycoprotein NMB	1.59	0.67	7.93E-04
Downregulated				
Q562R1	Beta-actin-like protein 2	0.323	-1.63	2.91E-08
P15531	Nucleoside diphosphate kinase A	0.491	-1.03	0.01
P30047	GTP cyclohydrolase 1 feedback regulatory protein	0.504	-0.99	9.89E-05
P04271	Protein S100-B	0.557	-0.85	1.11E-03
P49327	Fatty acid synthase	0.576	-0.8	5.31E-04
P07108	Acyl-CoA-binding protein	0.588	-0.77	1.08E-03

Table 6.19 (continued). Significant up- or down-regulated proteins in the infrapatellar fat pad of patients with a history of surgery.

Accession	Description	Abundance ratio	Abundance ratio (log2)	Abundance ratio adj. p-value
Downregulated				
P55083	Microfibril-associated glycoprotein 4	0.618	-0.69	5.30E-03
P02686	Myelin basic protein	0.628	-0.67	0.03
Q01469	Fatty acid-binding protein 5	0.653	-0.61	0.03
Q08170	Serine/arginine-rich splicing factor 4	0.661	-0.6	0.03

Table 6.20. Significant up- or down-regulated proteins in the infrapatellar fat pad of patients with high fibrosis.

Accession	Description	Abundance ratio	Abundance ratio (log2)	Abundance ratio adj. p-value
Upregulated				
P28906	Hematopoietic progenitor cell antigen CD34	5.97	2.58	5.64E-13
P50570	Dynamin-2	2.60	1.38	7.05E-03
P10620	Microsomal glutathione S-transferase 1	2.54	1.34	8.48E-05
P17612	cAMP-dependent protein kinase catalytic subunit alpha	2.41	1.27	0.01
P0DOX3	Immunoglobulin delta heavy chain	2.36	1.24	0.01
Q14767	Latent-transforming growth factor beta-binding protein 2	2.35	1.23	0.01
P68133	Actin, alpha skeletal muscle	2.31	1.21	2.71E-06
P15559	NAD(P)H dehydrogenase [quinone] 1	2.28	1.19	0.02
Q13596	Sorting nexin-1	2.24	1.16	0.01

Table 6.20 (continued). Significant up- or down-regulated proteins in the infrapatellar fat pad of patients with high fibrosis.

Accession	Description	Abundance ratio	Abundance ratio (log2)	Abundance ratio adj. p-value
Upregulated				
Q8IUL8	Cartilage intermediate layer protein 2	2.14	1.1	0.05
Downregulated				
P06702	Protein S100-A9	0.48	-1.08	1.98E-06
P02655	Apolipoprotein C-II	0.57	-0.81	8.45E-05
O00534	von Willebrand factor A domain-containing protein 5A	0.58	-0.8	0.01
O15144	Actin-related protein 2/3 complex subunit 2	0.58	-0.79	0.01
P04003	C4b-binding protein alpha chain	0.58	-0.79	1.11E-04
P01871	Immunoglobulin heavy constant mu	0.59	-0.75	2.35E-04
O75367	Core histone macro-H2A.1	0.61	-0.72	3.54E-03
P00738	Haptoglobin	0.61	-0.71	5.39E-04
P01861	Immunoglobulin heavy constant gamma 4	0.61	-0.71	5.39E-04
P01591	Immunoglobulin J chain	0.62	-0.68	1.19E-03
O43866	CD5 antigen-like	0.63	-0.66	1.55E-03
P00739	Haptoglobin-related protein	0.65	-0.63	0.01
P02671	Fibrinogen alpha chain	0.66	-0.59	0.01
P02675	Fibrinogen beta chain	0.67	-0.58	0.01

Can proteins in the infrapatellar fat pad predict patient outcome based on pre- and post-operative knee injury and osteoarthritis outcome score (KOOS) and visual analogue scale (VAS) score?

Looking at pre-operative patient outcome based on KOOS, 4 proteins were significantly upregulated in patients which had good KOOS scores prior to surgery

compared to bad KOOS scores, including collagen alpha-1(I) chain (COL1A1), collagen alpha-2(V) chain (COL5A2), urotensin-2, and TUBB4A (**Table 6.21**). No proteins were found significantly downregulated in the same group (**Table 6.21**).

Furthermore, for post-operative patient outcome based on KOOS, 13 proteins were significantly upregulated in patients with good KOOS scores after surgery compared to bad KOOS scores, including SPARC-related modular calcium-binding protein 1 (SMOC1-SPARC), collagen alpha-1(XIV) chain (COL14A1), and rho-related GTP-binding protein RHOC (**Table 6.22**). 13 proteins were found significantly downregulated in the same group, including CD34, hemoglobin gamma subunit 2 (HBG2), and epoxide hydrolase 1 (EPHX1) (**Table 6.22**).

Patients with bad surgical outcome (ΔKOOS < 10), four proteins were significantly upregulated in comparison to good surgical outcome, including CD34, CILP-2, TUBB4A and platelet basic protein (PBP) (**Table 6.23**). Nine proteins were significantly downregulated in the same group, including a top three of ACAN, hematopoietic lineage cell-specific protein (HCLS1), and gamma-interferon-inducible lysosomal thiol reductase (GILT) (**Table 6.23**).

Table 6.21. Significant upregulated proteins in the infrapatellar fat pad of patients with good pre-operative knee injury and osteoarthritis outcome scores (KOOS).

Accession	Description	Abundance ratio	Abundance ratio (log2)	Abundance ratio adj. p-value
Upregulated				
P02452	Collagen alpha-1(I) chain	1.62	0.69	0.69
P05997	Collagen alpha-2(V) chain	1.52	0.60	0.60
Downregulated				
O95399	Urotensin-2	0.34	-1.57	0.01
P04350	Tubulin beta-4A chain	0.01	-6.64	8.12E-16

Table 6.22. Significant up- or down-regulated proteins in the infrapatellar fat pad of patients with good post-operative knee injury and osteoarthritis outcome scores (KOOS).

Accession	Description	Abundance ratio	Abundance ratio (log2)	Abundance ratio adj. p-value
Upregulated				
Q9H4F8	SPARC-related modular calcium-binding protein 1	2.04	1.03	3.46E-03
Q05707	Collagen alpha-1(XIV) chain	1.77	0.83	1.32E-04
P08134	Rho-related GTP-binding protein RhoC	1.71	0.78	0.04
P14555	Phospholipase A2, membrane associated	1.71	0.78	0.01
Q4ZHG4	Fibronectin type III domain-containing protein 1	1.67	0.74	0.02
P14317	Hematopoietic lineage cell-specific protein	1.63	0.71	0.04
P42677	40S ribosomal protein S27	1.61	0.69	0.04
Q15651	High mobility group nucleosome-binding domain-containing protein 3	1.61	0.68	0.01
P62995	Transformer-2 protein homolog beta	1.56	0.64	0.03
P08311	Cathepsin G	1.56	0.64	0.01
P27695	DNA-(apurinic or apyrimidinic site) lyase	1.53	0.61	0.05
P16401	Histone H1.5	1.51	0.59	0.03
P15880	40S ribosomal protein S2	1.49	0.58	0.04
Downregulated				
P28906	Hematopoietic progenitor cell antigen CD34	0.139	-2.84	5.27E-16
P69892	Hemoglobin subunit gamma-2	0.30	-1.75	5.27E-16
P07099	Epoxide hydrolase 1	0.47	-1.1	3.42E-09
Q99972	Myocilin	0.52	-0.95	3.94E-12

Table 6.22 (continued). Significant up- or down-regulated proteins in the infrapatellar fat pad of patients with good post-operative knee injury and osteoarthritis outcome scores (KOOS).

Accession	Description	Abundance ratio	Abundance ratio (log2)	Abundance ratio adj. p-value
Downregulated				
P02775	Platelet basic protein	0.53	-0.92	1.12E-11
P07451	Carbonic anhydrase 3	0.54	-0.89	5.16E-05
P00915	Carbonic anhydrase 1	0.55	-0.87	1.73E-10
P01889	HLA class I histocompatibility antigen, B alpha chain	0.56	-0.85	4.41E-03
P16452	Erythrocyte membrane protein band 4.2	0.58	-0.79	4.81E-05
Q8IUL8	Cartilage intermediate layer protein 2	0.59	-0.75	3.46E-03
P01871	Immunoglobulin heavy constant mu	0.62	-0.68	4.02E-07
P15559	NAD(P)H dehydrogenase [quinone] 1	0.64	-0.65	0.05
P02042	Hemoglobin subunit delta	0.64	-0.65	1.35E-06
P69891	Hemoglobin subunit gamma-1	0.66	-0.6	8.53E-06
P00918	Carbonic anhydrase 2	0.66	-0.59	1.21E-05
P68871	Hemoglobin subunit beta	0.67	-0.59	1.32E-05
P21926	CD9 antigen	0.67	-0.59	1.35E-05

Table 6.23. Significant up- or down-regulated proteins in the infrapatellar fat pad of patients with bad surgical outcome (Δ knee injury and osteoarthritis outcome score (KOOS).

Accession	Description	Abundance ratio	Abundance ratio (log2)	Abundance ratio adj. p- value
Upregulated				
P28906	Hematopoietic progenitor cell antigen CD34	100	6.64	4.32E-16
Q8IUL8	Cartilage intermediate layer protein 2	2.98	1.58	2.49E-05
P04350	Tubulin beta-4A chain	2.14	1.1	5.52E-03
P02775	Platelet basic protein	1.60	0.68	3.18E-03
Downregulated				
P16112	Aggrecan core protein	0.01	-6.64	4.32E-16
P14317	Hematopoietic lineage cell-specific protein	0.36	-1.46	3.5E-05
P13284	Gamma-interferon-inducible lysosomal thiol reductase	0.37	-1.43	1.8E-05
P30047	GTP cyclohydrolase 1 feedback regulatory protein	0.40	-1.33	3.25E-03
P08571	Monocyte differentiation antigen CD14	0.42	-1.24	0.05
P14555	Phospholipase A2, membrane associated	0.42	-1.24	4.83E-04
P05413	Fatty acid-binding protein, heart	0.46	-1.12	0.01
Q07065	Cytoskeleton-associated protein 4	0.47	-1.09	0.01
Q92954	Proteoglycan 4	0.53	-0.93	0.05

A String pathway analysis of the proteins significantly different in patients with bad clinical outcome (ΔKOOS) showed 11 of 13 proteins (in red) to be related to the extracellular region (Cellular Component, Gene Ontology, false discovery rate (FDR) = 0.0035) (**Figure 6.9A**). In addition, eight proteins were related to the hematopoietic system (yellow, Tissue expression, TISSUES, FDR = 0.0273), four to bone marrow cells (green, Tissue expression, TISSUES, FDR = 0.0077), and two to synovia (red, Tissue expression, TISSUES, FDR = 0.0081), and rheumatoid arthritis disease specific synovial tissue (blue, Tissue expression, TISSUES, FDR = 0.0116) (**Figure 6.9B**).

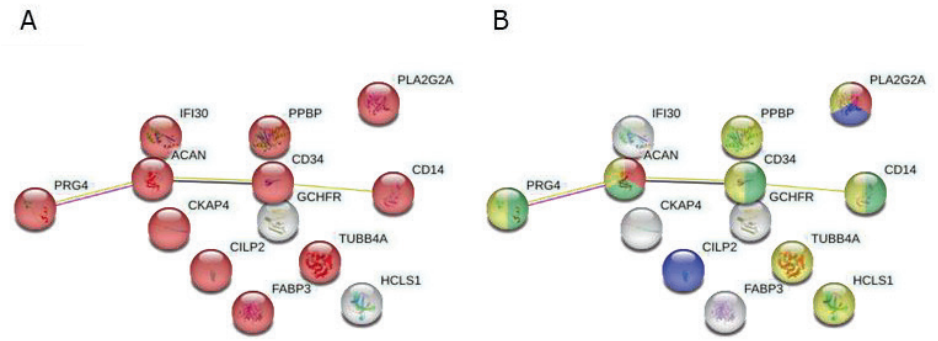

Figure 6.9. String pathway analysis of ΔKOOS with functional enrichments of the network in which (A) shows proteins related to the extracellular region (red) and (B) proteins related to synovia (red), rheumatoid arthritis disease specific synovial tissue (blue), bone marrow cells (green) and/or the hematopoietic system (yellow).

Patients with high pain scores (VAS) prior to surgery, showed seven proteins significantly upregulated compared to low VAS scores, including urotensin-2, fibrillin-1 and stromelysin-1 (**Table 6.24**). Four proteins were significantly downregulated in the same group: CD34, actin, phosphatidylinositol-binding clathrin assembly protein (PICALM), and nucleolar protein 3 (NOL3) (**Table 6.24**).

Post-operatively, high VAS scores were associated with a significant upregulation of 13 proteins, including CD34, PBP, and EPHX1 (**Table 6.25**). On the other hand, five proteins were significantly downregulated in the same group, including allograft inflammatory factor 1 (AIF1), PICALM, and agrin (**Table 6.25**).

Finally, high ΔVAS scores, or bad patient outcome, was associated with a significant upregulation of 12 proteins, among which insulin receptor substrate 1 (IRS1), GILT, and fatty acid-binding protein (FAB) (**Table 6.26**). 13 proteins were associated with a significant downregulation, including CD34, ACAN, and RHOG in the same group (**Table 6.26**).

Table 6.24. Significant up- or down-regulated proteins in the infrapatellar fat pad of patients with high pre-operative visual analogue scale (VAS) scores.

Accession	Description	Abundance ratio	Abundance ratio (log2)	Abundance ratio adj. p-value
Upregulated				
O95399	Urotensin-2	2.97	1.57	3.20E-06
P35555	Fibrillin-1	2.67	1.42	5.24E-05
P08254	Stromelysin-1	2.28	1.19	1.52E-03
Q8N163	Cell cycle and apoptosis regulator protein 2	2.13	1.09	0.01
P14555	Phospholipase A2, membrane associated	1.93	0.95	0.03
Q8IUL8	Cartilage intermediate layer protein 2	1.93	0.95	0.03
P09874	Poly [ADP-ribose] polymerase 1	1.89	0.91	0.04
Downregulated				
P28906	Hematopoietic progenitor cell antigen CD34	0.06	-3.98	6.30E-16
P68133	Actin, alpha skeletal muscle	0.41	-1.29	1.61E-04
Q13492	Phosphatidylinositol-binding clathrin assembly protein	0.54	-0.89	0.03
O60936	Nucleolar protein 3	0.55	-0.87	0.04

Table 6.25. Significant up- or down-regulated proteins in the infrapatellar fat pad of patients with high post-operative visual analogue scale (VAS) scores.

Accession	Description	Abundance ratio	Abundance ratio (log2)	Abundance ratio adj. p-value
Upregulated				
P28906	Hematopoietic progenitor cell antigen CD34	6.78	2.76	4.88E-16
P02775	Platelet basic protein	2.08	1.05	7.90E-10
P07099	Epoxide hydrolase 1	2.08	1.05	2.87E-06
P99999	Cytochrome c	1.89	0.92	1.60E-05
P69892	Hemoglobin subunit gamma-2	1.86	0.89	2.20E-06
P10620	Microsomal glutathione S-transferase 1	1.83	0.87	1.08E-3
Q8IUL8	Cartilage intermediate layer protein 2	1.67	0.74	0.04
P53814	Smoothelin	1.65	0.73	0.01
P20908	Collagen alpha-1(V) chain	1.60	0.67	2.80E-05
P23946	Chymase	1.54	0.62	9.31E-04
P02100	Hemoglobin subunit epsilon	1.52	0.61	0.02
Q99685	Monoglyceride lipase	1.52	0.60	0.02
P02730	Band 3 anion transport protein	1.49	0.58	1.85E-03
Downregulated				
P55008	Allograft inflammatory factor 1	0.45	-1.15	0.05
Q13492	Phosphatidylinositol-binding clathrin assembly protein	0.48	-1.06	0.03
O00468	Agrin	0.50	-1.00	0.05
P16401	Histone H1.5	0.54	-0.89	0.01
P13284	Gamma-interferon-inducible lysosomal thiol reductase	0.57	-0.82	0.04

Table 6.26. Significant up- or down-regulated proteins in the infrapatellar fat pad of patients with bad surgical outcome (Δ visual analogue scale (VAS)).

Accession	Description	Abundance ratio	Abundance ratio (log2)	Abundance ratio adj. p-value
Upregulated				
P35568	Insulin receptor substrate 1	2.22	1.15	7.51E-06
P13284	Gamma-interferon-inducible lysosomal thiol reductase	2.18	1.12	7.91E-06
P05413	Fatty acid-binding protein, heart	2.11	1.07	1.01E-04
Q96HN2	Adenosylhomocysteinase 3	2.07	1.05	0.03
P69892	Hemoglobin subunit gamma-2	2.00	1.00	2.52E-04
P06702	Protein S100-A9	1.97	0.98	0.01
P07919	Cytochrome b-c1 complex subunit 6, mitochondrial	1.97	0.98	0.01
P07451	Carbonic anhydrase 3	1.91	0.93	0.04
Q4ZHG4	Fibronectin type III domain-containing protein 1	1.87	0.90	0.01
Q92954	Proteoglycan 4	1.80	0.85	0.01
P28300	Protein-lysine 6-oxidase	1.74	0.80	0.01
P49746	Thrombospondin-3	1.73	0.79	0.035822
Downregulated				
P28906	Hematopoietic progenitor cell antigen CD34	0.01	-6.64	6.08E-16
P16112	Aggrecan core protein	0.51	-0.97	4.59E-03
P84095	Rho-related GTP-binding protein RhoG	0.52	-0.95	3.95E-05
P02686	Myelin basic protein	0.55	-0.88	3.05E-03
P53814	Smoothelin	0.56	-0.85	3.51E-04
Q9Y5X3	Sorting nexin-5	0.56	-0.84	0.01
P07099	Epoxide hydrolase 1	0.58	-0.78	1.25E-03
P15559	NAD(P)H dehydrogenase [quinone] 1	0.60	-0.73	0.04
Q99715	Collagen alpha-1(XII) chain	0.62	-0.68	4.57E-03
P00915	Carbonic anhydrase 1	0.64	-0.64	9.44E-04
P00738	Haptoglobin	0.64	-0.64	1.03E-03

Table 6.26 (continued). Significant up- or down-regulated proteins in the infrapatellar fat pad of patients with bad surgical outcome (Δ visual analogue scale (VAS)).

Accession	Description	Abundance ratio	Abundance ratio (log2)	Abundance ratio adj. p-value
Downregulated				
O14791	Apolipoprotein L1	0.65	-0.63	8.10E-04
P16452	Erythrocyte membrane protein band 4.2	0.65	-0.63	0.03

A String pathway analysis of the proteins significantly different in patients with bad clinical outcome (ΔVAS) showed 14 proteins to be related to biological processes, including the one-carbon metabolic process (red, Gene Ontology, FDR = 0.0437), cellular oxidant detoxification (blue, Gene Ontology, FDR = 0.0374), response to toxic substance (green, Gene Ontology, FDR = 0.0041), and connective tissue development (yellow, Gene Ontology, FDR = 0.0385) (**Figure 6.10A**). In addition, 11 proteins were related to the extracellular region (blue, Subcellular localization (COMPARTMENTS, FDR = 0.0402). Seven proteins were related to eicosanoids in the metabolic syndrome (red, Reference publications, PubMed, FDR = 0.0408) or proteoglycans (green, Annotated Keywords, UniProt, FDR = 0.0366) (**Figure 6.10B**). Finally, five, six and nine proteins were related to bone marrow cells (yellow, Tissue expression, TISSUES, FDR = 0.0047), bone marrow (pink, Tissue expression, TISSUES, FDR = 0.0125), and skeletal system (red, Tissue expression, TISSUES, FDR = 0.0101) respectively (**Figure 6.10C**).

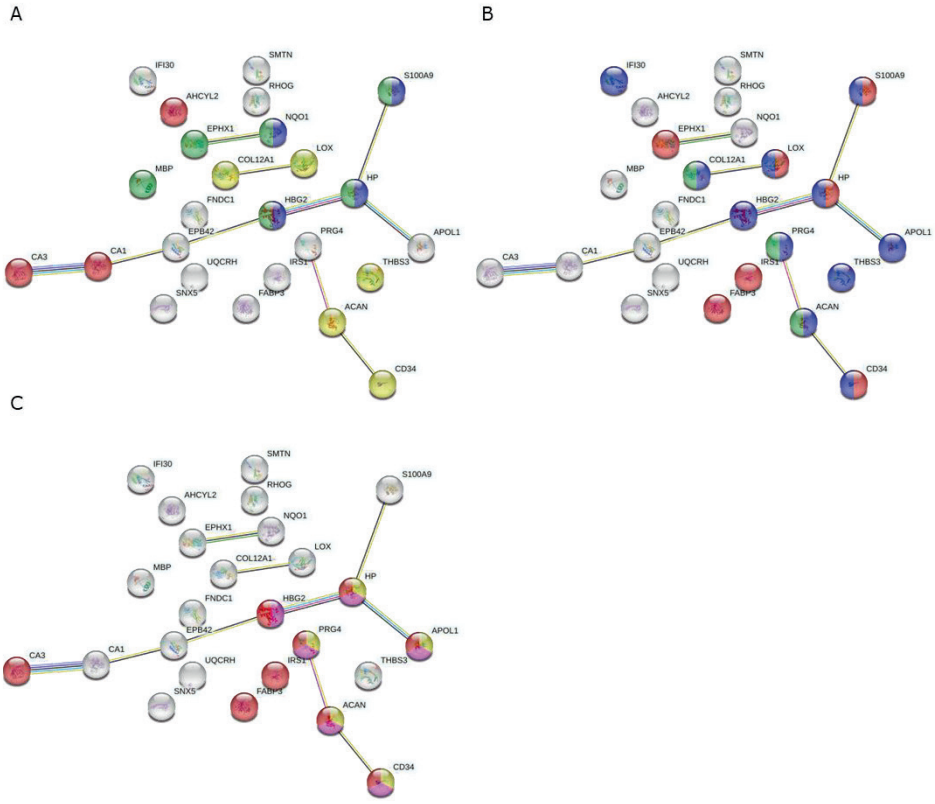

Figure 6.10. String pathway analysis of ΔVAS with functional enrichments of the network in which (A) shows proteins related to biological processes, including the one-carbon metabolic process (red), cellular oxidant detoxification (blue), response to toxic substance (green), and connective tissue development (yellow), (B) proteins related to the extracellular region (blue), eicosanoids in the metabolic syndrome (red), or proteoglycans (green), and (C) proteins related to bone marrow cells (yellow), bone marrow (pink), and/or the skeletal system (red).

Discussion

Rapid Evaporative Ionization Mass Spectrometry (REIMS) as potential tool for the detection of lipid-specific biomarkers for osteoarthritis and cartilage regeneration

First, REIMS was evaluated as potential diagnostic or prognostic tool for OA or (surgical outcome after) a cartilage defect. Based on the IPFPs lipid signature, LDA with confusion matrix showed an overall correct classification rate of 62.9% when comparing OA, and patients with a cartilage defect above or below the age of 35. Although no MS/MS was performed, some *m/z* (MS^1) were found more distinctive for either OA or cartilage defect patients. Comparable to the matrix-assisted laser desorption/ionization mass spectrometry imaging (MALDI-MSI) data described in **Chapter 5** of **this Thesis**, *m/z* 744.55 (identified as PE O-38:6), 766.55 (PE 38:4), 774.55 (PE O-40:7), and 746.55 (PE O-38:7) were found to be characteristic for OA patients. In addition, *m/z* 885.55 (phosphatidylinositol (PI) 38:4[320]), found characteristic for OA patients, as well as in cartilage defect patients with an age above 35, in this study, suggests the presence of an inflammatory profile in these patients. This implies that the group of patients, who are less likely to have high regenerative potential, are already showing a potential inflammatory profile associated with OA. PI is an important source of arachidonic acid, necessary for eicosanoid (and prostaglandin) synthesis, as has been described in **Chapter 3** and **Chapter 5**[198, 292, 294, 295].

In more detail, the least cuts made in the IPFP of OA patients were classified correctly in the OA group (only 37.1%). Better classification was acquired with cartilage defect patients. Namely, 71.4% of the cuts made in the IPFP of the group of cartilage defect patients older than 35 was correctly classified and 80% of the cuts made in the IPFP of the group of cartilage defect patients younger than 35. Potentially, factors such as age and previous surgery (possibly leading to fibrosis of the IPFP) play an important role in this discrimination, indicating the importance of taking into consideration the inter-patient variabilities in similar studies.

The results acquired from the cartilage defect patient cohort (n = 53), in which the lipid profile of the IPFP was studied, show a similar trend. Here, age has been shown one of the influencing factors when classifying patients based on their IPFP lipid profile. Patients could be classified in the correct age group with a correct overall classification rate of 65.5%. A better classification was again acquired in the younger age group. In this comparison, *m/z* 885.55 (PI 38:4, tentative assignment) popped

up in the older patient group as one of the important lipids in this separation, suggesting an increased inflammatory profile in these patients. With increasing age, already from the age of 30, the proliferation and differentiation of adipose progenitor cells and stem cells has been shown to decrease in white adipose tissue[321-323]. In addition, aging fat is associated with an accumulation of senescent cells[324], causing dysfunctions such as inflammation[321].

Furthermore, in this study, patients could not be classified in the correct group based on their IPFP lipid profile while looking at gender, BMI, previous trauma, previous surgery, or based on the fibrotic status of the IPFP. It is therefore suggested that for these factors the differences between patients are not substantial enough to be measured and classified using REIMS or that REIMS is not sensitive enough to measure differences at this moment.

Prediction of patient outcome prior to surgery would be beneficial for the patient, as well as the surgeon, as (personalized) therapeutic or clinical decisions could be taken accordingly. Therefore, it was investigated if patients with good or bad pre- and post-operative outcomes (VAS and KOOS) could be identified based on their IPFP lipid profile at the time of surgery. Patients could not be classified correctly based on the pre- or post-operative clinical outcome scores KOOS and VAS. In addition, it was investigated if the type of surgery performed had any measurable influence on the patient outcome and accompanying IPFP lipid profile. One group of patients, a ΔKOOS < 10 with use of own cartilage (regenerative) during surgery, showed a correct classification rate of 80%. However, only one patient belonged to this group.

Using REIMS, the intra-tissue heterogeneity of the IPFP has been shown of importance. While taking into account the lipid profiles of only the cuts made in adipose tissue or connective tissue, an overall classification rate of 90% was acquired. This suggests that REIMS can be used to discriminate between highly discriminative factors such as tissue type, as has been shown previously while comparing lipid profiles of different tissues[194], different diseases (OA vs cartilage defect, disease vs healthy), or tumor vs non-tumor in cancer research[305, 306]. Taking into account this intra-tissue heterogeneity while investigating patient outcome after surgery, it has been shown that correct classification rates increased above 70% while only taking into account the cuts made in adipose tissue or connective tissue for post-operative KOOS, and connective tissue for post-operative VAS.

It is less likely that REIMS, as has been utilized as such, can be used for the purpose of patient prediction models, improved clinical decision-making, and personalized

treatment for cartilage repair surgery at the operating theater. The inter-patient differences within this patient cohort were too small to predict patient outcome based on IPFP lipid profiles. Inter-patient variabilities might influence the results gathered in this study. Future studies should analyze large patient groups with limited inter-patient differences. In addition, improvements of the REIMS system as a clinical predictive tool would be necessary before implementation in the clinic would be possible. It would be beneficial to be able to guide, for example using microscopy, in which part of the tissue (or which tissue type) the probe cut. Eventually this might even lead to the development of a probe, which can analyze at single tissue-, or even, cell level.

Potential protein biomarkers for clinical response after cartilage repair

Multi-omics approaches are developed to do a variety of analysis (MALDI-MSI and proteomics) on the same tissue section[257]. It requires less tissue for analysis and is less destructive than REIMS with a diathermic knife or needle. In previous study, using MALDI-MSI and REIMS, we acknowledged the importance of the IPFP intra-tissue heterogeneity. Therefore, a variety in protocols for LMD were investigated to cut specific parts of the IPFP for proteome analysis. Whereas multiple washing steps with ethanol and chloroform improved the cutting ability of the IPFP with LMD, reducing the amount of lipids and drying the tissue section, only small amounts of proteins could be identified using LC-MS/MS. Instead, full-biopsy cryosections were acquired for LC-MS/MS analysis to be able to identify enough proteins for analysis and investigate the IPFP proteome.

Whereas our method requires a relatively large sample, generally consisting of hundreds to thousands of cells, methods for single-cell proteomics are being developed to overcome the cellular heterogeneity we acknowledged using advanced, simplified sample processing procedures[325].

In this study, it was shown that gender-related differences could be measured in the IPFP of patients with a cartilage defect. Women have been associated with better post-operative KOOS scores compared to men, despite the fact of a worse initial situation. On the contrary, women have also been associated with increased revision rates and discomfort[326]. A variety of proteins was significantly up- or downregulated in female patients compared to male patients. For example, increased levels of ACAN in the synovial fluid has been associated with cartilage destruction in OA patients[327]. ACAN is one of the building blocks of cartilage. A decrease of free ACAN in the intra-articular tissues suggests better regeneration of cartilage and better patient

outcome in female patients. A downregulation of ACAN was also associated with bad clinical outcome (ΔKOOS and ΔVAS) in this study.

CILP-1 and CILP-2 have been shown upregulated in patients older than 35, patients with a history of previous trauma, patients with IPFP fibrosis (only CILP-2), high pre- and post-operative VAS scores (only (CILP-2), and bad clinical outcome (ΔKOOS, only CILP-2), and downregulated in patients with good post-operative KOOS outcome (only CILP-2). CILP-2 is a glycoprotein most abundantly expressed in cartilaginous tissue and other connective tissues[328], where it contributes to the organization of tissue structure[329]. Whereas CILP-1 has been linked to cartilage degenerative diseases such as OA[328, 330-332], a decrease of CILP-2 expression has also been associated with OA pathology and might therefore function as possible biomarker for cartilage damage[328]. An increase of CILP-1 in patients older than 35 years might already indicate an indication of an OA-like phenotype in the joints of these patients.

Next, this study found a significant upregulation of CD34 in the IPFP of female patients compared to male patients, patients with a history of previous trauma, patients with high IPFP fibrosis, bad clinical outcome (ΔKOOS), and patients with high post-operative VAS scores. CD34 has been found downregulated in patients with good post-operative KOOS scores, as well as in patients with high pre-VAS and ΔVAS scores. These results suggest that CD34 might function as potential biomarker for bad post-operative clinical outcome after cartilage repair surgery. CD34 has been shown to play a role in the regulation of hematopoietic cell adhesion[333, 334] in human bone marrow[335]. The function on CD34 expressing hematopoietic stem cells is not fully understood, however, it is suggested that positive CD34 expression becomes apparent approaching cell division[335-338].

ACAN, as well as proteoglycan 4 (PRG4, lubricin) have been found downregulated in patients with bad surgical outcome (ΔKOOS). ACAN is a proteoglycan, one of the building blocks of the cartilage extracellular matrix (ECM) and plays an important role in articular cartilage function[327]. Its degradation is a factor contributing to the development of OA[327]. Lubricin, which has been found in synovial fluid and on articular cartilage surface, plays an important role in the lubrication of the joint. Lubricin plays an essential role in the regulation of macrophages in the synovium, as well as inflammatory joint infiltration of macrophages[339]. A reduction of lubricin has been associated with an increase in synovial pro-inflammatory M1 macrophages[339]. In patients with joint trauma or inflammatory arthritis, lubricin is not sufficient to prevent articular cartilage damage[340]. Its downregulation in patients with bad clinical

outcome after surgery might indicate that these patients have less lubrication in their joint, which might cause pain and damage corresponding to poor outcome[340].

Furthermore, the extracellular matrix protein cartilage oligomeric matrix protein (COMP)[341] was found upregulated in patients with a history of previous trauma, indicating cartilage turnover in these patients[342]. COMP has been considered a marker for cartilage breakdown and has been proposed as biomarker for OA[343]. In addition, a variety of collagens has been found upregulated in patients with good pre- and post-operative KOOS scores. Collagen alpha-1(XIV) (COL14A1, upregulated with good post-operative KOOS), for example, plays an important role in the adhesion of collagen bundles and has been shown to regulate fibrillogenesis (the development of fibrils in collagen fibers of connective tissue) in mice[344].

Related to pre-operative pain, stromelysin-1 (MMP-3) has been shown upregulated in patients with high pain vs low pain. MMP-3 is involved in the breakdown of extracellular matrix proteins such as fibronectin, proteoglycans, and denatured COL1[345].

Pathway analysis

Additional pathway analysis on proteins significantly different in patients with bad clinical outcome (ΔKOOS) showed that the majority of proteins were related to the extracellular region. An interaction between PRG4 (lubricin), ACAN, CD34, and CD14 was formed in this analysis. Although no direct link between these proteins has been described, PRG4, ACAN, and CD34 are involved in cartilage development and function. PRG4 and ACAN, secreted by chondrocytes, are important components of the ECM[327, 346]. CD34, as well as CD14, although not directly linked to OA, are both linked to the inflammatory process[347, 348]. All four proteins have also been shown related to bone marrow cells and the hematopoietic system.

For ΔVAS, differential proteins were related to biological processes, including the one-carbon metabolic process, cellular oxidant detoxification, response to toxic substance, and connective tissue development. A connection has been shown between carbonic anhydrase (CA) 1 and CA3. CAs are involved in a variety of biological processes, among which calcification and bone resorption[349, 350]. In addition, a connection was shown between HBG2, haptoglobin (HP), and S100A9 related to the extracellular region, cellular detoxification, response to toxic substances, as well as proteoglycans. HBG2 and S100A9 have been shown overexpressed in patients with bad surgical outcome (based on ΔVAS). HBG2 is usually present in the bone marrow and involved in oxygen and ion transport[351].

S100A9 is a calcium-binding protein, involved in the inflammatory process[352], and might contribute to cartilage matrix calcification[353].

Pathway analysis of ΔVAS also showed a connection between COL12A1 (downregulated) and protein-lysine 6-oxidase (LOX, upregulated) related to connective tissue development. LOX is essential for the cross-linking of extracellular matrix components such as collagen fibrils and elastin[354, 355], and is with that essential for the articular cartilage function[355]. In fibroblasts, prostaglandin E2 (PGE2) has been shown to reduce LOX expression[356]. PGE2, produced through cyclooxygenase (COX), as described in **Chapter 3** of **this Thesis**, is involved in the inflammatory process in OA and has been shown to suppress LOX expression in the inflammatory response occurring after injury[357].

Limitations

IPFPs collected from the operating theater were washed in PBS to reduce the contamination of blood. However, PBS, with its high salt content, has been shown to have a negative effect on electrospray ionization mass spectrometry (ESI-MS)[358]. Nevertheless, previous results in **Chapter 4** and **Chapter 5** did not show a reduction in signal intensity due to PBS washing.

In this study, we were able to identify the location of the cuts made in the IPFP with a diathermic knife, as well as the tissue type in which was cut for a large proportion of the data set. In general, the morphology of adipose tissue can change dependent on the method of storage, fixation, and preparation. Additionally, the IPFPs intra-tissue heterogeneity might have had an influence on the lipid signature and thus outcome of our analysis. Optimization of our method, in combination with an increased patient cohort, would be necessary to reduce the effect of patient variability and tissue heterogeneity. Further, although not determined in this study, a previous surgery in the same knee of a patient might have an influence on the IPFP as scarring of the tissue (or fibrosis) might occur.

Although the study size of the cartilage defect cohort was already of great value, it should be acknowledged that the degree of inter-patient and treatment (plan) heterogeneity might still have a big influence on the results. In the study performed, patients were matched for inter-patient differences as good as possible. Here, we were not able to perform LMD for multi-omics approaches, thus did not take into account the intra-tissue heterogeneity of the IPFP for LC-MS/MS analysis.

Conclusion

To our best knowledge, this is the first study utilizing REIMS on the IPFP as possible diagnostic or prognostic technology in the orthopedic research field of biomarker discovery. In conclusion, it was discussed that it is not likely that REIMS (as described in this Chapter) can be used as method to develop clinical prediction models for cartilage repair surgery after a cartilage defect. Differences in lipid profile between patients, measurable with REIMS, are too small compared to for example the difference seen in distinctive disease pathologies such as healthy and cancer. Further development of this technique and its use in the orthopedic operating theater could contribute to better understanding of patients' regenerative potential after a cartilage defect, better surgical outcome, and delay in OA development.

Although LMD is a promising technique for the development and implementation of multi-omics approaches, this method did not apply to the IPFP as has been described. Alternatively, proteomics results show promising potential biomarkers for the prediction of patient outcome after cartilage repair surgery including CILP-1 and CILP-2, CD34, COMP, and ACAN, among some less prominent proteins.

The results described in this Chapter suggests an interaction between the IPFP and cartilage, involved in OA development and cartilage repair. A variety of cartilage proteins related to cartilage degradation or OA could be measured in the IPFP, making it a promising, less invasive, and highly available tissue source for biomarker discovery. Before the IPFP can be used as biomarker source for OA or prediction models for cartilage regeneration, future studies should focus on even bigger patient cohorts. In addition, future research should take into account the IPFPs intra-tissue heterogeneity utilizing different MS approaches such as MSI, possibly at the cellular level.

Chapter 7

General discussion

This Thesis expands on the existing knowledge on diagnostic and prognostic biomarkers for cartilage repair and (early) osteoarthritis (OA) development, as well as currently existing treatment options. In addition, the possible application of different mass spectrometry (imaging) (MSI) techniques for novel biomarker discovery and prediction models for patient outcome after a cartilage defect, as well as its potential implementation in the clinic were investigated. First, this discussion focusses on the currently available biomarkers and treatment options for cartilage repair and OA development. The currently known (mass spectrometry-based) biomarkers, as well as the currently used treatment options for (early) OA will be discussed. Secondly, the use of mass spectrometry (imaging) for novel biomarker discovery in the infrapatellar fat pad (IPFP) using matrix-assisted laser desorption/ionization mass spectrometry imaging (MALDI-MSI), rapid evaporative ionization mass spectrometry (REIMS), or label free proteomics will be discussed in light of the discoveries in this Thesis. Finally, the use of mass spectrometry as diagnostic or predictive technology and its potential implementation in the clinic will be explored.

There is not one specific biomarker for osteoarthritis

The wide variety of MS techniques available makes it possible to identify molecular profiles in a variety of tissue types and disease states. These differences in MS techniques and approaches, tissue source, and targeted class of molecules, however, makes is difficult to determine which biomarker is most promising for OA. The results in Chapter 2 show that LC-MS is the most frequently used MS technique used in the search for OA biomarkers. LC-MS is a well-established technique, which provides important molecular information for a wide range of molecules. Alternatively, recent techniques still under development, such as MALDI-MSI, show promising potential in the search for local biomarkers as it allows the identification of molecules (lipids, metabolites, glycans, proteins, or peptides), while providing us with their spatial distribution throughout the tissue. A literature study provided a detailed overview of the currently known potential MS-based biomarkers for knee OA from a variety of different sample types. A variety of proteins, as well as metabolites and lipids were found specific for OA and therefore suggested as potential biomarkers for OA. The use of a molecular panel, rather than one single biomarker, increases the power of discriminating OA patients from non-OA patients. According to these results, it is likely that a combination of molecular classes or a group of proteins, lipids, and/or metabolites has added value as a biomarker profile for OA compared to the use of one single (molecular) biomarker[81].

Several OA phenotypes have been previously described[76, 78] and can be defined at the molecular level[160]. These phenotypes are the fundament of the development of personalized treatment plans for OA[81]. The differences between patients have an

influence on the biomarker profile measured. To reduce this inter-patient variability, patient groups analyzed should be large, representable for the population, and matched for features such as age, gender, or body mass index (BMI). In addition, the selection of the control group can also have an influence on the molecular profile. The use of healthy material is crucial in the search for a potential biomarker profile for OA, however, is usually not available as the procedure to collect the tissue is invasive. Analysis of blood or urine, or post-mortem tissue collection could be of added value, however come with certain drawbacks, possibly not representing the local changes (blood/urine), or tissue degradation (post-mortem)[81]. Tissue collection from the general population would be favored, but would ethically be prohibited. However, tissue collection post-mortem, or during autograft or allograft transplantation, as well as during (traumatic) surgery at the site near the unaffected knee, or contra-lateral biopsies during total knee arthroplasty (TKA) could possibly be taken into consideration as healthy alternative. A contra-lateral biopsy of the same patient helps to prevent inter-patient variabilities. For this, approval from the medical ethics committee (METC) as well as informed consent of the patient are needed. Specifically for the IPFP, taking a sample with a needle similar to a biopsy device for e.g. muscle, would be a minimally invasive option to acquire healthy material. In addition, analysis can be performed in a standardized way using a MS technique such as LC-MS. Still, the possibility of linking clinical and demographic data, with patient reported outcome measures (PROMs), magnetic resonance imaging (MRI) and X-ray information, as well as tissue analysis using MS, as has been performed in this study, is a unique way of researching the potential improvements in clinical decision making towards personalized treatment strategies.

There are already alternatives for healthy material available; however, they come with certain drawbacks. For example, degradation products can be visible in the analysis of material collected postmortem or inflammatory features in tissues derived from knee-related surgery such as anterior cruciate ligament (ACL) or meniscus surgery. Another option would be to collect tissue samples during bone-related trauma close to the joint of interest, although the sample size is usually low[81]. In **Chapter 2**, it was acknowledged that material collected from early vs late OA patients could contribute to the identification of biomarkers for OA stratification; estimation of the degree of OA, the progression of OA, or the possibility to alter the course of OA (e.g. by joint-preserving treatment such as lifestyle-changes, pharmacology, or surgery). However, to inhibit OA development and postpone TKA, it is of great importance to detect OA at the earliest moment possible. It would be beneficial to compare tissue samples from early OA patients to healthy material for the detection of biomarkers present at the earliest moment of development.

In **Chapter 5,** we compared the lipid profiles in the IPFP of patients undergoing surgery for a cartilage defect with patients undergoing TKA as a treatment for late

stage OA. In addition, in **Chapter 6**, we made steps towards clinical implementation of the use of the IPFP's lipid profile in patient profiling. Although tissues from cartilage defect patients can be considered as a healthy alternative, a traumatic incident in the knee can induce inflammation[69]. In our research, the IPFP was collected and studied. Whereas the IPFP is not frequently used as biopsy source in the search for OA biomarkers, compared to e.g. synovial fluid or cartilage, the IPFP is highly available and easily accessible (usually as waste material) during surgery. The IPFP has already been shown to play an important role in the pro-inflammatory signature of OA[164, 165, 171]. As it is located outside of the knee capsule and biopsy taking would be minimally invasive (apart from a potential bleed), this tissue type could be taken into consideration as healthy biopsy source. It has therefore been suggested that the IPFP would be a great source for the identification of possible diagnostic, prognostic, or therapeutic targets for OA.

As of today, there is no disease-modifying treatment for OA available. However, certain surgical interventions, such as joint distraction[359, 360], osteotomy[361, 362], or cartilage repair surgery[363] may be considered disease-modifying as they might result in changes which influence OA development or improve a patient's quality of life. Nevertheless, surgery increases the risk of side effects or complications such as pain, wound infection, nerve damage or thrombosis. The identification of biomarkers to predict OA development or patient outcome after surgery, might contribute to the development of individualized treatment plans. For example, a biomarker (profile) can help make clinical decisions such as if a surgery is necessary, or if this surgery should be conducted intra- or extra-articular. In addition, it might help estimate patient outcome by predicting regenerative potential, combined with a specific regenerative treatment. In addition, novel insights on the development and treatment of OA might contribute to the development of novel disease-modifying drugs for OA.

Early diagnosis of OA, or even the pre-stages of OA, is important. Early detection contributes to early treatment as has been shown in **Figure 1.5** (e.g. physical therapy, lifestyle/overweight, labor advise/participation, (anti-inflammatory) medication, or lubricating injections[364]) and possible delay in OA progression or development, and with this a delay in TKA and delay or even prevent possible revision surgery. Currently, joint-preserving surgery is the only proven way to delay OA development (e.g. the repair of an osteochondritis dissecans[66], joint-distraction[360], or osteotomy[279, 365]). In the search for biomarkers for OA, a variety of MS techniques with a diversity of sample preparation protocols are used in literature (**Chapter 2**). The variation in patient characteristics and material, sample storage and preparation, MS technique, and data analysis options complicates the discovery of potential biomarkers for OA. It is of great importance that standardized methods for biomarker discovery are applied on large patient cohorts and healthy, early OA and

late OA patients are defined in a more standardized manner (e.g. by the osteoarthritis research society international (OARSI) endorsed Early-stage Symptomatic Knee Osteoarthritis (EsSKOA) Classification Criteria) and that data is combined and shared via available databases. Preferably, patients that underwent (cartilage repair) surgery with high chances of developing OA early in life should be followed in time with among other testing questionnaires and MRI to be able to intervene and treat OA progression at the earliest moment possible. Appropriate treatment, together with lifestyle changes and physical therapy, inhibits OA progression, and will in turn postpone TKA surgery, reduce the chances of revision surgery, as well as surgery-related infections and patient's immobility, accompanied by long-term health costs.

In addition, new insights and the development of novel treatments or surgical techniques might lead to a reduction in health costs or better cost-effectiveness[366]. Novel techniques are evaluated in the health technology assessment (HTA), where all information about medical, economic, social, and ethical issues related to the technology (e.g. medicinal products, diagnostic and treatment equipment, or methods for prevention) are summarized.

Current treatments for cartilage repair and OA

The currently available options for cartilage repair surgery and early OA development are discussed in **Chapter 1** of **this Thesis**. Despite the fact that there is still no disease-modifying treatment for OA available, treatment of intra-articular damage and changes in lifestyle may contribute to a delay in OA development in these patients. The first line of treatment of OA focusses on diet, exercise and weight loss[35-37], and/or braces[38]. Symptoms such as pain and inflammation are treated pharmacologically using non-steroidal inflammatory drugs (NSAIDs)[39].

Chapter 3 elaborates on the use of celecoxib, a widely used NSAID to treat OA symptoms, and its potential chondroprotective potential. Celecoxib is known for its inhibition of pro-inflammatory mediators via the inhibition of cyclooxygenase-2 (COX-2)[40, 41]. Celecoxib has been shown to act chondroprotective in literature[42-47]. On the contrary, its lacking chondroprotective potential has been described[48-50].

As has been discussed in **this Thesis**, differences in study design could have an influence on the results acquired. Likewise, the contradiction in the chondroprotective effect of celecoxib found in literature can possibly be related to differences in study design, including the way of administration (e.g. oral or intra-articular injection) or dosage (e.g. repeated administration or single bolus injection). In **this Thesis** in **Chapter 3**, the chondroprotective effect of celecoxib on cartilage explants, as well as its chondroprotective effect in an OA mouse model,

administered as a single intra-articular bolus injection, was investigated. Although it has not been used in the clinic, an intra-articular bolus injection could have its advantages over oral administration, preventing adverse effects as a result of COX-2 and COX-1 inhibition, including cardiovascular or gastrointestinal complications[47, 52]. The methods developed in **this Thesis** could be directly employed to monitor treatment effect in such a study.

The anti-inflammatory effect of celecoxib has been confirmed in **Chapter 3.** This effect of celecoxib on the proteoglycan (PG) release of cartilage *ex vivo* has been shown previously by Dave et al[219]. These results suggest that PG production in cartilage is predominantly COX-2 driven[200]. It was suggested that PGs have an influence on chondrogenic differentiation of progenitor cells, indicating their anti-catabolic effect[220, 221]. It would be of great importance to further study the influence and effect of the different PG subtypes in cartilage as possible therapeutic target for inflammation or catabolic processes in OA.

In addition, celecoxib treatment of cartilage in an explant culture altered gene expression of proteolytic enzymes. The reduction of ADAMTS4 and ADAMTS5 could play an important role in the inhibition of OA by reducing aggrecan (ACAN) degradation in cartilage[222, 223]. In addition, the inhibition of MMP13 would reduce the collagen degradation process[223-225]. The regulation of enzymes involved in OA development by celecoxib indicates its potential anti-proteolytic effect[226]. The results in **this Thesis** on the effects of celecoxib, together with the substantiating results demonstrated in literature, show the importance of celecoxib, already used as NSAID in OA patients, as a potential chondroprotective drug, as well as COX-2 as a potential target for OA treatment. The increase of TIMP-2 in this study indicates that TIMP-2 contributed to the decrease in MMPs (the connection between TIMP-2 and MMP13 however, was not investigated in **this Thesis**), support the potential anti-inflammatory and anti-degenerative effect of celecoxib on cartilage[224, 228-230].

The experimental set-up described in **Chapter 3** of **this Thesis** does not take into account the adverse gastrointestinal or cardiovascular events of celecoxib *in vivo*[47]. Whereas intra-articular injections of celecoxib show contradictive results in literature, in **Chapter 3** the importance of study design, including dosage or concentration, way of administration, initiation, treatment duration, and scoring method were addressed. Although this study implies that a single intra-articular bolus injection of celecoxib acts chondroprotective in OA, the discussion on celecoxib's chondroprotective effect remains as long as study designs are not standardized and acquired results contravene. In literature, contrasting evidence on the chondroprotective effect of celecoxib, due to differences in drug concentration, timing, and other study-related factors, was reported. Additionally, the adverse effects of celecoxib might be due to its analgesic effect, improving mobility and

increasing cartilage wear and OA development[207]. It was suggested that administration by means of single intra-articular bolus injection positively influences the chondroprotective effect of celecoxib by better regulating the dosage at the affected site of the joint, while limiting potential adverse side effects[47, 238].

OA is a growing problem in the younger population

It is not only the elderly population that is increasingly affected by OA[33]. The incidence of OA in the younger population rises alarmingly[54] due to an increase in obesity and intra-articular trauma such as (osteo)chondral defects, ligament tears or patella luxations[28, 33, 54]. Taking into account the limited life-span of a total joint prosthesis and an increasing risk of revision surgery at younger age[56, 57], it is of high importance that joint damage is treated accordingly[66].

The type of treatment is dependent on its effectiveness, taking into account the patient's age, severity of the defect, and expected outcome, among others[61]. It is of great importance that the treating surgeon is aware of the latest insights concerning the treatment of an osteochondral defects[67]. Knowledge and availability of a variety of joint-preserving treatment strategies will contribute to better surgical decision-making and patient outcome[67, 68]. A better understanding of the (molecular) pathophysiology of OA has already contributed to the development of a variety of joint-preserving therapies[61]. Lipids are an important class of molecules involved in OA pathology[287]. Lipid deposits are found in the chondrocytes of OA articular cartilage[179, 287] and elevated levels of fatty acids are associated with OA severity[287]. Considering what has already been described in literature, it has been hypothesized that alterations in the lipid metabolism in the joint, could lead to a variety in OA related changes[367]. Therefore, in **Chapter 4**, a MALDI-MSI protocol for the IPFP was developed to identify potential lipid biomarkers for OA. Next, in **Chapter 5**, this protocol was implemented and the molecular lipid profile of the IPFP of cartilage repair and OA patients was investigated. Within the field of MSI, the analysis of lipids in adipose tissue is a growing field of research[244-246].

Current surgical decision-making on joint-preserving surgery is predominantly based on MRI and/or X-ray results, in combination with clinical aspects (e.g. medical history, age, and BMI), as well as the surgeons experience aligning to an individualized treatment plan including clinically and in literature proven, both surgical and non-surgical treatments. The discovery of a biomarker (panel) which can predict OA development and improve surgical decision-making would be of great benefit for a patient undergoing joint-preserving surgery to delay OA development. The MALDI-MSI method developed in **Chapter 4** and its implementation on a small patient cohort of cartilage repair and OA patients in **Chapter 5**, although of great value to identify possible biomarkers, requires multiple processing and analysis steps

which are too time-consuming for implementation in the clinic. Therefore, in Chapter 6, a near real-time MS method (REIMS) was connected to an electrocautery knife, comparable to the one used in the operating theater, to analyze the IPFP lipid profile and identify possible lipid profiles that could be used as diagnostic or predictive tool in the clinic.

Application of MALDI-MSI as possible diagnostic/prognostic tool

MALDI-MSI is one of the most frequently used MSI techniques in the biomedical field[239]. Among other applications, MALDI-MSI has been used to detect and identify molecules (e.g. lipids, metabolites, or proteins) and their distribution throughout a tissue section for clinical diagnostics and biomarker discovery in a variety of pathological conditions and biological samples[240-242], as well as for the analysis of drugs or compounds[101, 243], or find treatment targets[22, 101].

Chapter 4 describes a sample preparation method for MALDI-MSI on IPFP. Subsequently in Chapter 5, this method was applied on fresh-frozen IPFP of cartilage defect and OA patients to find (a) possible biomarker(s) profile for OA. The biggest challenge in Chapter 4 to overcome was the challenge of matrix application without the delocalization of molecules[252]. The IPFP has a heterogeneous morphology, consisting of synovium, connective tissue (including blood vessels), and adipose tissue. Adipose tissue is prone to melting. Therefore, sample handling and preparation of the tissue are important factors to take into consideration. Another important factor to be taken into account is that a possible trauma or previous surgery at the same area as the taken biopsy could have led to the development of scar tissue or IPFP fibrosis.

The general MALDI-MSI sample preparation workflow includes cryosectioning of snap-frozen tissue samples at a few micrometers and low temperatures. Subsequently, mounting on the glass slide can be done using a variety of methods including thaw mounting, coating of the slide, gluing, or tape transfer[251-253]. The tissue is dried under vacuum before a matrix, dependent on the molecule of interest, is applied using spraying or sublimation[258]. Usually, a scan of the slide is made at room temperature for co-registration of the MALDI-MSI image to histological staining. Delocalization of molecules happens most likely during one of the sample handling steps, including mounting, drying, or matrix application. Mounting of the tissue sample on the slide is important as it is possible that the tissue detaches during either one of the sample preparation steps. Thaw-mounting is a widely used method to attach a tissue section to a slide. During this procedure, the section is placed on top of a slide and heated from below using body-heat. Thawing and re-freezing of the tissue can have a negative effect on the morphology, as well as the delocalization of the molecules in the tissue because the tissue is likely to expand and shrink. Other

methods to mount a tissue section to a slide using a type of coating, glue or tape might contaminate the sample because of the existence of polymers or interfere with histological examination. Frozen tissue sections are subsequently dried under vacuum to prevent delocalization of molecules before matrix application. Usually, the slide is taken out of the freezer, into room temperature, and placed in a desiccator for a certain time to dry. Subsequently, the slide is taken out of the desiccator and matrix is applied. The spraying application of the matrix is performed at room temperature. The matrix is usually dissolved in a fast-drying spraying solvent such as methanol. The nozzle used for spraying is commonly heated, causing the matrix to reach the tissue at high temperature. The time it takes for the matrix to dry is dependent on the solvent used.

In **Chapter 4**, a method was described which prevented molecule delocalization of adipose-like tissue as has been seen before when using spray deposition[252], without the addition of a slide coating, polymer-containing tape, or glue[251-253]. Samples were collected as waste material, washed in phosphate-buffered saline (PBS) to remove blood residue, and snap-frozen in liquid nitrogen directly after dissection at the surgical theater to prevent tissue degradation. The IPFP is highly vascularized, causing blood to be present throughout the tissue sample. Performing a PBS wash prior to snap-freezing removes the majority of blood present in the sample. Heme and hemoglobin are two molecules highly present in the blood that can considerably disturb the MS analysis because these molecules prevent the ionization of other molecules of interest. The use of PBS as washing solution might not be optimal for MALDI-MSI[255], but did not disturb MS analysis in negative ion mode. Alternative washing solutions, containing less salt molecules would be more favorable; however its use is limited by strict regulations and protocols within the hospital.

In the method described in **Chapter 4**, tissue sections were cut at 15 µm thickness at a temperature of below -30°C. The anti-roll system inside the cryotome prevented the tissue from rolling up or sticking to the knife. Tissue sections were thaw mounted onto cooled (in the chamber of the cryotome) indium tin oxide (ITO) coated glass slides using the body heat of a finger. To prevent delocalization of the lipids in the tissue, the slide was directly refrozen on the cooled stage of the cryotome. Again, the slides were transported on dry ice to the ultra-low temperature freezer (ULF) and stored at -80°C until matrix application and MALDI-MSI.

Compared to other sample preparation methods for MALDI-MSI, thaw mounting prevents the use of tape transfer[251] or additional slide coating[252]. Nevertheless, it was not ruled out that different (adipose-like) tissue types need a different sample preparation approach. Another important step in the sample preparation approach described is transportation from the ULF to the laboratory for matrix application. Slides were transported horizontally in a cooled silica carrier box[258, 259]. These in-

house developed carrier boxes are employed to prevent molecule delocalization from condensation of the frozen sample when it is taken out of the freezer into room temperature. These closed carrier boxes contain a case with silica gel granules, which absorb the condensation moisture coming from the sample, preventing molecules from delocalizing throughout the tissue section. Subsequently, the carrier box containing a sample was placed slightly open in a desiccator to dry. To prevent sudden changes in air pressure, the desiccator stayed closed for the total drying time of 30 min. When dry, the silica carrier box was closed and taken out of the desiccator. Norharmane matrix was applied using sublimation. Furthermore, using Norharmane as a matrix, lipids can be measured in both, negative and positive, polarities. The matrix application protocol was adjusted according to the IPFP. Since the IPFP is a fatty tissue and thus prone to melting, the slide with tissue sections was removed from the silica carrier box and placed into the sublimator at the latest moment possible. Before placing the slide, it was made sure that the slide holder of the sublimator was cooled using the in-built water-cooling system. The vacuum created in the sublimator prevents molecules from delocalizing when the chamber is heated. Sublimation was performed at a temperature of 140°C for 200 s. Although keeping the tissue as dry as possible while applying the matrix, leaving the sample for a longer period under vacuum (either in the desiccator or sublimator) might increase the subtraction of volatile compounds from the tissue. Although application of the matrix by spraying is described to be more efficient, enhancing the extraction of molecules and thus the signal measured[253]. Concerning the IPFP this was not favored because of potential melting of the tissue with accompanied molecule delocalization[252]. Sufficiently dried matrix should prevent molecules from delocalizing when handling the slides at room temperature. Nevertheless, the silica carrier boxes were used for transportation.

Utilizing MALDI-MSI, a variety of lipid species were identified inside the IPFP. Based on the lipid profiles of each separate tissue type within the IPFP, using principal component analysis (PCA), adipose tissue, connective tissue, and synovial tissue could be distinguished. MALDI-MSI has been shown an excellent method to visualize specific lipids, as well as their spatial distribution throughout the tissue section, along with the identification of specific lipid profiles within the different IPFP tissue types, showing its intra-tissue heterogeneity.

Subsequently in **Chapter 5**, the method described in **Chapter 4** was applied to the IPFPs of a small patient cohort consisting of 7 cartilage repair and 7 OA patients as a proof of concept and to identify possible biomarkers for OA. Lipid profiles of the IPFP of cartilage defect and OA patients were investigated. Additionally, the IPFPs intra-tissue heterogeneity was explored. According to the patients' IPFP lipid profile, a clear differential distribution between cartilage defect and OA patients could be visualized, independent from tissue type. Likewise, a different distribution between

adipose tissue and connective tissue within the IPFP could be appreciated, independent from disease state (cartilage defect or OA). This separation between patient groups and tissue types was acquired in both polarities (negative and positive ion mode), though the analysis in negative ion mode was more distinctive.

Additionally, a higher abundance of phospholipids was found to be present in OA patients compared to cartilage defect patients, as has been described before by Kosinska et al comparing lipids in early and late OA synovial fluid[155]. The most discriminate lipid species found for OA patients included ether-linked phosphatidylethanolamines (PE O-s) and phosphatidylethanolamines (PEs), as well as a sphingomyelin (SM). There were no specific lipid species found for cartilage defect patients. Most likely this is due to the fact that the intensity of lipids in the OA patient samples was substantially higher than in the cartilage repair patient samples. The fact that no distinguishing lipids could be identified for the cartilage defect patient group in **Chapter 5** was also observed in **Chapter 6**, where the lipid profile of the IPFP of patients with a cartilage defect measured with REIMS was not sufficient to discriminate patient groups based on clinical outcome.

Phospholipids are important species contributing to healthy joint homeostasis[289-291]. In line with the findings in the IPFP described in **Chapter 5**, in synovial fluid, elevated levels of phospholipids induced the formation of lipid aggregates, disturbing lubrication[291] or modulating inflammation[289]. In addition, PE O-s, including the fatty acid arachidonic acid, were found to be highly abundant in OA patients. Ether-linked lipids such as PE O-s are known to play an important role in the pro-inflammatory response via prostaglandins and thromboxanes[292, 368, 369] (as described in **Chapter 3** of **this Thesis**). Prostaglandins, derived from arachidonic acid, play an important role in the inflammatory response in OA[51, 198, 292-295]. According to these results, PE O-s are suggested as possible biomarker group for OA. Furthermore, the SM (SM 40:2;O2) was found to be specific for OA in **Chapter 5**. Sphingolipids have been shown to be involved in synovial inflammation and joint repair responses and are therefore suggested as possible biomarker for OA[156]. The discovery of biomarkers for OA is of great importance, as they would help with early detection and possible prediction of treatment outcome. A predictive biomarker could indicate which joint-preserving treatment could have a disease-modifying effect in each patient and would facilitate clinical decision-making and improve patient outcome.

Chapter 5 shows the IPFPs intra-tissue and inter-patient heterogeneity. The combination of MALDI-MSI with histology provides us with additional information of the spatial distribution of specific lipids throughout the different tissue types of the IPFP. Arachidonic acid, as part of a PE O- was found mainly in the connective tissue of the IPFP, suggesting that the connective tissue is most likely involved in the pro-inflammatory phenotype of OA. A higher amount of connective, or fibrous tissue in

the IPFP was present in the tissue sections of OA patients. Fibrosis of cartilage and synovium has been shown of importance with OA[298, 299]. Similarly, fibrosis in the IPFP is characteristic for OA patients, indicating that molecular and biomechanical alterations in the IPFP might have an influence on OA development[124, 300]. The correlation between cartilage repair patient outcome and fibrosis and its influence on lipid and protein profiles has been described in **Chapter 6**.

MALDI-MSI allows us to identify analytes of interest and their spatial distribution throughout different tissue types. The MS instrument used in **Chapter 4** and **Chapter 5** (RapifleX Tissue Typer, Bruker Daltonics, Bremen, Germany) provides us with molecular distributions molecular profiles which might contribute to the discovery of potential prognostic or diagnostic biomarkers. Although sample preparation consists a variety of steps including sample handling, storage, sectioning, and matrix application, this method provides us with a fast and complete overview of the lipidome of the IPFP in a variety of tissue sections and patients. The samples in **Chapter 5** were measured at a lateral resolution of 50 µm. MALDI-MSI is an evolving MS method, progressing towards measurements with a lateral resolution of < 5 µm. The IPFP mainly consists relatively large adipocytes (~0.1 mm) compared to other cells. As these experiments mainly focused on adipocytes, it was not necessary to measure at a higher spatial resolution. High mass resolution measurements using e.g. an Orbitrap instrument are still necessary for tandem MS (MS/MS) analysis and identification of molecules. Additionally, multi-omics approaches, combining MS analysis, histology, laser microdissection (LMD), and liquid-chromatography MS (LC-MS) for proteomics, are being developed to identify a variety of molecules on the same tissue section, reducing the amount of tissue necessary for analysis[257]. Combining lipid with protein analysis increases the molecular information in these samples. Pathway analysis on a combination of molecular species would provide us with a more complete overview of the disease pathology of interest and possible treatment targets. LMD on the IPFP has been briefly addressed in **Chapter 6**, however, was not implemented in the final experimental set-up. Nevertheless, the role of spatial biology (including spatial multi-omics studies) in molecular biological studies is increasing[370, 371].

Ultimately, it would be of great value if these methods could be implemented in the clinic. While measurements performed at higher resolution provide us with higher specificity, the time it takes to run the experiment, as well as the data analysis, should be taken into account. In addition, sample preparation is time-consuming and requires optimization, making this method less likely to be used in the clinic. Therefore in **Chapter 6**, a real-time MS method which can be implemented in the clinic directly by measuring (explant) tissue samples at the site of the defect in the operating theater was described.

Application of REIMS as potential diagnostic/prognostic tool in the clinical setting (& protein analysis)

REIMS is a near real-time MS method, which allows us to analyze lipids in a variety of tissue types to make a molecular discrimination between healthy and disease (e.g. cancer), detect drug compounds, or identify potential predictive or diagnostic biomarkers. Connected to an electrocautery device, as has been used in the clinic, it could function as a potential tool to predict patient outcome after surgery and work towards personalized treatment for cartilage repair.

Although REIMS has great potential to be used in the operating theater for on-the-spot lipid analysis, the results in **Chapter 6** did not show clear separation of patients with OA or a cartilage defect, or cartilage defect patients based on their clinical outcome. Although REIMS has been used successfully to discriminate between different organs (e.g. muscle and liver), or different tissue pathologies (e.g. healthy and cancer), the differences in IPFP lipid profiles of the OA and cartilage defect patients in current study might be too small to detect. Nevertheless, using this technique, it was possible to distinguish patients with an age above 35 from patients with an age below 35 based on their IPFP lipid profile with a correct classification rate of 65%, suggesting that the IPFPs lipid profile changes with increasing age.

In addition, the importance of tissue type has been acknowledged. The cuts made in adipose tissue could be distinguished from the ones made in connective tissue with a correct classification rate of 90%. While taking into account these intra-tissue differences, cuts made in the IPFP of patients with good or bad post-operative clinical outcome (knee injury and osteoarthritis outcome score (KOOS), adipose tissue or connective tissue; and visual analogue scale (VAS), connective tissue) were correctly classified with a rate of > 70%.

REIMS cannot yet be, according to these results, implemented in the clinic as predictive or prognostic tool; however, shows great potential. REIMS has already been used in a clinical setting[372]. No major alterations to the system are necessary to make the transition from a laboratory setting to a clinical setting as REIMS can already be connected to a diathermic knife as is used in the operating theater. It would be a great implementation as REIMS gives (additional) information about a patient on the molecular level, instead of only at macro-level by MRI. Whereas REIMS at this moment is not yet suitable to predict patient outcome based on the lipid profile of the IPFP of patients with a cartilage defect and more research needs to be conducted (including bigger patient cohorts with more distinctive patient groups), other techniques might already be applicable. The lack of sensitivity of REIMS on the IPFP is most likely caused by the IPFP's intra-tissue heterogeneity. A combination with microscopy would make it possible to visualize in which tissue of

the IPFP is cut. In addition, recognition and prediction models for the tissue of interest could contribute to the identification of a tissue type at the time of cutting.

As has been shown in **Chapter 6**, distinctive protein profiles of the IPFP, with clear (already known) markers, could function as predictive tool to facilitate clinical decision-making and personal treatment after a cartilage defect. LC-MS is already a well-developed technique to identify protein biomarkers in any type of tissue or disease. In combination with a potential biopsy tool, which can already be used pre-operatively or in outpatient clinic[373], protein analysis might be able to predict a patients clinical outcome after surgery or help determining which cartilage repair treatment should be conducted. Whereas lipids are a very interesting type of molecules to investigate and the IPFP is full of them, a lot more is known about the relation of proteins in cartilage repair and OA development[374]. Not only proteomics approaches are used to analyze the proteome of OA patients, other methods such as immunoassays are also conducted to identify novel biomarkers in the field of OA[375].

Although LC-MS analysis demands time-consuming sample preparation (including long waiting steps) and is more prone to mistakes (many sample preparation steps), for now, it might be the best way to predict patient outcome after surgery. However, it is doubtlessly worth further developing REIMS for the same purpose, as it is fast, gives immediate information on the molecular status of the patient, and can be implemented in a clinical setting immediately.

The IPFP as potential biomarker source for OA stratification

OA has been acknowledged as whole joint disease, affecting most, if not all intra-articular tissues, including cartilage, meniscus, synovium, synovial fluid, and IPFP[16, 283, 284]. The IPFP is located underneath the patella and patella tendon[16]. During intra-articular surgery the IPFP is removed (partially) to gain access into the knee capsule and improve visibility and therefore highly available as surgical waste material. The IPFP is not located inside the knee capsule and therefore easily accessible with limited risk of infection, proposing it as potential biopsy target and biomarker source for OA. **Chapter 2** describes that, with regard to MS research, the IPFP is not (commonly) used as biomarker source for OA[81], although its importance in OA already has been acknowledged[16, 20, 124, 300]. The IPFPs lipid profile and its role in OA has not been studied thoroughly. Therefore, the results described in **this Thesis** might contribute to a better understanding of the IPFPs lipid profile and identification of a possible biomarker (profile) for OA. These findings might provide more insight in the future prognostic and diagnostic application of MS on the IPFP for OA development, as well as prediction of patient-related treatment outcome and potential treatment targets.

A drawback or potential future challenge in the use of the IPFP for OA biomarker discovery is its intra-tissue and inter-patient heterogeneity. At this moment, histological analysis (in combination with MSI) should be used to identify possible fibrosis, inflammation, or other influencing factors before drawing conclusions. Another drawback is the fact that the IPFP is affected when an intra-articular surgery, or even arthroscopy, is performed. A previous surgery shows scarring or fibrosis of the IPFP, has a negative effect on surgical outcome, increases the risk of a failure of cartilage repair[376], and might increase the risk at pre/early OA development in these patients. A previous surgery might therefore influence the IPFP in such way, that it can no longer be used as predictable biopsy target or for biomarker discovery. If this is not the case, and the IPFP is not affected and can be used as biomarker source for clinical decision making, it might be thinkable to already perform a diagnostic arthroscopy (e.g. using the NanoScope[377] (Arthrex, Naples, FL, USA) in outpatient clinic to gain the information necessary for treatment.

Conclusions and (clinical) outlook

Biomarkers for OA stratification

The results described in **this Thesis** need to be validated in future studies in independent cohorts before being implemented in the clinic. Predictive and diagnostic biomarkers have been shown of importance in cartilage regeneration (surgery) and early development and diagnosis of OA. In **Chapter 2** the currently known biomarkers for OA, measured with MS, were described. It is not likely that one single biomarker will be specific enough to diagnose OA or predict its development. Instead, a panel of dry (e.g. patient characteristics or previous surgery) and wet (e.g. lipids or proteins) biomarkers is presumed to serve as diagnostic or predictive model for OA (development). With the existence of a biomarker panel, which can be used as model for early OA diagnosis or prediction of clinical outcome after joint-preserving surgery/treatment, clinical decision making, as well as patient outcome will be improved. In addition, novel biomarkers might contribute to the discovery of unique therapeutic targets and potential personalized treatment for cartilage repair and OA. A combined biomarker panel of dry and wet biomarkers is likely an optimal strategy to predict patient outcome after surgery or OA development.

It is important that surgeons and rheumatologists, as well as the first line of care (including family doctors and physiotherapists) are well informed on the recent findings and new applications regarding the treatment of a cartilage defect and/or OA that follows. This is not only paramount in the clinic, but also transmural and inter-specialist collaborations are needed. Although this might lead to competition, some competitive forces are necessary to feel rewarded, rather than only treating a patient.

Treatment strategies for cartilage repair and OA

Before surgical intervention, the first lines of treatment for OA focuses on exercise, diet, the use of braces, and/or medication (e.g. NSAIDs). In Chapter 3, the anti-inflammatory and chondroprotective effect of one of these NSAIDs, celecoxib, has been investigated. Implementation in the clinic of the results described on the use of celecoxib as single intra-articular bolus injection, would potentially inhibit or reverse OA development and avoid the known adverse events linked to oral administration. NSAIDs such as celecoxib are already used in the first lines of treatment for OA to inhibit the inflammatory response in OA. It has been shown in Chapter 3 that celecoxib reduces the inflammatory profile, which is present in OA patients, in a cartilage explant culture via the COX-2 signaling pathway. *In vivo*, it was shown that celecoxib acts chondroprotective, inhibiting OA development. This experiment was conducted in mice. The chondroprotective effect of celecoxib found in this Thesis could be further explored in larger animal models such as equine, or possibly even using organ-on-a-chip set-ups taking into account the physiology of the tissue, to represent better the human situation. It is important that dose, time of application after OA development, OA state, and frequency of administration are taken into consideration before applying this method in the clinic.

The step towards clinical implementation should not be too complicated as celecoxib has already been used for the treatment of OA symptoms in patients. A limitation of this newly explored therapy using intra-articular injections of celecoxib for OA to treat not only inflammation, but also prevent cartilage from degrading, would be that it is a more invasive way of administration. The positive results we acquired from the animal model after a single bolus injection in Chapter 3 might not reflect the clinical and/or pharmacological legislation for intra-articular joint injections. The difficulty with animal studies like this is that there is no consensus on which OA animal model represents which human OA phenotype best. In addition, celecoxib is a lipophilic drug with low pH, potentially harmful with poor pharmacokinetics in the joint. Another option would be the use of a drug-delivery system such as nanoparticles for controlled drug delivery and release, and to target a specific area or cell type[378-380]. However, if an intra-articular injection of celecoxib overcomes the adverse effects of oral administration, it would be of great importance to explore its intra-articular use for future clinical purpose. Additionally, if this treatment would also have a chondroprotective effect in human studies, OA development is inhibited, TKA is postponed, and revision surgery is prevented, high health care costs, as well as long waiting lists could be avoided.

The application of MALDI-MSI and REIMS in the clinic

In **Chapter 4** and **Chapter 5** of **this Thesis**, the (pre-) clinical application of MALDI-MSI was investigated. In **Chapter 6**, the first steps towards clinical implementation of REIMS for predictive patient outcome measures were addressed.

There are still some hurdles to overcome before MALDI-MSI and REIMS can be implemented in a clinical setting for cartilage repair and OA. Standardization and automating of the different workflows, including sample preparation, laser, and detector settings for MALDI-MSI, would contribute to an improvement in reproducibility of experiments. In addition, quality control measurements should be performed to address performance of the instrument, as well as for the sample preparation method used. Experiments utilizing MALDI-MSI are often performed on small sample sizes or cohorts with a variety in sample preparation and instrumentation methods. Results should therefore be confirmed in validation experiments including large cohorts and large sample sizes, ideally acquired in multi-center studies.

MS experiments are prone to batch effects, caused by day-to-day differences in laboratory environmental factors such as temperature and humidity, affecting sample preparation and instrument performance. Laboratory circumstances should be taken into account when performing experiments. Variance caused by these differences should be addressed during data analysis before drawing conclusions.

Another subject that needs to be addressed before MALDI-MSI and REIMS can be implemented in the clinic is quantification of a specific analyte of interest. In **Chapter 5** and **Chapter 6**, it has been acknowledged that intra-tissue heterogeneity is of great importance when comparing data sets and searching for biomarkers. Each molecule type has a different ion suppression, complicating the quantification of specific molecules. If the compound of interest is known, for example in drug assessment, quantification is performed utilizing a calibrant, spiked homogenate, or stable isotope[381-383]. In **this Thesis**, the untargeted analysis of unknown compounds was performed, making quantification difficult. Quantification for REIMS is even more difficult as detection of molecules is dependent on the smoke aspirated, sample volume, intra-tissue heterogeneity, and contamination of the system in time. On the contrary, LC-MS/MS, used for proteomic analysis on the IPFP in **Chapter 6**, and on medium samples in **Chapter 3**, has already been extensively used in clinic for diagnostic purposes, including secretome and proteome analysis.

In **Chapter 4,** a sample preparation method for MALDI-MSI on the IPFP was described. In **Chapter 5**, this method was applied to the IPFP of a small cohort

cartilage repair and OA patients. Whereas this technique has not been applied on the IPFP in the search for OA biomarkers, future experiments utilizing MALDI-MSI on IPFP gives the opportunity to describe novel biomarkers or therapeutic targets for cartilage repair and OA. One of the biggest challenges in biomedical research is the implementation of a healthy control group. With the analysis of the lipid profile of a larger cohort of healthy, cartilage defect, early OA, and late OA patients would provide information on the profile changes throughout the development of disease with the incorporation of a healthy control. In addition, the effect of celecoxib on the lipid profile, as has been described *ex vivo* and *in vivo* in an OA mouse model on cartilage in Chapter 3, could be analyzed utilizing MALDI-MSI. Using MSI, combined with histology, this effect or these changes can be visualized, providing additional spatial information. This Thesis only focused on measuring lipids with MALDI-MSI, though the analysis of metabolites, proteins, or peptides could be of interest as has been reviewed in Chapter 2.

With the information acquired, (joint) pathway analysis can be conducted. Molecular pathways that could be of interest for analyzing the pathophysiology of OA, as well as potential novel treatment targets. Importantly, for the IPFP, the different steps in the MALDI-MSI workflow, including sample handling and matrix application, as well as reproducibility of the experiments should be taken into account. In this Thesis, in Chapter 4, the challenges regarding sample preparation for MALDI-MSI on the IPFP were described. Delocalization of molecules has been described as one of the most challenging aspects. Currently, MALDI-MSI stays a tool for biomedical research. Application of this technique as diagnostic tool in the field of OA is unlikely at this moment due to its workload and expertise needed. However, MALDI-MSI is a fast MS technique, providing spatial information of the molecules of interest throughout a tissue section. Optimized for the tissue type of interest, MALDI-MSI could provide supporting molecular information to the pathological analysis. MALDI-MSI was able to discriminate cartilage repair patients from OA patients in Chapter 5.

REIMS, as has been described in Chapter 6, has most potential to be utilized in a clinical setting, possibly for *in situ* analysis at the operating theater. Although this technique is very promising, it needs to be further developed before it can be used in the clinic as prognostic or diagnostic tool for cartilage repair or OA. At this moment, the development of a biopsy device (for the IPFP), in combination with LC-MS (proteomics) analysis is most likely the best way to define a patients potential to regenerate and predict patient outcome after cartilage repair surgery, or even define OA phenotypes. However, more research is needed before this technique can be implemented.

Chapter 8

Impact

Social and economic impact

Understanding the molecular roots of a disease could advance (personalized) treatment, improve a patient's quality of life, and contribute to better (public) health care. A biomarker (panel) for cartilage repair patient outcome and early osteoarthritis (OA) development would improve accurate diagnosis, surgical decision making, and facilitate personalized treatment, inhibiting OA development and improving a patient's quality of life by increasing its ability to move. This will eventually lead to a reduction in OA-related comorbidities, a reduction in total knee arthroplasty (TKA) revision surgery accompanied with a reduction in surgery-related infections, and a reduction in health costs. However, it will take years before these benefits are accessible for the patient, as scientific studies need to be converted into clinical trials and money needs to be invested to make it applicable for the patient.

Unlike for example in cardiology, where asymptomatic patients are treated according to e.g. blood pressure or blood lipid levels, there is no proper measurement control in the diagnosis of pre-, early, or moderate OA. When OA is diagnosed early in its development, preventive measures, such as an already used anti-inflammatory drug like celecoxib, with a chondroprotective potential, could contribute to this delay in OA development. Additional research on the effect of celecoxib on the pathways involved in OA development could lead to a better understanding of the molecular changes happening in OA and facilitate the development of (novel) therapeutic targets and treatments. Potential injection with disease modifying OA drugs (DMOADs) in an early phase of the disease is of interest, however, the outcome might only be visible on MRI (structural changes), rather than improving quality of life by e.g. reducing pain, where pain is often not existing in early stages of disease. Therefore, at this moment, the FDA (Food and Drug Administration) dictates that (injectable) drugs should act on both pain as well as structural changes.

Early diagnosis of OA would give the opportunity to intervene early in the disease development and postpone TKA and revision surgery. MALDI-MSI can give us a better understanding of the molecular changes, as well as the molecular distributions of OA development. Knowledge on the molecular profiles can be applied to point-of-care *in situ* analysis techniques such as REIMS for the development of pattern recognition models for early diagnosis of OA or prediction models for cartilage repair. According to the results acquired, a clinician can adjust treatment to the patient's profile, start OA treatment early in its development, and possibly prevent OA from developing further. This would lead to a reduction in TKA

surgeries, TKA revision surgeries, and health care costs, while improving a patient's quality of life and public health. The biggest risk of losing an implant are stress shielding – a reduction in bone density – or bacterial infection. Especially prosthetic joint infections are difficult to treat as patients are often too weak for additional surgery and antibiotics alone do not eradicate the infection, leading to bacterial resistance. The FDA has acknowledged this problem and pays special attention to the majority of joint-preserving treatments.

In this research, we address the importance of data sharing, as well as the importance of collaborations between research institutes and clinical facilities. In the field of biomedical research, studies are conducted to find answers to clinical questions and improve patient care. The fundamental research conducted throughout this Thesis provides us with results, which can lead to a better understanding of disease development and pathways involved. Working closely together with a university medical center, the lines between fundamental findings in the laboratory and its application in the clinic are kept close. Here, the clinic provided us with the essential patient samples for the identification of molecular pathways involved in the closest human situation available. Knowledge should not only be shared between research institute and hospital, but also between research institutes. Providing other researchers with information on protocol development, application, and data acquirement (even if it is not working) is of great importance as usually only small optimization steps (dependent on the tissue type, materials, and techniques available) have to be taken prior to utilization. This would eventually save time, reduce workload, and experimental costs.

The biomedical research conducted in this Thesis would not have been possible without the financial funding of a variety of instances and companies. Not only have we been collaborating between the Laboratory for Experimental Orthopedics, the department of Orthopedic Surgery of the MUMC+ (Joint-Preserving clinic), and the Maastricht Multimodal molecular imaging institute (M4i), our data has also been presented to the instances and companies financially involved. Collaborations between research facilities and companies makes it possible to get new developments patented, further developed, and produced for clinical implementation. In addition, changes in design of the instruments used (e.g. for application in the clinic), can be made by the owner company who is invested in a type of treatment or a novel method. Whereas companies have the best interest in helping the patient, developing new treatment strategies, incurred costs from many years of research have to be repaid, bringing potential high health care costs. The patient and provider (e.g. the surgeon or hospital) is caught between the incentive

of articles showing promising results and patents of products on the other hand. In this Thesis we showed that with a close collaboration between the patient (having a problem), the surgeon (bringing the question), researchers (providing the research and results), funds, and companies (providing money), this gap might be closed. However, the risk vs benefit, as well as data vs ownership coming with this type of research are still under debate.

Scientific impact

Early detection of OA development is of great importance to intervene in its progression and outcome by treating the early stages of the disease. Biomarkers might contribute to the development of novel therapeutic treatment options. In this Thesis, we provide further knowledge on the (lipid and protein profile of the) infrapatellar fat pad (IPFP) and acknowledge its function as biochemical organ in maintaining (healthy) joint homeostasis. Fat pads are present in every joint and are highly available and accessible for research or as biopsy target. This in contrast to the widely studied synovial fluid, which is not easy to harvest in a healthy, pre-, or early OA patient.

Importantly, we found through our review in Chapter 2 that most likely, a combination of proteins, lipids, and metabolites would contribute to a biomarker profile for OA, rather than one single biomarker. Additionally, we are stressing the importance of the use of large patient cohorts for analysis, the use of standardized methods, and allocation of acquired information through shared and open databases. These statements should be taken into account in future scientific research while searching for novel OA biomarkers.

According to the results on celecoxib described in this Thesis, future studies should focus on the use of a single intra-articular bolus injection of celecoxib in bigger animal models, such as equine, to make implementation in the human situation possible. It is difficult to translate these findings in animal studies to the clinic, as there is no consensus on which animal model corresponds to which “theoretical” OA phenotype best. These OA phenotypes should then be connected to a treatment algorithm, as for example has been described by the Dutch Orthopedic Association (NOV) for surgical treatment of (osteo)chondral defects in the knee in 2019. The results described in this Thesis on celecoxib were presented during the International Cartilage Regeneration and Joint Preservation Society (ICRS) in 2022, where the broad impact of this research was acknowledged. Celecoxib is an example of a possible disease-modifying drug still under debate, which may benefit from the

results in **this Thesis,** as our results are not modifying, but thriving the discussion towards the benefits of celecoxib as a disease-modifying drug for OA. Our findings on potential biomarkers for cartilage repair and OA might contribute to new or additional therapeutic targets and possibly identify which patient population might benefit from the use of celecoxib in the clinic.

A variety of methods were optimized for the analysis of the IPFP lipid and protein profile in a variety of patients, with a variety of (pre-)OA pathologies. The further scientific impact of the results described in **this Thesis** is based on the methodological development of the use of matrix-assisted laser desorption/ionization mass spectrometry imaging (MALDI-MSI) on the IPFP of OA and cartilage defect patients. Additionally, the differences in lipid profiles between OA and cartilage repair patients were described. Furthermore, a considerable step towards clinical implementation of mass spectrometry (MS) as a potential point-of-care technique in the form of rapid evaporative ionization MS (REIMS) was made by analyzing differences in lipid profiles of OA and cartilage defect patients, as well as differences in lipid profiles in a cartilage defect patient cohort for prediction profiling. Proteomics analysis on this same patient cohort was performed to get a better insight in the changes occurring in the IPFP of patients after a cartilage defect, as well as after surgery.

The sample preparation and MALDI-MSI analysis to measure lipid profiles in the IPFP of patients with OA or a cartilage defect has not been described before. This method allows for the sectioning of fresh-frozen IPFP and application of matrix with limited delocalization of molecules. The results contributing to this future publication have been presented during the European Orthopedic Research Society (EORS) in 2019 and 2020, as well as during the Mass Spectrometry School in Biotechnology and Medicine (MSBM) Summer School in 2019, and the LipidMaps Spring School and Tissue Engineering and Regenerative Medicine International Society (TERMIS) in 2021. By presenting our results at a variety of conferences in a variety of cities with a variety of researchers, we were able to share and discuss our knowledge on the current status of biomarkers in cartilage repair and OA. It is of great importance to share knowledge in an honest and public way to, in the end, provide the patient with the best care possible.

The method for MALDI-MSI on the IPFP has a multipurpose application, as it can be used as basis for the development of sample preparation and MALDI-MSI protocols on other fatty tissue such as abdominal fat or breast tissue. Among other applications, the use of MALDI-MSI on the IPFP has the potential to identify possible

biomarkers for cartilage regeneration, prediction models, OA development, or OA phenotyping. The IPFP is a type of tissue which is easy accessible and usually removed as waste material during cartilage repair surgery or TKA. This makes the IPFP a promising tissue type for biomarker discovery. In addition, the IPFP might be easily biopsied during out-patient clinic visits prior to surgery, as the risk at infection or other complications is relatively low. Pre-clinically, the MALDI-MSI analysis on the IPFP might contribute to a broader knowledge and better molecular understanding of the development of OA, as well as the effect of cartilage repair surgery on patient outcome.

While we slightly addressed the use of MS in the clinical setting, utilizing REIMS on the IPFP for diagnostic or prognostic purposes, this field of research needs optimization in future experiments. REIMS is a highly potential tool which can be used *in situ* in a variety of surgical applications such as cancer or cartilage repair surgery. When connected to a diathermic knife, as is already been used in the surgical theater for electrocautery cutting, no big alterations have to be made for implementation in the clinical setting. This Thesis describes the first application of the use of REIMS, connected to a diathermic knife, on the IPFP of OA and cartilage defect patients. The preliminary results have been presented at TERMIS 2020 and the European Society of Tissue Regeneration in Orthopedics and Traumatology (ESTROT) in 2022. Furthermore, the results are planned to be presented at the European Society for Biomaterials (ESB) in 2023. In (pre)clinical setting and future biomedical research, REIMS is used to study the molecular profiles in a variety of tissues and a variety of disease pathologies, allowing it to be used in a wide range of applications. Utilizing this technique on the IPFP of OA and cartilage defect patients can improve the understanding of impaired molecular pathways and pathologies. The data acquired could be used to construct accurate pattern recognition and prediction models to, for example, identify different molecular OA phenotypes, or predict patient outcome after cartilage repair surgery to improve surgical decision making and possibly contribute to the development of (novel) personal treatment strategies.

Not only can REIMS be used on the IPFP, with the right optimization, it can be used on many other tissue types, using less destructive techniques such as laser-assisted REIMS on cartilage[384]. Moreover, REIMS can be applied in the food industry to, for example, study food quality and safety, or for the identification of specific types of species in flora and fauna, or accompanying (resistance to) parasites, bacteria, and fungi. Its application is unlimited, as long as ablation of the tissue and the ionization of molecules is possible with REIMS.

Chapter 9

Summary

Nederlandse samenvatting

Summary

Osteoarthritis (OA) is not only affecting the elderly population, but also more and more affecting the younger population, causing not only disability, but also co-existing conditions such as heart disease, diabetes, or mental health problems. Its incidence is expected to increase due to an ageing population, an increase in obesity, and an increase in sport injuries. A variety of intra-articular tissues, including the infrapatellar fat pad (IPFP), contributes to a healthy joint homeostasis. The IPFP is an important inflammatory mediator in the knee joint and has been associated to knee pain after injury, as well as progression of knee OA. A disturbed joint homeostasis due to e.g. injury or an inflammatory event can cause OA in this joint. OA is characterized by a progressive loss of cartilage and has a negative impact on a patient's quality of life. OA is usually diagnosed in late stage of the disease.

At this moment, there is no specific biomarker for early diagnosis of OA, OA progression, or prognosis after cartilage repair surgery. Most studies focus on biomarkers in cartilage, synovium, or synovial fluid. However in **this Thesis**, the potential of the IPFP as biomarker discovery was addressed. In addition, in **Chapter 2**, it was discussed that, rather than one specific biomarker, a group of molecules (including lipids, proteins, and metabolites) would provide us with a biomarker panel that gives better insight in OA development and potential therapeutic targets. The use of untargeted mass spectrometry (MS) techniques could contribute to gaining more knowledge on the molecular understanding of OA. Early detection and treatment of OA are of great importance. Life-style changes, as well as joint-preserving surgeries have been shown to slow down, stop, or reverse OA development. As soon as a patient suffers from end-stage OA, the only treatment option available is total knee arthroplasty (TKA). Whereas this treatment has a limited lifespan, postponing OA progression and TKA in patients is of great importance.

The first line of treatment options for OA include exercise and dietary changes, as well as the use of non-steroidal anti-inflammatory drugs (NSAIDs) to treat symptoms. One of these NSAIDs is celecoxib, a selective cyclooxygenase-2 (COX-2) inhibitor. In **Chapter 3**, the anti-inflammatory and chondroprotective effect of celecoxib were studied in a human cartilage explant culture, as well as an OA animal model by ways of intra-articular single bolus administration. Celecoxib reduced the secretion of pro-inflammatory prostaglandins, as well as proteins, and altered gene expression in human articular cartilage explants. *In vivo*, in a rat OA model, celecoxib acted chondroprotective after a single intra-articular bolus injection.

To investigate the potential of the IPFP in the search for biomarkers for OA, in Chapter 4, a method for the analysis of lipids in the IPFP using matrix-assisted laser desorption/ionization mass spectrometry imaging (MALDI-MSI) was optimized. The biggest challenge lays within the sample preparation. The IPFP is an adipose-like tissue and is therefore prone to melt. Melting tissue during various steps of the sample preparation, including cryosectioning, transportation, or matrix application would cause delocalization of molecules. To prevent this from happening and to keep the IPFPs spatial molecule information, cryosections were made at very low temperatures. Thaw mounting and refreezing were performed at very fast rates and transportation was always performed using silica gel carrier boxes. The main different tissue types within the IPFP explant (adipose tissue, connective tissue, and synovium) could be identified with MALDI-MSI. Subsequently in Chapter 5, this method was applied to visualize the differences in lipid profiles in the IPFP of OA and cartilage defect patients. Different lipid profiles were identified for OA and cartilage defect patients. In addition, the IPFPs intra-tissue heterogeneity was acknowledged, as it might be associated to patient phenotypes. Arachidonic acid-containing, ether-linked phosphatidylethanolamines (PE-O-s) in the connective tissue of the IPFP were suggested specific for OA.

In Chapter 6, we worked towards a point-of-care device for diagnosis of OA, as well as prediction of OA development after a cartilage defect. Rapid evaporative ionization mass spectrometry (REIMS) was used to visualize the lipid profiles of OA, as well as a variety of cartilage defect patients. REIMS was only able to correctly classify cuts made in the IPFP of patients with an age above 35 or below 35 years (65%). Further, as has been shown previously in Chapter 4 and Chapter 5, the IPFPs intra-tissue heterogeneity was of importance. Cuts made in either adipose tissue or connective tissue could be correctly classified with a rate of 90%. Taking into account this intra-tissue heterogeneity while looking at clinical outcome after surgery, the highest correct classifications were acquired with post-operative knee injury and osteoarthritis outcome score (KOOS) for adipose tissue (70%) and connective tissue (73%), as well as for post-operative visual analogue scale (VAS) scores for connective tissue (73%). According to these results, it is not likely that REIMS will be used as method to develop clinical prediction models for cartilage repair surgery. More research and optimization of the technique is necessary to identify the small changes occurring in the IPFP after a cartilage defect.

Proteomic results in Chapter 6 suggest that there is an interaction between the IPFP and cartilage as a variety of cartilage proteins related to cartilage degradation or OA were measured in the IPFP. The IPFP could therefore been seen as promising tissue source for (OA) biomarker discovery. Future studies however, should take into account the IPFP's intra-tissue heterogeneity when drawing conclusions.

Nederlandse samenvatting

Artrose treft niet alleen de oudere bevolking, maar treft ook steeds meer de jongere bevolking. Het veroorzaakt niet alleen handicaps, maar ook bestaande aandoeningen zoals hartaandoeningen, diabetes of psychische problemen. De incidentie zal naar verwachting toenemen als gevolg van een vergrijzende bevolking, een toename van obesitas en een toename van sportblessures. Een verscheidenheid aan intra-articulaire weefsels, waaronder het infrapatellaire vetkussentje, draagt bij aan een gezonde gewrichtshomeostase. Het infrapatellaire vetkussentje is een belangrijke ontstekingsmediator in het kniegewricht en wordt in verband gebracht met kniepijn na een blessure, evenals progressie van knieartrose. Een verstoorde gewrichtshomeostase door b.v. letsel of een ontstekingsgebeurtenis kan artrose in dit gewricht veroorzaken. Artrose wordt gekenmerkt door een progressief verlies van kraakbeen en heeft een negatieve invloed op de kwaliteit van leven van een patiënt. Artrose wordt meestal gediagnosticeerd in een laat stadium van de ziekte.

Op dit moment is er geen specifieke biomarker voor vroege diagnose van artrose, artrose-progressie of prognose na kraakbeenherstelchirurgie. De meeste onderzoeken richten zich op biomarkers in kraakbeen, synovia of synoviaal vocht. In dit proefschrift werd echter aandacht besteed aan het potentieel van het infrapatellaire vetkussentje voor de ontdekking van biomarkers. Bovendien werd in Hoofdstuk 2 besproken dat, in plaats van één specifieke biomarker, een groep moleculen (waaronder lipiden, eiwitten en metabolieten) ons een biomarkerpaneel zou opleveren dat een beter inzicht geeft in de ontwikkeling van artrose en potentiële therapeutische doelen. Het gebruik van ongerichte massaspectrometrie (MS)-technieken zou kunnen bijdragen aan het verkrijgen van meer kennis over het moleculaire begrip van artrose. Vroege opsporing en behandeling van artrose zijn van groot belang. Het is aangetoond dat veranderingen in levensstijl, evenals operaties die de gewrichten beschermen, de ontwikkeling van artrose vertragen, stoppen of omkeren. Zodra een patiënt lijdt aan artrose in het eindstadium, is de enige beschikbare behandelingsoptie een totale knieartroplastiek. Waar deze behandeling een beperkte levensduur heeft, is het uitstellen van artrose-progressie en totale knieartroplastiek bij patiënten van groot belang.

De eerste lijn van behandelingsopties voor artrose omvat lichaamsbeweging en dieetveranderingen, evenals het gebruik van niet-steroïde anti-inflammatoire geneesmiddelen (NSAIDs) om symptomen te behandelen. Een van deze NSAIDs is celecoxib, een selectieve cyclo-oxygenase-2 (COX-2)-remmer. In Hoofdstuk 3 werden het ontstekingsremmende en chondroprotectieve effect van celecoxib bestudeerd in een menselijke kraakbeenexplantcultuur, evenals in een diermodel voor artrose door middel van intra-articulaire enkelvoudige bolustoediening.

Celecoxib verminderde de secretie van pro-inflammatoire prostaglandinen, evenals eiwitten, en veranderde genexpressie in explantaten van menselijk gewrichtskraakbeen. *In vivo*, in een artrosse-model bij ratten, werkte celecoxib chondroprotectief na een enkele intra-articulaire bolusinjectie.

Om het potentieel van het infrapatellaire vetkussentje in de zoektocht naar biomarkers voor artrose te onderzoeken, werd in Hoofdstuk 4 een methode voor de analyse van lipiden in het infrapatellaire vetkussentje met behulp van matrix-geassisteerde laserdesorptie/ionisatie massaspectrometrie-beeldvorming (MALDI-MSI) geoptimaliseerd. De grootste uitdaging ligt bij de sample voorbereiding. Het infrapatellaire vetkussentje is een vetachtig weefsel en is daarom vatbaar voor smelten. Het smelten van weefsel tijdens verschillende stappen van de monstervoorbereiding, inclusief cryosectie, transport of matrixtoepassing, zou delokalisatie van moleculen veroorzaken. Om dit te voorkomen en om de ruimtelijke molecuulinformatie van het infrapatellaire vetkussentje te behouden, werden cryosecties gemaakt bij zeer lage temperaturen. Het ontdooien en opnieuw invriezen gebeurde met zeer hoge snelheden en het transport gebeurde altijd met behulp van draagdozen met silicagel. De belangrijkste verschillende weefseltypen binnen het vetkussentje-explantaat (vetweefsel, bindweefsel en synovium) konden worden geïdentificeerd met MALDI-MSI. Vervolgens werd deze methode in Hoofdstuk 5 toegepast om de verschillen in lipidenprofielen in het infrapatellaire vetkussentje van patiënten met artrose en kraakbeendefecten te visualiseren. Er werden verschillende lipidenprofielen geïdentificeerd voor patiënten met artrose en kraakbeendefecten. Bovendien werd de intra-weefselheterogeniteit van het infrapatellaire vetkussentje erkend, omdat deze mogelijk verband houdt met patiëntfenotypes. Arachidonzuur-bevattende, ether-gekoppelde fosfatidylethanolamines (PE-O-s) in het bindweefsel van het infrapatellaire vetkussentje werden voorgesteld als specifiek voor artrose.

In Hoofdstuk 6 hebben we gewerkt aan een point-of-care-apparaat voor de diagnose van artrose en voor het voorspellen van de ontwikkeling van artrose na een kraakbeendefect. Snelle verdamping-ionisatie-massaspectrometrie (REIMS) werd gebruikt om de lipidenprofielen van artrose te visualiseren, evenals een verscheidenheid aan patiënten met kraakbeendefecten. REIMS was alleen in staat om de sneden in het infrapatellaire vetkussentje van patiënten met een leeftijd boven de 35 of onder de 35 jaar (65%) correct te classificeren. Verder, zoals eerder is aangetoond in Hoofdstuk 4 en Hoofdstuk 5, was de intra-weefselheterogeniteit van het infrapatellaire vetkussentje van belang. Sneden gemaakt in vetweefsel of bindweefsel konden correct worden geclassificeerd met een percentage van 90%. Rekening houdend met deze heterogeniteit binnen het weefsel, terwijl gekeken werd naar de klinische uitkomst na een operatie, werden de hoogste correcte classificaties verkregen met postoperatieve knieblessure en osteoartritis

uitkomstscore (KOOS) voor vetweefsel (70%) en bindweefsel (73%), evenals voor postoperatieve visuele analoge schaal (VAS) scores voor bindweefsel (73%). Volgens deze resultaten is het niet waarschijnlijk dat REIMS zal worden gebruikt als methode om klinische voorspellingsmodellen voor kraakbeenhersteloperaties te ontwikkelen.

Meer onderzoek en optimalisatie van de techniek is nodig om de kleine veranderingen in het infrapatellaire vetkussentje na een kraakbeendefect te identificeren. Eiwit-resultaten in Hoofdstuk 6 suggereren dat er een interactie is tussen het infrapatellaire vetkussentje en kraakbeen, aangezien een verscheidenheid aan kraakbeeneiwitten die gerelateerd zijn aan kraakbeenafbraak of artrose werden gemeten. Het infrapatellaire vetkussentje kan daarom worden gezien als een veelbelovende weefselbron voor de ontdekking van (artrose) biomarkers. Toekomstige studies zouden echter bij het trekken van conclusies rekening moeten houden met de intra-weefselheterogeniteit van het infrapatellaire vetkussentje.

Appendix

List of abbreviations

References

List of publications & presentations

Acknowledgements

Biography

List of abbreviations

1 H NMR	1 H nuclear magnetic resonance
2D-DIGE-MS	Two-dimensional difference gel electrophoresis mass spectrometry
2DE	Two-dimensional gel electrophoresis
ABC	Ammonium bicarbonate
ABI3BP	Target of Nesh-SH3
ACAN	Aggrecan
ACL	Anterior cruciate ligament
ACLT/pMMx	Anterior cruciate ligament and partial medial meniscectomy
ACN	Acetonitrile
ACT	Articular chondrocyte transplantation
ACTBL	Beta-actin-like protein
ADAMTS	A disintegrin and metalloproteinase with thrombospondin motifs
ADL	Activities of daily living
AIF	Allograft inflammatory factor
APCI	Atmospheric pressure chemical ionization
APO	Apolipoprotein
APPI	Atmospheric pressure photoionization
ARRIVE	Animal research reporting of in vivo experiments
BMI	Body mass index
B/W	Between/within
CA	Carbonic anhydrase
CD	Hematopoietic progenitor cell antigen
CI	Collision induced
CID	Collision-induced dissociation
CILP	Cartilage intermediate layer protein
COL	Collagen
COMP	Cartilage oligomeric matrix protein
COX	Cyclooxygenase
COPE	Coatomer subunit epsiloon
CytC	Cytochrome C
DDA	Data-dependent acquisition
DEC	Animal ethics committee
DEFA	Neutrofil defensin
DF	Discriminant function
DMEM	Dulbecco’s modified Eagle’s medium
DMOAD	Disease modifying osteoarthritis drug
DMSO	Dimethyl sulfoxide
DOC	Deoxycholate
DTT	Dithiothreitol
ECM	Extracellular matrix
EDTA	Ethylenediaminetetraacetic acid

EI	Electron ionization
ELISA	Enzyme-linked immunosorbent assay
eOA	Early osteoarthritis
EORS	European orthopedic research society
EPHX	Epoxide hydrolase
ESB	European society for biomaterials
ESI	Electrospray ionization
EsSKOA	Early-stage Symptomatic Knee Osteoarthritis
ESTROT	European society of tissue regeneration in orthopedics and traumatology
lOA	Late osteoarthritis
FA	Formic acid
FAB	Fatty acid-binding protein
FAS	Fatty acid synthase
FDA	Food and drug administration
FDR	False discovery rate
FFPE	Formalin-fixed and paraffin embedded
GAG	Glycosaminoglycan
GAPDH	Glyceraldehyde 3-phosphate dehydrogenase
GC-MS	Gas chromatography
GFRP	GTP cyclohydrolase 1 feedback regulatory protein
GILT	Gamma-interferon-inducible lysosomal thiol reductase
H&E	Hematoxylin and eosin
HB	Hemoglobin
HCD	Higher-energy collisional dissociation
HCLS	Hematopoietic lineage cell-specific protein
HFP	Hoffa's fat pad
HP	Haptoglobin
HPLC	High performance liquid chromatography
HTA	Health technology assessment
IAM	Iodoacetamide
ICRS	International cartilage regeneration and joint preservation society
IPFP	Infrapatellar fat pad
IQR	Inter quartile range
IRS	Insulin receptor substrate
ITO	Indium tin oxide
ITS	Insulin-transferrin-selenite
KL	Kellgren-Lawrence
KOOS	Knee injury and osteoarthritis outcome score
LC-MS	Liquid chromatography mass spectrometry
LC-MS/MS	Liquid chromatography tandem mass spectrometry
LDA	Linear discriminant analysis
Leu-Enk	Leucine-Encephalin
LMD	Laser microdissection

LOX	Protein-lysine 6-oxidase
MAGP	Microfibril-associated glycoprotein
MALDI	Matrix-assisted laser desorption/ionization
MBP	Myelin basic protein
MCID	Minimal clinically important difference
MEC	Medical ethics committee
METC	Medical ethics testing committee
MGST	Microsomal glutathione S-transferase
MMP	Matrix metalloproteinase
MPS1	40S ribosomal protein S27
MRI	Magnetic resonance imaging
MS	Mass spectrometry
MS^1	Mass spectrometry
MS/MS	Tandem mass spectrometry
MS^2	Tandem mass spectrometry
MSBM	Mass spectrometry school in biotechnology and medicine
m/z	Mass-to-charge ratio
MSI	Mass spectrometry imaging
MUMC+	Maastricht university medical center +
NCE	Normalized collision energy
NDPKA	Nucleoside diphosphate kinase
NOL	Nucleolar protein
NOV	Dutch orthopedic association
NS	Not stated
NSAID	Non-steroidal anti-inflammatory drug
OA	Osteoarthritis
OARSI	Osteoarthritis research society international
OPLS-DA	Orthogonal partial least squares discriminant analysis
P36269	Glutathione hydrolase 5 proenzyme
PA	Phosphatidic acid
PBP	Platelet basic protein
PBS	Phosphate buffered saline
PC	Principal component
PCA	Principal component analysis
PD	Proteome discoverer
PE	Phosphatidylethanolamine
PEN	Polyethylene naphthalate
PE O-	Ether-linked phosphatidylethanolamine
PG	Prostaglandin
PI	Phosphatidylinositol
PICALM	Phosphatidylinositol-binding clathrin assembly protein
PPIA	Peptidylprolyl isomerase A
PPS	Polyphenylene sulfide

PRG	Proteoglycan
PRISMA	Preferred reporting items for systematic reviews and meta-analysis
PROM	Patient reported outcome measure
PS	Phosphatidylserine
PTOA	Post-traumatic osteoarthritis
QOL	Quality of life
Q-TOF	Quadrupole time-of-flight
REIMS	Rapid evaporative ionization mass spectrometry
RHOC	Rho-related GTP-binding protein
ROI	Region of interest
RP-LC-MS	Reversed phase liquid chromatography mass spectrometry
rRNA	Ribosomal RNA
RT-qPCR	Quantitative real-time polymerase chain reaction
SA	Serum amyloid
SDS-PAGE	Sodium dodecyl sulfate polyacrylamide gel electrophoresis
SIMS	Secondary ion mass spectrometry
SM	Sphingomyelin
SMOC	SPARC-related modular calcium-binding protein
SOP	Standard operating procedure
SPARC	Secreted protein acidic and rich in cysteine
SWATH-MS	SWATH mass spectrometry
T2DM	Type 2 diabetes mellitus
TCA	Trichloroacetic acid
TERMIS	Tissue engineering and regenerative medicine international society
TIMP	Tissue inhibitor of metalloproteinase
TKA	Total knee arthroplasty
TNX	Tenascin-X
TOF	Time-of-flight
TUB	Tubulin
TX	Thromboxane
UHPLC	Ultra high performance liquid chromatography
ULC/MS	Ultra liquid chromatography/mass spectrometry
ULF	Ultra-low temperature freezer
VAS	Visual analogue scale
VW	Von Willebrand
WMO	Wet medisch-wetenschappelijk onderzoek

References

1. Hunter DJ, March L, Chew M. Osteoarthritis in 2020 and beyond: a Lancet Commission. Lancet. 2020;396(10264):1711-2.
2. Plotz B, Bomfim F, Sohail MA, Samuels J. Current Epidemiology and Risk Factors for the Development of Hand Osteoarthritis. Curr Rheumatol Rep. 2021;23(8):61.
3. Cho HJ, Morey V, Kang JY, Kim KW, Kim TK. Prevalence and Risk Factors of Spine, Shoulder, Hand, Hip, and Knee Osteoarthritis in Community-dwelling Koreans Older Than Age 65 Years. Clin Orthop Relat Res. 2015;473(10):3307-14.
4. Marshall M, Watt FE, Vincent TL, Dziedzic K. Hand osteoarthritis: clinical phenotypes, molecular mechanisms and disease management. Nat Rev Rheumatol. 2018;14(11):641-56.
5. Disease GBD, Injury I, Prevalence C. Global, regional, and national incidence, prevalence, and years lived with disability for 310 diseases and injuries, 1990-2015: a systematic analysis for the Global Burden of Disease Study 2015. Lancet. 2016;388(10053):1545-602.
6. Cui A, Li H, Wang D, Zhong J, Chen Y, Lu H. Global, regional prevalence, incidence and risk factors of knee osteoarthritis in population-based studies. EClinicalMedicine. 2020;29-30:100587.
7. Booth FW, Roberts CK, Laye MJ. Lack of exercise is a major cause of chronic diseases. Compr Physiol. 2012;2(2):1143-211.
8. Veronese N, Cereda E, Maggi S, Luchini C, Solmi M, Smith T, et al. Osteoarthritis and mortality: A prospective cohort study and systematic review with meta-analysis. Semin Arthritis Rheum. 2016;46(2):160-7.
9. Luyten FP, Lories RJ, Verschueren P, de Vlam K, Westhovens R. Contemporary concepts of inflammation, damage and repair in rheumatic diseases. Best Pract Res Clin Rheumatol. 2006;20(5):829-48.
10. Lories RJ. Joint homeostasis, restoration, and remodeling in osteoarthritis. Best Pract Res Clin Rheumatol. 2008;22(2):209-20.
11. Sophia Fox AJ, Bedi A, Rodeo SA. The basic science of articular cartilage: structure, composition, and function. Sports Health. 2009;1(6):461-8.
12. Gee SM, Posner M. Meniscus Anatomy and Basic Science. Sports Med Arthrosc Rev. 2021;29(3):e18-e23.
13. Noyes FR. The function of the human anterior cruciate ligament and analysis of single- and double-bundle graft reconstructions. Sports Health. 2009;1(1):66-75.
14. Smith MD. The normal synovium. Open Rheumatol J. 2011;5:100-6.
15. Dragoo JL, Johnson C, McConnell J. Evaluation and treatment of disorders of the infrapatellar fat pad. Sports Med. 2012;42(1):51-67.
16. Timur UT, Caron MMJ, Bastiaansen-Jenniskens YM, Welting TJM, van Rhijn LW, van Osch G, et al. Celecoxib-mediated reduction of prostanoid release in Hoffa's fat pad from donors with cartilage pathology results in an attenuated inflammatory phenotype. Osteoarthritis Cartilage. 2018;26(5):697-706.
17. Labusca L, Zugun-Eloae F. The Unexplored Role of Intra-articular Adipose Tissue in the Homeostasis and Pathology of Articular Joints. Front Vet Sci. 2018;5:35.
18. Ottaviani E, Malagoli D, Franceschi C. The evolution of the adipose tissue: a neglected enigma. Gen Comp Endocrinol. 2011;174(1):1-4.

19. Coelho M, Oliveira T, Fernandes R. Biochemistry of adipose tissue: an endocrine organ. Arch Med Sci. 2013;9(2):191-200.
20. Ioan-Facsinay A, Kloppenburg M. An emerging player in knee osteoarthritis: the infrapatellar fat pad. Arthritis Res Ther. 2013;15(6):225.
21. do Amaral R, Almeida HV, Kelly DJ, O'Brien FJ, Kearney CJ. Infrapatellar Fat Pad Stem Cells: From Developmental Biology to Cell Therapy. Stem Cells Int. 2017;2017:6843727.
22. Oppenheimer SR, Wehr AY. Imaging mass spectrometry in drug discovery and development. Bioanalysis. 2015;7(20):2609-10.
23. Hunter W. Of the structure and disease of articulating cartilages. 1743. Clin Orthop Relat Res. 1995(317):3-6.
24. Abramoff B, Caldera FE. Osteoarthritis: Pathology, Diagnosis, and Treatment Options. Med Clin North Am. 2020;104(2):293-311.
25. Mandl LA. Osteoarthritis year in review 2018: clinical. Osteoarthritis Cartilage. 2019;27(3):359-64.
26. Disease GBD, Injury I, Prevalence C. Global, regional, and national incidence, prevalence, and years lived with disability for 354 diseases and injuries for 195 countries and territories, 1990-2017: a systematic analysis for the Global Burden of Disease Study 2017. Lancet. 2018;392(10159):1789-858.
27. Centers for Disease C, Prevention. Prevalence and impact of arthritis among women--United States, 1989-1991. MMWR Morb Mortal Wkly Rep. 1995;44(17):329-34.
28. Musumeci G, Aiello FC, Szychlinska MA, Di Rosa M, Castrogiovanni P, Mobasheri A. Osteoarthritis in the XXIst century: risk factors and behaviours that influence disease onset and progression. Int J Mol Sci. 2015;16(3):6093-112.
29. Blagojevic M, Jinks C, Jeffery A, Jordan KP. Risk factors for onset of osteoarthritis of the knee in older adults: a systematic review and meta-analysis. Osteoarthritis Cartilage. 2010;18(1):24-33.
30. Felson DT, Zhang Y, Hannan MT, Naimark A, Weissman BN, Aliabadi P, et al. The incidence and natural history of knee osteoarthritis in the elderly. The Framingham Osteoarthritis Study. Arthritis Rheum. 1995;38(10):1500-5.
31. Thomas AC, Hubbard-Turner T, Wikstrom EA, Palmieri-Smith RM. Epidemiology of Posttraumatic Osteoarthritis. J Athl Train. 2017;52(6):491-6.
32. Kujala UM, Kettunen J, Paananen H, Aalto T, Battie MC, Impivaara O, et al. Knee osteoarthritis in former runners, soccer players, weight lifters, and shooters. Arthritis Rheum. 1995;38(4):539-46.
33. Zhang Y, Jordan JM. Epidemiology of osteoarthritis. Clin Geriatr Med. 2010;26(3):355-69.
34. Kellgren JH, Lawrence JS. Radiological assessment of osteo-arthrosis. Ann Rheum Dis. 1957;16(4):494-502.
35. Uthman OA, van der Windt DA, Jordan JL, Dziedzic KS, Healey EL, Peat GM, et al. Exercise for lower limb osteoarthritis: systematic review incorporating trial sequential analysis and network meta-analysis. BMJ. 2013;347:f5555.
36. Messier SP, Legault C, Loeser RF, Van Arsdale SJ, Davis C, Ettinger WH, et al. Does high weight loss in older adults with knee osteoarthritis affect bone-on-bone joint loads and muscle forces during walking? Osteoarthritis Cartilage. 2011;19(3):272-80.
37. Pai YC, Rymer WZ, Chang RW, Sharma L. Effect of age and osteoarthritis on knee proprioception. Arthritis Rheum. 1997;40(12):2260-5.

38. Rannou F, Poiraudeau S, Beaudreuil J. Role of bracing in the management of knee osteoarthritis. Curr Opin Rheumatol. 2010;22(2):218-22.
39. Fransen M, McConnell S, Harmer AR, Van der Esch M, Simic M, Bennell KL. Exercise for osteoarthritis of the knee: a Cochrane systematic review. Br J Sports Med. 2015;49(24):1554-7.
40. Zarghi A, Arfaei S. Selective COX-2 Inhibitors: A Review of Their Structure-Activity Relationships. Iran J Pharm Res. 2011;10(4):655-83.
41. Nakata K, Hanai T, Take Y, Osada T, Tsuchiya T, Shima D, et al. Disease-modifying effects of COX-2 selective inhibitors and non-selective NSAIDs in osteoarthritis: a systematic review. Osteoarthritis Cartilage. 2018;26(10):1263-73.
42. Mastbergen SC, Lafeber FP, Bijlsma JW. Selective COX-2 inhibition prevents proinflammatory cytokine-induced cartilage damage. Rheumatology (Oxford). 2002;41(7):801-8.
43. Alvarez-Soria MA, Herrero-Beaumont G, Sanchez-Pernaute O, Bellido M, Largo R. Diacerein has a weak effect on the catabolic pathway of human osteoarthritis synovial fibroblast - comparison to its effects on osteoarthritic chondrocytes. Rheumatology. 2008;47(5):627-33.
44. de Boer TN, Huisman AM, Polak AA, Niehoff AG, van Rinsum AC, Saris D, et al. The chondroprotective effect of selective COX-2 inhibition in osteoarthritis: ex vivo evaluation of human cartilage tissue after in vivo treatment. Osteoarthr Cartilage. 2009;17(4):482-8.
45. Jiang DH, Zou J, Huang LX, Shi Q, Zhu XS, Wang GL, et al. Efficacy of Intra-Articular Injection of Celecoxib in a Rabbit Model of Osteoarthritis. International Journal of Molecular Sciences. 2010;11(10):4106-13.
46. Welting TJ, Caron MM, Emans PJ, Janssen MP, Sanen K, Coolsen MM, et al. Inhibition of cyclooxygenase-2 impacts chondrocyte hypertrophic differentiation during endochondral ossification. Eur Cell Mater. 2011;22:420-36; discussion 36-7.
47. Zweers MC, de Boer TN, van Roon J, Bijlsma JWJ, Lafeber FPJG, Mastbergen SC. Celecoxib: considerations regarding its potential disease-modifying properties in osteoarthritis. Arthritis Research & Therapy. 2011;13(5).
48. Mastbergen SC, Marijnissen AC, Vianen ME, Zoer B, van Roermund PM, Bijlsma JW, et al. Inhibition of COX-2 by celecoxib in the canine groove model of osteoarthritis. Rheumatology (Oxford). 2006;45(4):405-13.
49. Raynauld JP, Martel-Pelletier J, Beaulieu A, Bessette L, Morin F, Choquette D, et al. An open-label pilot study evaluating by magnetic resonance imaging the potential for a disease-modifying effect of celecoxib compared to a modelized historical control cohort in the treatment of knee osteoarthritis. Semin Arthritis Rheum. 2010;40(3):185-92.
50. Fukai A, Kamekura S, Chikazu D, Nakagawa T, Hirata M, Saito T, et al. Lack of a chondroprotective effect of cyclooxygenase 2 inhibition in a surgically induced model of osteoarthritis in mice. Arthritis Rheum. 2012;64(1):198-203.
51. Haartmans MJJ, Timur UT, Emanuel KS, Caron MMJ, Jeuken RM, Welting TJM, et al. Evaluation of the Anti-Inflammatory and Chondroprotective Effect of Celecoxib on Cartilage Ex Vivo and in a Rat Osteoarthritis Model. Cartilage. 2022;13(3):19476035221115541.
52. Hawkey CJ. COX-2 inhibitors. Lancet. 1999;353(9149):307-14.
53. Skou ST, Roos EM, Laursen MB, Rathleff MS, Arendt-Nielsen L, Simonsen O, et al. A Randomized, Controlled Trial of Total Knee Replacement. N Engl J Med. 2015;373(17):1597-606.

54. Driban JB, Harkey MS, Liu SH, Salzler M, McAlindon TE. Osteoarthritis and Aging: Young Adults with Osteoarthritis. Curr Epidemiol Rep. 2020;7(1):9-15.
55. Learmonth ID, Young C, Rorabeck C. The operation of the century: total hip replacement. Lancet. 2007;370(9597):1508-19.
56. Bayliss LE, Culliford D, Monk AP, Glyn-Jones S, Prieto-Alhambra D, Judge A, et al. The effect of patient age at intervention on risk of implant revision after total replacement of the hip or knee: a population-based cohort study. Lancet. 2017;389(10077):1424-30.
57. Li CS, Karlsson J, Winemaker M, Sancheti P, Bhandari M. Orthopedic surgeons feel that there is a treatment gap in management of early OA: international survey. Knee Surg Sports Traumatol Arthrosc. 2014;22(2):363-78.
58. Zhang L, Hu J, Athanasiou KA. The role of tissue engineering in articular cartilage repair and regeneration. Crit Rev Biomed Eng. 2009;37(1-2):1-57.
59. Oegema TR, Jr., Carpenter RJ, Hofmeister F, Thompson RC, Jr. The interaction of the zone of calcified cartilage and subchondral bone in osteoarthritis. Microsc Res Tech. 1997;37(4):324-32.
60. Kwon H, Brown WE, Lee CA, Wang D, Paschos N, Hu JC, et al. Surgical and tissue engineering strategies for articular cartilage and meniscus repair. Nat Rev Rheumatol. 2019;15(9):550-70.
61. Jeuken RM, van Hugten PPW, Roth AK, Timur UT, Boymans T, van Rhijn LW, et al. A Systematic Review of Focal Cartilage Defect Treatments in Middle-Aged Versus Younger Patients. Orthop J Sports Med. 2021;9(10):23259671211031244.
62. Ward BD, Lubowitz JH. Basic knee arthroscopy part 4: chondroplasty, meniscectomy, and cruciate ligament evaluation. Arthrosc Tech. 2013;2(4):e507-8.
63. Armiento AR, Alini M, Stoddart MJ. Articular fibrocartilage - Why does hyaline cartilage fail to repair? Adv Drug Deliv Rev. 2019;146:289-305.
64. Brittberg M, Lindahl A, Nilsson A, Ohlsson C, Isaksson O, Peterson L. Treatment of deep cartilage defects in the knee with autologous chondrocyte transplantation. N Engl J Med. 1994;331(14):889-95.
65. Inderhaug E, Solheim E. Osteochondral Autograft Transplant (Mosaicplasty) for Knee Articular Cartilage Defects. JBJS Essent Surg Tech. 2019;9(4).
66. Sanders TL, Pareek A, Obey MR, Johnson NR, Carey JL, Stuart MJ, et al. High Rate of Osteoarthritis After Osteochondritis Dissecans Fragment Excision Compared With Surgical Restoration at a Mean 16-Year Follow-up. Am J Sports Med. 2017;45(8):1799-805.
67. Jeuken RM, van Hugten PPW, Roth AK, Boymans T, Caron J, Weber A, et al. Cartilage repair strategies in the knee according to Dutch Orthopedic Surgeons: a survey study. Arch Orthop Trauma Surg. 2023.
68. van Tuijn IM, Emanuel KS, van Hugten PPW, Jeuken R, Emans PJ. Prognostic Factors for the Clinical Outcome after Microfracture Treatment of Chondral and Osteochondral Defects in the Knee Joint: A Systematic Review. Cartilage. 2023;14(1):5-16.
69. Punzi L, Galozzi P, Luisetto R, Favero M, Ramonda R, Oliviero F, et al. Post-traumatic arthritis: overview on pathogenic mechanisms and role of inflammation. RMD Open. 2016;2(2):e000279.
70. Stiebel M, Miller LE, Block JE. Post-traumatic knee osteoarthritis in the young patient: therapeutic dilemmas and emerging technologies. Open Access J Sports Med. 2014;5:73-9.

71. Vincent KR, Conrad BP, Fregly BJ, Vincent HK. The pathophysiology of osteoarthritis: a mechanical perspective on the knee joint. PM R. 2012;4(5 Suppl):S3-9.
72. Kim YM, Joo YB. Patellofemoral osteoarthritis. Knee Surg Relat Res. 2012;24(4):193-200.
73. Dell'Isola A, Allan R, Smith SL, Marreiros SS, Steultjens M. Identification of clinical phenotypes in knee osteoarthritis: a systematic review of the literature. BMC Musculoskelet Disord. 2016;17(1):425.
74. Yu SP, Hunter DJ. Managing osteoarthritis. Aust Prescr. 2015;38(4):115-9.
75. Mahmoudian A, Lohmander LS, Mobasheri A, Englund M, Luyten FP. Early-stage symptomatic osteoarthritis of the knee - time for action. Nat Rev Rheumatol. 2021;17(10):621-32.
76. Van Spil WE, Kubassova O, Boesen M, Bay-Jensen AC, Mobasheri A. Osteoarthritis phenotypes and novel therapeutic targets. Biochem Pharmacol. 2019;165:41-8.
77. Deveza LA, Nelson AE, Loeser RF. Phenotypes of osteoarthritis: current state and future implications. Clin Exp Rheumatol. 2019;37 Suppl 120(5):64-72.
78. Mobasheri A, Saarakkala S, Finnila M, Karsdal MA, Bay-Jensen AC, van Spil WE. Recent advances in understanding the phenotypes of osteoarthritis. F1000Res. 2019;8.
79. Strimbu K, Tavel JA. What are biomarkers? Curr Opin HIV AIDS. 2010;5(6):463-6.
80. Detalle L, Vanheusden K, Sargentini-Maier ML, Stöhr T. 2.20 - Translational Aspects in Drug Discovery. In: Chackalamannil S, Rotella D, Ward SE, editors. Comprehensive Medicinal Chemistry III. Oxford: Elsevier; 2017. p. 495-529.
81. Haartmans MJJ, Emanuel KS, Tuijthof GJM, Heeren RMA, Emans PJ, Cillero-Pastor B. Mass Spectrometry-based Biomarkers for Knee Osteoarthritis: A Systematic Review. Expert Rev Proteomics. 2021;18(8):693-706.
82. Boffa A, Merli G, Andriolo L, Lattermann C, Salzmann GM, Filardo G. Synovial Fluid Biomarkers in Knee Osteoarthritis: A Systematic Review and Quantitative Evaluation Using BIPEDs Criteria. Cartilage. 2021;13(1_suppl):82S-103S.
83. Convill JG, Tawy GF, Freemont AJ, Biant LC. Clinically Relevant Molecular Biomarkers for Use in Human Knee Osteoarthritis: A Systematic Review. Cartilage. 2021;13(1_suppl):1511S-31S.
84. Hoch JM, Mattacola CG, Medina McKeon JM, Howard JS, Lattermann C. Serum cartilage oligomeric matrix protein (sCOMP) is elevated in patients with knee osteoarthritis: a systematic review and meta-analysis. Osteoarthritis Cartilage. 2011;19(12):1396-404.
85. Mobasheri A, Henrotin Y. Biomarkers of (osteo)arthritis. Biomarkers. 2015;20(8):513-8.
86. Jungmann PM, Baum T, Bauer JS, Karampinos DC, Erdle B, Link TM, et al. Cartilage repair surgery: outcome evaluation by using noninvasive cartilage biomarkers based on quantitative MRI techniques? Biomed Res Int. 2014;2014:840170.
87. Han EH, Chen SS, Klisch SM, Sah RL. Contribution of proteoglycan osmotic swelling pressure to the compressive properties of articular cartilage. Biophys J. 2011;101(4):916-24.
88. Bodzon-Kulakowska A, Suder P. Imaging mass spectrometry: Instrumentation, applications, and combination with other visualization techniques. Mass Spectrom Rev. 2016;35(1):147-69.
89. Chughtai K, Heeren RM. Mass spectrometric imaging for biomedical tissue analysis. Chem Rev. 2010;110(5):3237-77.

90. Buchberger AR, DeLaney K, Johnson J, Li L. Mass Spectrometry Imaging: A Review of Emerging Advancements and Future Insights. Anal Chem. 2018;90(1):240-65.
91. Haartmans MJJ, Claes BSR, Emanuel KS, Tuijthof GJM, Heeren RMA, Emans PJ, et al. Sample preparation for lipid analysis of intra-articular adipose tissue by using matrix-assisted laser desorption/ionization imaging. Anal Biochem. 2023;662:115018.
92. Cuypers E, Claes BSR, Biemans R, Lieuwes NG, Glunde K, Dubois L, et al. 'On the Spot' Digital Pathology of Breast Cancer Based on Single-Cell Mass Spectrometry Imaging. Anal Chem. 2022;94(16):6180-90.
93. Vaysse PM, Heeren RMA, Porta T, Balluff B. Mass spectrometry imaging for clinical research - latest developments, applications, and current limitations. Analyst. 2017;142(15):2690-712.
94. Glish GL, Vachet RW. The basics of mass spectrometry in the twenty-first century. Nat Rev Drug Discov. 2003;2(2):140-50.
95. Goodwin RJA. Sample preparation for mass spectrometry imaging: small mistakes can lead to big consequences. J Proteomics. 2012;75(16):4893-911.
96. Genangeli M, Heeren RMA, Porta Siegel T. Tissue classification by rapid evaporative ionization mass spectrometry (REIMS): comparison between a diathermic knife and CO(2) laser sampling on classification performance. Anal Bioanal Chem. 2019;411(30):7943-55.
97. Van Hese L, De Vleeschouwer S, Theys T, Lariviere E, Solie L, Sciot R, et al. Towards real-time intraoperative tissue interrogation for REIMS-guided glioma surgery. J Mass Spectrom Adv Clin Lab. 2022;24:80-9.
98. Boesl U. Time-of-flight mass spectrometry: Introduction to the basics. Mass Spectrom Rev. 2017;36(1):86-109.
99. Weickhardt C, Moritz F, Grotemeyer J. Time-of-flight mass spectrometry: State-of the-art in chemical analysis and molecular science. Mass Spectrom Rev. 1996;15(3):139-62.
100. Wells JM, McLuckey SA. Collision-induced dissociation (CID) of peptides and proteins. Methods Enzymol. 2005;402:148-85.
101. Karlsson O, Hanrieder J. Imaging mass spectrometry in drug development and toxicology. Arch Toxicol. 2017;91(6):2283-94.
102. Crecelius AC, Vitz J, Schubert US. Mass spectrometric imaging of synthetic polymers. Anal Chim Acta. 2014;808:10-7.
103. Dudley E. MALDI Profiling and Applications in Medicine. Adv Exp Med Biol. 2019;1140:27-43.
104. Duenas ME, Lee YJ. Single-Cell Metabolomics by Mass Spectrometry Imaging. Adv Exp Med Biol. 2021;1280:69-82.
105. Zhu X, Xu T, Peng C, Wu S. Advances in MALDI Mass Spectrometry Imaging Single Cell and Tissues. Front Chem. 2021;9:782432.
106. Ahlf Wheatcraft DR, Liu X, Hummon AB. Sample preparation strategies for mass spectrometry imaging of 3D cell culture models. J Vis Exp. 2014(94).
107. Wang S, Chen X, Luan H, Gao D, Lin S, Cai Z, et al. Matrix-assisted laser desorption/ionization mass spectrometry imaging of cell cultures for the lipidomic analysis of potential lipid markers in human breast cancer invasion. Rapid Commun Mass Spectrom. 2016;30(4):533-42.
108. Wang Y, Hummon AB. MS imaging of multicellular tumor spheroids and organoids as an emerging tool for personalized medicine and drug discovery. J Biol Chem. 2021;297(4):101139.

109. Liu X, Flinders C, Mumenthaler SM, Hummon AB. MALDI Mass Spectrometry Imaging for Evaluation of Therapeutics in Colorectal Tumor Organoids. J Am Soc Mass Spectrom. 2018;29(3):516-26.
110. Hart PJ, Clench MR. MALDI-MSI of Lipids in Human Skin. Methods Mol Biol. 2017;1618:29-36.
111. Mezger STP, Mingels AMA, Soulie M, Peutz-Kootstra CJ, Bekers O, Mulder P, et al. Protein Alterations in Cardiac Ischemia/Reperfusion Revealed by Spatial-Omics. Int J Mol Sci. 2022;23(22).
112. Tang W, Chen J, Zhou J, Ge J, Zhang Y, Li P, et al. Quantitative MALDI Imaging of Spatial Distributions and Dynamic Changes of Tetrandrine in Multiple Organs of Rats. Theranostics. 2019;9(4):932-44.
113. Susniak K, Krysa M, Gieroba B, Komaniecka I, Sroka-Bartnicka A. Recent developments of MALDI MSI application in plant tissues analysis. Acta Biochim Pol. 2020;67(3):277-81.
114. Sturtevant D, Lee YJ, Chapman KD. Matrix assisted laser desorption/ionization-mass spectrometry imaging (MALDI-MSI) for direct visualization of plant metabolites in situ. Curr Opin Biotechnol. 2016;37:53-60.
115. Nguyen HN. Visualization of Food Polyphenols. J Nutr Sci Vitaminol (Tokyo). 2022;68(Supplement):S116-S8.
116. Schwartz SA, Reyzer ML, Caprioli RM. Direct tissue analysis using matrix-assisted laser desorption/ionization mass spectrometry: practical aspects of sample preparation. J Mass Spectrom. 2003;38(7):699-708.
117. Marcos J, Pozo OJ. Current LC-MS methods and procedures applied to the identification of new steroid metabolites. J Steroid Biochem Mol Biol. 2016;162:41-56.
118. Seger C, Salzmann L. After another decade: LC-MS/MS became routine in clinical diagnostics. Clin Biochem. 2020;82:2-11.
119. Jones EA, Simon D, Karancsi T, Balog J, Pringle SD, Takats Z. Matrix Assisted Rapid Evaporative Ionization Mass Spectrometry. Anal Chem. 2019;91(15):9784-91.
120. Schafer KC, Denes J, Albrecht K, Szaniszlo T, Balog J, Skoumal R, et al. In vivo, in situ tissue analysis using rapid evaporative ionization mass spectrometry. Angew Chem Int Ed Engl. 2009;48(44):8240-2.
121. de Windt TS, Vonk LA, Brittberg M, Saris DB. Treatment and Prevention of (Early) Osteoarthritis Using Articular Cartilage Repair-Fact or Fiction? A Systematic Review. Cartilage. 2013;4(3 Suppl):5S-12S.
122. Kraus VB, Karsdal MA. Osteoarthritis: Current Molecular Biomarkers and the Way Forward. Calcif Tissue Int. 2021;109(3):329-38.
123. Poole AR. Osteoarthritis as a whole joint disease. HSS J. 2012;8(1):4-6.
124. Zeng N, Yan ZP, Chen XY, Ni GX. Infrapatellar Fat Pad and Knee Osteoarthritis. Aging Dis. 2020;11(5):1317-28.
125. Moher D, Liberati A, Tetzlaff J, Altman DG, Group P. Preferred reporting items for systematic reviews and meta-analyses: the PRISMA statement. Int J Surg. 2010;8(5):336-41.
126. Ouzzani M, Hammady H, Fedorowicz Z, Elmagarmid A. Rayyan-a web and mobile app for systematic reviews. Syst Rev. 2016;5(1):210.
127. Ahmed U, Anwar A, Savage RS, Thornalley PJ, Rabbani N. Protein oxidation, nitration and glycation biomarkers for early-stage diagnosis of osteoarthritis of the knee and typing and progression of arthritic disease. Arthritis Res Ther. 2016;18(1):250.

128. Ahrman E, Lorenzo P, Holmgren K, Grodzinsky AJ, Dahlberg LE, Saxne T, et al. Novel cartilage oligomeric matrix protein (COMP) neoepitopes identified in synovial fluids from patients with joint diseases using affinity chromatography and mass spectrometry. J Biol Chem. 2014;289(30):20908-16.
129. Brophy RH, Cai L, Duan X, Zhang Q, Townsend RR, Nunley RM, et al. Proteomic analysis of synovial fluid identifies periostin as a biomarker for anterior cruciate ligament injury. Osteoarthr Cartilage. 2019;27(12):1778-89.
130. Gobezie R, Kho A, Krastins B, Sarracino DA, Thornhill TS, Chase M, et al. High abundance synovial fluid proteome: distinct profiles in health and osteoarthritis. Arthritis Res Ther. 2007;9(2):R36.
131. Kamphorst JJ, van der Heijden R, DeGroot J, Lafeber FP, Reijmers TH, van El B, et al. Profiling of endogenous peptides in human synovial fluid by NanoLC-MS: method validation and peptide identification. J Proteome Res. 2007;6(11):4388-96.
132. Liao W, Li Z, Li T, Zhang Q, Zhang H, Wang X. Proteomic analysis of synovial fluid in osteoarthritis using SWATH-mass spectrometry. Mol Med Rep. 2018;17(2):2827-36.
133. Roller BL, Monibi F, Stoker AM, Bal BS, Cook JL. Identification of Novel Synovial Fluid Biomarkers Associated with Meniscal Pathology. J Knee Surg. 2016;29(1):47-62.
134. Steinbeck MJ, Nesti LJ, Sharkey PF, Parvizi J. Myeloperoxidase and chlorinated peptides in osteoarthritis: potential biomarkers of the disease. J Orthop Res. 2007;25(9):1128-35.
135. Timur UT, Jahr H, Anderson J, Green DC, Emans PJ, Smagul A, et al. Identification of tissue-dependent proteins in knee OA synovial fluid. Osteoarthritis Cartilage. 2021;29(1):124-33.
136. Corigliano A, Preiano M, Terracciano R, Savino R, De Gori M, Galasso O, et al. C3f is a potential tool for the staging of osteoarthritis. J Biol Regul Homeost Agents. 2017;31(4 suppl 1):29-35.
137. Liao W, Li Z, Wang H, Wang J, Fu Y, Bai X. Proteomic analysis of synovial fluid: insight into the pathogenesis of knee osteoarthritis. Int Orthop. 2013;37(6):1045-53.
138. Liao W, Li Z, Zhang H, Li J, Wang K, Yang Y. Proteomic analysis of synovial fluid as an analytical tool to detect candidate biomarkers for knee osteoarthritis. Int J Clin Exp Pathol. 2015;8(9):9975-89.
139. Ritter SY, Subbaiah R, Bebek G, Crish J, Scanzello CR, Krastins B, et al. Proteomic Analysis of Synovial Fluid From the Osteoarthritic Knee: Comparison With Transcriptome Analyses of Joint Tissues. Arthritis Rheum-Us. 2013;65(4):981-92.
140. Cillero-Pastor B, Eijkel GB, Kiss A, Blanco FJ, Heeren RM. Matrix-assisted laser desorption ionization-imaging mass spectrometry: a new methodology to study human osteoarthritic cartilage. Arthritis Rheum. 2013;65(3):710-20.
141. Guo D, Tan W, Wang F, Lv Z, Hu J, Lv T, et al. Proteomic analysis of human articular cartilage: identification of differentially expressed proteins in knee osteoarthritis. Joint Bone Spine. 2008;75(4):439-44.
142. Hsueh MF, Khabut A, Kjellstrom S, Onnerfjord P, Kraus VB. Elucidating the Molecular Composition of Cartilage by Proteomics. J Proteome Res. 2016;15(2):374-88.
143. Rosenthal AK, Gohr CM, Ninomiya J, Wakim BT. Proteomic analysis of articular cartilage vesicles from normal and osteoarthritic cartilage. Arthritis Rheum. 2011;63(2):401-11.

144. Wu J, Liu W, Bemis A, Wang E, Qiu Y, Morris EA, et al. Comparative proteomic characterization of articular cartilage tissue from normal donors and patients with osteoarthritis. Arthritis Rheum. 2007;56(11):3675-84.
145. Cillero-Pastor B, Eijkel GB, Blanco FJ, Heeren RM. Protein classification and distribution in osteoarthritic human synovial tissue by matrix-assisted laser desorption ionization mass spectrometry imaging. Anal Bioanal Chem. 2015;407(8):2213-22.
146. Tang S, Deng S, Guo J, Chen X, Zhang W, Cui Y, et al. Deep Coverage Tissue and Cellular Proteomics Revealed IL-1beta Can Independently Induce the Secretion of TNF-Associated Proteins from Human Synoviocytes. J Immunol. 2018;200(2):821-33.
147. Folkesson E, Turkiewicz A, Ali N, Ryden M, Hughes HV, Tjornstrand J, et al. Proteomic comparison of osteoarthritic and reference human menisci using data-independent acquisition mass spectrometry. Osteoarthritis Cartilage. 2020;28(8):1092-101.
148. Roller BL, Monibi F, Stoker AM, Bal BS, Stannard JP, Cook JL. Characterization of Meniscal Pathology Using Molecular and Proteomic Analyses. J Knee Surg. 2015;28(6):496-505.
149. Carlson AK, Rawle RA, Adams E, Greenwood MC, Bothner B, June RK. Application of global metabolomic profiling of synovial fluid for osteoarthritis biomarkers. Biochem Biophys Res Commun. 2018;499(2):182-8.
150. Carlson AK, Rawle RA, Wallace CW, Brooks EG, Adams E, Greenwood MC, et al. Characterization of synovial fluid metabolomic phenotypes of cartilage morphological changes associated with osteoarthritis. Osteoarthritis Cartilage. 2019;27(8):1174-84.
151. Kim S, Hwang J, Kim J, Ahn JK, Cha HS, Kim KH. Metabolite profiles of synovial fluid change with the radiographic severity of knee osteoarthritis. Joint Bone Spine. 2017;84(5):605-10.
152. Mickiewicz B, Kelly JJ, Ludwig TE, Weljie AM, Wiley JP, Schmidt TA, et al. Metabolic analysis of knee synovial fluid as a potential diagnostic approach for osteoarthritis. J Orthop Res. 2015;33(11):1631-8.
153. Zheng K, Shen N, Chen H, Ni S, Zhang T, Hu M, et al. Global and targeted metabolomics of synovial fluid discovers special osteoarthritis metabolites. J Orthop Res. 2017;35(9):1973-81.
154. Cillero-Pastor B, Eijkel G, Kiss A, Blanco FJ, Heeren RM. Time-of-flight secondary ion mass spectrometry-based molecular distribution distinguishing healthy and osteoarthritic human cartilage. Anal Chem. 2012;84(21):8909-16.
155. Kosinska MK, Liebisch G, Lochnit G, Wilhelm J, Klein H, Kaesser U, et al. A lipidomic study of phospholipid classes and species in human synovial fluid. Arthritis Rheum. 2013;65(9):2323-33.
156. Kosinska MK, Liebisch G, Lochnit G, Wilhelm J, Klein H, Kaesser U, et al. Sphingolipids in human synovial fluid--a lipidomic study. PLoS One. 2014;9(3):e91769.
157. Kosinska MK, Ludwig TE, Liebisch G, Zhang R, Siebert HC, Wilhelm J, et al. Articular Joint Lubricants during Osteoarthritis and Rheumatoid Arthritis Display Altered Levels and Molecular Species. PLoS One. 2015;10(5):e0125192.
158. Van de Vyver A, Clockaerts S, van de Lest CHA, Wei W, Verhaar J, Van Osch G, et al. Synovial Fluid Fatty Acid Profiles Differ between Osteoarthritis and Healthy Patients. Cartilage. 2020;11(4):473-8.

159. Xia J, Psychogios N, Young N, Wishart DS. MetaboAnalyst: a web server for metabolomic data analysis and interpretation. Nucleic Acids Res. 2009;37(Web Server issue):W652-60.
160. Eveque-Mourroux MR, Emans PJ, Boonen A, Claes BSR, Bouwman FG, Heeren RMA, et al. Heterogeneity of Lipid and Protein Cartilage Profiles Associated with Human Osteoarthritis with or without Type 2 Diabetes Mellitus. J Proteome Res. 2021;20(5):2973-82.
161. Courtney P, Doherty M. Joint aspiration and injection and synovial fluid analysis. Best Pract Res Clin Rheumatol. 2013;27(2):137-69.
162. Friel NA, Chu CR. The role of ACL injury in the development of posttraumatic knee osteoarthritis. Clin Sports Med. 2013;32(1):1-12.
163. Rai MF, Brophy RH, Sandell LJ. Osteoarthritis following meniscus and ligament injury: insights from translational studies and animal models. Curr Opin Rheumatol. 2019;31(1):70-9.
164. Mathiessen A, Conaghan PG. Synovitis in osteoarthritis: current understanding with therapeutic implications. Arthritis Res Ther. 2017;19(1):18.
165. Belluzzi E, Stocco E, Pozzuoli A, Granzotto M, Porzionato A, Vettor R, et al. Contribution of Infrapatellar Fat Pad and Synovial Membrane to Knee Osteoarthritis Pain. Biomed Res Int. 2019;2019:6390182.
166. Barr AJ, Campbell TM, Hopkinson D, Kingsbury SR, Bowes MA, Conaghan PG. A systematic review of the relationship between subchondral bone features, pain and structural pathology in peripheral joint osteoarthritis. Arthritis Research & Therapy. 2015;17.
167. Kovacs B, Vajda E, Nagy EE. Regulatory Effects and Interactions of the Wnt and OPG-RANKL-RANK Signaling at the Bone-Cartilage Interface in Osteoarthritis. International Journal of Molecular Sciences. 2019;20(18).
168. Dakin SG, Martinez FO, Yapp C, Wells G, Oppermann U, Dean BJF, et al. Inflammation activation and resolution in human tendon disease. Sci Transl Med. 2015;7(311).
169. Le Quesne JPC, Spriggs KA, Bushell M, Willis AE. Dysregulation of protein synthesis and disease. J Pathol. 2010;220(2):140-51.
170. Corradi V, Mendez-Villuendas E, Ingolfsson HI, Gu RX, Siuda I, Melo MN, et al. Lipid-Protein Interactions Are Unique Fingerprints for Membrane Proteins. Acs Central Sci. 2018;4(6):709-17.
171. Ioan-Facsinay A, Kloppenburg M. Bioactive lipids in osteoarthritis: risk or benefit? Current Opinion in Rheumatology. 2018;30(1):108-13.
172. Klont F, Bras L, Wolters JC, Ongay S, Bischoff R, Halmos GB, et al. Assessment of Sample Preparation Bias in Mass Spectrometry-Based Proteomics. Analytical Chemistry. 2018;90(8):5405-13.
173. Gundry RL, White MY, Murray CI, Kane LA, Fu Q, Stanley BA, et al. Preparation of proteins and peptides for mass spectrometry analysis in a bottom-up proteomics workflow. Curr Protoc Mol Biol. 2009;Chapter 10:Unit10 25.
174. Hardin JA, Cobelli N, Santambrogio L. Consequences of metabolic and oxidative modifications of cartilage tissue. Nat Rev Rheumatol. 2015;11(9):521-9.
175. Cohen A. Mass Spectrometry, Review of the Basics: Electrospray, MALDI and Commonly Used Mass Analyzers (vol 44, pg 210, 2009). Appl Spectrosc Rev. 2009;44(4):362-
.

176. Domon B, Aebersold R. Mass spectrometry and protein analysis. Science. 2006;312(5771):212-7.
177. Kiraly M, Dalmadine Kiss B, Vekey K, Antal I, Ludanyi K. [Mass spectrometry: past and present]. Acta Pharm Hung. 2016;86(1):3-11.
178. Perkel J. Mass Spectrometry Ionization Sources: labCompare 2009 [Available from: https://www.labcompare.com/18-Mass-Spectrometry-Ionization-Sources/.
179. Gkretsi V, Simopoulou T, Tsezou A. Lipid metabolism and osteoarthritis: lessons from atherosclerosis. Prog Lipid Res. 2011;50(2):133-40.
180. Rockel JS, Kapoor M. The Metabolome and Osteoarthritis: Possible Contributions to Symptoms and Pathology. Metabolites. 2018;8(4).
181. Fontanella CG, Macchi V, Carniel EL, Frigo A, Porzionato A, Picardi EEE, et al. Biomechanical behavior of Hoffa's fat pad in healthy and osteoarthritic conditions: histological and mechanical investigations. Australas Phys Eng S. 2018;41(3):657-67.
182. Goracci L, Tortorella S, Tiberi P, Pellegrino RM, Di Veroli A, Valeri A, et al. Lipostar, a Comprehensive Platform-Neutral Cheminformatics Tool for Lipidomics. Analytical Chemistry. 2017;89(11):6258-65.
183. Lahm A, Mrosek E, Spank H, Erggelet C, Kasch R, Esser J, et al. Changes in content and synthesis of collagen types and proteoglycans in osteoarthritis of the knee joint and comparison of quantitative analysis with Photoshop-based image analysis. Arch Orthop Traum Su. 2010;130(4):557-64.
184. Miosge N, Hartmann M, Maelicke C, Herken R. Expression of collagen type I and type II in consecutive stages of human osteoarthritis. Histochem Cell Biol. 2004;122(3):229-36.
185. Smyth EM, Grosser T, Wang M, Yu Y, FitzGerald GA. Prostanoids in health and disease. J Lipid Res. 2009;50:S423-S8.
186. Paduszynski W, Jeskiewicz M, Uchanski P, Gackowski S, Radkowski M, Demkow U. Hoffa's Fat Pad Abnormality in the Development of Knee Osteoarthritis. Current Concepts in Medical Research and Practice. 2018;1039:95-102.
187. Loeser RF. Molecular mechanisms of cartilage destruction: Mechanics, inflammatory mediators, and aging collide. Arthritis Rheum-Us. 2006;54(5):1357-60.
188. Ushiyama T, Chano T, Inoue K, Matsusue Y. Cytokine production in the infrapatellar fat pad: another source of cytokines in knee synovial fluids. Annals of the Rheumatic Diseases. 2003;62(2):108-12.
189. Hoff P, Buttgereit F, Burmester GR, Jakstadt M, Gaber T, Andreas K, et al. Osteoarthritis synovial fluid activates pro-inflammatory cytokines in primary human chondrocytes. International Orthopaedics. 2013;37(1):145-51.
190. Xu D, Xu Y. Protein databases on the internet. Curr Protoc Protein Sci. 2004;Chapter 2:2 6 1-2 6 15.
191. Bruford EA, Braschi B, Denny P, Jones TEM, Seal RL, Tweedie S. Guidelines for human gene nomenclature. Nat Genet. 2020;52(8):754-8.
192. Liebisch G, Fahy E, Aoki J, Dennis EA, Durand T, Ejsing CS, et al. Update on LIPID MAPS classification, nomenclature, and shorthand notation for MS-derived lipid structures. J Lipid Res. 2020;61(12):1539-55.
193. Liebisch G, Vizcaino JA, Kofeler H, Trotzmuller M, Griffiths WJ, Schmitz G, et al. Shorthand notation for lipid structures derived from mass spectrometry. J Lipid Res. 2013;54(6):1523-30.

194. Balog J, Sasi-Szabo L, Kinross J, Lewis MR, Muirhead LJ, Veselkov K, et al. Intraoperative tissue identification using rapid evaporative ionization mass spectrometry. Sci Transl Med. 2013;5(194):194ra93.
195. Kloppenburg M, Berenbaum F. Osteoarthritis year in review 2019: epidemiology and therapy. Osteoarthritis Cartilage. 2020;28(3):242-8.
196. Rodriguez-Merchan EC. Patient dissatisfaction after total knee arthroplasty for hemophilic arthropathy and osteoarthritis (non-hemophilia patients). Expert Rev Hematol. 2016;9(1):59-68.
197. Oo WM, Hunter DJ. Disease modification in osteoarthritis: are we there yet? Clinical and Experimental Rheumatology. 2019;37(5):135-40.
198. Ricciotti E, FitzGerald GA. Prostaglandins and inflammation. Arterioscler Thromb Vasc Biol. 2011;31(5):986-1000.
199. Attur M, Al-Mussawir HE, Patel J, Kitay A, Dave M, Palmer G, et al. Prostaglandin E2 exerts catabolic effects in osteoarthritis cartilage: evidence for signaling via the EP4 receptor. J Immunol. 2008;181(7):5082-8.
200. Hardy MM, Seibert K, Manning PT, Currie MG, Woerner BM, Edwards D, et al. Cyclooxygenase 2-dependent prostaglandin E2 modulates cartilage proteoglycan degradation in human osteoarthritis explants. Arthritis Rheum. 2002;46(7):1789-803.
201. Li X, Ellman M, Muddasani P, Wang JH, Cs-Szabo G, van Wijnen AJ, et al. Prostaglandin E2 and its cognate EP receptors control human adult articular cartilage homeostasis and are linked to the pathophysiology of osteoarthritis. Arthritis Rheum. 2009;60(2):513-23.
202. Sato T, Konomi K, Fujii R, Aono H, Aratani S, Yagishita N, et al. Prostaglandin EP2 receptor signalling inhibits the expression of matrix metalloproteinase 13 in human osteoarthritic chondrocytes. Ann Rheum Dis. 2011;70(1):221-6.
203. Nishitani K, Ito H, Hiramitsu T, Tsutsumi R, Tanida S, Kitaori T, et al. PGE2 inhibits MMP expression by suppressing MKK4-JNK MAP kinase-c-JUN pathway via EP4 in human articular chondrocytes. J Cell Biochem. 2010;109(2):425-33.
204. Manferdini C, Maumus M, Gabusi E, Piacentini A, Filardo G, Peyrafitte JA, et al. Adipose-Derived Mesenchymal Stem Cells Exert Antiinflammatory Effects on Chondrocytes and Synoviocytes From Osteoarthritis Patients Through Prostaglandin E-2. Arthritis Rheum-Us. 2013;65(5):1271-81.
205. Martel-Pelletier J, Pelletier JP, Fahmi H. Cyclooxygenase-2 and prostaglandins in articular tissues. Semin Arthritis Rheum. 2003;33(3):155-67.
206. Goldenberg MM. Celecoxib, a selective cyclooxygenase-2 inhibitor for the treatment of rheumatoid arthritis and osteoarthritis. Clin Ther. 1999;21(9):1497-513; discussion 27-8.
207. Timur UT, Caron MMJ, Jeuken RM, Bastiaansen-Jenniskens YM, Welting TJM, van Rhijn LW, et al. Chondroprotective Actions of Selective COX-2 Inhibitors In Vivo: A Systematic Review. Int J Mol Sci. 2020;21(18).
208. Dong J, Jiang D, Wang Z, Wu G, Miao L, Huang L. Intra-articular delivery of liposomal celecoxib-hyaluronate combination for the treatment of osteoarthritis in rabbit model. Int J Pharm. 2013;441(1-2):285-90.
209. Janssen M, Timur UT, Woike N, Welting TJ, Draaisma G, Gijbels M, et al. Celecoxib-loaded PEA microspheres as an auto regulatory drug-delivery system after intra-articular injection. J Control Release. 2016;244(Pt A):30-40.

210. Tellegen AR, Rudnik-Jansen I, Pouran B, de Visser HM, Weinans HH, Thomas RE, et al. Controlled release of celecoxib inhibits inflammation, bone cysts and osteophyte formation in a preclinical model of osteoarthritis. Drug Deliv. 2018;25(1):1438-47.
211. Mehana EE, Khafaga AF, El-Blehi SS. The role of matrix metalloproteinases in osteoarthritis pathogenesis: An updated review. Life Sci. 2019;234:116786.
212. Pfaffl MW, Tichopad A, Prgomet C, Neuvians TP. Determination of stable housekeeping genes, differentially regulated target genes and sample integrity: BestKeeper--Excel-based tool using pair-wise correlations. Biotechnol Lett. 2004;26(6):509-15.
213. Gerwin N, Bendele AM, Glasson S, Carlson CS. The OARSI histopathology initiative - recommendations for histological assessments of osteoarthritis in the rat. Osteoarthritis Cartilage. 2010;18 Suppl 3:S24-34.
214. Kilkenny C, Browne WJ, Cuthill IC, Emerson M, Altman DG. Improving bioscience research reporting: the ARRIVE guidelines for reporting animal research. PLoS Biol. 2010;8(6):e1000412.
215. Sachs L. Applied statistics: a handbook of techniques: Springer Science & Business Media; 2012.
216. Mankin HJ, Dorfman H, Lippiello L, Zarins A. Biochemical and metabolic abnormalities in articular cartilage from osteo-arthritic human hips. II. Correlation of morphology with biochemical and metabolic data. J Bone Joint Surg Am. 1971;53(3):523-37.
217. Benjamini Y, Hochberg Y. Controlling the False Discovery Rate - a Practical and Powerful Approach to Multiple Testing. J R Stat Soc B. 1995;57(1):289-300.
218. Goldring MB. Articular cartilage degradation in osteoarthritis. HSS J. 2012;8(1):7-9.
219. Dave M, Amin AR. Yin-Yang regulation of prostaglandins and nitric oxide by PGD2 in human arthritis: reversal by celecoxib. Immunol Lett. 2013;152(1):47-54.
220. Jakob M, Demarteau O, Suetterlin R, Heberer M, Martin I. Chondrogenesis of expanded adult human articular chondrocytes is enhanced by specific prostaglandins. Rheumatology. 2004;43(7):852-7.
221. Caron MM, Emans PJ, Sanen K, Surtel DA, Cremers A, Ophelders D, et al. The Role of Prostaglandins and COX-Enzymes in Chondrogenic Differentiation of ATDC5 Progenitor Cells. PLoS One. 2016;11(4):e0153162.
222. Fosang AJ, Little CB. Drug insight: aggrecanases as therapeutic targets for osteoarthritis. Nat Clin Pract Rheum. 2008;4(8):420-7.
223. Verma P, Dalal K. ADAMTS-4 and ADAMTS-5: Key Enzymes in Osteoarthritis. Journal of Cellular Biochemistry. 2011;112(12):3507-14.
224. Hu QC, Ecker M. Overview of MMP-13 as a Promising Target for the Treatment of Osteoarthritis. International Journal of Molecular Sciences. 2021;22(4).
225. Nagase H, Kashiwagi M. Aggrecanases and cartilage matrix degradation. Arthritis Research & Therapy. 2003;5(2):94-103.
226. Yang SF, Hsieh YS, Lue KH, Chu SC, Chang IC, Lu KH. Effects of nonsteroidal anti-inflammatory drugs on the expression of urokinase plasminogen activator and inhibitor and gelatinases in the early osteoarthritic knee of humans. Clinical Biochemistry. 2008;41(1-2):109-16.
227. Tsutsumi R, Ito H, Hiramitsu T, Nishitani K, Akiyoshi M, Kitaori T, et al. Celecoxib inhibits production of MMP and NO via down-regulation of NF-kappaB and JNK in a PGE2 independent manner in human articular chondrocytes. Rheumatol Int. 2008;28(8):727-36.

228. Pruitt KD, Tatusova T, Klimke W, Maglott DR. NCBI Reference Sequences: current status, policy and new initiatives. Nucleic Acids Res. 2009;37(Database issue):D32-6.
229. Troeberg L, Nagase H. Analysis of TIMP expression and activity. Methods Mol Med. 2007;135:251-67.
230. Cabral-Pacheco GA, Garza-Veloz I, Castruita-De la Rosa C, Ramirez-Acuna JM, Perez-Romero BA, Guerrero-Rodriguez JF, et al. The Roles of Matrix Metalloproteinases and Their Inhibitors in Human Diseases. International Journal of Molecular Sciences. 2020;21(24).
231. Latini FRM, Hemerly JP, Oler G, Riggins GJ, Cerutti JM. Re-expression of ABI3-binding protein suppresses thyroid tumor growth by promoting senescence and inhibiting invasion. Endocr-Relat Cancer. 2008;15(3):787-99.
232. Martin JA, Buckwalter JA. The role of chondrocyte senescence in the pathogenesis of osteoarthritis and in limiting cartilage repair. Journal of Bone and Joint Surgery-American Volume. 2003;85a:106-10.
233. Price JS, Waters JG, Darrah C, Pennington C, Edwards DR, Donell ST, et al. The role of chondrocyte senescence in osteoarthritis. Aging Cell. 2002;1(1):57-65.
234. Hissnauer TN, Baranowsky A, Pestka JM, Streichert T, Wiegandt K, Goepfert C, et al. Identification of molecular markers for articular cartilage. Osteoarthr Cartilage. 2010;18(12):1630-8.
235. Giudici C, Raynal N, Wiedemann H, Cabral WA, Marini JC, Timpl R, et al. Mapping of SPARC/BM-40/osteonectin-binding sites on fibrillar collagens. Journal of Biological Chemistry. 2008;283(28):19551-60.
236. Lane TF, Sage EH. The Biology of Sparc, a Protein That Modulates Cell-Matrix Interactions. Faseb J. 1994;8(2):163-73.
237. Nanba Y, Nishida K, Yoshikawa T, Sato T, Inoue H, Kuboki Y. Expression of osteonectin in articular cartilage of osteoarthritic knees. Acta Med Okayama. 1997;51(5):239-43.
238. Mateos JL. Selective Inhibitors of Cyclooxygenase-2 (Cox-2) Celecoxib and Parecoxib: A Systematic Review. Drug Today. 2010;46:1-25.
239. Tuck M, Grelard F, Blanc L, Desbenoit N. MALDI-MSI Towards Multimodal Imaging: Challenges and Perspectives. Front Chem. 2022;10:904688.
240. Michno W, Wehrli PM, Blennow K, Zetterberg H, Hanrieder J. Molecular imaging mass spectrometry for probing protein dynamics in neurodegenerative disease pathology. J Neurochem. 2019;151(4):488-506.
241. Hanrieder J, Ljungdahl A, Andersson M. MALDI imaging mass spectrometry of neuropeptides in Parkinson's disease. J Vis Exp. 2012(60).
242. Heijs B, Holst-Bernal S, de Graaff MA, Briaire-de Bruijn IH, Rodriguez-Girondo M, van de Sande MAJ, et al. Molecular signatures of tumor progression in myxoid liposarcoma identified by N-glycan mass spectrometry imaging. Lab Invest. 2020;100(9):1252-61.
243. Kwon HJ, Kim Y, Sugihara Y, Baldetorp B, Welinder C, Watanabe K, et al. Drug compound characterization by mass spectrometry imaging in cancer tissue. Arch Pharm Res. 2015;38(9):1718-27.
244. Miniewska K, Godzien J, Mojsak P, Maliszewska K, Kretowski A, Ciborowski M. Mass spectrometry-based determination of lipids and small molecules composing adipose tissue with a focus on brown adipose tissue. J Pharm Biomed Anal. 2020;191:113623.
245. Baker RC, Nikitina Y, Subauste AR. Analysis of adipose tissue lipid using mass spectrometry. Methods Enzymol. 2014;538:89-105.

246. Lopez-Bascon MA, Calderon-Santiago M, Sanchez-Ceinos J, Fernandez-Vega A, Guzman-Ruiz R, Lopez-Miranda J, et al. Influence of sample preparation on lipidomics analysis of polar lipids in adipose tissue. Talanta. 2018;177:86-93.
247. Engin A. The Pathogenesis of Obesity-Associated Adipose Tissue Inflammation. Adv Exp Med Biol. 2017;960:221-45.
248. Stolarczyk E. Adipose tissue inflammation in obesity: a metabolic or immune response? Curr Opin Pharmacol. 2017;37:35-40.
249. Fantuzzi G. Adipose tissue, adipokines, and inflammation. J Allergy Clin Immunol. 2005;115(5):911-9; quiz 20.
250. Zhou S, Maleitzke T, Geissler S, Hildebrandt A, Fleckenstein FN, Niemann M, et al. Source and hub of inflammation: The infrapatellar fat pad and its interactions with articular tissues during knee osteoarthritis. J Orthop Res. 2022;40(7):1492-504.
251. Fernandez-Vega A, Chicano-Galvez E, Prentice BM, Anderson D, Priego-Capote F, Lopez-Bascon MA, et al. Optimization of a MALDI-Imaging protocol for studying adipose tissue-associated disorders. Talanta. 2020;219:121184.
252. Fournelle F, Yang E, Dufresne M, Chaurand P. Minimizing Visceral Fat Delocalization on Tissue Sections with Porous Aluminum Oxide Slides for Imaging Mass Spectrometry. Anal Chem. 2020;92(7):5158-67.
253. Good CJ, Neumann EK, Butrico CE, Cassat JE, Caprioli RM, Spraggins JM. High Spatial Resolution MALDI Imaging Mass Spectrometry of Fresh-Frozen Bone. Anal Chem. 2022;94(7):3165-72.
254. Anderson DM, Floyd KA, Barnes S, Clark JM, Clark JI, McHaourab H, et al. A method to prevent protein delocalization in imaging mass spectrometry of non-adherent tissues: application to small vertebrate lens imaging. Anal Bioanal Chem. 2015;407(8):2311-20.
255. Annesley TM. Ion suppression in mass spectrometry. Clin Chem. 2003;49(7):1041-4.
256. Ross MA, Kohut L, Loughran PA. Cryosectioning. Curr Protoc. 2022;2(1):e342.
257. Mezger STP, Mingels AMA, Bekers O, Heeren RMA, Cillero-Pastor B. Mass Spectrometry Spatial-Omics on a Single Conductive Slide. Anal Chem. 2021;93(4):2527-33.
258. Huizing LRS, Ellis SR, Beulen B, Barre FPY, Kwant PB, Vreeken RJ, et al. Development and evaluation of matrix application techniques for high throughput mass spectrometry imaging of tissues in the clinic. Clin Mass Spectrom. 2019;12:7-15.
259. Scupakova K, Balluff B, Tressler C, Adelaja T, Heeren RMA, Glunde K, et al. Cellular resolution in clinical MALDI mass spectrometry imaging: the latest advancements and current challenges. Clin Chem Lab Med. 2020;58(6):914-29.
260. Ellis SR, Paine MRL, Eijkel GB, Pauling JK, Husen P, Jervelund MW, et al. Automated, parallel mass spectrometry imaging and structural identification of lipids. Nat Methods. 2018;15(7):515-8.
261. Tortorella S, Tiberi P, Bowman AP, Claes BSR, Scupakova K, Heeren RMA, et al. LipostarMSI: Comprehensive, Vendor-Neutral Software for Visualization, Data Analysis, and Automated Molecular Identification in Mass Spectrometry Imaging. J Am Soc Mass Spectrom. 2020;31(1):155-63.
262. Pauling JK, Hermansson M, Hartler J, Christiansen K, Gallego SF, Peng B, et al. Proposal for a common nomenclature for fragment ions in mass spectra of lipids. PLoS One. 2017;12(11):e0188394.

263. Ibrahim MM. Subcutaneous and visceral adipose tissue: structural and functional differences. Obes Rev. 2010;11(1):11-8.
264. Greif DN, Kouroupis D, Murdock CJ, Griswold AJ, Kaplan LD, Best TM, et al. Infrapatellar Fat Pad/Synovium Complex in Early-Stage Knee Osteoarthritis: Potential New Target and Source of Therapeutic Mesenchymal Stem/Stromal Cells. Front Bioeng Biotechnol. 2020;8:860.
265. Sun K, Tordjman J, Clement K, Scherer PE. Fibrosis and adipose tissue dysfunction. Cell Metab. 2013;18(4):470-7.
266. Cieza A, Causey K, Kamenov K, Hanson SW, Chatterji S, Vos T. Global estimates of the need for rehabilitation based on the Global Burden of Disease study 2019: a systematic analysis for the Global Burden of Disease Study 2019. Lancet. 2021;396(10267):2006-17.
267. Heidari B. Knee osteoarthritis diagnosis, treatment and associated factors of progression: part II. Caspian J Intern Med. 2011;2(3):249-55.
268. Heidari B. Knee osteoarthritis prevalence, risk factors, pathogenesis and features: Part I. Caspian J Intern Med. 2011;2(2):205-12.
269. Snoeker B, Turkiewicz A, Magnusson K, Frobell R, Yu D, Peat G, et al. Risk of knee osteoarthritis after different types of knee injuries in young adults: a population-based cohort study. Br J Sports Med. 2020;54(12):725-30.
270. Muthuri SG, McWilliams DF, Doherty M, Zhang W. History of knee injuries and knee osteoarthritis: a meta-analysis of observational studies. Osteoarthritis Cartilage. 2011;19(11):1286-93.
271. Jeuken RM, Roth AK, Peters R, Van Donkelaar CC, Thies JC, Van Rhijn LW, et al. Polymers in Cartilage Defect Repair of the Knee: Current Status and Future Prospects. Polymers (Basel). 2016;8(6).
272. Loeser RF. Age-related changes in the musculoskeletal system and the development of osteoarthritis. Clin Geriatr Med. 2010;26(3):371-86.
273. Johnson VL, Hunter DJ. The epidemiology of osteoarthritis. Best Pract Res Clin Rheumatol. 2014;28(1):5-15.
274. Brandt KD, Dieppe P, Radin EL. Etiopathogenesis of osteoarthritis. Rheum Dis Clin North Am. 2008;34(3):531-59.
275. Salzmann GM, Ossendorff R, Gilat R, Cole BJ. Autologous Minced Cartilage Implantation for Treatment of Chondral and Osteochondral Lesions in the Knee Joint: An Overview. Cartilage. 2021;13(1_suppl):1124S-36S.
276. Mistry H, Connock M, Pink J, Shyangdan D, Clar C, Royle P, et al. Autologous chondrocyte implantation in the knee: systematic review and economic evaluation. Health Technol Assess. 2017;21(6):1-294.
277. Jeuken RM, Vles GF, Jansen EJP, Loeffen D, Emans PJ. The Modified Hedgehog Technique to Repair Pure Chondral Shear-off Lesions in the Pediatric Knee. Cartilage. 2021;13(1_suppl):271S-9S.
278. Richter DL, Schenck RC, Jr., Wascher DC, Treme G. Knee Articular Cartilage Repair and Restoration Techniques: A Review of the Literature. Sports Health. 2016;8(2):153-60.
279. van der Woude JAD, Wiegant K, van Heerwaarden RJ, Spruijt S, van Roermund PM, Custers RJH, et al. Knee joint distraction compared with high tibial osteotomy: a randomized controlled trial. Knee Surg Sports Traumatol Arthrosc. 2017;25(3):876-86.

280. Brouwer RW, Raaij van TM, Bierma-Zeinstra SM, Verhagen AP, Jakma TS, Verhaar JA. Osteotomy for treating knee osteoarthritis. Cochrane Database Syst Rev. 2007(3):CD004019.
281. Glyn-Jones S, Palmer AJ, Agricola R, Price AJ, Vincent TL, Weinans H, et al. Osteoarthritis. Lancet. 2015;386(9991):376-87.
282. Henrotin Y, Sanchez C, Bay-Jensen AC, Mobasheri A. Osteoarthritis biomarkers derived from cartilage extracellular matrix: Current status and future perspectives. Ann Phys Rehabil Med. 2016;59(3):145-8.
283. Hunter DJ, Felson DT. Osteoarthritis. BMJ. 2006;332(7542):639-42.
284. Dieppe PA, Lohmander LS. Pathogenesis and management of pain in osteoarthritis. Lancet. 2005;365(9463):965-73.
285. Clockaerts S, Bastiaansen-Jenniskens YM, Runhaar J, Van Osch GJ, Van Offel JF, Verhaar JA, et al. The infrapatellar fat pad should be considered as an active osteoarthritic joint tissue: a narrative review. Osteoarthritis Cartilage. 2010;18(7):876-82.
286. Bastiaansen-Jenniskens YM, Clockaerts S, Feijt C, Zuurmond AM, Stojanovic-Susulic V, Bridts C, et al. Infrapatellar fat pad of patients with end-stage osteoarthritis inhibits catabolic mediators in cartilage. Ann Rheum Dis. 2012;71(2):288-94.
287. Lippiello L, Walsh T, Fienhold M. The association of lipid abnormalities with tissue pathology in human osteoarthritic articular cartilage. Metabolism. 1991;40(6):571-6.
288. Aspden RM, Scheven BA, Hutchison JD. Osteoarthritis as a systemic disorder including stromal cell differentiation and lipid metabolism. Lancet. 2001;357(9262):1118-20.
289. Villalvilla A, Gomez R, Largo R, Herrero-Beaumont G. Lipid transport and metabolism in healthy and osteoarthritic cartilage. Int J Mol Sci. 2013;14(10):20793-808.
290. Sarma AV, Powell GL, LaBerge M. Phospholipid composition of articular cartilage boundary lubricant. J Orthop Res. 2001;19(4):671-6.
291. Petelska AD, Kazimierska-Drobny K, Janicka K, Majewski T, Urbaniak W. Understanding the Unique Role of Phospholipids in the Lubrication of Natural Joints: An Interfacial Tension Study. Coatings. 2019;9(4).
292. Donovan EL, Pettine SM, Hickey MS, Hamilton KL, Miller BF. Lipidomic analysis of human plasma reveals ether-linked lipids that are elevated in morbidly obese humans compared to lean. Diabetol Metab Syndr. 2013;5(1):24.
293. Harizi H, Corcuff JB, Gualde N. Arachidonic-acid-derived eicosanoids: roles in biology and immunopathology. Trends Mol Med. 2008;14(10):461-9.
294. Yui K, Imataka G, Nakamura H, Ohara N, Naito Y. Eicosanoids Derived From Arachidonic Acid and Their Family Prostaglandins and Cyclooxygenase in Psychiatric Disorders. Curr Neuropharmacol. 2015;13(6):776-85.
295. Bar-Or D, Rael LT, Thomas GW, Brody EN. Inflammatory Pathways in Knee Osteoarthritis: Potential Targets for Treatment. Curr Rheumatol Rev. 2015;11(1):50-8.
296. Gilbert SJ, Blain EJ, Jones P, Duance VC, Mason DJ. Exogenous sphingomyelinase increases collagen and sulphated glycosaminoglycan production by primary articular chondrocytes: an in vitro study. Arthritis Res Ther. 2006;8(4):R89.
297. Gilbert SJ, Blain EJ, Duance VC, Mason DJ. Sphingomyelinase decreases type II collagen expression in bovine articular cartilage chondrocytes via the ERK signaling pathway. Arthritis Rheum. 2008;58(1):209-20.

298. Remst DF, Blaney Davidson EN, Vitters EL, Blom AB, Stoop R, Snabel JM, et al. Osteoarthritis-related fibrosis is associated with both elevated pyridinoline cross-link formation and lysyl hydroxylase 2b expression. Osteoarthritis Cartilage. 2013;21(1):157-64.
299. Rim YA, Ju JH. The Role of Fibrosis in Osteoarthritis Progression. Life (Basel). 2020;11(1).
300. Favero M, El-Hadi H, Belluzzi E, Granzotto M, Porzionato A, Sarasin G, et al. Infrapatellar fat pad features in osteoarthritis: a histopathological and molecular study. Rheumatology (Oxford). 2017;56(10):1784-93.
301. Eiersbrock FB, Orthen JM, Soltwisch J. Validation of MALDI-MS imaging data of selected membrane lipids in murine brain with and without laser postionization by quantitative nano-HPLC-MS using laser microdissection. Anal Bioanal Chem. 2020;412(25):6875-86.
302. Gelber AC, Hochberg MC, Mead LA, Wang NY, Wigley FM, Klag MJ. Joint injury in young adults and risk for subsequent knee and hip osteoarthritis. Ann Intern Med. 2000;133(5):321-8.
303. Jiang LF, Fang JH, Wu LD. Role of infrapatellar fat pad in pathological process of knee osteoarthritis: Future applications in treatment. World J Clin Cases. 2019;7(16):2134-42.
304. Van Hese L, Vaysse PM, Siegel TP, Heeren R, Rex S, Cuypers E. Real-time drug detection using a diathermic knife combined to rapid evaporative ionisation mass spectrometry. Talanta. 2021;221:121391.
305. Marcus D, Phelps DL, Savage A, Balog J, Kudo H, Dina R, et al. Point-of-Care Diagnosis of Endometrial Cancer Using the Surgical Intelligent Knife (iKnife)-A Prospective Pilot Study of Diagnostic Accuracy. Cancers (Basel). 2022;14(23).
306. Tzafetas M, Mitra A, Paraskevaidi M, Bodai Z, Kalliala I, Bowden S, et al. The intelligent knife (iKnife) and its intraoperative diagnostic advantage for the treatment of cervical disease. Proc Natl Acad Sci U S A. 2020;117(13):7338-46.
307. Delgado DA, Lambert BS, Boutris N, McCulloch PC, Robbins AB, Moreno MR, et al. Validation of Digital Visual Analog Scale Pain Scoring With a Traditional Paper-based Visual Analog Scale in Adults. J Am Acad Orthop Surg Glob Res Rev. 2018;2(3):e088.
308. Roos EM, Lohmander LS. The Knee injury and Osteoarthritis Outcome Score (KOOS): from joint injury to osteoarthritis. Health Qual Life Outcomes. 2003;1:64.
309. Feist P, Hummon AB. Proteomic challenges: sample preparation techniques for microgram-quantity protein analysis from biological samples. Int J Mol Sci. 2015;16(2):3537-63.
310. Szklarczyk D, Kirsch R, Koutrouli M, Nastou K, Mehryary F, Hachilif R, et al. The STRING database in 2023: protein-protein association networks and functional enrichment analyses for any sequenced genome of interest. Nucleic Acids Res. 2023;51(D1):D638-D46.
311. Filardo G, Andriolo L, Sessa A, Vannini F, Ferruzzi A, Marcacci M, et al. Age Is Not a Contraindication for Cartilage Surgery: A Critical Analysis of Standardized Outcomes at Long-term Follow-up. Am J Sports Med. 2017;45(8):1822-8.
312. Mezhov V, Ciccutini FM, Hanna FS, Brennan SL, Wang YY, Urquhart DM, et al. Does obesity affect knee cartilage? A systematic review of magnetic resonance imaging data. Obes Rev. 2014;15(2):143-57.
313. Keng A, Sayre EC, Guermazi A, Nicolaou S, Esdaile JM, Thorne A, et al. Association of body mass index with knee cartilage damage in an asymptomatic population-based study. BMC Musculoskelet Disord. 2017;18(1):517.

314. Bolia IK, Mertz K, Faye E, Sheppard J, Telang S, Bogdanov J, et al. Cross-Communication Between Knee Osteoarthritis and Fibrosis: Molecular Pathways and Key Molecules. Open Access J Sports Med. 2022;13:1-15.
315. Saxena S, Patel DD, Shah A, Doctor M. Fat Chance for Hidden Lesions: Pictorial Review of Hoffa's Fat Pad Lesions. Indian J Radiol Imaging. 2021;31(4):961-74.
316. Loef M, Gademan MGJ, Latijnhouwers D, Kroon HM, Kaptijn HH, Marijnissen W, et al. Comparison of KOOS Scores of Middle-Aged Patients Undergoing Total Knee Arthroplasty to the General Dutch Population Using KOOS Percentile Curves: The LOAS Study. J Arthroplasty. 2021;36(8):2779-87 e4.
317. de Groot IB, Favejee MM, Reijman M, Verhaar JA, Terwee CB. The Dutch version of the Knee Injury and Osteoarthritis Outcome Score: a validation study. Health Qual Life Outcomes. 2008;6:16.
318. Jensen MP, Chen C, Brugger AM. Interpretation of visual analog scale ratings and change scores: a reanalysis of two clinical trials of postoperative pain. J Pain. 2003;4(7):407-14.
319. Boonstra AM, Schiphorst Preuper HR, Balk GA, Stewart RE. Cut-off points for mild, moderate, and severe pain on the visual analogue scale for pain in patients with chronic musculoskeletal pain. Pain. 2014;155(12):2545-50.
320. Bakker B, Eijkel GB, Heeren RMA, Karperien M, Post JN, Cillero-Pastor B. Oxygen-Dependent Lipid Profiles of Three-Dimensional Cultured Human Chondrocytes Revealed by MALDI-MSI. Anal Chem. 2017;89(17):9438-44.
321. Ou MY, Zhang H, Tan PC, Zhou SB, Li QF. Adipose tissue aging: mechanisms and therapeutic implications. Cell Death Dis. 2022;13(4):300.
322. Schipper BM, Marra KG, Zhang W, Donnenberg AD, Rubin JP. Regional anatomic and age effects on cell function of human adipose-derived stem cells. Ann Plast Surg. 2008;60(5):538-44.
323. Kirkland JL, Tchkonia T, Pirtskhalava T, Han J, Karagiannides I. Adipogenesis and aging: does aging make fat go MAD? Exp Gerontol. 2002;37(6):757-67.
324. de Magalhaes JP, Passos JF. Stress, cell senescence and organismal ageing. Mech Ageing Dev. 2018;170:2-9.
325. Kelly RT. Single-cell Proteomics: Progress and Prospects. Mol Cell Proteomics. 2020;19(11):1739-48.
326. Faber S, Zinser W, Angele P, Spahn G, Loer I, Zellner J, et al. Does Gender Influence Outcome in Cartilage Repair Surgery? An Analysis of 4,968 Consecutive Patients from the German Cartilage Registry (Knorpel Register DGOU). Cartilage. 2021;13(1_suppl):837S-45S.
327. Roughley PJ, Mort JS. The role of aggrecan in normal and osteoarthritic cartilage. J Exp Orthop. 2014;1(1):8.
328. Bernardo BC, Belluoccio D, Rowley L, Little CB, Hansen U, Bateman JF. Cartilage intermediate layer protein 2 (CILP-2) is expressed in articular and meniscal cartilage and down-regulated in experimental osteoarthritis. J Biol Chem. 2011;286(43):37758-67.
329. Wu T, Zhang Q, Wu S, Hu W, Zhou T, Li K, et al. CILP-2 is a novel secreted protein and associated with insulin resistance. J Mol Cell Biol. 2019;11(12):1083-94.
330. Lorenzo P, Bayliss MT, Heinegard D. Altered patterns and synthesis of extracellular matrix macromolecules in early osteoarthritis. Matrix Biol. 2004;23(6):381-91.

331. Seki S, Kawaguchi Y, Chiba K, Mikami Y, Kizawa H, Oya T, et al. A functional SNP in CILP, encoding cartilage intermediate layer protein, is associated with susceptibility to lumbar disc disease. Nat Genet. 2005;37(6):607-12.
332. Valdes AM, Hart DJ, Jones KA, Surdulescu G, Swarbrick P, Doyle DV, et al. Association study of candidate genes for the prevalence and progression of knee osteoarthritis. Arthritis Rheum. 2004;50(8):2497-507.
333. Healy L, May G, Gale K, Grosveld F, Greaves M, Enver T. The stem cell antigen CD34 functions as a regulator of hemopoietic cell adhesion. Proc Natl Acad Sci U S A. 1995;92(26):12240-4.
334. Gangenahalli GU, Singh VK, Verma YK, Gupta P, Sharma RK, Chandra R, et al. Hematopoietic stem cell antigen CD34: role in adhesion or homing. Stem Cells Dev. 2006;15(3):305-13.
335. AbuSamra DB, Aleisa FA, Al-Amoodi AS, Jalal Ahmed HM, Chin CJ, Abuelela AF, et al. Not just a marker: CD34 on human hematopoietic stem/progenitor cells dominates vascular selectin binding along with CD44. Blood Adv. 2017;1(27):2799-816.
336. Gotze KS, Schiemann M, Marz S, Jacobs VR, Debus G, Peschel C, et al. CD133-enriched CD34(-) (CD33/CD38/CD71)(-) cord blood cells acquire CD34 prior to cell division and hematopoietic activity is exclusively associated with CD34 expression. Exp Hematol. 2007;35(9):1408-14.
337. Nakamura Y, Ando K, Chargui J, Kawada H, Sato T, Tsuji T, et al. Ex vivo generation of CD34(+) cells from CD34(-) hematopoietic cells. Blood. 1999;94(12):4053-9.
338. Sato T, Laver JH, Ogawa M. Reversible expression of CD34 by murine hematopoietic stem cells. Blood. 1999;94(8):2548-54.
339. Qadri M, Jay GD, Zhang LX, Schmidt TA, Totonchy J, Elsaid KA. Proteoglycan-4 is an essential regulator of synovial macrophage polarization and inflammatory macrophage joint infiltration. Arthritis Res Ther. 2021;23(1):241.
340. Jay GD, Waller KA. The biology of lubricin: near frictionless joint motion. Matrix Biol. 2014;39:17-24.
341. Paulsson M, Heinegard D. Purification and structural characterization of a cartilage matrix protein. Biochem J. 1981;197(2):367-75.
342. Petersen SG, Saxne T, Heinegard D, Hansen M, Holm L, Koskinen S, et al. Glucosamine but not ibuprofen alters cartilage turnover in osteoarthritis patients in response to physical training. Osteoarthritis Cartilage. 2010;18(1):34-40.
343. Tseng S, Reddi AH, Di Cesare PE. Cartilage Oligomeric Matrix Protein (COMP): A Biomarker of Arthritis. Biomark Insights. 2009;4:33-44.
344. Ansorge HL, Meng X, Zhang G, Veit G, Sun M, Klement JF, et al. Type XIV Collagen Regulates Fibrillogenesis: PREMATURE COLLAGEN FIBRIL GROWTH AND TISSUE DYSFUNCTION IN NULL MICE. J Biol Chem. 2009;284(13):8427-38.
345. Lee M, Shimizu E, Krane SM, Partridge NC. Chapter 19 - Bone Proteinases. In: Bilezikian JP, Raisz LG, Martin TJ, editors. Principles of Bone Biology (Third Edition). San Diego: Academic Press; 2008. p. 367-84.
346. Damen AHA, van Donkelaar CC, Cardinaels RM, Brandt JM, Schmidt TA, Ito K. Proteoglycan 4 reduces friction more than other synovial fluid components for both cartilage-cartilage and cartilage-metal articulation. Osteoarthritis Cartilage. 2021;29(6):894-904.

347. Lee HR, Lee S, Yoo IS, Yoo SJ, Kwon MH, Joung CI, et al. CD14+ monocytes and soluble CD14 of synovial fluid are associated with osteoarthritis progression. Arch Rheumatol. 2022;37(3):335-43.
348. Rodrigues CR, Moga S, Singh B, Aulakh GK. CD34 Protein: Its expression and function in inflammation. Cell Tissue Res. 2023.
349. Supuran CT. Carbonic anhydrases--an overview. Curr Pharm Des. 2008;14(7):603-14.
350. Schultz M, Jin W, Waheed A, Moed BR, Sly W, Zhang Z. Expression profile of carbonic anhydrases in articular cartilage. Histochem Cell Biol. 2011;136(2):145-51.
351. Goldoni I, Ibelli AMG, Fernandes LT, Peixoto JO, Hul LM, Cantao ME, et al. Comprehensive Analyses of Bone and Cartilage Transcriptomes Evince Ion Transport, Inflammation and Cartilage Development-Related Genes Involved in Chickens' Femoral Head Separation. Animals (Basel). 2022;12(6).
352. Ryckman C, Vandal K, Rouleau P, Talbot M, Tessier PA. Proinflammatory activities of S100: proteins S100A8, S100A9, and S100A8/A9 induce neutrophil chemotaxis and adhesion. J Immunol. 2003;170(6):3233-42.
353. Zreiqat H, Howlett CR, Gronthos S, Hume D, Geczy CL. S100A8/S100A9 and their association with cartilage and bone. J Mol Histol. 2007;38(5):381-91.
354. Chen W, Yang A, Jia J, Popov YV, Schuppan D, You H. Lysyl Oxidase (LOX) Family Members: Rationale and Their Potential as Therapeutic Targets for Liver Fibrosis. Hepatology. 2020;72(2):729-41.
355. Lin W, Xu L, Li G. Corrigendum: Molecular Insights Into Lysyl Oxidases in Cartilage Regeneration and Rejuvenation. Front Bioeng Biotechnol. 2020;8:598323.
356. Liu C, Zhu P, Wang W, Li W, Shu Q, Chen ZJ, et al. Inhibition of lysyl oxidase by prostaglandin E2 via EP2/EP4 receptors in human amnion fibroblasts: Implications for parturition. Mol Cell Endocrinol. 2016;424:118-27.
357. Roy R, Polgar P, Wang Y, Goldstein RH, Taylor L, Kagan HM. Regulation of lysyl oxidase and cyclooxygenase expression in human lung fibroblasts: interactions among TGF-beta, IL-1 beta, and prostaglandin E. J Cell Biochem. 1996;62(3):411-7.
358. Donnelly DP, Rawlins CM, DeHart CJ, Fornelli L, Schachner LF, Lin Z, et al. Best practices and benchmarks for intact protein analysis for top-down mass spectrometry. Nat Methods. 2019;16(7):587-94.
359. Jansen MP, Mastbergen SC. Joint distraction for osteoarthritis: clinical evidence and molecular mechanisms. Nat Rev Rheumatol. 2022;18(1):35-46.
360. van Roermund PM, Marijnissen AC, Lafeber FP. Joint distraction as an alternative for the treatment of osteoarthritis. Foot Ankle Clin. 2002;7(3):515-27.
361. Peng H, Ou A, Huang X, Wang C, Wang L, Yu T, et al. Osteotomy Around the Knee: The Surgical Treatment of Osteoarthritis. Orthop Surg. 2021;13(5):1465-73.
362. Hussain SM, Neilly DW, Baliga S, Patil S, Meek R. Knee osteoarthritis: a review of management options. Scott Med J. 2016;61(1):7-16.
363. Jungmann PM, Gersing AS, Baumann F, Holwein C, Braun S, Neumann J, et al. Cartilage repair surgery prevents progression of knee degeneration. Knee Surg Sports Traumatol Arthrosc. 2019;27(9):3001-13.
364. Emans PJ SG, Haverkamp D, Bentin J, Chausson M, Schifflers M and Portelange N. KiOmedine® CM-Chitosan is Effective for Treating Advanced Symptomatic Knee

Osteoarthritis up to Six Months Following a Single Intra-Articular Injection: A Post Hoc Analysis of Aproove Clinical Study. Open Rheumatol J. 2023;17.
365. Hoorntje A, Kuijer P, Koenraadt KLM, Waterval-Witjes S, Kerkhoffs G, Mastbergen SC, et al. Return to Sport and Work after Randomization for Knee Distraction versus High Tibial Osteotomy: Is There a Difference? J Knee Surg. 2022;35(9):949-58.
366. Snow M, Mandalia V, Custers R, Emans PJ, Kon E, Niemeyer P, et al. Cost-effectiveness of a new ACI technique for the treatment of articular cartilage defects of the knee compared to regularly used ACI technique and microfracture. J Med Econ. 2023;26(1):537-46.
367. Aspden RM, Scheven BAA, Hutchison JD. Osteoarthritis as a systemic disorder including stromal cell differentiation and lipid metabolism. Lancet. 2001;357(9262):1118-20.
368. Bosetti F. Arachidonic acid metabolism in brain physiology and pathology: lessons from genetically altered mouse models. J Neurochem. 2007;102(3):577-86.
369. xPharm: The Comprehensive Pharmacology Reference. Enna S, editor. Amsterdam: Elsevier; 2008.
370. Park J, Kim J, Lewy T, Rice CM, Elemento O, Rendeiro AF, et al. Spatial omics technologies at multimodal and single cell/subcellular level. Genome Biol. 2022;23(1):256.
371. Vandereyken K, Sifrim A, Thienpont B, Voet T. Methods and applications for single-cell and spatial multi-omics. Nat Rev Genet. 2023;24(8):494-515.
372. Balog J, Kumar S, Alexander J, Golf O, Huang J, Wiggins T, et al. In vivo endoscopic tissue identification by rapid evaporative ionization mass spectrometry (REIMS). Angew Chem Int Ed Engl. 2015;54(38):11059-62.
373. Fuentes-Braesch M, Tuijthof GJM, Emans PJ, Emanuel KS. The preferred technique for knee synovium biopsy and synovial fluid arthrocentesis. Rheumatol Int. 2022.
374. Paz-Gonzalez R, Lourido L, Calamia V, Fernandez-Puente P, Quaranta P, Picchi F, et al. An Atlas of the Knee Joint Proteins and Their Role in Osteoarthritis Defined by Literature Mining. Mol Cell Proteomics. 2023;22(8):100606.
375. Fuentes M, Ruiz-Romero C, Misiego S, Juanes-Velasco P, Landeira-Vinuela A, Torres-Roda A, et al. Exploring High-Throughput Immunoassays for Biomarker Validation in Rheumatic Diseases in the Context of the Human Proteome Project. J Proteome Res. 2023;22(4):1105-15.
376. Janssen MPF, van der Linden EGM, Boymans T, Welting TJM, van Rhijn LW, Bulstra SK, et al. Twenty-Two-Year Outcome of Cartilage Repair Surgery by Perichondrium Transplantation. Cartilage. 2021;13(1_suppl):860S-7S.
377. Bradsell H, Lencioni A, Shinsako K, Frank RM. In-Office Diagnostic Needle Arthroscopy Using the NanoScope Arthroscopy System. Arthrosc Tech. 2022;11(11):e1923-e7.
378. Alajami HN, Fouad EA, Ashour AE, Kumar A, Yassin AEB. Celecoxib-Loaded Solid Lipid Nanoparticles for Colon Delivery: Formulation Optimization and In Vitro Assessment of Anti-Cancer Activity. Pharmaceutics. 2022;14(1).
379. Wen J, Li H, Dai H, Hua S, Long X, Li H, et al. Intra-articular nanoparticles based therapies for osteoarthritis and rheumatoid arthritis management. Mater Today Bio. 2023;19:100597.
380. Pontes AP, Welting TJM, Rip J, Creemers LB. Polymeric Nanoparticles for Drug Delivery in Osteoarthritis. Pharmaceutics. 2022;14(12).

381. Huizing LRS, McDuffie J, Cuyckens F, van Heerden M, Koudriakova T, Heeren RMA, et al. Quantitative Mass Spectrometry Imaging to Study Drug Distribution in the Intestine Following Oral Dosing. Anal Chem. 2021;93(4):2144-51.
382. Porta T, Lesur A, Varesio E, Hopfgartner G. Quantification in MALDI-MS imaging: what can we learn from MALDI-selected reaction monitoring and what can we expect for imaging? Anal Bioanal Chem. 2015;407(8):2177-87.
383. Schulz S, Becker M, Groseclose MR, Schadt S, Hopf C. Advanced MALDI mass spectrometry imaging in pharmaceutical research and drug development. Curr Opin Biotechnol. 2019;55:51-9.
384. Nauta SP, Huysmans P, Tuijthof GJM, Eijkel GB, Poeze M, Siegel TP, et al. Automated 3D Sampling and Imaging of Uneven Sample Surfaces with LA-REIMS. J Am Soc Mass Spectrom. 2022;33(1):111-22.

Publications

Kaj S Emanuel, Luojiao Huang, **Mirella J J Haartmans**, Javier Sanmartin Martinez, Frank Zijta, Ron M A Heeren, Gino M M J Kerkhoffs, Pieter J Emans, Berta Cillero-Pastor. *Identification of patient-responsive protein biomarkers in the infrapatellar fat pad for cartilage degeneration and repair*. In preparation.

Mirella J J Haartmans*, Kaj S Emanuel*, Sylvia P Nauta, Eva Cuypers, Gabrielle J M Tuijthof, Ron M A Heeren, Pieter J Emans, Berta Cillero-Pastor. *Rapid Evaporative Ionization Mass Spectrometry (REIMS) with electrocautery device as a diagnostic tool in cartilage defect and osteoarthritis patient*s. In preparation.

Mirella J J Haartmans, Maxime R Eveque-Mourroux, Gert B Eijkel, Britt S R Claes, Kaj S Emanuel, Gabrielle J M Tuijthof, Lodewijk W van Rhijn, Ron M A Heeren, Pieter J Emans, and Berta Cillero-Pastor. *Matrix-Assisted Laser Desorption/Ionization Mass Spectrometry Imaging (MALDI-MSI) identifies Osteoarthritis and Cartilage Defect Markers in the infrapatellar fat pad*. Anal. Bioanal. Chem. 2023.

Mirella J J Haartmans, Britt S R Claes, Kaj S Emanuel, Gabrielle J M Tuijthof, Ron M A Heeren, Pieter J Emans, Berta Cillero-Pastor. *Sample preparation of Intra-articular Adipose Tissue for measuring Lipids using Matrix-assisted Laser Desorption/Ionization Mass spectrometry Imaging*. Anal. Biochem. 2022.

Kaj S Emanuel, Lukas J Kellner, Marloes J M Peters, **Mirella J J Haartmans**, Melissa T Hooijmans, Pieter J Emans. *The relation between the biochemical composition of knee articular cartilage and quantitative MRI: a systematic review and meta-analysis.* Osteoarthritis Cartilage. 2021.

Mirella J J Haartmans*, Ufuk Tan Timur*, Kaj S Emanuel, Marjolein M J Caron, Ralph M Jeuken, Tim J M Welting, Gerjo J V M van Osch, Ron M A Heeren, Berta Cillero-Pastor, Pieter J Emans. *Evaluation of the Anti-Inflammatory and Chondroprotective Effect of Celecoxib on Cartilage Ex Vivo and in a Rat Osteoarthritis Model.* Cartilage. 2021.

Mirella J J Haartmans, Kaj S Emanuel, Gabrielle J M Tuijthof, Ron M A Heeren, Pieter J Emans, Berta Cillero-Pastor. *Mass Spectrometry-based Biomarkers for Knee Osteoarthritis: A Systematic Review.* Expert Rev. Proteomics. 2021.

Marjolein M J Caron, Tessy M R Castermans, Bert van Rietbergen, **Mirella J J Haartmans**, Lodewijk W van Rhijn, Adhiambo M A Witlox, Tim J M Welting. *Impairment of Cyclo-oxygenase-2 Function Results in Abnormal Growth Plate Development and Bone Microarchitecture but Does Not Affect Longitudinal Growth of the Long Bones in Skeletally Immature Mice.* J. Orthop. Res. 2021

Anne-Marije Hulshof, Minka J A Vries, Paul W M Verhezen, Rick J H Wetzels, **Mirella J J Haartmans**, Renske H Olie, Hugo Ten Cate, Yvonne M C Henskens. *The Influence of Prostaglandin E1 and Use of Inhibitor Percentage on the Correlation between the Multiplate and VerifyNow in Patients on Dual Antiplatelet Therapy*. Platelets, 2021.

Marjolein M J Caron, Bert van Rietbergen, Tessy M R Castermans, **Mirella J J Haartmans**, Lodewijk W van Rhijn, Tim J M Welting, Adhiambo M A Witlox. *Evaluation of impaired growth plate development of long bones in skeletally immature mice by antirheumatic agents*. J. Orthop. Res. 2021.

Presentations

Claire Polain, Freek G Bouwman, Timo Rademakers, **Mirella J J Haartmans**, Christian Plank, Berta Cillero Pastor, Martijn van Griensven, Elizabeth R Balmayor. *Novel chemically modified RNA encoding for nerve growth factor shows therapeutic potential to induce innervation for bone regeneration in vitro.* Orthopaedic Research Society (ORS) 2024. Long Beach, California, USA. Podium.

Kaj S Emanuel, **Mirella J J Haartmans**, Benjamin D Balluff, Sylvia P Nauta, Gabrielle J M Tuijthof, Ron M A Heeren, Pieter J Emans, Berta Cillero-Pastor. *Molecular profiles of Hoffa's Fat pad, regulators of cartilage repair?* International Cartilage Regeneration and Joint Preservation Society (ICRS) 2023. Barcelona, Spain. Podium.

Mirella J J Haartmans, Kaj S Emanuel, Sylvia P Nauta, Gabrielle J M Tuijthof, Ron M A Heeren, Pieter J Emans, Berta Cillero-Pastor. *Multimodal method to predict patient outcome after cartilage repair surgery.* European Society for Biomaterials (ESB) 2023. Davos, Switzerland. Poster.

Mirella J J Haartmans, Kaj S Emanuel, Sylvia P Nauta, Gabrielle J M Tuijthof, Ron M A Heeren, Pieter J Emans, Berta Cillero-Pastor. *Rapid Evaporative Ionization Mass Spectrometry (REIMS) with diathermic knife as a potential diagnostic tool in cartilage defect and osteoarthritis patients.* European Society of Tissue Regeneration in Orthopedics and Traumatology (ESTROT) 2022. Maastricht, Nederland. Poster.

Kaj S Emanuel, Lukas J Kellner, Marloes J M Peters, **Mirella J J Haartmans**, Melissa T Hooijmans, Pieter J Emans. *The relation between the biochemical composition of the knee articular cartilage and quantitative MRI: a systematic review and meta-analysis.* International Cartilage Regeneration and Joint Preservation Society (ICRS) 2022. Berlin, Germany. Poster.

Mirella J J Haartmans, Ufuk T Timur, Marjolein M J Caron, Kaj S Emanuel, Tim J M Welting, Lodewijk W van Rhijn, Ron M A Heeren, Berta Cillero-Pastor, Pieter J Emans. *Evaluation of the effect of Celecoxib on cartilage in vitro and in a rat osteoarthritis model.* International Cartilage Regeneration and Joint Preservation Society (ICRS) 2022. Berlin, Germany. Podium.

Mirella J J Haartmans, Britt S R Claes, Maxime R Eveque-Mourroux, Gert B Eijkel, Kaj S Emanuel, Gabrielle J M Tuijthof, Lodewijk W van Rhijn, Ron M A Heeren, Pieter J Emans, Berta Cillero-Pastor. *Hoffa's fat pad as a possible target for biomarker research in osteoarthritis.* Tissue Engineering and Regenerative Medicine International Society (TERMIS) 2021. Online. Poster.

Mirella J J Haartmans, Maxime R Eveque-Mourroux, Gert B Eijkel, Britt S R Claes, Kaj S Emanuel, Gabrielle J M Tuijthof, Lodewijk W van Rhijn, Ron M A Heeren, Pieter J Emans, Berta Cillero-Pastor. *Lipid profiles in Hoffa's fat pad of osteoarthritic vs cartilage defect patients.* LipidMaps Spring School 2021. Online. Poster.

Mirella J J Haartmans, Maxime R Eveque-Mourroux, Kaj S Emanuel, Gabrielle J M Tuijthof, Ron M A Heeren, Pieter J Emans, Berta Cillero-Pastor. *Lipid profiles in Hoffa's fat pad as biomarker for cartilage regeneration and osteoarthritis development.* Osteoarthritis Research Society International (OARSI) 2020. Vienna, Austria. Cancelled.

Mirella J J Haartmans, Maxime R Eveque-Mourroux, Gert B Eijkel, Kaj S Emanuel, Gabrielle J M Tuijthof, Lodewijk W van Rhijn, Ron M A Heeren, Pieter J Emans, Berta Cillero-Pastor. *Human Hoffa's fat pad lipid profiles as read out of cartilage damage*. Orthopaedic Research Society (EORS) 2020. Online. Podium.

Mirella J J Haartmans, Kaj S Emanuel, Sylvia P Nauta, Gabrielle J M Tuijthof, Eva Cuypers, Ron M A Heeren, Pieter J Emans, Berta Cillero-Pastor. *Rapid Evaporative Ionization Mass Spectrometry (REIMS) with diathermic knife as a potential diagnostic tool in cartilage defect and osteoarthritis patients.* Tissue Engineering and Regenerative Medicine International Society (TERMIS) 2020. Manchester, UK. Poster.

Mirella J J Haartmans, Berta Cillero-Pastor, Kaj S Emanuel, Maxime R Eveque-Mourroux, Gabrielle J M Tuijthof, Ron M A Heeren, Pieter J Emans. *Lipid Profiles in Hoffa's Fat Pad of Osteoarthritic vs Osteochondral Defect Patients.* European Orthopaedic Research Society (EORS) 2019. Maastricht, the Netherlands. Podium & poster.

Mirella J J Haartmans, Maxime R Eveque-Mourroux, Gert B Eijkel, Kaj S Emanuel, Gabrielle J M Tuijthof, Lodewijk W van Rhijn, Ron M A Heeren, Pieter J Emans, Berta Cillero-Pastor. Id*entifying Lipid Profiles in Hoffa's Fat Pad – Detect before It melts!* Mass Spectrometry School in Biotechnology and Medicine (MSBM) Summer School 2019. Dubrovnik, Croatia. Podium & poster.

Marjolein M J Caron, Tessy M R Castermans, Bert van Rietbergen, Mirella J J Haartmans, Lodewijk van Rhijn, Tim J M Welting, Adhiambo M A Witlox. *Anti-rheumatic agents naproxen and methotrexate affect skeletal development in skeletally immature mice.* Osteoarthritis Research Society International (OARSI) 2018. Liverpool, UK. Poster.

Mirella J J Haartmans, Nicole A P van Gestel, Sandra Hofmann, Chris (J J) Arts, Keita Ito. Bone grafting - Unravelling the angiogenic potential of human umbilical vein endothelial cells by elucidating cell communication in an in vitro (co-)culture with human bone marrow stromal cells, osteoblasts and chondrocytes. Mosa Conference 2018. Maastricht, the Netherlands. Poster.

Marjolein M J Caron, Tessy M R Castermans, Bert van Rietbergen, Mirella J J Haartmans, Lodewijk W van Rhijn, Adhiambo M A Witlox, Tim J M Welting. Celecoxib leads to impaired cartilage and bone extracellular matrix formation in the growth plate of skeletally immature mice. European Orthopaedic Research Society (EORS) 2017. Munich, Germany. Podium.

Acknowledgements

While writing my acknowledgements, I discovered that I got to know and work with many people over the past years. Although not everyone is mentioned below, I still want to thank every one of you for your part in my PhD trajectory. I enjoyed and appreciated working with every single one of you. I would not be able to have finished my PhD without you, nor would I be the person I am today.

First, I want to thank **Prof. Dr. Poeze**, **Prof. Dr. van Griensven**, **Prof. Dr. Boonen**, **Prof. Dr. Karperien**, and **Dr. Creemers** for being part of the assessment committee and your time reviewing my thesis.

Secondly, I want to thank my promotion team **Prof. Dr. Heeren**, **Dr. Emans**, and **Dr. Cillero-Pastor** for giving me the opportunity to perform my promotion trajectory within your outstanding research groups.

Beste **Ron**. Ik wil toch starten met je te bedanken voor de mogelijkheid om dit promotietraject voor het grootste deel binnen M4i te mogen uitvoeren. Jouw kennis en kunde, openheid, motivatie en toegankelijkheid hebben mij meermaals versteld doen staan. Jij zorgde ervoor dat er af en toe een pasje op de plaats werd gemaakt wanneer we te hard van stapel liepen. Bedankt voor je supervisie en ondersteuning en dat ik altijd even binnen mocht lopen voor vragen.

Beste **Pieter**. Bedankt dat jij in mij geloofde en mij deze kans hebt geboden. Ik vond het fantastisch dat ik (op mijn tweede dag al) met jou mee mocht naar de OK. Wat heb ik veel mensen leren kennen en heb ik veel mogen leren. Jouw enthousiasme en motivatie om voor elke patiënt het beste resultaat te verkrijgen werkt aanstekelijk en drijft mij nog steeds. Jij zet je in om het onmogelijke voor de patiënt mogelijk te maken. Bedankt dat ik altijd bij jou terecht kon en je tijd voor mij vrij maakte.

Dear **Berta**. Thank you for being you, for always being there for me, and helping me with everything I needed. Thank you expanding our research topic to MERLN, where I got to know many other great researchers that broadened our view on the topic. I am amazed by your work and how you motivate me and other researchers to bring the best out of themselves. Thank you for your kindness and your efforts for women in science. You are an example for women combining their family with a career.

Beste **Kaj**, de andere helft van Team MALDI. Bedankt voor jouw motivatie en doorzettingsvermogen. Bedankt dat je ons onderzoek altijd in goede banen hebt

geleid. Jouw hulp bij experimenten en data-analyse, alsook jouw hulp bij het schrijven van manuscripten hebben een veelzijdige bijdrage geleverd aan de totstandkoming van mijn thesis. Ik heb waardering voor hoe jij je werkzaamheden in Maastricht en Amsterdam combineerde en hoe jouw connecties tot nieuwe samenwerkingen leiden.

Beste **Prof. Dr. Welting**, beste **Tim**. Bedankt dat ik mijn onderzoek ook binnen jouw afdeling Laboratory for Experimental Orthopedics mocht uitvoeren. Bedankt voor al je hulp en vooral ook voor je gastvrijheid tijdens de lab-uitjes.

Beste **Prof. Dr. Tuijthof**, en **Prof. Dr. Van Rhijn**, beste **Gabrielle** en **Lodewijk**. Hoewel wij ons project niet samen hebben kunnen afmaken wil ik jullie toch bedanken voor alles dat jullie voor mij hebben betekend. Ik heb grote waardering voor jullie kennis en kunde en wil jullie dan ook hartelijk bedanken voor alle input die ik van jullie heb gekregen tijdens de verschillende bijeenkomsten.

Lieve **Vera**. Bedankt dat jij niet alleen tijdens mijn grote dag naast mij wilde staan als getuige, maar ook binnenkort als paranimf tijdens mijn verdediging. Grappig dat wij na lange tijd onze eigen weggetjes te hebben bewandeld, elkaar bij de orthopedie weer tegen kwamen. Fijn dat we in onze drukke agenda's toch altijd even tijd vinden om gezellig een koffietje te doen. Bedankt dat wij altijd even kunnen kletsen over ditjes en datjes, maar ook over de serieuzere onderwerpen.

Lieve **Sylvia**. Bedankt voor jouw warm ontvangst op kantoor bij M4i. Het was heel fijn om te kunnen discussiëren over onze projectjes, maar het ook over andere dingen konden hebben. Bedankt voor al jouw hulp op het lab en jouw steun tijdens de moeilijkere momenten. Ik vond het fijn dat we zo nu en dan even aan iets anders konden denken dan ons werk tijdens de lunch of een etentje. Bedankt dat je me zo helpt en jij mijn paranimf wilt zijn.

Dear **Anjusha**. I am grateful for how well I got to know you over the past years. Your talks on work (if I understood), as well as your stories about your life and culture were very appealing. I really appreciate the fact that, after you made us smell your food for months, you made this great Indian dinner for Sylvia and me. It was an honor to be one of your paranymphs at your promotion (I am very happy I did not have to answer your questions). Please stay the person you are today (okay maybe try to share the blanket in the future). Take care of yourself and do not forget to take some downtime every now and then.

Natuurlijk mag ik mijn andere kantoorgenootjes van M4i (en chirurgie) ook niet vergeten. Lieve Romy, Lars, Pien en zo nu en dan aanwezige student of gast. Heel erg bedankt voor jullie gezelligheid, wijze woorden en wonderlijke verhalen. Ik heb genoten van onze tijd samen op kantoor en wens jullie heel veel succes met jullie nieuwe uitdagingen en Lars met het afronden van je PhD.

Dear colleagues of M4i. It is not possible to finish a PhD without the help and support of your colleagues. Thank you all, Aljoscha, Andrej, Andrew, Ben, Benjamin (for helping with complicated data analysis), Bo, Brenda (for your tips on histology), Bryn, Charles, Christel (for your time and help on the QE), Darya, Eva (for all your help with the iKnife), Fabian, Florian (it can be worse than cartilage), Fred, Helen (for always finding the best time slots in Ron's agenda), Ian, Isabeau (for all your help with proteomics and data analysis), Jian-Hua, Kasper, Kasper, Kim (for your help with the proteomics approach), Klára, Laura, Laura, Layla, Lennart, Lidia, Lieke, Lucia, Maarten, Maxime (for helping me through the first part of my PhD and (with my lack of knowledge) on mass spectrometry), Michele, Michiel, Mudita (please stay the happy, energetic person you are, success met het leren van de Nederlandse taal!), Naomi, Peiliang, Philippe, Pieter, P-max (for your time and help with the iKnife), Rob, Roel, Sebastiaan, Shane, Stephanie, Tialfi, Tiffany (for your time and help with the iKnife), Tim (for your time and help with the iKnife), Yuandi, and all other students and guests. I wish you all the best in your future (career)!

Lieve Annet en Britt. Wat is het fijn om af en toe met iemand te kunnen overleggen die hetzelfde doormaakt. Heel erg bedankt voor jullie hulp, advies en luisterend oor, in het lab met het uitvoegen van experimenten, alsook daarbuiten. Ik wens jullie heel veel succes met het afronden van jullie proefschrift en natuurlijk met de nieuwe uitdagingen die op jullie pad komen!

Lieve Gert, Frans, Ronny en Annemarie. Zonder jullie geen M4i. Bedankt voor jullie hulp met het opzetten van experimenten in het lab, data-analyse en het zorgen dat altijd alles aanwezig was. Gert, jouw expertise in data-analyse was onmisbaar. Bedankt voor de gesprekken en gezelligheid die ik tijdens de vele uren en dagen heb mogen beleven bij Frans en jou op kantoor. Ik wens jullie allen het beste toe!

Dear PhD colleagues and roomies at the Laboratory for Experimental Orthopedics. Over the years, I have seen many people come and go. Lieve Ralph, Pieter, Bas, Arjan, en Remco. Wat maakten jullie er altijd een feestje van op kantoor en wat heb ik met jullie kunnen lachen. Dear Ellen, Alzbeta, and Lotte. Thank you for keeping the balance in this office full of testosterone. Thank you for always being kind and for

our conversations over the years. Lieve Roderick, Jane, Jessica, Julia en Sanne. Wat heb ik een fijne tijd gehad met jullie op kantoor. Waar er veel werd gekletst en gelachen hebben we gelukkig ook af en toe serieus kunnen werken. Bedankt voor jullie hulp en gezelligheid. In addition, I want to say thank you to dear Marian, Bianca, Mingzheng, Abdullah, and Amin. Good luck with your PhD journey! Lieve Maarten, Annemarijn, Thomay en Florance. Ondanks dat ik jullie niet zo heel veel heb gezien en gesproken wil ik jullie bedanken en wens ik jullie het beste toe voor jullie toekomst! Lieve Christine, Eva en Anna. Bedankt voor jullie vrolijkheid en het initiëren van de etentjes. Heel veel succes bij de orthopedie!

Of course, also a big thank you to the other members of the Laboratory for Experimental Orthopedics. Thank you Prof. Dr. Chris Arts, beste Chris, Marjolein, Alex, Raymond, Marloes (voor jouw hulp en begeleiding tijdens de eerste maanden van mijn PhD), Audrey (voor jouw hulp met het plannen van meetings of uitjes), Candice, Guus, Ilona, and Majid.

Lieve Andy, Don en Laura. Wat was het fijn om jullie als collega's te hebben. Bedankt dat jullie deur altijd open stond. Lieve Laura. Wie had gedacht dat toen we samen als stagiaires begonnen in de keuken van het lab, we er 5 jaar later nog steeds samen rondliepen. Bedankt voor al jouw hulp op het lab, maar ook voor jouw luisterend oor en de fijne gesprekken die we hebben gehad. Lieve Andy, jij zorgde er altijd voor dat het lab goed georganiseerd en veilig was. Bedankt dat ik bij jou niet alleen terecht kon voor werk-gerelateerde, maar ook voor persoonlijke zaken. Ik hoef je gelukkig niet te missen en zie je graag met regelmaat in de sporthal.

Mijn onderzoek was niet mogelijk zonder de lieve mensen van de afdeling orthopedische chirurgie van het MUMC+. Lieve Chantalle. Wat heb ik het jou soms moeilijk gemaakt. Het aanmelden op OK en het plannen van afspraken (samen met Denise en Helen) met vele personen en drukke agenda's. Mijn waardering is groot dat jij dit steeds maar voor elkaar hebt gekregen en dat ik altijd bij jou terecht kon voor een praatje. Natuurlijk mag ik ook de medewerkers op OK en OK-planning niet vergeten te bedanken voor al hun hulp en interesse tijdens het verzamelen van materiaal (weer op een andere manier dan die andere mensen van het lab). Lieve Liesbeth. Wat was het fijn dat er altijd iemand op de hoogte was van alle regels omtrent medisch-wetenschappelijk onderzoek. Bedankt dat jij alle vragen en informatie omtrent patiënten aan ons door wilde geven.

Beste chirurgen, beste Tim, Peter, Maarten, Eva, Baris, en alle andere artsen die mij hebben geholpen met het verzamelen van materiaal of het begeleiden van

studenten op OK. Bedankt dat ik altijd welkom was in jullie OK en jullie altijd klaar stonden om een bijdragen te leveren aan het onderzoek. Beste **Ufuk**. Bedankt voor de fijne samenwerking voor het Celecoxib artikel en bedankt voor jouw gezelligheid wanneer je op kantoor of in het lab aanwezig was.

I also want to thank my colleagues at MERLN, who I got to know in the last part of my PhD. Dear **Betzabeth** and **Luojiao**, thank you for your input during our meetings, for your help with data-analysis, and for taking over part of my project. Good luck in the future! Beste **Timo**, beste **Claire**, bedankt voor de fijne samenwerking en het wegwijs maken op het lab bij MERLN.

En dan, mijn lieve **vrienden** en **familie**. Wat hebben jullie vaak naar mijn gezeur moeten luisteren, maar wat ben ik dankbaar dat ik jullie heb. Lieve **mama**, lieve **Jos**. Bedankt dat jullie altijd voor mij klaar staan, mij weten te motiveren en mij steunen in alles wat ik doe. Bedankt dat ik altijd aan tafel mag aanschuiven. Lieve **Melvin**. Wat zou ik toch zonder jou moeten. Bedankt dat jij er altijd voor mij bent en naar mij luistert (ook wanneer je al twaalf uur naar (het gezeur van) anderen hebt moeten luisteren). Bedankt dat jij mij altijd weet te motiveren om het beste uit mijzelf te halen en door te pakken. Bedankt voor jouw geduld en je lieve berichtjes, die mij steeds weer op de been houden.

Mirella

Biography

Mirella Haartmans was born in Heerlen, the Netherlands on January 24, 1995. In 2013, she graduated from pre-university education (Gymnasium, Grotius College Heerlen) with a combined profile Nature & Technique and Nature & Health. She started a Bachelor in Biomedical Sciences (Biological Healthy Sciences) at Maastricht University and performed an internship on platelet function tests at CARIM, School for Cardiovascular Diseases and the Laboratory for Central Diagnostics at Maastricht University and Maastricht University Medical Center under the supervision of Dr. Minka Vries and Prof. Dr. Ir. Yvonne Henskens.

From 2016 to 2018, Mirella attended the Master in Biomedical Sciences at the Transnational University Limburg (collaboration between Maastricht University and Hasselt University) with a specialization in Clinical Molecular Sciences. For her junior practical internship, she investigated skeletal development in immature mice at the department of Orthopedic Surgery, Maastricht University, under the supervision of Dr. Marjolein Caron and Prof. Dr. Tim Welting. Finally, for her senior practical internship, Mirella studied the angiogenic potential of human umbilical vein endothelial cells by investigating direct and indirect interactions with bone regenerative cells in 2D and 3D. This research was performed at the Orthopaedic Biomechanics Group of the department of Biomedical Engineering at Eindhoven, University of Technology, under the supervision of Dr. Nicole van Gestel, Dr. Sandra Hofmann, Dr. Chris Arts and Prof. Dr. Keita Ito.

Since September 2018, Mirella worked as a PhD candidate with her promotors Prof. Dr. Ron Heeren and her co-promotors Dr. Berta Cillero-Pastor and Dr. Pieter Emans on a collaborative project between the Maastricht MultiModal Molecular Imaging Institute M4I and the department of Orthopedic Surgery/Laboratory for Experimental Orthopedics at Maastricht University. This PhD position was part of the William Hunter Revisited project, leaded by Prof. Dr. Marcel Karperien. She searched for molecular characteristics and biomarkers for osteochondral defect and osteoarthritis patients using multiple mass spectrometry techniques, as part of this Thesis.

From February 2024, Mirella will start working at Philips Healthcare – Imaging Guided Therapy through Bright Society.